SSC-351

AN INTRODUCTION TO STRUCTURAL RELIABILITY THEORY
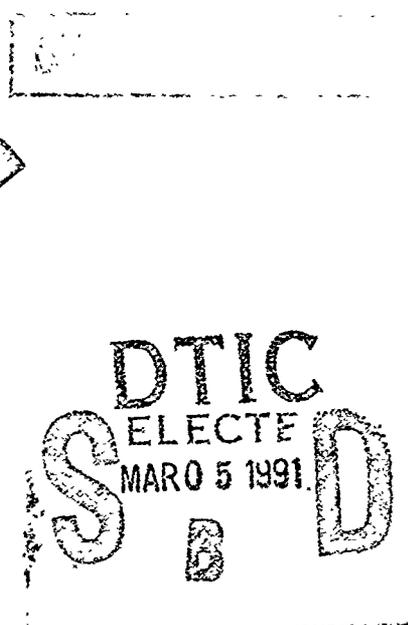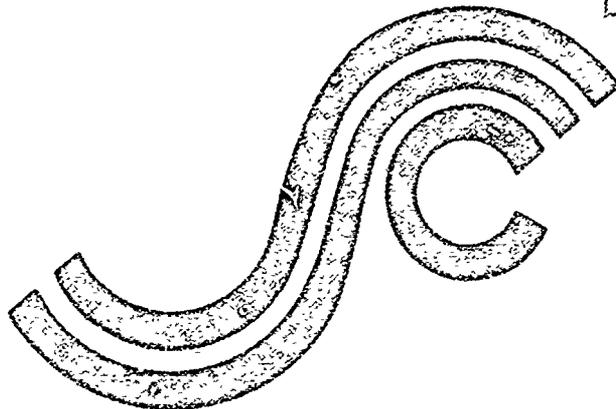
DTIC
SELECTE
MAR 0 5 1991
B D

SHIP STRUCTURE COMMITTEE
1990

SHIP STRUCTURE COMMITTEE

The SHIP STRUCTURE COMMITTEE is constituted to prosecute a research program to improve the ull structures of ships and other marine structures by an extension of knowledge pertaining to design. materials, and methods of construction.

RADM J. D. Sipes, USCG, (Chairman)
Chief, Office of Marine Safety, Security
  and Environmental Protection
U. S. Coast Guard

Mr. Alexander Malakhoff
Director, Structural Integrity
  Subgroup (SEA 55Y)
Naval Sea Systems Command

Dr. Donald Liu
Senior Vice President
American Bureau of Shipping

Mr. H T. Haller
Associate Administrator for Ship-
  building and Ship Operations
Maritime Administration

Mr. Thomas W. Allen
Engineering Officer (N7)
Military Sealift Command

CDR Michael K. Parmelee, USCG,
Secretary, Ship Structure Committee
U. S. Coast Guard

CONTRACTING OFFICER TECHNICAL REPRESENTATIVES

Mr. William J. Siekierka
SEA 55Y3
Naval Sea Systems Command

Mr. Greg D. Woods
SEA 55Y3
Naval Sea Systems Command

SHIP STRUCTURE SUBCOMMITTEE

The SHIP STRUCTURE SUBCOMMITTEE acts for the Ship Structure Committee on technical matte s by providing technical coordination for determinating the goals and objectives of the program and by evaluating and interpreting the results in terms of structural design, construction, and operation

AMERICAN BUREAU OF SHIPPING

Mr. Stephen G. Arntson (Chairman)
Mr John F. Conlon
Mr. William Hanzalek
Mr. Philip G. Rynn

MILITARY SEALIFT COMMAND

Mr. Albert J. Attermeyer
Mr Michael W. Touma
Mr. Jeffery E. Beach

MARITIME ADMINISTRATION

Mr. Frederick Seibold
Mr. Norman O. Hammer
Mr. Chao H. Lin
Dr. Walter M. Maclean

NAVAL SEA SYSTEMS COMMAND

Mr. Robert A. Sielski
Mr. Charles L. Null
Mr. W. Thomas Packard
Mr. Allen H. Engle

U. S. COAST GUARD

CAPT T. E. Thompson
CAPT Donald S. Jensen
CDR Mark E. Noll

SHIP STRUCTURE SUBCOMMITTEE LIAISON MEMBERS

U. S. COAST GUARD ACADEMY

LT Bruce Mustain

U. S. MERCHANT MARINE ACADEMY

Dr. C. B. Kim

U. S. NAVAL ACADEMY

Dr Ramswar Bhattacharyya

STATE UNIVERSITY OF NEW YORK MARITIME COLLEGE

Dr. W. R. Porter

WELDING RESEARCH COUNCIL

Dr. Martin Prager

NATIONAL ACADEMY OF SCIENCES - MARINE BOARD

Mr. Alexander B. Stavovy

NATIONAL ACADEMY OF SCIENCES - COMMITTEE ON MARINE STRUCTURES

Mr. Stanley G. Stiansen

SOCIETY OF NAVAL ARCHITECTS AND MARINE ENGINEERS - HYDRODYNAMICS COMMITTEE

Dr. William Sandberg

AMERICAN IRON AND STEEL INSTITUTE

Mr. Alexander D. Wilson

Ship Structure Committee

An Interagency Advisory Committee
Dedicated to the Improvement of Marine Structures

December 3, 1990

SSC-351
SR-1310

AN INTRODUCTION TO STRUCTURAL RELIABILITY THEORY

As structural designs and analysis techniques evolve, we find that there is a need to more rationally assess uncertainties associated with marine structures. Naval architects and structural engineers recognize that it necessary to gain a greater understanding of structural reliability as it relates to the safety and serviceability of marine structures. This report provides an excellent introduction to structural reliability theory. It was developed as a tutorial and should prove to be a valuable reference document.
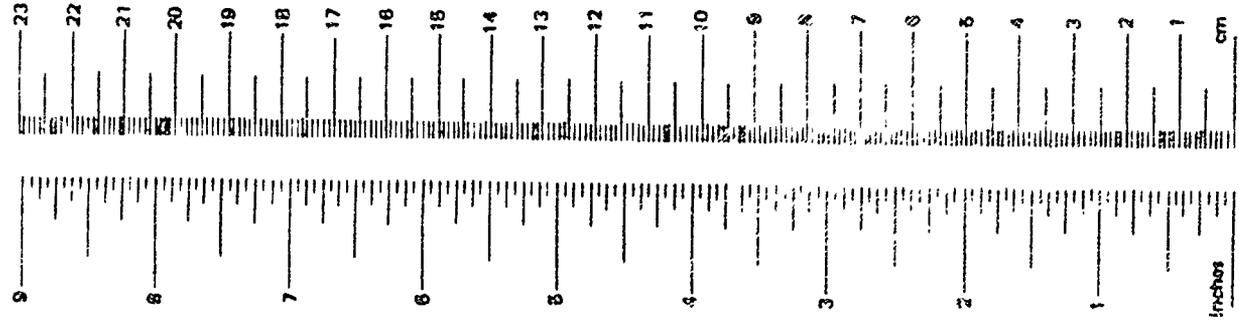
J. D. SIPES
Rear Admiral, U.S. Coast Guard
Chairman, Ship Structure Committee

1. Report No. SSC-351	2. Government Accession No.	3. Recipient's Catalog No.
4. Title and Subtitle AN INTRODUCTION TO STRUCTURAL RELIABILITY THEORY		5. Report Date JANUARY 1989
		6. Performing Organization Code
7. Author's) ALAA E. MANSOUR		8. Performing Organization Report No SR-1310
9. Performing Organization Name and Address MANSOUR ENGINEERING, INC BERKELEY, CA 94708		10. Work Unit No. (TRAIS)
		11. Contract or Grant No. DTCG23-86-C-20054
12. Sponsoring Agency Name and Address SHIP STRUCTURE COMMITTEE U.S. COAST GUARD 2100 SECOND STREET, SW, WASHINGTON, DC 20593		13. Type of Report and Period Covered FINAL
		14. Sponsoring Agency Code G-M

15. Supplementary Notes

This work was carried out under the sponsorship of the Ship Structure Committee and its member agencies.

16. Abstract

This report provides an introduction to the state-of-the-art in structural reliability theory directed specifically toward the marine industry. Comprehensive probabilistic models are described for the environment, wave loads acting on a marine structure, its failure modes, reliability under extreme load, system reliability, and fatigue reliability. Application examples of various models are presented including the necessary information required to perform such reliability analyses. A description of a computer programs for calculating the reliability level of a marine structure is provided as an appendix.

17. Key Words Reliability Theory Probability Reliability Models System Reliability Fatigue Reliability		18. Distribution Statement Available to the public from: National Technical Information Service Springfield, VA 22161 or Marine Technical Information Facility National Maritime Research Center Kings Point, NY 10024-1699	
19. Security Classif. (of this report) UNCLASSIFIED	20. Security Classif. (of this page) UNCLASSIFIED	21. No. of Pages 354	22. Price

Form DOT F 1700.7 (8-72)   Reproduction of completed page authorized

METRIC CONVERSION FACTORS

Approximate Conversions to Metric Measures

Symbol	When You Know	Multiply by	To Find	Symbol
LENGTH				
in	inches	*2.5	centimeters	cm
ft	feet	30	centimeters	cm
yd	yards	0.9	meters	m
mi	miles	1.6	kilometers	km
AREA				
in²	square inches	6.5	square centimeters	cm²
ft²	square feet	0.09	square meters	m²
yd²	square yards	0.8	square meters	m²
mi²	square miles	2.6	square kilometers	km²
	acres	0.4	hectares	ha
MASS (weight)				
oz	ounces	28	grams	g
lb	pounds	0.45	kilograms	kg
	short tons (2000 lb)	0.9	tonnes	t
VOLUME				
tsp	teaspoons	5	milliliters	ml
Tbsp	tablespoons	15	milliliters	ml
fl oz	fluid ounces	30	milliliters	ml
c	cups	0.24	liters	l
pt	pints	0.47	liters	l
qt	quarts	0.95	liters	l
gal	gallons	3.8	liters	l
ft³	cubic feet	0.03	cubic meters	m³
yd³	cubic yards	0.76	cubic meters	m³
TEMPERATURE (exact)				
°F	Fahrenheit temperature	5/9 (after subtracting 32)	Celsius temperature	°C

*1 in. = 2.54 cm (exactly). For other exact conversions and more detail tables see NBS Misc. Publ. 286, Units of Weight and Measures. Price $2.25 SD Catalog No. C13 10 286.

Approximate Conversions from Metric Measures

Symbol	When You Know	Multiply by	To Find	Symbol
LENGTH				
mm	millimeters	0.04	inches	in
cm	centimeters	0.4	inches	in
m	meters	3.3	feet	ft
m	meters	1.1	yards	yd
km	kilometers	0.6	miles	mi
AREA				
cm²	square centimeters	0.16	square inches	in²
m²	square meters	1.2	square yards	yd²
km²	square kilometers	0.4	square miles	mi²
ha	hectares (10,000 m²)	2.5	acres	
MASS (weight)				
g	grams	0.035	ounces	oz
kg	kilograms	2.2	pounds	lb
t	tonnes (1000 kg)	1.1	short tons	
VOLUME				
ml	milliliters	0.03	fluid ounces	fl oz
l	liters	2.1	pints	pt
l	liters	1.06	quarts	qt
l	liters	0.26	gallons	gal
m³	cubic meters	35	cubic feet	ft³
m³	cubic meters	1.3	cubic yards	yd³
TEMPERATURE (exact)				
°C	Celsius temperature	9/5 (then add 32)	Fahrenheit temperature	°F

TEMPERATURE scale:
°F -40   0   32   80   98.6   160   212
°C -40 -20   0   20   37   60 80 100

TABLE OF CONTENTS

v

NOTATION

The following list defines the main symbols appearing in this report.

L = ship length

X = random variable

μ_x = mean of X

σ_x = standard deviation of X

$f_x(\cdot)$ = probability density function of X

$F_x(\cdot)$ = distribution function of X

E_x = mean square value of X

λ = parameter of exponential distribution

l, k = parameters of Weibull distribution

ω = wave frequency

$H(\omega)$ = frequency response function

$S_x(\omega)$ = wave spectrum

$S_y(\omega)$ = response spectrum

N, n = number of records or encounters

Z_n = random variable representing extreme amplitude of total bending moment in n-records

$\phi z_n(\cdot)$ = probability density function of Z_n

p_f = probability of failure

$p_f|n=1$ = probability of failure for n = 1

$[A_1 \cup A_2]$ = union of two events A_1 and A_2

$\bar{A}_i$ = complementary event of A_i

$[A_1 \cap A_2]$ = intersection of the two events A_1 and A_2

C_g = generalized cost

C_i = initial cost of construction plus maintenance

C_f = cost due to failure

M = safety margin

S = random variable representing strength

Z = random variable representing total bending moment

$g(\cdot)$ = limit state function or performance function

x_i^* = coordinates of most likely failure point in original space

$y_i{}^*$ = coordinates of most likely failure point in reduced space

v_x = coefficient of variation of a random variable X

θ = central safety factor

$\phi(\ ),\Phi(\ )$ = standard normal probability density and distribution functions

ρ_{ij} = correlation coefficient

α_i = direction cosine

β = safety index

Δ_i = partial safety factors associated with a random variable

Metric Conversion Table

1 ft	=	0.3048 m
1 in.	=	25.4 mm
1 psi	=	6.894 kPa
1 ksi	=	6.894 MPa
1 lb-in.	=	0.113 N·m
1 ton-ft	=	0.309 t·m

1. INTRODUCTION AND SUMMARY

Structural reliability theory is concerned with the rational treatment of uncertainties associated with design of structures and with assessing the safety and serviceability of these structures. The subject has grown rapidly in the last decade as can be seen from the many recent books and proceedings published on the subject [1,2,3,4]. It has evolved from a research topic to procedures and methodologies of wide range of practical applications and has been used in code development.

There is a need for naval architects and structural engineers to develop an understanding of structural reliability theory and its application to marine structure. The aim of the application is usually to achieve economy together with an appropriate degree of safety. However, like other tools, structural reliability theory can be misused if not well understood. It cannot be thought of as the solution to all safety problems and it cannot be applied in a mechanical fashion. There are also several shortcomings that must be clearly identified and examined.

The objective of this work is to provide an introduction and summary of the state-of-the-art in structural reliability theory <u>directed specifically towards the marine industry</u>. To this end, consideration is given to: (a) the kind and <u>nature of existing data</u> on the design variables of a marine structure, and (b) the <u>numerical nature of the analysis</u> of complex structures that typically exist in the marine environment.

1.1   Role of Reliability Analysis in a General Probabilistic Design Procedure

In order to define the role of reliability analysis in a general probabilistic procedure for the design of marine structures, Figure 1.1 is introduced.

Starting with a configuration of the marine structure and using random ocean waves as input, the wave loads acting on the structure can be determined (please refer to Figure 1.1). Generally, for primary design analysis the most important loads are the large ones. Extrapolation procedures are usually used to determine the characteristics of these large loads. In the case of ocean-going

vessels, for example, this is done either through the determination of a long-term distribution of the wave loads [5,6,7] or through the evaluation of an extreme load distribution [8,9,10,11] that may occur in a specific storm condition.

In general, wave loads acting on an ocean-going vessel include low-frequency loads due to the motion of the vessel in waves as a rigid body. They also include higher frequency loads (and response) due to slamming and springing which can be determined by considering the ship as a flexible body. In principle, these loads should be combined stochastically to determine the total wave load as, for example, developed in [12,13].

Referring back to Figure 1.1, other loads beside wave loads occur on a marine structure. These loads may be important in magnitude, though usually less random in nature (except possibly for wind loads on offshore structures). For example, in the case of ocean-going vessels, these loads consist mainly of stillwater loads and thermal loads.

Following Figure 1.1, the response of the marine structure to the total combined loads is determined and compared with the resistance or capability of the structure. This comparison may be conducted through one of several reliability methods. Based on these methods, safety indices or probabilities of failure are estimated and compared with acceptable ones. A new cycle may be necessary if the estimated indices are below the acceptable ones.

1.2   Basic Concept in Reliability

In order to illustrate some aspects of the procedure described in figure 1.1 and to introduce the basic concept in the reliability analysis, the following example is given. Consider a simple beam subjected to a loading induced by the environment, e.g. wave load. Traditionally, in the design of such a beam, practitioners and designers have used fixed deterministic values for the load acting on the beam and for its strength. In reality these values are not unique values but rather have probability distributions that reflect many uncertainties in the load and the strength of the beam. Structural reliability theory deals mainly with the assessment of these uncertainties and the methods of quantifying and

2
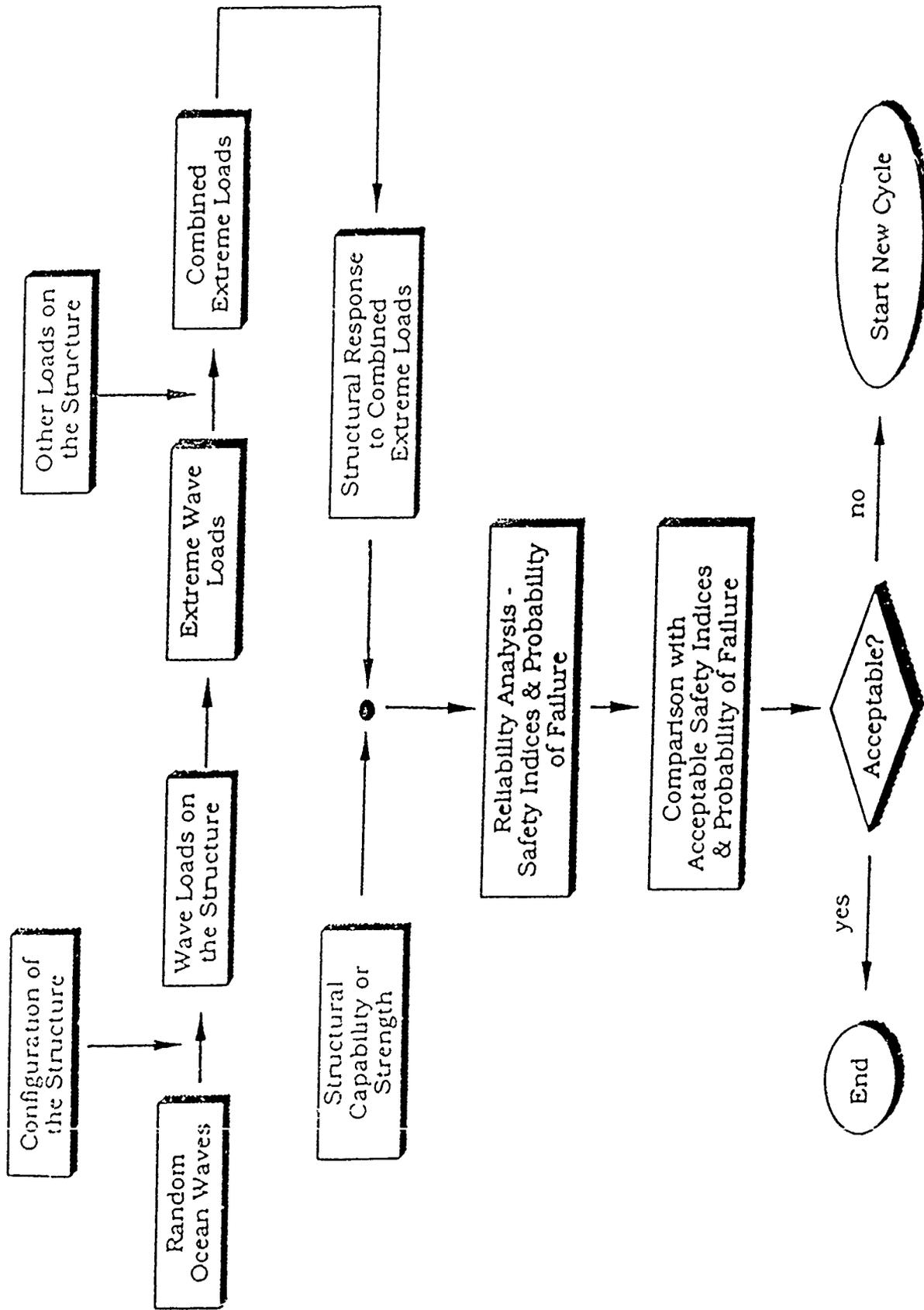
Figure 1.1- Probabilistic Analysis of Marine Structures

rationally including them in the design process. The load and the strength are thus modelled as random variables.

Figure 1.2 shows the probability density functions of the load and the strength of the beam in terms of applied bending moment and ultimate moment capacity of the beam, respectively. Both, the load "Z" and the strength "S" are assumed in this example to follow the normal (Gaussian) probability distribution with mean values μ_Z=20,000 ft-ton and μ_S=30,000 ft-ton, respectively, and standard deviations of σ_Z=2,500 ft-ton and σ_S=3,000 ft-ton, respectively.
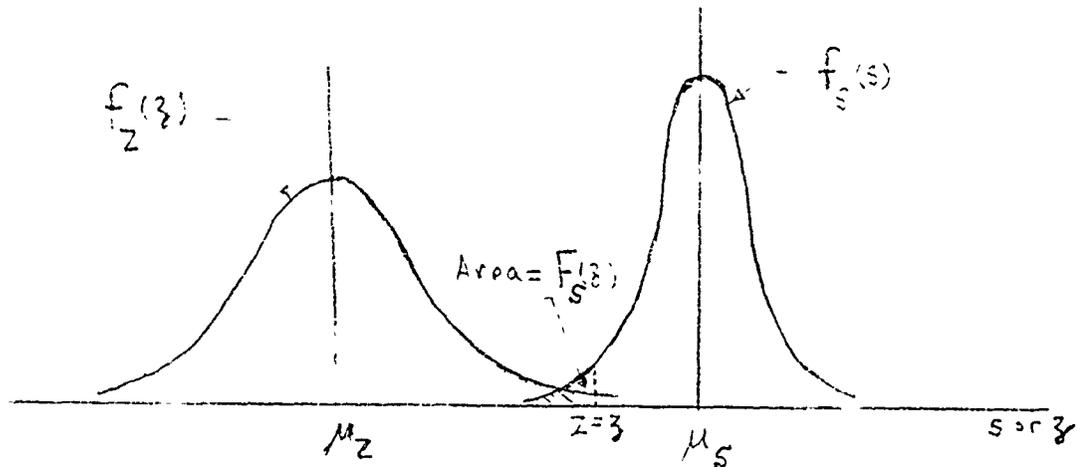
Figure 1.2. Load and Strength Probability Density Functions

We may now construct a simple function g(s,z), called the limit state function, which describes the safety margin "M" between the strength of the beam and the load acting on it, i.e.,

$$M = g(s,z) = S\text{-}Z \tag{1.1}$$

Both S and Z are random variables and may assume several values. Therefore, the following events or conditions describe the possible states of the beam,

4

(i) M = g(s,z) < 0   represents a failure state since this means that the load Z exceeds the strength S.

(ii) M = g(s,z) > 0   represents a safe state

(iii) M = g(s,z) = 0   represents the limit state surface (line in this case) or the border line between the safe and failure states.

The probability of failure implied in (i) above can be computed from :

$$p_f = P[M = g(s,z) \leq 0] = \iint\limits_{g(s,z) \leq 0} f_{S,Z}(s,z)\, ds\, dz \qquad (1.2)$$

where $f_{S,Z}(s,z)$ is the joint probability density function of S and Z and the domain of integration is over all values of s and z where the margin M is not positive, i.e., not in the safe state. If the applied load on the beam is statistically independent from the beam strength the above equation can be simplified and interpreted easily as:

$$p_f = \int_0^\infty F_S(z)\, f_Z(z)\, dz \qquad (1.3)$$

where $F_S(.)$ and $f_Z(.)$ are the cumulative distribution function of S and the probability density function of Z, respectively, both in this example, are Gaussian.

Equation (1.3) is the convolution integral with respect to z and can be interpreted with reference to Figure 1.2. If Z=z, the conditional probability of failure would be $F_S(z)$. But since $z<Z\leq z+dz$ is associated with probability $f_Z(z)dz$, integration of all values of z results in equation (1.3).

In our example, S and Z are both statistically independent and normally distributed. Equation (1.3) can be thus shown to reduce to:

5

$$p_f = \Phi(-\beta) \tag{1.4}$$

where $\Phi(\cdot)$ is the standard normal cumulative distribution function and β is called a safety index defined as:

$$\beta = \frac{\mu_s - \mu_z}{\sqrt{\sigma_s^2 + \sigma_z^2}} \tag{1.5}$$

Notice that as the safety index β increases the probability of failure p_f as given by (1.4) decreases. The safety of the beam as measured by the safety index β can be thus increased (see equation 1.5) by increasing the difference between the means μ_s-μ_z or decreasing the standard deviations σ_s and σ_z.

Substituting in equation (1.5) the numerical values for μ_s, μ_z, σ_s and σ_z given in our simple beam example results in a safety index $\beta = 2.56$. Equation (1.4) can be then used in conjunction with tables of standard normal cumulative distribution function to yield a probability of failure = 5.23×10^{-3}.

1.3   Necessary Information for Reliability Analysis of Marine Structures

The preceding example and Figure 1.1 indicate that certain specific load and strength information are necessary for performing reliability analysis of marine structures. It is mostly in this area that reliability analysis of marine structures differs from typical civil engineering structures. In this report emphasis is placed on developing the required load and strength information for marine structures.

Prior to estimating the loads acting on ships or marine structures a statistical representation of the environment is necessary. This includes waves, wind, ice, seismic and current. The last four items are more important for fixed offshore structures than for floating vessels. The environmental information can then be used as input to determine the loads acting on the structure. Typically, an input/output spectral analysis procedure is used to determine the "short-term" loads in a specific sea condition (stationary condition). The required transfer

function is determined from strip theory using the equations of motion of the vessel or from a towing tank experiment. In offshore structures, Morison's equation is usually used to determine the wave load transfer function.

Short term prediction of the loads is not sufficient for the reliability analysis. Extreme values and long-term prediction of the maximum loads and their statistics are more valuable. For this purpose order statistics and statistics of extremes play a very important role. Gumbel's theory of asymptotic distributions is often used in this regard. In the long-term prediction, the fatigue loads, i.e., the cyclic repetitive loads which cause cumulative damage to the structure must also be considered.

For complete description of this aspect of reliability analysis, methods of combining the loads such as static and dynamic, including high and low frequency loads, must be considered. In nature, many of these loads act simultaneously, therefore, their combination must be evaluated for a meaningful reliability analysis. The environment and load aspects are discussed in Chapter 2 of this report.

The second major component in the reliability analysis is the strength (or resistance) of the marine structure and the evaluation of its modes of failure. In this regard several limit states may be defined such as the ultimate limit state, fatigue limit state and serviceability limit state. The first is related to the maximum load carrying capacity of the structure, the second to the damaging effect of repeated loading and the third to criteria governing normal use and durability. Each of these limit states include several modes; for example, the ultimate limit state includes excessive yielding (plastic mechanisms) and instability (buckling failure).

Methods of analyzing uncertainties associated with the loads and the strength of marine structures are important aspects of reliability analysis [14,15]. Generally, these uncertainties are quantified by coefficients of variation since in most cases lack of data prevents the estimation of complete probability distributions. Strength, modes of failure and uncertainty analysis of marine structures are discussed in Chapter 3 of the report.

Chapters 4, 5 and 6 present three different levels of reliability analysis based on the load and strength information discussed in Chapters 2 and 3. Examples of application to ships are also provided in these chapters. Chapter 7 introduces simulation and Monte Carlo techniques as a tool for use in the reliability analysis. System reliability, which deals with redundancy of structures and multiplicity of failure modes is discussed in Chapter 8. Chapter 9 describes a procedure for fatigue reliability which requires separate treatment from reliability under extreme load. Several application examples to ships and offshore structures are given in Chapter 10. The last chapter of the report discusses some shortcomings and offers concluding remarks. Appendices are given at the end of the report one of which includes some helpful information and another describes a computer program for performing reliability analysis.

The reader of this report can get full benefit of the material presented if he/she has a background (one course) in basic probability theory and statistics including probability distributions, random variables, expectation of a random variable, sampling theory, and estimation methods.

REFERENCES

1.1 Madsen, H. O., Krenk, S. and Lind, N. C., Methods of Structural Safety, Prentice-Hall, Inc., Englewood Cliffs, 1986.

1.2 Ang, A. H.-S., and Tang, W. H., Probability Concepts in Engineering Planning and Design - Volume II. Decision, Risk and Reliability, John Wiley and Sons, Inc., New York, 1984.

1.3 Thoft-Christensen, P. and Baker, M., Structural Reliability Theory and Its Application, Springer-Verlag, Berlin, 1982.

1.4 Konishi, I., Ang, A. H.-S. and Shinozuka, M. (editors), Structural Safety and Reliability, Volumes I, II and III, Proceedings of ICOSSAR, Kobe, Japan, 1985.

1.5 Mansour, A., "Methods of Computing the Probability of Failure Under Extreme Values of Bending Moment," M.I.T Report No. 70-15, Sept. 1970; also Journal of Ship Research, Vol. 16, No. 2, June 1972.

1.6 Lewis, E., "Predicting Long-Term Distributions of Wave-Induced Bending Moment on Ship Hulls," Spring Meeting, SNAME, 1967.

1.7 Mansour, A., "Probabilistic Design Concepts in Ship Structural Safety and Reliability," Transactions, SNAME, 1972.

1.8 Ochi, M. and Motter, E., "Prediction of Extreme Values of Impact Pressure Associated with Ship Slamming," Journal of Ship Research, Vol. 13, No. 2, June 1969.

1.9 Mansour, A. and Faulkner, D., "On Applying the Statistical Approach to Extreme Sea Loads and Ship Hull Strength," RINA Transactions, 1973.

1.10 Ochi, M. K., "Principles of Extreme Value Statistics and Their Application," Proc. Extreme Loads Symposium., Oct. 1981.

1.11 Mansour, A. and Lozow, J., "Stochastic Theory of Marine Vehicles Slamming Response in Random Seas," Journal of Ship Research, Vol. 26, No. 4, Dec. 1982.

1.12 Ferro, G. and Mansour, A., "Probabilistic Analysis of the Combined Slamming and Wave-Induced Responses," Journal of Ship Research, Vol. 29, No. 3, Sept. 1985, p.170.

1.13 Mansour, A., "Combining Extreme Environmental Loads for Reliability-based Designs," Proceedings of the Extreme Loads Response Symposium, SSC and SNAME, Arlington, VA, October 1981, pp. 63-74.

1.14 Faulkner, D. and Sadden, J. A., "Toward a Unified Approach to Ship Structural Safety," Trans. Royal Institution of Naval Architects, Vol. 121, 1979, pp. 1-38.

1.15 Guesdes Soares, C. and Moan, T., "Statistical Analysis of Stillwater Load Effects in Ship Structures," Trans. SNAME, Vol. 96, 1988.

2. LOAD INFORMATION REQUIRED IN RELIABILITY ANALYSIS OF MARINE STRUCTURES

2.1 Probabilistic Representation of Environment

Prior to discussing the loads acting on a ship or a marine structure, a discussion of a probabilistic representation of the environment is essential. Information on the environment can be then used as input to determine the loads acting on the structure. A complete description of the environment entails description of waves, wind, ice, seismic and current. The last four items are more important for fixed offshore structures than for floating vessels. Since the main emphasis in this work is floating vessels, only waves will be thoroughly investigated in this report.

The sea surface is irregular and never repeats itself. An exact mathematical representation of it as function of time, wind speed, wind direction, current, etc. is not possible. A representation, however, using a probabilistic model is possible and more suitable. By means of the theory of random processes one may represent the sea surface and determine certain statistical averages and extreme values suitable for design.

Such a probabilistic representation of a random phenomenon has been well developed in electrical engineering to analyze random noise (see reference [2.1]) and was used successfully in mechanical engineering to investigate random vibration (e.g. [2.2]). It has been also used in civil engineering for earthquake analysis. In the next section a few definitions related to random processes and the associated probability distributions are discussed.

2.1.1. Definitions:

Deterministic process: If an experiment is performed many times under identical conditions and the records obtained are always alike, the process is said to be deterministic. For example, sinusoidal or

predominantly sinusoidal time history of a measured quantity are records of a deterministic process [2.2].

Random process: If the experiment is performed many times when all conditions under the control of the experimenter are kept the same, but the records continually differ from each other, the process is said to be random [2.2].

The degree of randomness in a process depends on: (1) the understanding of effects of the factors involved in the experiment, and (2) the ability to control them.

As an example of a random process, consider a test is being performed to determine the wave elevation as a function of time at a given location in the ocean. Figure 2.1 is a record of the wave elevation as recorded for a period of approximately 18 minutes.

WAVE ELEVATION RECORDS

$x^{(1)}(t)$

TIME (sec)
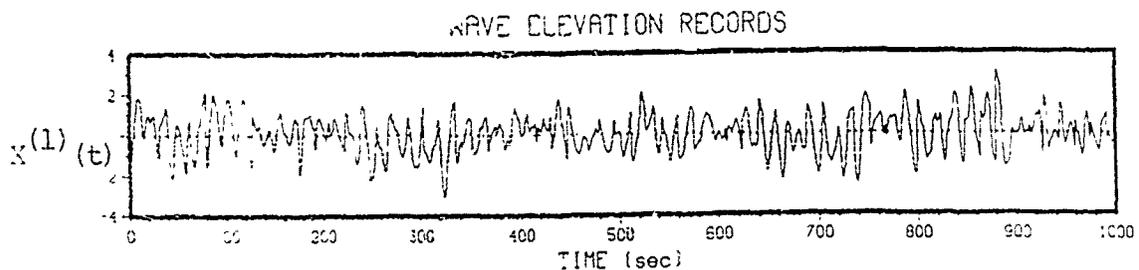
Figure 2.1

The same test was repeated under identical conditions as far as is known, that is, under the same wind speed   and   a record as shown in Figure 2.2 was obtained. The striking feature is that the two records are not identical, If the test is repeated several times under identical conditions as far as is known, records will be obtained that are not identical. This randomness in the records is

12

due to factors beyond one's control and ability to measure. The elevation of the water surface at any time is due to the entire history of the meteorological conditions in that area and surrounding areas. Therefore, under given macroscopic parameters such as wind direction, speed, duration, etc., one cannot predict exactly the wave surface at the given point. The wave elevation records can be thus treated as records of a random process.

$X^{(2)}(t)$
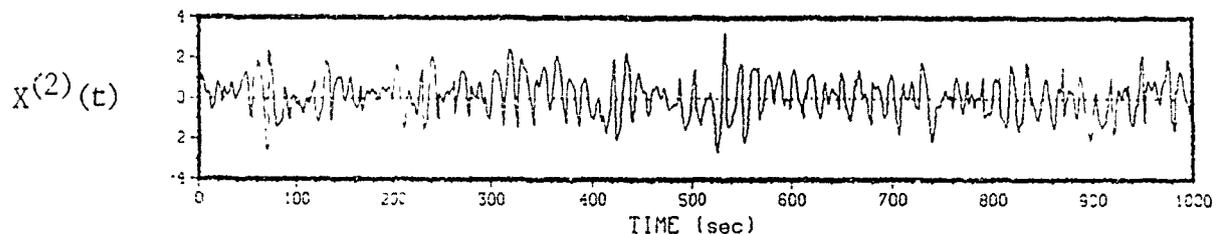
Figure 2.2

Another example of a random process is an ensemble of time history records of a strain gage installed in a ferry boat operating between, say, San Francisco and San Rafael. In any given day, a record during each trip between these two neighboring cities is obtained. The resulting ensemble of records can be treated as records of a random process.

As discussed above, the most important notion involved in the concept of a random process $X^{(i)}(t)$ is that not just one time history is described, but the whole family or ensemble of possible time histories which might have been the outcome of the same test are described. In the example of recording wave elevation at a given point in the ocean, the end result is an ensemble of records of wave variation as a function of time (see Figure 2.3).

Each of the above records is called a "sample." Some of these samples are more probable than others, and in order to describe the random process further it is necessary to give probability information.

It should be noted that a sinusoid in a deterministic process can be characterized completely by its amplitude and frequency (phase is unimportant in many cases). Similarly, the random samples can be characterized by some average amplitude (root mean square) and a decomposition in frequency (spectral density) as will be discussed later.
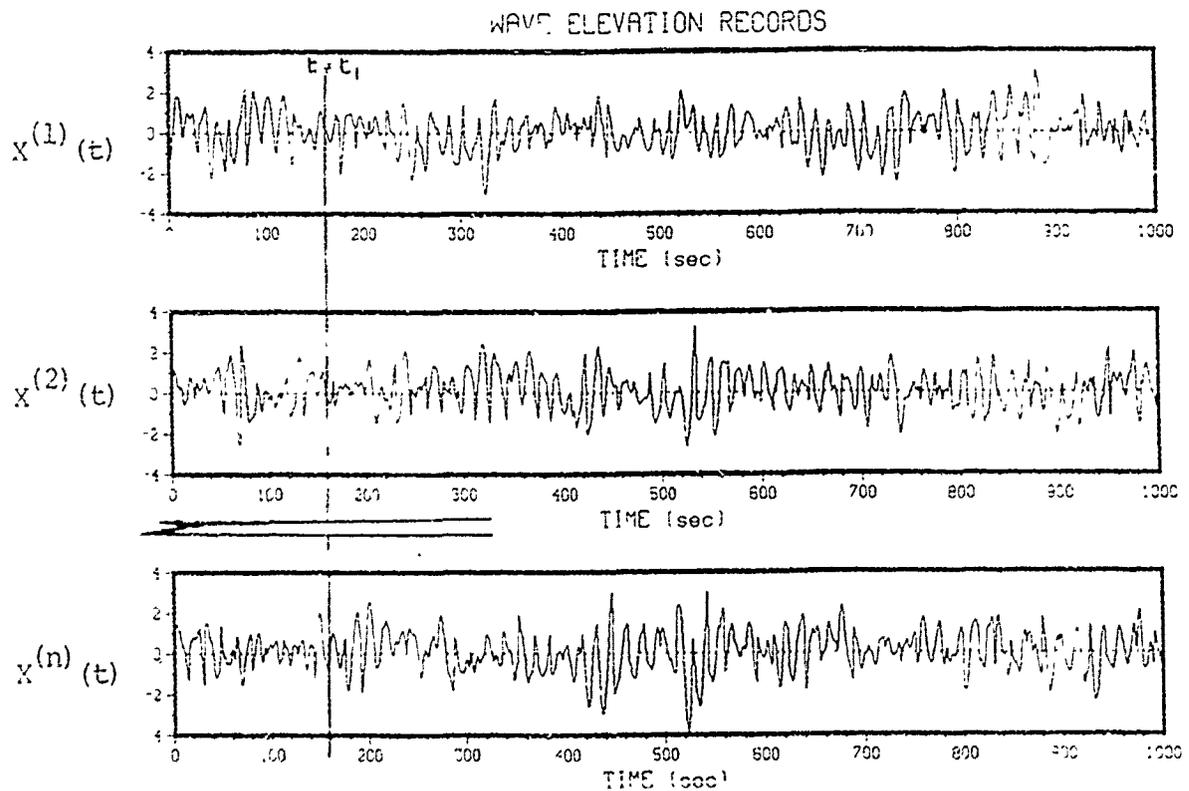
Figure 2.3.

A designer given the record ensemble shown in Figure 2.3 may:

a. Select the largest value in the ensemble and use it for his new design with a factor of safety. In this case he will make no use of all information he is given except for one value, i.e., the maximum value, or,

b. Try to obtain statistical information from all the records and use such information in his new design.

If "b" is selected, a probability description of the random process is necessary.

First and Second Order Probability Distributions:

At a fixed value, $t = t$, (see Figure 2.3) the values of $X^{(i)}(t_1)$, which represent wave elevation, can be described by a graph such as in Figure 2.4. This graph shows the probability density function[1] (p.d.f.) $f [x (t_1)]$ or simply $f(x)$ which has the following properties:

PROBABILITY DENSITY FUNCTION
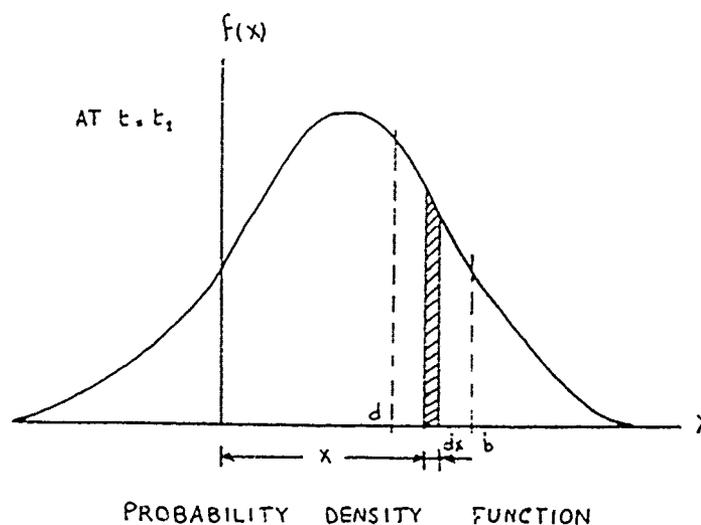
Figure 2.4.

---

1 First order probability distribution

1)   The fraction of the ensemble members for which the wave elevation X, treated as a random variable, lies between x and x + dx is f(x) dx , i.e.,

$$P[x < X \le x + dx] = f(x)\, dx$$

2)   The probability that a sample of wave elevation lies between a and b is

$$P[a < X \le b] = \int_{a}^{b} f(x)\, dx$$

3)   The probability that X lies between $-\infty$ and $+\infty$ is one, that is,

$$P[-\infty < X \le \infty] = \int_{-\infty}^{+\infty} f(x)\, dx = 1$$

4) $P[x = a] = 0.$

where "a" is a constant.

If, at two time instants t_1 and t_2, the wave elevations treated as random variables are denoted $X(t_1)$ and $X(t_2)$, or simply X_1 and X_2, the probability distribution[2] of these (called joint probability density function) is given by a surface $f(x_1, x_2)$ and has the properties (Figure 2.5):

1) $P[x_1 < X_1 \le x_1 + dx_1 \text{ and } x_2 < X_2 \le x_2 + dx_2] = f(x_1, x_2)\, dx_1 dx_2$

2) $P[a_1 < X_1 \le b_1 \text{ and } a_2 < X_2 \le b_2] = \int_{a_2}^{b_2} \int_{a_1}^{b} f(x_1, x_2)\, dx_1 dx_2$

3) $P[-\infty < X_1 < +\infty, -\infty < X_2 < +\infty] = \int_{-\infty}^{+\infty} \int_{-\infty}^{+\infty} f(x_1, x_2)\, dx_1 dx_2 = 1$

---

2 Second order probability distribution.

Ensemble Averages:

For a given function g(x), it may be defined:

$$E[g(x)] = \text{expected value of } g(x) = \int_{-\infty}^{+\infty} g(x)f(x)dx$$
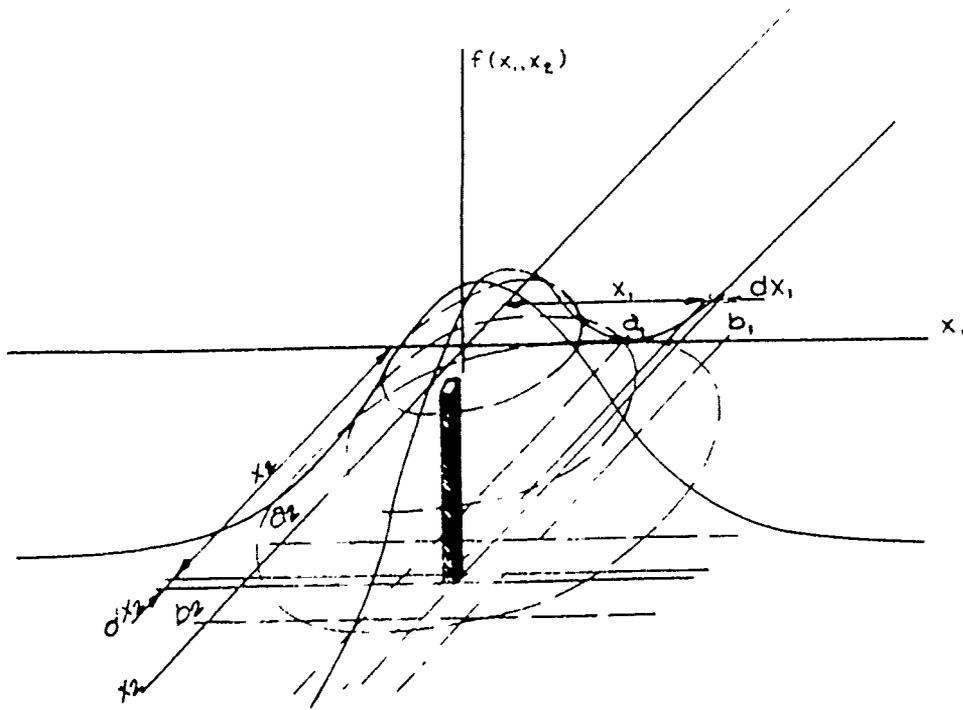
JOINT PROBABILITY DENSITY FUNCTION

Figure 2.5.

For a given p.d.f. f(x), the following definitions will be used for the wave elevation treated as a random variable X. When g(x) is simply x, then

$$E[x] = \int_{-\infty}^{+\infty} xf(x)dx \quad = \quad \text{mean or ensemble average} \quad (2.1)$$

= expected value of X (analogous to moment about origin or distance from origin to center of mass of a rod of unit mass)

When $g(x) = x^2$, then

$$E[x^2] = \int_{-\infty}^{+\infty} x^2 f(x)dx = \text{mean square of the random variable X} \quad (2.2)$$

(analogous to moment of inertia or square of radius of gyration about origin)

Root mean square (r.m.s.) = $\sqrt{E[x^2]}$

Setting $g(x) = (x - E[x])^2$

$$\sigma^2 \quad = E(x - E[x])^2 \quad = \quad \int_{-\infty}^{+\infty} (x-E[x])^2 f(x)dx \quad (2.3)$$

$= E[x^2] - (E[x])^2 = $ variance of the random variable X (analogous to moment of inertia or square of radius of gyration about center of mass)

$$\sigma = \sqrt{\sigma^2} \quad = \text{standard deviation of the random variable X.}$$

At two fixed values t_1 and t_2, let x_1 and x_2 denote $x(t_1)$ and $x(t_2)$ respectively, then the autocorrelation and covariance functions are defined by:

$$\text{Autocorrelation} = E[x_1,x_2] = \int_{-\infty}^{+\infty} \int_{-\infty}^{+\infty} x_1 x_2 f(x_1,x_2)dx_1 dx_2 \quad (2.4)$$

18

(analogous to a product of inertia of a plate of unit mass about origin)

Covariance $\mu_{x_1 x_2} = E\{ [x_1 - E[x_1]][x_2 - E[x_2]] \}$

$$= \int_{-\infty}^{+\infty} \int_{-\infty}^{+\infty} [x_1 - E[x_1]][x_2 - E[x_2]] \, f(x_1, x_2) dx_1 dx_2$$

$$= E[x_1 x_2] - E[x_1]E[x_2] \qquad (2.5)$$

(analogous to the product of inertia of a plate of unit mass about the center of mass)

It should be noted that the covariance is equal to the autocorrelation minus the product of the means. Therefore, if one of the means is zero then the covariance is equal to the autocorrelation. The correlation coefficient $\rho_{x_1 x_2}$ can be defined as:

$$\rho_{x_1 x_2} = \frac{\mu_{x_1 x_2}}{\sigma_{x_1} \sigma_{x_2}} \qquad (2.6)$$

that is, a non-dimensional covariance.

The two random variables X_1 and X_2 are said to be independent if:

$$f(x_1, x_2) = f(x_1) f(x_2) \qquad (2.7)$$

therefore, from the definition of the autocorrelation function. it is easy to show, in this case, that

$$E[x_1 x_2] = E[x_1] E[x_2] \qquad (2.8)$$

and, thus, both the correlation coefficient $\rho_{x_1 x_2}$ and the covariance $\mu_{x_1 x_2}$ are zero. This means that independent random variables must necessarily be also uncorrelated (the converse is not necessarily true).

Note that when $t_2 = t_1$ the covariance becomes identical with the variance and the autocorrelation becomes identical with the mean square.

It is interesting to notice that in rigid body dynamics we need to know only the gross moments of inertia, but in vibration analysis more detailed information on the inertia distribution is necessary. Similarly, the average quantities derived above (mean, autocorrelation, covariance, etc.) give only gross statistical estimates of a random process. More refined estimates require more detailed information about the probability distribution.

2.1.2 Stationary and Ergodic Processes:

A random process is an infinite ensemble of sample functions. In the foregoing, the properties of the random process representing the wave generation at fixed instants t_1, t_2, etc., have been examined. Next, the variation of these properties when t_1, t_2 are assumed to vary is briefly discussed.

A random process is said to be <u>stationary</u> if its distributions are invariant under a shift of time scale, that is, independent of the origin.

This implies that the first order p.d.f. $f(x)$ becomes a universal distribution independent of time and $E(x)$ and σ^2 are also constants independent of time.

In addition, the second order p.d.f. is invariant under translation of time scale; therefore, it must be a function of the lag between t_1 and t_2 only, and not t_1 and t_2 individually. This implies

that the autocorrelation function is also a function of $\tau = t_2 - t_1$ only (see definition of the autocorrelation function given by equation 2.4).

$$E[x_1 x_2] = E[x(t)x(t+\tau)] = R(\tau) \qquad (2.9)$$

where $R(\tau)$ will be used to denote the autocorrelation function of a stationary random process. Note that $R(0) = E[x^2(t)] = $ mean square of the process.

$R(\tau)$ is an important function because it correlates the random process at any instant of time with its past (or future). $R(\tau)$ has the following properties (see figure 2.6):

i - $R(0)$ $=$ $E[x^2]$ $=$ mean square of the process

ii - $R(+\tau)$ $=$ $R(-\tau)$ ie, an even function of τ

iii - $R(0)$ $\geq$ $|R(\tau)|$
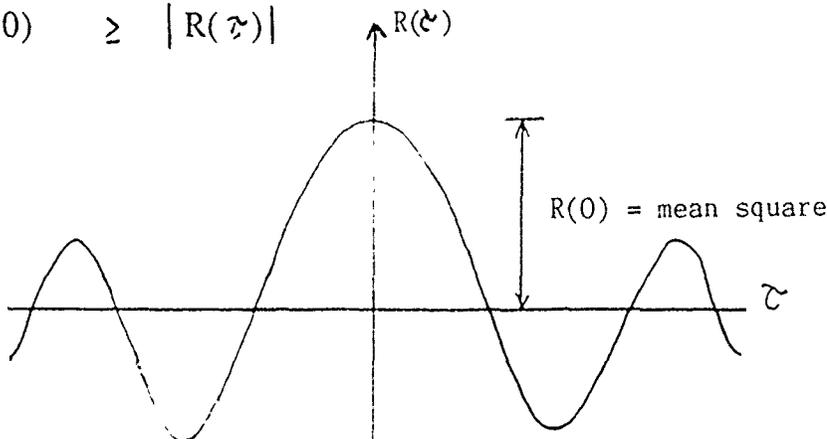
Figure 2.6. Autocorrelation function $R(\tau)$.

If changes in the statistical properties of a random process occur slowly with time then it is possible to subdivide the process into several processes of shorter duration, each of which may be considered stationary. It is usual to represent ocean waves as a stationary random process over a period of about 30 minutes to two hours.

The ergodic hypothesis states that a single sample function is quite typical of all other sample functions; therefore, we can estimate

various statistics of interest by averaging over time instead of averaging over the ensemble.
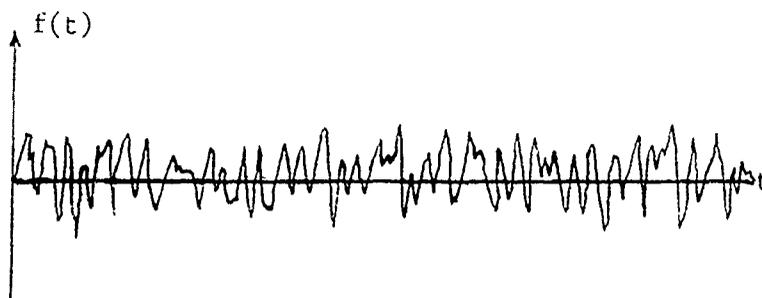
Figure 2.7. A sample function f(t).

If f(t) represents such a sample function (Fig.2.7), then the following temporal averages can be determined.

The temporal mean is,

$$<f> = \lim_{T \to \infty} \frac{1}{T} \int_{-T/2}^{+T/2} f(t)\,dt \qquad (2.10)$$

The temporal autocorrelation function $\phi(\tau)$ is,

$$\phi(\tau) = \lim_{T \to \infty} \frac{1}{T} \int_{-T/2}^{+T/2} f(t)f(t + \tau)\,dt \qquad (2.11)$$

The temporal mean square is,

$$<f^2> = \lim_{T \to \infty} \frac{1}{T} \int_{-T/2}^{+T/2} f^2(t)\,dt \qquad (2.12)$$

An ergodic process implies that $E[x] = <f>$ and $R(\tau) = \phi(\tau)$. An ergodic process is necessarily stationary since $<f>$ is a constant while $E[x]$ is generally a function of the time $t = t_1$ at which the ensemble average is performed except in the case of stationary process. However, a random process can be stationary without being ergodic.

22

For ocean waves, it may be necessary to assume the ergodic hypothesis if there is only one sample function of the process.

2.1.3 Spectral Density of a Stationary Random Process:

In many engineering problems it is customary to conduct a Fourier analysis of periodic functions. This simplifies the problem, because linearity permits treating each single frequency Fourier component separately and finally combining to obtain the total response.

A frequency decomposition of the autocorrelation function $R(\tau)$ of the ocean waves can be made:

$$R(\tau) = \int_{-\infty}^{+\infty} S(\omega) e^{i\omega\tau} d\omega \quad -\infty < \tau < \infty \tag{2.13}$$

where $S(\omega)$ is essentially the Fourier transform of $R(\tau)$ (except for the factor 2π) given by

$$S(\omega) = \frac{1}{2\pi} \int_{-\infty}^{+\infty} R(\tau) e^{-i\omega\tau} d\tau \quad -\infty < \omega < \infty \tag{2.14}$$

Relations (2.13) and (2.14) are known as Wiener-Khintchine relations. It can be shown that $S(\omega)$ is a non-negative even function of ω [2.2]. A physical meaning can be given to $S(\omega)$ by considering the limiting case when $\tau = 0$.

$$R(0) = \text{mean square} = [Ex^2] = \int_{-\infty}^{+\infty} S(\omega) \, d\omega ,$$

that is, the mean square of the process = the sum over all frequencies of $S(\omega)d\omega$, so that $S(\omega)$ can be interpreted as a mean square spectral density.

The mean square (area under the spectral density curve) is the average of the square of the wave elevation and the root mean square (rms) is the square root of that value. Physically, the larger the mean square (or the r.m.s. value), the larger is the wave elevation and the higher is the sea state.

Since the spectral density is an important function in ocean waves, the following remarks are made:

1) The units of ocean waves' spectral density are $[ft^2 \cdot sec]$ since

$$R(0) = E[x^2] = \int_{-\infty}^{+\infty} S(\omega) \, d\omega : [ft^2] \; ; \text{ therefore}$$

$$S(\omega) = [ft^2]/\text{units of circular frequency} = [ft^2 \cdot sec]$$

2) From the properties of a Fourier transform, it can be shown that $S(\omega)$ is a real and even function of ω. It can be represented by a curve as shown in Figure 2.8.
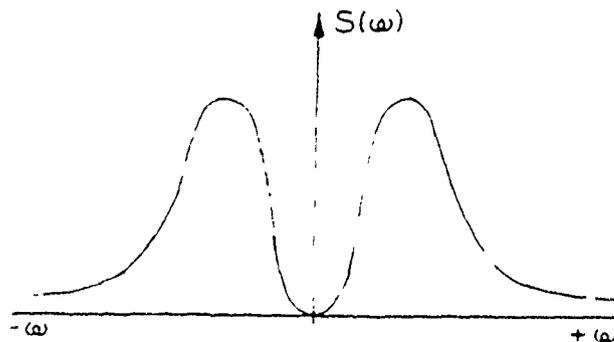
Figure 2.8. Two-sided Spectral Density.

3) In practice, the negative frequency obviously has no significance. It appeared in the mathematical model only to make the sums easier. Because of the shape of $S(\omega)$, it is called a two-sided spectrum.

24

4)   In practice, a "one-sided spectrum" can be defined by simply folding the $S(\omega)$ curve about the $\omega = 0$ axis, that is,

$$\int_{-\infty}^{+\infty} S(\omega)d\omega = \int_0^\infty 2S(\omega)d\omega = \int_0^\infty S^+(\omega)d\omega = \text{mean}$$

square of the process, where

$$S^+(\omega) = \text{one-sided spectrum} = 2S(\omega) \quad \omega \geq 0$$

$$= 0 \quad \omega < 0$$

$S^+(\omega)$ is shown in Figure 2.9.
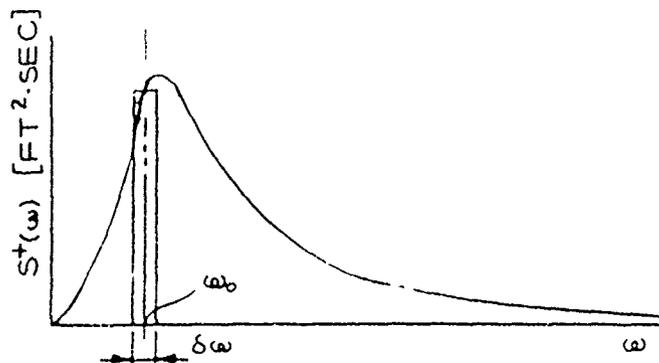
Figure 2.9.   Energy Spectrum.

5)   It can be shown that the area under the ocean waves' spectral density, that is, the mean square is proportional to the total energy per unit area of the waves' surface which is given by:

Total energy per unit area of the waves' surface =

$$\rho g \int_0^\infty S^+(\omega)\,d\omega \quad [\text{lb ft/ft}^2]$$

For this reason $S^+(\omega)$ is sometimes called the energy spectrum.

The energy in an increment $\delta\omega$ of wave frequencies at a central frequency ω_0 is

$$\rho g \ S^+(\omega_0) \ \delta\omega \qquad\qquad (2.15)$$

6)   From simple gravity waves, the total energy which is composed of half kinetic energy and half potential energy is,

Energy per unit area $= \dfrac{1}{2}\rho g \zeta_a^2$, where $\zeta_a =$ wave amplitude.

It follows that the square of the amplitude of a wave having the same energy as all the wave components in the band of frequencies represented by $\delta\omega$ is:[3]

$$\frac{1}{2}\rho g \zeta_a^2 = \rho g \cdot S^+(\omega_0) \cdot \delta\omega$$

therefore,

$\zeta_a^2 = 2S^+(\omega_c) \ \delta\omega =$ double the incremental area under the $S^+(\omega)$ curve

7)   For this reason, oceanographers define a new spectral density called the amplitude spectral density obtained by doubling the $S^+(\omega)$ ordinates. The incremental area will then represent component wave amplitudes as $\delta\omega \to 0$. The area under the amplitude spectrum

$$= \quad 2\int_0^\infty S^+(\omega) \ d\omega = 2E[x^2]$$

$$= \quad 2 \quad \text{mean square of the process.} \qquad (2.16)$$

In this report the energy rather than the amplitude spectral density will be used.

---

3 Valid only for the limiting case when $\delta\omega \to 0$.

It should be noted that, both the spectral density and the autocorrelation function are measurable quantities that can be indeed determined from time history records of ocean waves.

2.1.4 Narrow and Wide Band Random Processes:

A random process is said to be a narrow-band process if $S(\omega)$ has significant values only in a band or range of frequencies whose width is small compared with the magnitude of the center frequency of the band ω_0. Figure 2.10 shows $S^+(\omega)$ of a narrow band process and the corresponding time history of a sample function. It should be noted that a narrow band of frequencies appears in the sample and it is meaningful to speak of individual cycles.
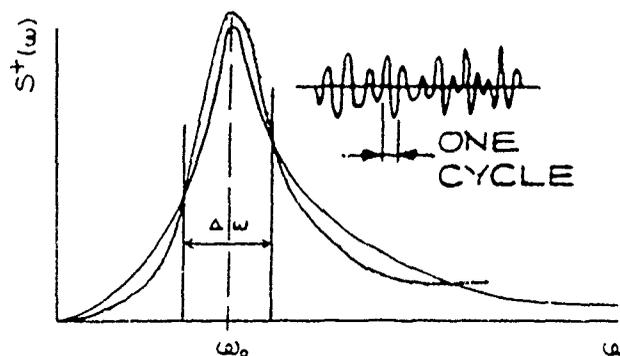
Figure 2.10.   Spectrum of a Narrow Band Process
(The sample shows a narrow band of frequencies.)

A random process is said to be a wide-band process if $S(\omega)$ has significant values over a band range of frequencies which is roughly the same order of magnitude as the center frequency ω_0. Figure 2.11 shows a typical $S^+(\omega)$ and the corresponding sample function of a wide-band process. Notice that a wide range of frequencies appears in the sample function.
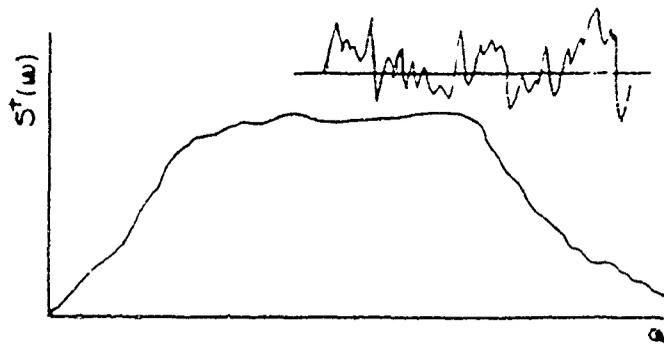
Figure 2.11.   Spectrum of a Wide Band Process.
(A broad range of frequencies are shown in the sample.)

2.1.5 Additional Statistics of a Random Process:

The rate of crossing a certain level of wave height or, in general, a threshold is an important information in design. Similarly, the probability distribution of the wave peaks can be useful in estimating probabilities of exceedence of specified wave heights in a given sea state. Because of their importance the rate of crossing a threshold and the peak distribution of a random process will be discussed in the next two sections:

a.   Rate of Crossing a Threshold:

The problem of crossing a threshold was examined extensively by Rice[2.1]. Some of the important results of his work will be given here without proof. Consider a random process $x^{(t)}(t)$ representing wave heights and the process has a zero mean, i.e., E [x] = 0. The mean rate of crossing a given level "a" denoted by ν_a^+ with positive slope, that is, from below (see figure 2.12) was derived by Rice [2.1] as:

$$\nu_a^+(t) = \int_0^\infty \dot{x} \; f_{X,\dot{X}} \; (a,\dot{x},t) \; d\dot{x} \qquad (2.17)$$
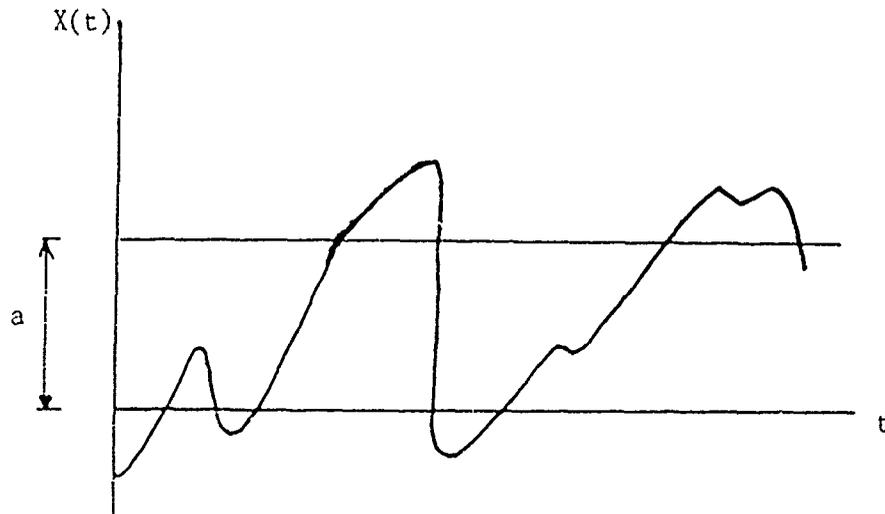
Figure 2.12. Crossing a Level "a".

where $\dot{x} = \dfrac{dx}{dt}$ and $f_{X,\dot{X}}(\,.,\,.,\,.)$ is the j.p.d.f. of x and $\dot{x}$

Similarly, the mean rate of crossing, that is, the average number of crossing per unit time with a negative slope (from above) is

$$v_a^-(t) = \int_{-\infty}^{0} |\dot{x}|\; f_{X,\dot{X}}\; (a,\dot{x},t)d\dot{x} \tag{2.18}$$

If the threshold level "a" is zero, the corresponding mean rate of crossing (from above and below) is

$$v_0(t) = \int_{-\infty}^{\infty} |\dot{x}|\; f_{X,\dot{X}}(0,\dot{x},t)\; d\dot{x} \tag{2.19}$$

If the process is stationary and narrow band, then v_0^+ or v_0^- is the apparent (mean) frequency of the process and from the stationarity property they are constant, i.e., independent of time.

b.   Peak distribution of a stationary narrow band random process:

For a narrow band random process (e.g. ocean waves) every zero crossing from below is followed by a positive peak (crest), and every zero crossing from above is followed by a negative peak (trough). Therefore, the proportion of the positive zero crossings that also cross the level "a" with a positive slope represents the probability that the positive peak is larger than "a", that is,

$$P[p>a] = 1 - P[p\leq a] = 1 - F_p(a) = \frac{\nu_a^+}{\nu_o^+} \quad (2.20)$$

where $F_p(a)$ is the cumulative probability distribution function of the peak values. The corresponding p.d. f. "$f_p(a)$" is obtained as:

$$f_p(a) = \frac{dF_p(a)}{da} = - \frac{1}{\nu_o^+} \frac{d\nu_a^+}{da} \quad (2.21)$$

As will be discussed later, ocean waves can be considered as a stationary narrow band Gaussian process with zero mean. It can be shown that for such a process x and $\dot{x}$ are statistically independent, i.e., the slope $\dot{x}$ is independent of the magnitude x . Therefore, the j.p.d.f. is given by:

$$f_{X,\dot{X}}(x,\dot{x}) = f_X(x) \cdot f_{\dot{X}}(\dot{x}) = \frac{1}{2\pi\,\sigma_X\sigma_{\dot{X}}} e^{-\frac{1}{2}\left(\frac{x^2}{\sigma_X^2}+\frac{\dot{x}^2}{\sigma_{\dot{X}}^2}\right)} \quad (2.22)$$

where the individual variances σ_X^2 and $\sigma_{\dot{X}}^2$ are given in terms of the wave spectral density[4] $S(\omega)$ by

$$\sigma_X^2 = \int_0^\infty S(\omega)\ d\omega \quad (2.23)$$

and

$$\sigma_{\dot{X}}^2 = \int_0^\infty \omega^2 S(\omega)\ d\omega \quad (2.24)$$

---

4. $S(\omega)$ represents the one-sided energy spectral density. The "+" superscript will be dropped to simplify the notation.

Thus, from equation (2.17) and (2.22) the mean rate of positive crossing of an amplitude of level "a" is

$$\nu_a^+ = \frac{1}{2\pi} \frac{\sigma_{\dot{X}}}{\sigma_X} e^{-\frac{1}{2}\left(\frac{a}{\sigma_X}\right)^2} \qquad (2.25)$$

Due to symmetry of the Gaussian process about zero $\nu_a^- = \nu_a^+$, therefore

$$\nu_a = \frac{1}{\pi} \frac{\sigma_{\dot{X}}}{\sigma_X} e^{-\frac{1}{2}\left(\frac{a}{\sigma_X}\right)^2} \qquad (2.26)$$

and

$$\nu_0^+ = \nu_0^- = \frac{1}{2\pi} \frac{\sigma_{\dot{X}}}{\sigma_X}$$

Since a wave spectral density is a relatively narrow-banded spectrum, its apparent (mean) circular frequency "ω_e" is

$$\omega_e = 2\pi \nu_0^+ = \frac{\sigma_{\dot{X}}}{\sigma_X} = \left[\frac{\int_0^\infty \omega^2 S(\omega) \, d\omega}{\int_0^\infty S(\omega) \, d\omega}\right]^{\frac{1}{2}} \qquad (2.27)$$

Furthermore, the p.d.f. of the peaks from equations (2.21) and (2.26) is given by

$$f_p(a) = \frac{a}{\sigma_X^2} e^{-\frac{1}{2}\left(\frac{a}{\sigma_X}\right)^2} \qquad (2.28)$$

which is the Rayleigh distribution with a parameter $= \sigma_X$

Both equation (2.25) and (2.28) are important results for ocean waves. Equation (2.25) gives the average number per unit time (mean rate) of crossing a wave amplitude of level "a" and equation (2.28) gives the p.d.f. of the peaks. In general, the following important result was obtained: <u>The peaks of a stationary,</u>

narrowband Gaussian process (e.g. ocean waves) follow a Rayleigh distribution with parameter "E_X" given by

$$E_X = \sigma_X^2 = E[X^2] = \int_0^\infty S(\omega) \, d\omega$$

$$= \text{area under the energy (mean square) spectral density} \quad (2.29)$$

2.1.6 Typical Wave Data

From sea data, oceanographers found that:

1) Over a short period of time (one hour) the wave records can be assumed to be stationary, relatively narrow-band random process.

2) At any time "t" the elevation of the wave surface from the mean follows a normal (i.e., Gaussian) distribution given by (see Figure 2.13).

$$f(x) = \frac{1}{\sigma_X \sqrt{2\pi}} \cdot e^{-\frac{1}{2}\left(\frac{x}{\sigma_X}\right)^2} \quad (2.30)$$

where σ_X = standard deviation

$$\sigma_X^2 = \int_{-\infty}^{+\infty} x^2 \, f(x) \, dx = E[x^2]$$

Notice that the variance is equal to the mean square since the mean of the wave elevation $E[x]$ is taken equal to zero.

3) The peak amplitude is found to follow closely the Rayleigh distribution given by

$$f_f(a) = \frac{a}{E_X} \cdot e^{-\frac{a^2}{2E_X}} \qquad a \geq 0 \qquad (2.31)$$

where E_X is a parameter (see figure 2.14).

It has been shown in the previous section that for a narrow-band normal process, with zero mean, the distribution of the peaks follows a Rayleigh distribution with parameter

$$E_x = E[x^2] = \sigma_x^2 = \text{mean square of the process}$$

$$= \text{area under the energy spectrum}$$
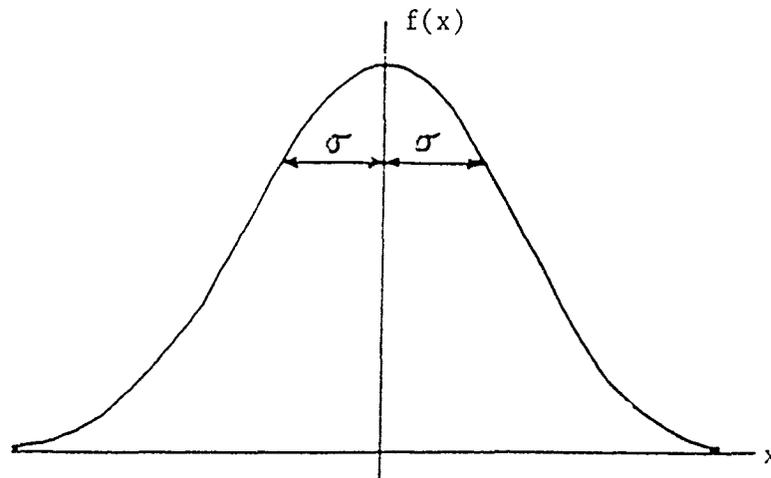
Figure 2.13. Probability Density Function of Wave Elevation

This shows the importance of these spectra. Several wave statistics regarding wave amplitudes can be derived from the Rayleigh distribution. For example:

$$\text{Average wave amplitude} = 1.25 \sqrt{E_x}$$

$$\text{Average wave height} = 2.5 \sqrt{E_x}$$

$$\text{Average of 1/3 highest waves (significant wave height)} = 4.0 \sqrt{E_x}$$

$$\text{Average of 1/10 highest waves} = 5.1 \sqrt{E_x} \quad \text{(double amplitude)}$$

$$\text{Average of 1/1000 highest waves} = 7.7 \sqrt{E_x} \quad \text{(double amplitude)}$$
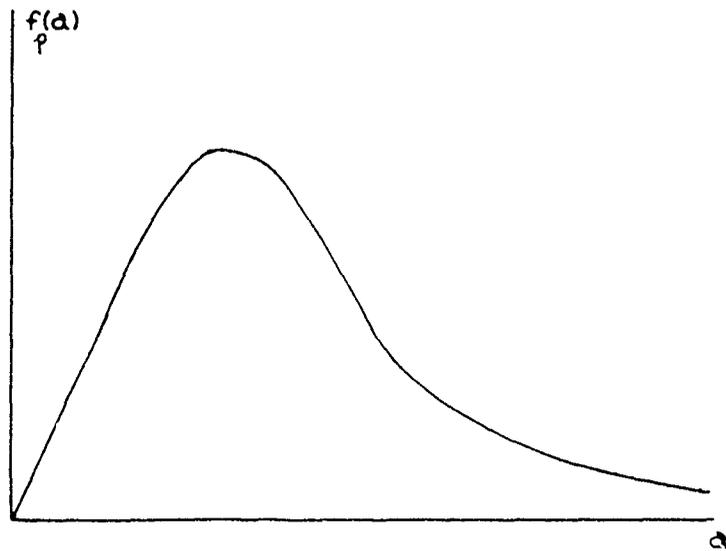
Figure 2.14. Rayleigh Distribution of the Peaks.

2.1.7 Typical Wave Spectra

It is useful for design purposes to obtain many representative spectra for different wind velocities or significant wave heights. A number of formulations are presented next.

i. Pierson-Moskowitz (1964)

Moskowitz [2.4] selected spectra from available data in the North Atlantic and grouped them in a family of five wind speeds equal to 20, 25, 30, 35, and 40.

Pierson arrived at the following analytical formulation to fit these spectra (see Figure 2.15).

$$S(\omega) = \frac{\alpha g^2}{\omega^5} \cdot e^{-\beta (g/V\omega)^4} \qquad (2.32)$$

where:

$S(\omega)$	=	spectral density (energy spectrum)
ω	=	frequency, rad/sec

$$\alpha = 8.1 \times 10^{-3}$$

$$\beta = 0.74$$

$$g = \text{acceleration of gravity, ft/sec}^2$$

$$V = \text{wind speed, ft/sec}$$

Any other consistent units could be used in (2.32)
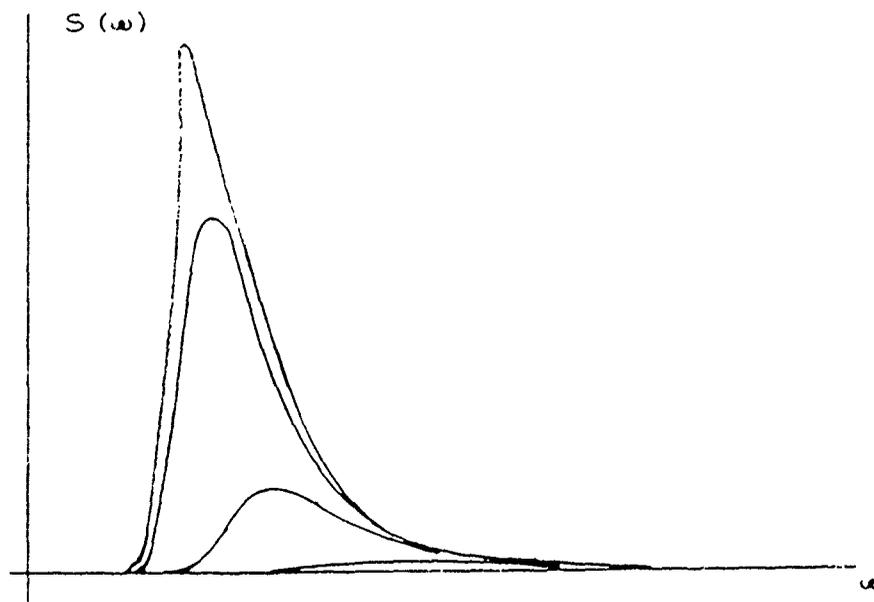
Figure 2.15.   Pierson-Moskowitz Spectrum.

2.   Bretschneider Spectrum

The proposed wave spectrum developed by Bretschneider [2.5] can describe developing and decaying seas, unlike Pierson-Moskowitz spectrum which describes fully developed seas. Bretschneider spectrum can be written in the form

$$S(\omega) = \alpha \, \omega^{-5} \, e^{-\beta \omega^{-4}} \qquad (2.33)$$

where α and β are given by

$$\alpha = \frac{5}{16} \, \omega_p^4 \, (\, \bar{H}_{1/3} \,)^2$$

$$\beta = \frac{5}{4} \, \omega_p^4$$

It should be noted that Pierson-Moskowitz spectrum is completely specified by wind velocity (one parameter) while Bretschneider spectrum is specified by two parameters; the significant wave height $\bar{H}_{1/3}$ and the peak frequency ω_p.

3. The International Ship Structure Congress Spectrum (1967)

The ISSC [2.6] adopted a two parameter spectrum given by

$$S(\omega) = A \, B \, \omega^{-5} \, e^{-B\omega^{-4}} \tag{2.34}$$

where

$$A = 0.25 \, (\, \bar{H}_{1/3} \,)^2$$
$$B = (\, 0.817 \, \frac{2\pi}{T} \,)^4$$

T = mean wave period

$\bar{H}_{1/3}$ = significant wave height

This spectrum is intended to be used in conjunction with observed wave heights and periods.

In general, the shape of the wave spectrum depends on:

1)   Wind speed (most important parameter)

2)   Wind duration

3)   Fetch (distance over which the wind blows)

4)   Location of other storm areas from which swell may travel

It should be noted that waves may attain their fully developed state for winds up to 32 knots. Beyond that, it is unlikely for waves to attain their fully developed state. For example, according to Pierson, a fully developed sea would result if a wind of 52 knots blew for 80 hours over a fetch of 1800 n. miles. Such conditions are not common.

2.1.8   Directional Spectra:

So far the so-called point spectrum (1-D) has been discussed. This is obtained from records taken at a fixed point with no indication of the direction of wave components, that is, no indication of how much each of the components of the wave in different directions contributes to the energy (spectrum). Such a representation is adequate for long-created seas, but a more complete representation is given by a 2-D spectrum $S(\omega,\mu)$ where μ = angle between wave components' direction and prevailing wind direction (see Figure 2.16).
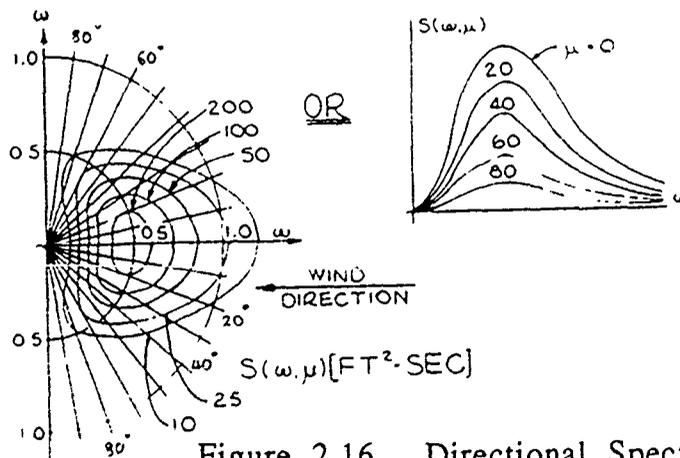
Figure 2.16.   Directional Spectrum

The angular integration of this spectrum will yield the same one-directional spectrum as would be obtained from a record taken at a fixed point.

The 2-D spectrum is much more difficult to obtain and sometimes it is assumed that a directional spectrum can be approximated by two independent functions.

$$S(\omega, \mu) = S(\omega) \cdot f(\mu) \qquad (2.35)$$

where $f(\mu)$ is called the "spreading function" and $S(\omega)$ is the one directional spectrum. The spreading function $f(\mu)$ can be assumed to be:

$$f(\mu) = (2/\pi) \cos^2\mu \qquad (2.36)$$

Thus,

$$\int_{-\pi/2}^{+\pi/2} \int_0^\infty S(\omega, \mu) \, d\omega d\mu = \int_0^\infty S(\omega) d\omega \int_{-\pi/2}^{\pi/2} f(\mu) d\mu$$

$$= \int_0^\infty S(\omega) d\omega \cdot \int_{-\pi/2}^{+\pi/2} (2/\pi) \cos^2\mu d\mu = \int_0^\infty S(\omega) d\omega$$

that is, integration of the directional spectrum with respect to ω and μ = integration of point spectrum with respect to ω.

2.1.9 Peak Distribution of a General Stationary Gaussian Random Process:

In a few cases of wave spectra (and vessel response) the narrow band assumption may not be adequate. Therefore in this section the probability distribution of the peaks of a stationary Gaussian (normal) random process with zero mean that is not necessarily narrow-banded is presented. The following results were

first obtained by Rice [2.1] and then used by Cartwright and Longuet-Higgins [2.7] and their proof is given in reference [2.1].

Instead of the Rayleigh distribution obtained earlier (equations (2.28) or (2.31)), the p.d.f. for the peaks is given by:

$$f_p(a,\epsilon) = \frac{\epsilon}{\sqrt{2\pi m_0}} e^{-\frac{a^2}{2\epsilon^2 m_0}} + \sqrt{1-\epsilon^2}\; \frac{a}{m_0} e^{-\frac{a^2}{2m_0}}.$$

$$\cdot\; \Phi\left[\frac{\sqrt{1-\epsilon^2}}{\epsilon} \cdot \frac{a}{\sqrt{m_0}} \right] \tag{2.37}$$

and, by integration, the corresponding cumulative distribution function of the peaks is given by

$$F_p(a,\epsilon) = \Phi\left[\frac{a}{\epsilon\sqrt{m_0}} \right] - \sqrt{1-\epsilon^2}\; e^{-\frac{a^2}{2m_0}} \cdot \Phi\left[\frac{\sqrt{1-\epsilon^2}}{\epsilon} \frac{a}{\sqrt{m_0}} \right] \tag{2.38}$$

where

$$\epsilon^2 = \text{bandwidth parameter} = 1 - \frac{m_2^2}{m_0 m_4}$$

$$\Phi(u) = \int_{-\infty}^{u} \frac{1}{\sqrt{2\pi}} e^{-\frac{z^2}{2}}\; dz$$

$$m_n = \int_0^{\infty} \omega^n S(\omega)\; d\omega = \text{nth moment of the spectrum} \quad n=0,2,4$$

It should be noted that m_0 is equal to the mean square or variance of the process σ_x^2.

As ϵ approaches zero the process approaches the ideal narrow band process and both equations (2.37) and (2.38) reduce to the p.d.f. and cumulative distribution function (c.d.f.) of the Rayleigh probability law. On the other hand, as ϵ approaches one the two equations reduce to the Gaussian (Normal) probability law, that is, the peak distribution reduces to the distribution of the surface itself. It should be noted that both positive maxima and negative maxima are included in equations (2.37) and (2.38) as can be seen from figure 2.17.
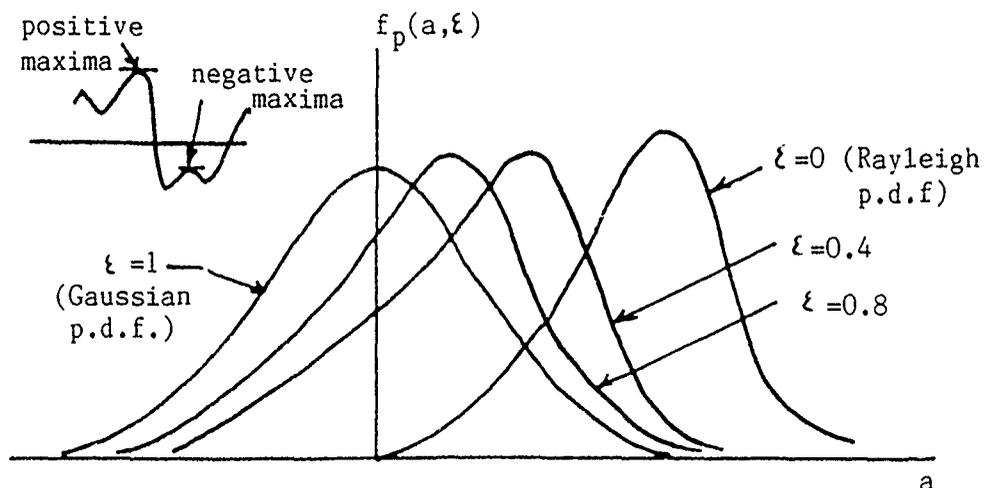
Figure 2.17. P.D.F. of the Peaks of a General Gaussian Process

2.2 Dynamic Loads and Response of a Floating Vessel Considered as a Rigid Body:

The objective now is to determine a floating vessel response (output) for a given state of ocean waves (input) probabilistically described as discussed in the previous sections. In order to do this, some preliminary definitions are necessary.

A fixed parameter or time invariant system means that if a deterministic input $x(t)$ produces an output $y(t)$ then $x(t+ \tau)$ produces $y(t+ \tau)$ where τ is a time shift. A linear system means that if $x_i(t)$ produces $y_i(t)$, then $x(t) = a_1 x_1(t) + a_2 x_2(t)$ produces $y(t) = a_1 y_1(t) + a_2 y_2(t)$ where a_1 and a_2 are constants. Such a system is governed by a set of linear differential equations with constant coefficients.

Some of the properties of such a linear system include:

If the input $x(t) = e^{i\omega t}$ then $y(t) = Ae^{i\omega t}$

where A does not depend on time t. If the input has an amplitude $X(\omega)$ dependent on the frequency ω, then the output amplitude $Y(\omega)$ will also depend on ω, i.e.

If $x(t) = X(\omega) e^{i\omega t}$

then $y(t) = Y(\omega) e^{i\omega t}$

where $\dfrac{Y(\omega)}{X(\omega)} \equiv H(\omega)$ \hfill (2.39)

$H(\omega)$ is called the transfer function or frequency response function or Response Amplitude Operator (RAO). The last terminology usually refers to the modulus $|H(\omega)|$. The transfer function is thus an output measure of unit input amplitude.

2.2.1 Random Input- Output Relations for Floating Vessels:

OCEAN WAVES   VESSEL SYSTEM   SHIP RESPONSE

$X(t)$ ASSUMED $Y(t)$

or   (INPUT)   LINEAR   (OUTPUT)   or

$S_x(\omega)$ $S_y(\omega)$
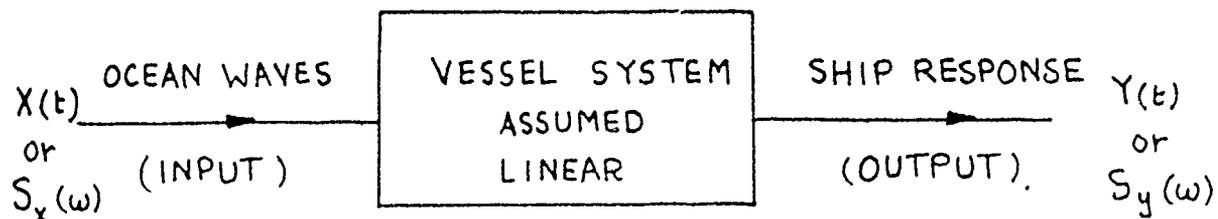
Figure 2.18. Input/Output System.

We will proceed now to determine the ship response (output) for a given state of ocean waves (input). Since the input $X(t)$ is random, we expect to get a random output $Y(t)$ (see Figure 2.18). Some statistics of the random output may then be useful for design. A floating vessel response could be vessel motions such as pitch, heave, roll, etc., the corresponding velocities and accelerations, bending moments (vertical and horizontal), torque or shear forces.

In order to determine the vessel response, the following assumption is made (introduced first by St. Dennis and Pierson [2.8]). The ship is assumed to behave linearly so that the response can be described by the superposition of the response to all regular wave components that make up the irregular sea.

It should be noted that in very severe seas certain responses may not be linear and non-linear analysis must be conducted.

Using the linearity assumption, the following conclusions will be stated and the proof can be found in [2.2]:

41

1. If the excitation (wave input) is a stationary random process, the response (output) is also a stationary random process.

2. If the input is a normally distributed random process, the output is also a normally distributed random process.

3. If the mean of the input process is zero, the mean of the output process is also zero.

4. If the input is an ergodic process, the output is also an ergodic process.

Notice that if the input process is narrow band, the output is not necessarily a narrow band process. For ocean waves, we have assumed over a short period of time a stationary normal random process with zero mean. The process could be completely characterized by the spectral density $S_x(\omega)$. The area under the spectrum is related to the mean square of the process, therefore certain averages such as average wave height, average of 1/3 highest waves, etc., can be determined. (The subscript x in the wave spectrum $S_x(\omega)$ is used in order to distinguish it from the output (response) spectrum $S_y(\omega)$).

Using 1, 2 and 3 above, it can be concluded that a floating vessel response is a normally distributed, stationary random process with zero mean over a short period of time. Again, just as in the input waves, if the spectral density of the vessel response is obtained, the mean square value, certain averages and other statistics of the vessel response can be determined.

It is thus important now to find the relationship between the wave spectrum and the response spectrum. For linear systems, it can be shown [2.2] that this relation is generally given in the form

$$S_y(\omega) = |H(\omega)|^2 S_x(\omega) \qquad (2.40)$$

where $H(\omega)$ is the "frequency response function" or the "transfer function" and its modulus $|H(\omega)|$ is the Response Amplitude Operator (RAO) - see also equation (2.39).

Equation (2.40) gives the input-output-relation in a frequency domain, i.e., between the spectra of the input (waves) and the output (vessel response). Similar relation can be obtained in the time domain between the response time history $y(t)$ and the wave time history $x(t)$. This relation as well as other relations in the time and frequency domains are developed in [2.2]. The important results are given here as follows.

The response of a vessel $y(t)$ (time domain) for any arbitrary - known wave excitation $x(t)$ is

$$y(t) = \int_0^\infty x(t - \theta) \, h(\theta) \, d\theta \qquad (2.41)$$

and the mean of the response $E[y(t)]$ in terms of the mean of the stationary excitation $E[x(t)]$ (if different from zero) is

$$E[y(t)] = E[x(t)] \int_0^\infty h(\theta) \, d\theta \qquad (2.42)$$

where $h(\theta)$ is called the impulse response function which is the response of the vessel due to unit excitation. Notice that $E[y(t)]$ is actually independent of time since $E[x(t)]$ is independent of time if the process is stationary.

The relation (time domain) between the autocorrelation functions of the response $R_y(\tau)$ and the wave $R_x(\tau)$ is given by [2.2].

$$R_y(\tau) = \int_{-\infty}^{+\infty} \int_{-\infty}^{+\infty} R_x(\tau + \theta_1 - \theta_2) h(\theta_1) h(\theta_2) d\theta_1 \ d\theta_2 \qquad (2.43)$$

The impulse response function $h(t)$ and the transfer function $H(\omega)$ are not independent. In fact, together they form a Fourier pair.

$$h(t) = \frac{1}{2\pi} \int_{-\infty}^{+\infty} H(\omega) e^{i\omega t} d\omega \qquad (2.44)$$

and

$$H(\omega) = \int_{-\infty}^{+\infty} h(t) e^{-i\omega t} dt \qquad (2.45)$$

Load and response determination for floating vessels is usually done in frequency domain. Therefore emphasis will be given on this in the following sections.

The frequency response function $H(\omega)$ or the RAO's are functions that give the vessel response to a regular wave of unit

amplitude. For example, if the response under consideration is the bending moment, then the bending moment can be calculated for the vessel in regular waves of different frequencies and for different vessel speeds. The RAO curves would appear as shown in Figure 2.19.

$$|H(\omega)|^2 = \left(\frac{M}{\zeta}\right)^2$$
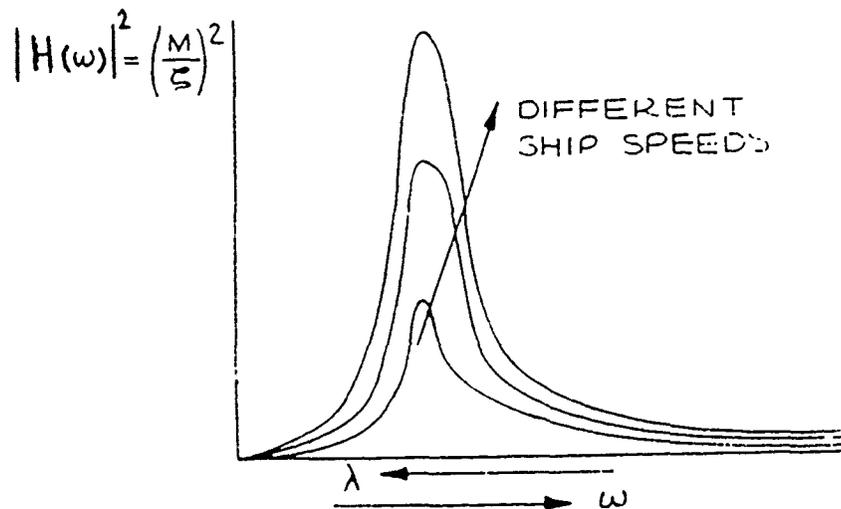
Figure 2.19. Response Amplitude Operator

Notice that the ordinate of $|H(\omega)|^2$ is the square of the bending moment per unit wave amplitude " ζ ". This can be given in the nondimensional form

$$|H(\omega)|^2 = [\frac{M/\zeta}{\rho g B L^2}]^2$$

where

ρ = water mass density
g = acceleration of gravity
B = vessel beam
L = vessel length

The RAO of other responses such as shear force could be obtained in the form $|H(\omega)|^2 = (V/\zeta)^2$ or the nondimensional form

$$|H(\omega)|^2 = (\frac{V/\zeta}{\rho g B L})^2$$

where V is the shear force.

In general the RAO's can be obtained either from:

a) Calculations using the equations of motion of the ship
b) Towing tank experiments

Each of these will be discussed briefly in the following.

The general dynamic equations of motion of a vessel in regular waves can be obtained by applying Newton's Law of Motion for a rigid body. If the origin is taken at the center of gravity of the body, then

$$\overline{F} = \frac{d}{dt}(m \cdot \overline{v})$$

and

$$\overline{M} = \frac{d}{dt}(I \cdot \overline{\omega})$$

where

$$
\begin{array}{lcl}
\overline{V} &=& \text{velocity vector} \\
\overline{F} &=& \text{force vector} \\
m &=& \text{mass} \\
\overline{M} &=& \text{moment acting on the body} \\
\overline{\omega} &=& \text{angular velocity vector} \\
I &=& \text{moment of inertia about the coordinates axes}
\end{array}
$$

The first of these equations give the three force equations in the x, y, and z directions (surge, sway, and heave equations). The second gives the three moment equations about the x, y, and z axes (roll, pitch and yaw equations).

These general six coupled differential equations for the six degrees of freedom are highly nonlinear and difficult to solve exactly. However, approximate solutions after decoupling some of the motions from each other and going through a linearization procedure are available, for example, in [2.9] and [2.10]. The decoupling of the equations is usually done by decoupling the motions in a vertical plane (surge, heave, and pitch) from the rest and neglecting the surge degree of freedom. The solution of these equations permits the calculation of the vessel motions and accelerations in regular waves of different frequencies. For further information on this subject, see references [2.11, 2.12, 2.13, 2.14,

2.15]. Once the vessel motions and accelerations are determined, the shear force and bending moment (or any other loads) can be computed. The values of these responses (including loads) due to waves of unit amplitude and different frequencies give the required RAO's. There are several computer programs to perform these rather lengthy computations, for example, [2.16, 2.17, 2.18, 2.19].

The RAO's can also be determined by simply running a model in regular waves at various speeds, headings and wave frequencies. The model has to be scaled properly to represent the ship mass distribution and structural geometry. The model motion, velocities, accelerations, shear forces, bending moment, etc., are then measured and plotted versus the wave frequency [2.20]. If the bending moment needs to be measured at the midship section only, then one may use a rigid wooden model jointed at the midship section with a dynamometer calibrated to read the bending moment acting on a bar connecting the two parts. If the bending moment is desired at more than one location, then a segmented model is usually used with a bar equipped with several strain gauges [2.21].

With the RAO determined, equation (2.40) can be applied to determine the energy spectrum of the response in long-crested seas. This is usually represented graphically, as shown in Figure 2.20, for the bending moment case taken as an example.
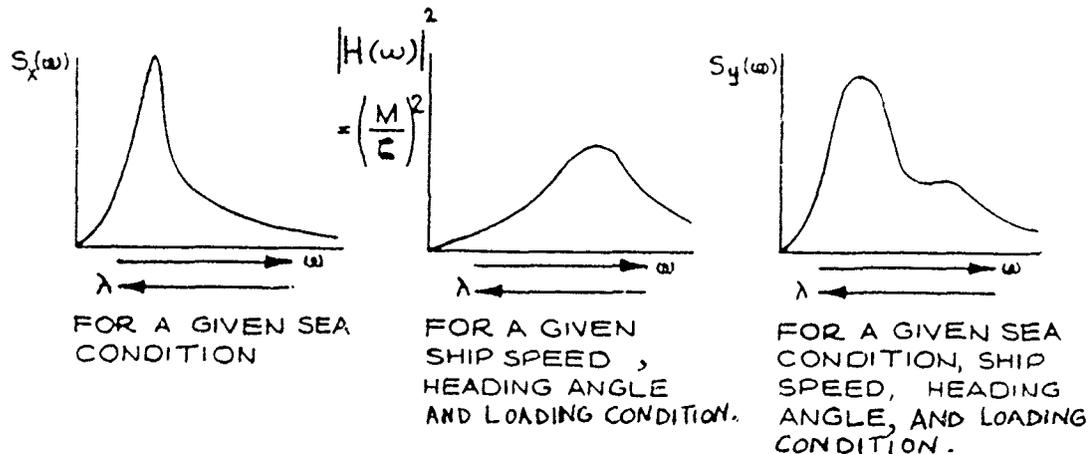
Figure 2.20. Response Spectrum.

Equation (2.40) indicates that ordinates of the bending moment spectrum are obtained by multiplying the ordinates of the wave spectrum by the square of the ordinate of the response amplitude operator. Since over a short period of time the response is a

46

stationary normal process, then the response spectrum characterizes the process completely. If the resulting wave bending moment spectrum is narrow-band as is the case usually, then the amplitudes of the wave bending moment follow the Rayleigh distribution (equation 2.28) with a parameter E_y related to the area under the bending moment spectrum.

$$E_y = \text{area under the energy spectrum of the bending moment}$$
$$= \int_0^\infty S_x(\omega)|H(\omega)|^2 d\omega$$

Some statistics of the bending moment can be thus obtained:
average amplitude of bending moment $= 1.25 \sqrt{E_y}$

average of 1/3 highest amplitude of bending moment $= 2.0 \sqrt{E_y}$

average of 1/10 highest amplitude of bending moment $= 2.55 \sqrt{E_y}$

In general if the response spectrum is not narrow-band, then the peaks (including negative maxima) will follow Rice distribution given by equations (2.37) and (2.38) with the band width parameter ε determined from the moments of the response spectrum. It should be noted that the assumption of a narrow-band spectrum produces more conservative results and simplifies the analysis considerably.

2.2.2 Frequency Mapping:

The response spectrum discussed, $S_y(\omega)$, is not the spectrum that would be obtained by records taken of bending moment aboard a vessel and analyzing them. This is because, when the vessel is moving, the waves are encountered at different frequencies to their absolute frequencies. Consider a vessel moving with velocity V and heading θ in regular waves of frequency ω (see Figure 2.21).

47
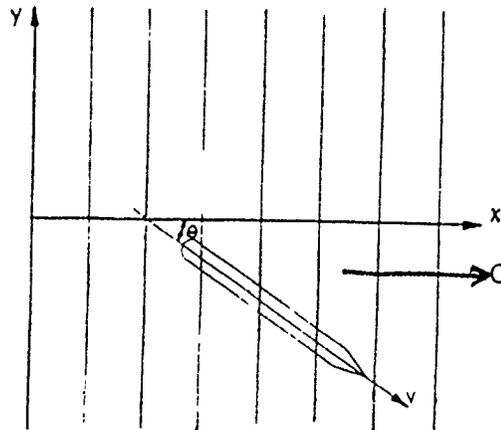
Figure 2.21. Heading Angle in Regular Waves.

The wave velocity C in the x-direction = ω/k, where k = wave number = $2\pi/\lambda$. The relative velocity between waves and the ship = C - V cos θ = encountered wave velocity. Therefore, the encountered wave frequency ω_e= (C - V cos θ) k or ω_e = ω- kV cos θ. For gravity waves

$$\omega^2 = \frac{2\pi g}{\lambda} = kg$$

where λ is the wave length
then, $\omega_e = \omega - \frac{\omega^2}{g} V \cos \theta$ $\qquad$ (2.46)

Now the wave spectrum can be plotted to a base of the encountered frequency rather than the wave frequency. However, a change in the base will necessitate a change in the ordinate of the spectrum such that [2.10]:

$$S_y(\omega)\delta\omega = S_y(\omega_e)\,\delta\omega_e \qquad (2.47)$$

Therefore, on integration

$$E_y = \int_0^\infty S_y(\omega)d\omega = \int_c^\infty S_y(\omega_e)d\omega_e$$

48

But from equation (2.46) $\delta\omega_e = [1 - \frac{2\omega}{g}V\cos\theta]\,\delta\omega$
substituting in equation (2.47)

$$S_y(\omega_e) = S_y(\omega)\ \frac{1}{[1 - \frac{2\omega}{g}V\cos\theta]} \qquad (2.48)$$

Thus, for a given $S_y(\omega)$ and vessel velocity V, $S_y(\omega_e)$ can be obtained from equation (2.48).

The input-output relation in the frequency of encounter domain becomes:

$$S_y(\omega_e) = |\rho(\omega_e)|^2\, S_x(\omega_e)$$

where $\rho(\omega_e)$ is the response amplitude operator obtained as a function of the frequency of encounter, and the response spectrum $S_y(\omega_e)$ relates to records taken on board the vessel.

It should be noticed that $E_y = \int_0^{\infty} S_y(\omega)\,d\omega = \int_c^{\infty} S_y(\omega_e)\,d\omega_e$

2.2.3 Response Spectrum in Short-Crested Seas:

In short-crested seas, when two-dimensional wave spectrum $S(\omega,\mu)$ is used, the input-output relation becomes:

$$S_y(\omega,\mu) = |\rho(\omega,\alpha-\mu)|^2\, S_x(\omega,\mu) \qquad (2.49)$$

where μ =   angle between wave component under consideration and the prevailing wind direction.

$\alpha - \mu$ =   angle between the vessel velocity vector and wave component (see Figure 2.22).

The response of the vessel for all wave components can be then obtained by integration over μ

$$S_y(\omega) = \int_{-\pi/2}^{+\pi/2} S_y(\omega,\mu)\,d\mu$$

49
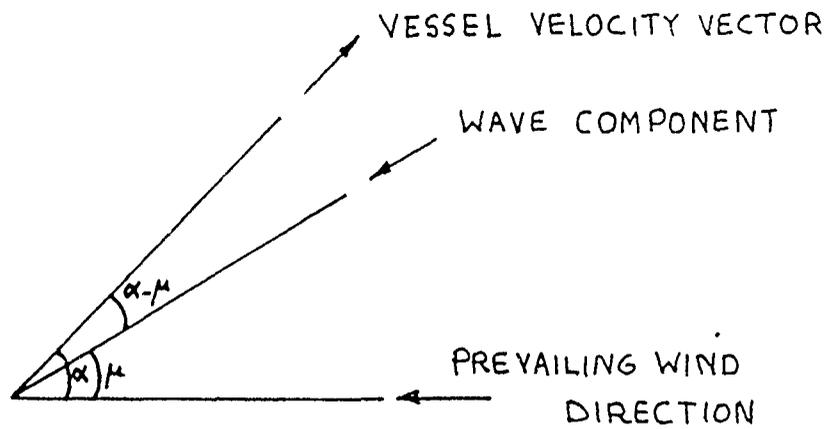
Figure 2.22. Angle Between Wave Component and Prevailing Wind Direction.

It should be noted that several computer programs are available to determine the response spectrum of a vessel based on the above or similar analysis. Such computer programs include SCORES [2.16], SPRINGSEA [2.17], and MIT Ship Motion Program [2.18].

2.3 Long-Term Prediction of Wave Loads:

In the previous discussion, one of the major restrictions has been the assumption of stationarity which limits the validity of the analysis to short periods of time. This leads to Rayleigh distribution of the peaks for narrow band spectra. For design purposes, however, it may be important to determine the distribution of the wave load peaks over long periods of time (years) in order to determine design values of the load.

The long term distribution can be determined by adding statistically several short-term (Rayleigh) distributions, or, by taking records of wave loads and determining what probability distribution gives the best fit of the data. Several statistical methods can be used to estimate the parameters of the candidate distributions and tests are available to examine the goodness-of-fit and to determine which distribution fits the data best.

Several investigators, [2.22, 2.23, 2.24, 2.25, 2.26] examined long-term wave loads data with the aim of determining the long-term distribution of the peaks. It was found that the Weibull distribution is general enough and fits well the wave bending moment data on ships. The p.d.f. and c.d.f. of the Weibull distribution are given by:

$$f(x) = (\frac{\ell}{k}) (\frac{x}{k})^{\ell - i} \, e^{-(x/k)^{\ell}} \qquad x \geq 0 \qquad (2.50)$$

50

and

$$F(x) = 1 - e^{-\left(x/k\right)^{\ell}} \qquad\qquad x \geq 0 \qquad (2.51)$$

where ℓ and k are parameters to be determined from the wave load data (e.g. strain gages installed on deck of a ship).

It should be noted that the Weibull distribution is a generalized Rayleigh distribution and if one inserts $\ell = 2$ and $k = \sqrt{2E}$ in equations (2.50) and (2.51) one obtains directly the Rayleigh distribution p.d.f. and c.d.f. (see equation (2.31)).

It has also been shown that in many cases of long-term wave load data, the parameter ℓ of the Weibull distribution is approximately equal to one. When $\ell = 1$, the Weibull distribution reduces to the Exponential distribution given by:

$$f(x) = \frac{1}{\lambda} e^{-\left(x/\lambda\right)} \qquad\qquad x \geq 0 \qquad (2.52)$$

$$F(x) = 1 - e^{-\left(x/\lambda\right)} \qquad\qquad x \geq 0 \qquad (2.53)$$

where $\lambda = k$ = mean or expected value of the wave load amplitude. Section A1.1 of Appendix 1 describes how to determine the parameters k and 1 and how to construct and use a probability paper.

2.4 Prediction of Extreme Wave Loads:

If the wave loads acting on a marine structure can be represented as a stationary Gaussian process (short period), then at least four methods are available to predict the distribution of the maximum load. These methods are developed for application to marine structures and are given in more detail in [2.27]. In the first method the peaks are assumed to be statistically independent and identically distributed, and the extreme value distribution of the largest in N-peaks is determined using classical order statistics. In the second, a discrete point process is assumed in order to determine the asymptotic type-I distribution based on Rice's [2.1] initial distribution. Cramer's procedure [2.28, 2.29] can be used for determining the resulting aysmptotic distribution. Conventional upcrossing analysis n.ay be used in the third method for determining the extreme value distribution. Finally a two-stage description of the

51

random process which leads to an extreme distribution derived by Vanmarcke [2.30] is the basis for the fourth method.

Each. one of these methods will be described briefly in the following sections.

A. Distribution of the largest peak in a sequence of N peaks using order statistics

The distribution of the largest peak in a sequence of N peaks can be determined using standard order statistics. Consider a sequence of random variables $Z_1, Z_2, \ldots Z_n$ representing the peaks of a load on a marine structure. Assuming that these peaks are identically distributed and statistically independent, the cumulative distribution function (cdf) of the largest one using order statistics is given by [2.31]:

$$F_{Z_N}(z) = P\left[\max (z_1, z_2, \ldots, z_N) \leq z \right] = \left[F_Z(z, \varepsilon) \right]^N \qquad (2.54)$$

where $F_Z(z, \varepsilon)$ is the initial cumulative distribution function of the load peaks (maxima) and ε is the spectral width parameter defined as:

$$\varepsilon^2 = 1 - \frac{m_2^2}{m_0 m_4}$$

$$m_n = \int_{-\infty}^{+\infty} \omega^n S(\omega) d\omega , \qquad n = 0,2,4 \qquad (2.55)$$

The probability density function (pdf) of the largest peak is determined by differentiating equation (2.54) with respect to z, thus:

$$f_{Z_N}(z) = N\left[F_Z(z, \varepsilon) \right]^{N-1} \cdot f_Z(z, \varepsilon) \qquad (2.56)$$

where $f_Z(z, \varepsilon)$ is the initial p.d.f. of the load peaks. For any band-width load process, Rice's distribution should be used as the initial

distribution, thus equations (2.37) and (2.38) hold for f_Z (z,ε) and F_Z (z,ε), respectively.

Based on the above analysis, the expected value of the maximum load peak in a sequence of N-peaks was determined by Cartwright and Longuet-Higgins and is approximated by:

$$\frac{E [\max (z_1, z_2, \ldots z_n)]}{\sqrt{m_0}} \simeq [2 \ln (\sqrt{1 - \varepsilon^2} N)]^{\frac{1}{2}}$$
$$+ C [2 \ln (\sqrt{1 - \varepsilon^2} N)]^{-\frac{1}{2}} \quad (2.57)$$

where $C = 0.5772 = $ Euler's constant .

The extreme load peak with a probability of exceedence α is given by [2.32]:

$$Z_\alpha \simeq \left[2 m_0 \left(\ln N + \ln \left[1 / \ln (\frac{1}{1-\alpha}) \right] \right) \right]^{-\frac{1}{2}} \quad (2.58)$$

which is independent of ε (for small α).

(B)   Asymptotic type I distribution

It is known that as the number of peaks   N   increases without bound a   limiting   or   asymptotic   form   of   the   extreme   value distribution (equations (2.54)   and (2.56)) is reached.   The asymptotic form of an extreme value distribution does not depend, in general, on the exact form of the initial distribution; it depends only on the tail behavior of the initial distribution.   The parameters of the asymptotic distribution depend   however on the exact form of the initial distribution.

In reference [2.27], Cramer's method was used to derive the asymptotic distribution based on Rice's distribution as an initial distribution.   The derived extreme value c.d.f. is

$$F_{Z_N}(z, \varepsilon) = \exp\left\{ -N \left[\Phi\left(\frac{m_S - z}{\varepsilon\sqrt{m_0}}\right) + \sqrt{1 - \varepsilon^2}\, e^{-\frac{1}{2}\left(\frac{z - m_S}{\sqrt{m_0}}\right)^2} \right.\right.$$

$$\left.\left. \cdot \Phi\left(\frac{\sqrt{1 - \varepsilon^2}}{\varepsilon} \cdot \frac{z - m_S}{\sqrt{m_0}}\right) \right] \right\} \qquad (2.59)$$

that is, the asymptotic form is double exponential and the cumulative distribution itself depends on N. m_S is the mean value of the load if different from zero.

Several years after the appearance of Cramer's book Gumbel [2.31] classified the asymptotic distribution of extremes in three types: (type I) a double exponential form, (type II) an exponential form, and (type III) an exponential form with an upper bound. Convergence of an initial distribution to one of the three types depends largely on the tail behavior of the initial distribution. An initial distribution with an exponentially decaying tail in direction of the extreme will converge to type I asymptotic distribution, i.e., the double exponential form.

Gumbel's analysis and classification provide another method for deriving the asymptotic distribution and may be in a form easier to handle than that given by equation (2.59). The cdf of type I asymptotic form as given by Gumbel is:

$$F_{Z_N}(z) = \exp\left[- e^{-\alpha_N(z - u_N)} \right] \qquad (2.60)$$

where u_N is the characteristic largest value of the initial variate Z and α_N is an inverse measure of dispersion of Z_N. These parameters, u_N and α_N, have to be determined and depend on the form of the initial distribution.

The corresponding pdf is given by:

$$f_{Z_N}(z) = \alpha_N\, e^{-\alpha_N(z - u_N)} \cdot \exp\left[- e^{-\alpha_N(z - u_N)} \right] \qquad (2.61)$$

The mean and standard deviation of the extreme value Z_N are given, respectively, by:

$$\mu_{Z_n} = u_N + \frac{0.5772}{\alpha_N} \qquad (2.62)$$

$$\sigma_{Z_n} = \frac{\pi}{\sqrt{6}\ \alpha_N} \qquad (2.63)$$

The parameters u_N and α_N were determined in [2.27] for Rice's distribution given by equations (2.37) and (2.38) as an initial distribution.

The results for u_N and α_N are:

$$u_N = m_S \pm \left\{ 2\, m_0\ \ln\left[\frac{\sqrt{1-\varepsilon^2}\ \Phi(\beta)}{\frac{1}{N} - \Phi(-\alpha)} \right] \right\}^{\frac{1}{2}} \qquad (2.64)$$

$$\alpha_N = \frac{N\,\varepsilon}{\sqrt{2\pi\, m_0}}\, e^{-\frac{\alpha^2}{2}} + \frac{N\,\varepsilon\,\beta}{\sqrt{m_0}}\, e^{-\frac{\alpha^2}{2}\varepsilon^2}\cdot \Phi(\beta) \qquad (2.65)$$

where

$$\alpha = \frac{u_N - m_S}{\varepsilon\sqrt{m_0}}$$

and

$$\beta = \sqrt{1-\varepsilon^2}\cdot\alpha \qquad (2.66)$$

The plus sign in equation (2.64) should be used if the mean value m_s is positive in order to obtain the larger characteristic value. It should be noted that both α and β contain u_N as defined in (2.66); therefore, an iterative procedure must be used for determining u_N. To start the iterative procedure an initial value for u_N is necessary and may be taken as $u_N = m_s + \sqrt{\lambda m_0 \ln N}$. The corresponding values of α, β, $\Phi(-\alpha)$ and $\Phi(\beta)$ can then be determined. Equation (2.64) is then checked to see if the right side is equal to the left side, otherwise a new value of u_N equals the right side of equation (2.64) should be used in the second step of the iterative procedure. Three or four steps are usually sufficient for convergence.

(C)   Extreme value distribution based on upcrossing analysis

The distribution of the largest peak can be determined from upcrossing analysis of a time history of a stationary random process instead of the peak analysis presented above. For example, the number of N peaks can be changed to a time interval T in the upcrossing analysis and the problem of determining the characteristics of the largest peak in N peaks becomes that of evaluating the characteristics of the maximum crest of a stationary ergodic Gaussian random process X(t) during a period T. The assumption of the statistical independence of the peaks is usually replaced by the assumption that upcrossing of a level x by X(t) are statistically independent. This leads to the Poisson's upcrossing process which is true only in the asymptotic sense (as $x \to \infty$; $T \to \infty$).

From upcrossing analysis it can be shown (see for example [2.1]) that the probability that the largest value is less than a certain level x during a period T is given by:

$$P\left[\max\left(X(t) \; ; \; 0 \le t \le T \right) \le x \right] = e^{-v_x^+ T} \qquad (2.67)$$

where

56

$$v_x^{\tau} = v_0 \, e^{-\frac{1}{2}\left(\frac{x - m_s}{\sqrt{m_0}}\right)^2} \tag{2.68}$$

and

$$v_0 = \frac{1}{2\pi} \sqrt{\frac{m_2}{m_0}} \qquad 1 \, / \, \text{sec} \tag{2.69}$$

Therefore the cdf of the largest X is

$$F_X(x) = \exp\left[-v_0 T \, e^{-\frac{1}{2}\left(\frac{x - m_s}{\sqrt{m_0}}\right)^2} \right] \tag{2.70}$$

that is, it has a double exponential form although quite different from equation (2.60) with u_N and α_N given by (2.64) and (2.65).

(D) Extreme value distribution based on a two-state description of a random process

Vanmarcke [2.30] estimated the probability distribution of the time to first passage across a specified barrier for a Gaussian stationary random process. In his analysis he considered a two-state description of the time history X(t) relative to the specified barrier. Based on his results the distribution of the extreme value may be determined from:

$$F_X(x) = \exp\left[-\nu_0 T \left(\frac{1 - e^{-\sqrt{2\pi}\, q \left(\frac{x - m_S}{\sqrt{m_0}} \right)}}{1 - e^{-\frac{1}{2}\left(\frac{x - m_S}{\sqrt{m_0}} \right)^2}} \right) \cdot e^{-\frac{1}{2}\left(\frac{x - m_S}{\sqrt{m_0}} \right)^2} \right] \qquad (2.71)$$

where q is a band width parameter defined as

$$q = \sqrt{1 - \frac{m_1^2}{m_0\, m_2}} \qquad 0 \le q \le 1 \qquad (2.72)$$

Distributions given in (A), (B), (C) and (D) above, are valid for a load process represented by a stationary Gaussian process of any band width. Reference [2.33] shows the corresponding equations for the special cases of a narrow-band process (ε = o or q = o) and a wide-band process (ε = 1 or q = 1). It should be noted that the narrow-band case gives a conservative estimate of the extreme wave load distribution and the resulting equations may be used for values of ε up to 0.60 since they are insensitive to ε in the range 0 to 0.60.

Application Example and Comparisons:

The extreme value distributions of the wave loads discussed above differ from each other in their basic derivation and underlying assumptions. The forms of their equations are drastically different as can be seen by comparing equations (2.54), (2.59), (2.60), (2.70) and (2.71). It would be interesting now to compare some typical results obtained from the different methods when applied to a marine structure. For this purpose a tanker of length = 763 feet, breadth = 125 feet and depth = 54.5 feet is considered. We will compare the distribution of the extreme wave bending moment acting on the tanker under a storm condition specified by a significant wave height of 38.75 feet and an average wave period of 11.5 seconds. The storm is assumed to be stationary under these

58

conditions for a period of one hour. The following parameters were computed for an earlier application given in [2.33]:

Still water bending moment (full load)

$$m_s = 669,037 \text{ ft-tons}$$

RMS of wave bending moment

$$\sqrt{m_0} = 286,300 \text{ ft-tons}$$

Average wave moment period $= 13.0$ seconds

Band width parameter of wave moment spectral
density $\varepsilon = 0.364$

Number of wave moment peaks in one hour

$$N = \frac{60 \times 60}{13.0} = 276.9$$

The application given in reference [2.33] shows that if ε is assumed to be zero (ideal narrow-band) instead of the 0.364 given above, the resulting error in the expected maximum wave bending moment in N peaks is less than 0.5 percent. This gives an indication that for $\varepsilon = 0.364$, it is sufficiently accurate to use the ideal narrow-band equations for our comparison.

Using this assumption and the above values for m_s, $\sqrt{m_0}$ and N, a comparison is made of the distribution functions of the four extreme value distributions as given in the preceding sections (A), (B), (C) and (D).

The results of the comparison are shown and plotted on a standard extremal probability paper and on a regular graph paper in figures 2.23, 2.24 and 2.25.

59

Based on these results, one surprising conclusion can be drawn. All extreme value distributions of the wave loads considered produce similar results even though their basic assumptions and derivations differ drastically. In fact, if one inspects the equations representing the cumulative distribution functions of these distributions one sees that these equations are not similar in form and may conclude erroneously that they would produce very different results.

The extreme distributions based on the largest peak in N peaks (distribution A), upcrossing analysis (distribution C) and a two-state description (distribution D) produce almost identical results as far as the probability of exceedence is concerned as can be seen by inspecting figures 2.23 and 2.24. The asymptotic type I distribution (distribution B) results in slightly higher values of probability of exceedence. This is to be expected since the asymptotic distribution is an upper bound extreme distribution and becomes more accurate as the number of load peaks approaches infinity. In the example shown for the tanker, the number of wave bending moment peaks N is approximately 277.

As an example of the differences between the asymptotic distribution and the other distributions, the probability of exceedence of a total bending moment of 2,069,000 ft-ton (including still water bending moment of 669,000 ft-ton) is 0.006 according to the asymptotic distribution (B) and 0.002 according to the other three distributions (A, C, and D).
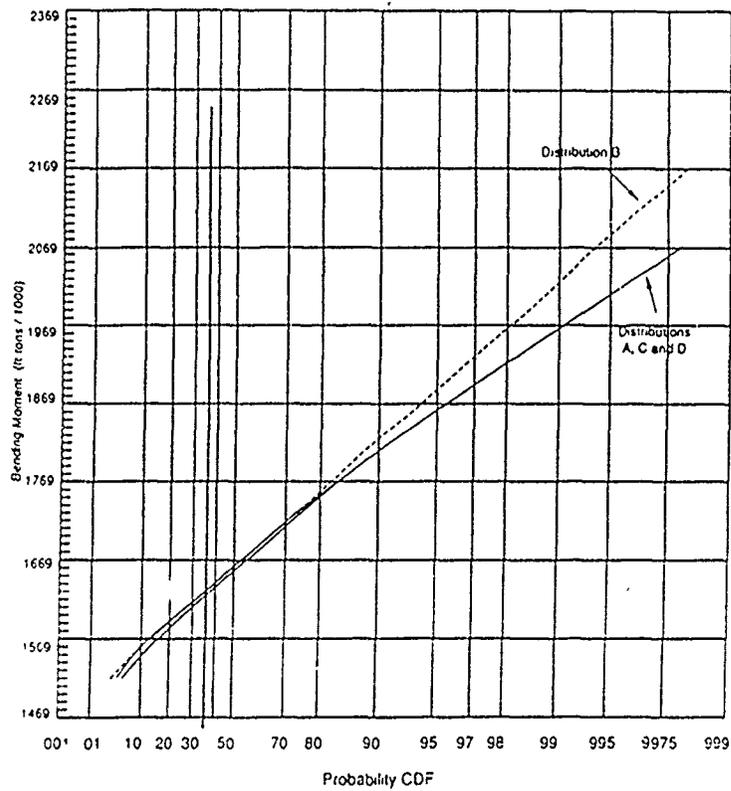
Figure 2.23. Standard Extremal Variate - Bending Moment on a Tanker.
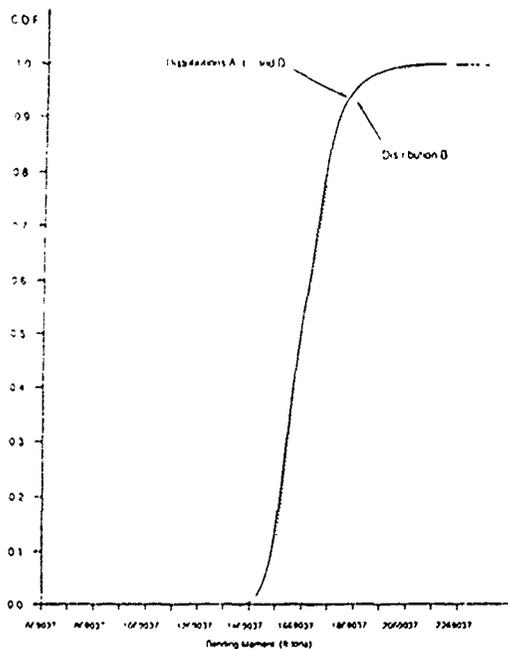
Figure 2.24 - Cumulative Distribution Functions of Extreme Bending Moment on a Tanker

61
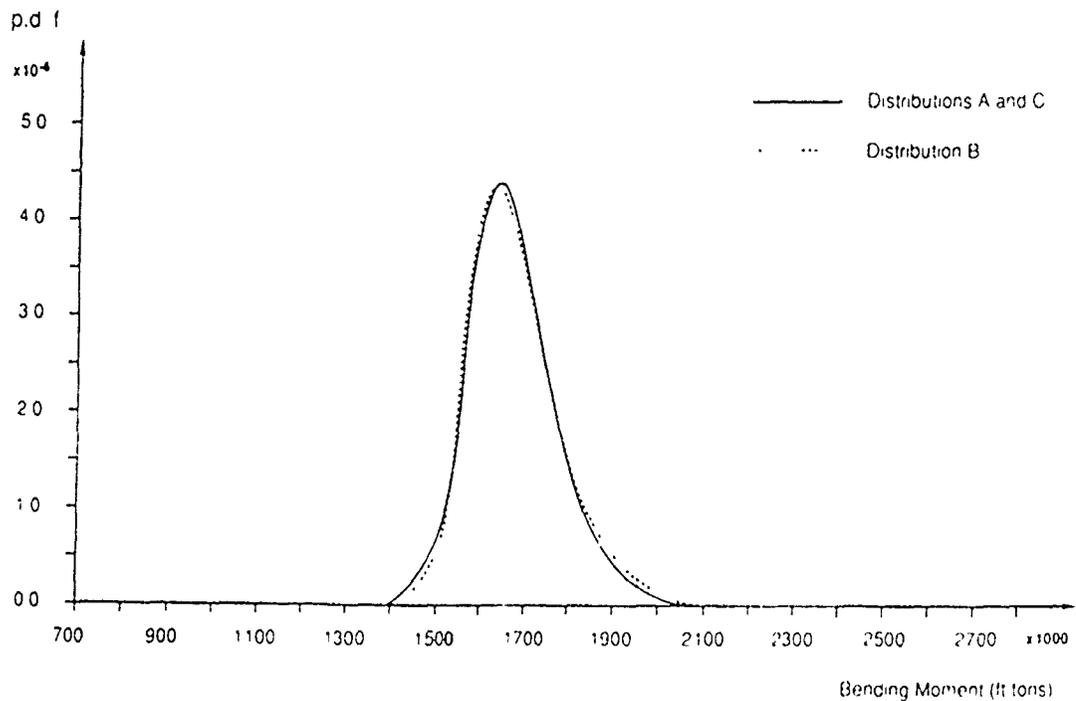
Figure 2.25. Probability Density Function of Extreme Total Bending
Moment on a Tanker

2.5 Return Periods of Extreme Events and Non-Encounter Probabilities:

The probability that an extreme value of an event (say wave
height x) will not be encountered during the life "L" of a marine
structure is called non-encounter probability "NE(x)".   This, in
general, is given by [2.34]:

$$NE(x) \quad = \quad P \text{ [no exceedence of x occurs during life L]}$$
$$= \quad P\,[X_{max} \leq x \;] = [\,F_X\,(x)\,]^{\,L}$$

$$(2.73)$$

where X_{max} = maximum value during life L

$\qquad$ L   = life in years

$\qquad F_X\,(x)$ =   distribution function of annual maximum.

The waiting or return period, R, is the average length of time
between exceedence.   Thus one may speak of a 100 year wave height
or 50 year wind velocity.

The waiting period in years has a probability law given by

$$P [W = w] = F_X^{w-1}(x) [1 \cdot F_X (x)]$$

and therefore, the average waiting period, i.e., the return period "R" is

$$R = E [W] = [1 - F_X (x)]^{-1} \qquad (2.74)$$

The relation between the non-encounter probability "NE(x)" and the return period "R" can be determined by eliminating $F_X (x)$ from equations (2.73) and (2.74) , thus,

$$NE(x) = P [X_{max} \leq x] = [1 - R^{-1}]^{L} \qquad (2.75)$$

If $R = L$, then $NE(x) \simeq e^{-1}$

The probability of exceedence in this case $= 1 - e^{-1} = 0.632$, that is, there is a high probability (0.632) of exceeding the event with a return period L during the "L" life years of the structure.

In selecting return periods, one must distinguish between an annual interruption of operation of the structure (L = one year) and ultimate failure during life time (L = 20 to 30 years). In the former case a return period R = 10 years may be adequate. Using equation (2.75) with L = 1 and R = 10 we obtain a nonencounter probability of 90%. If R is increased to 100, the non-encounter probability becomes 99%.

In the latter case where failure during life of, say 20 years, is considered, and the return period is 100 years, then the non-encounter probability, from (2.75) is 81.8%. If the return period is increased to 1000 years, the non-encounter probability becomes 98.0%.

2.6 Stochastic Combination of Loads on a Marine Structure

Undoubtedly, there are certain similarities between decomposing ship response records of full-scale measurements into their basic components and combining analytically calculated components to obtain the total response. Since decomposing full scale measurements can be done with a certain degree of success, it is possible to invert the procedure in order to compute the combined response from the analytically determined components.

In this section, a brief discussion is given of the decomposition of full-scale records into their basic components. In the following section, a method is presented to combine analytically-determined response components.

A. Decompositions of measured records into their basic components

A typical measured stress time history of a bulk carrier is shown in figure 2.26 (from reference [2.35]). Usually, such a record consists of a rapidly varying time history of random amplitude and frequency, oscillating about a mean value. The mean value itself is a weakly time-dependent function and may shift from positive to negative (sagging to hogging). The two dominant factors which affect the mean value are:

1   The stillwater loads which can be accurately determined from the loading condition of the ship floating in stillwater.

2   The thermal loads which arise due to variations in ambient temperatures and differences in water and air temperatures.

A closer look at the rapidly varying part shows that it also can be decomposed into components. Figures 2.27 and 2.28 illustrate

records taken over shorter periods of time (larger scale). Two main central frequencies appear in these records. The smaller central frequency is associated with the loads resulting from the motion of the ship as a rigid body (primarily heave and pitch motions). This lower central frequency is, therefore, close in magnitude to the wave encounter frequencies for wave length nearly equal to ship length.
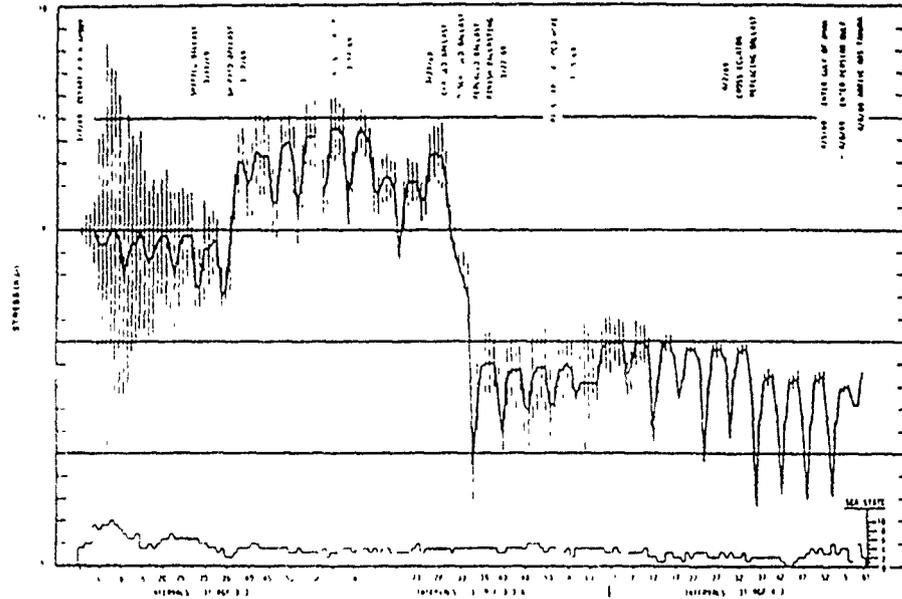
Fig. 2.26   Typical voyage variation of midship vertical bending stress for a bulk carrier. From reference [2.35]
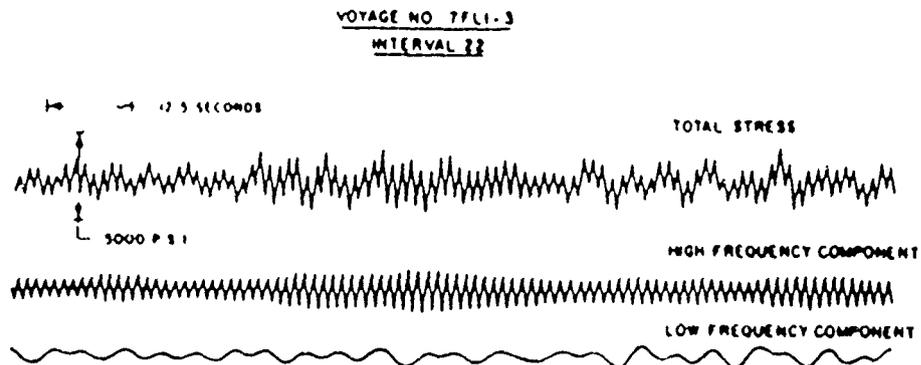
Figure 2.27.   Decomposition of a stress time history of a Great Lakes vessel into low and high frequency components.

65
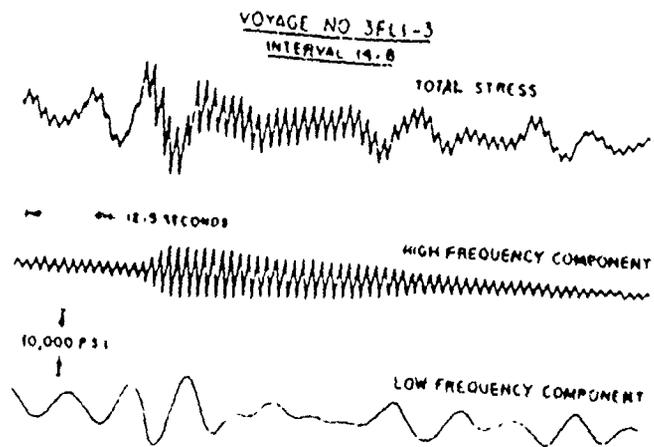
Figure 2.28. Decomposition of a stress time history of an ocean going bulk carrier.

The higher central frequency is associated with loads resulting from the two-node mode response of the ship when it vibrates as a flexible body. This higher central frequency is thus close to the two-node mode natural frequency of the ship. The high frequency response itself can be due to "springing" of the flexible ship when excited by the energy present in the high-frequency wave components as shown in figure 2.27. It can be due, also to the impact of the ship bow on the water as the ship moves into the waves, i.e., slamming (possibly together with low-speed machinery-induced vibrations), see figure 2.28. Though springing and slamming may occur simultaneously, it is unusual to see records which exhibit both clearly. These two responses can be distinguished from each other by inspecting the records' envelope. In general, a decaying envelope (see figure 2.28) indicates a slamming response whereas a continuous envelope of varying amplitude, as shown in figure 2.27, indicates a springing response.

The rigid body and the high frequency responses do not always occur simultaneously in the same record. Quite often only the rigid

66

body response appears in a record; particularly, in that of a smaller ship which has a high two-node mode frequency. Occasionally, only the high frequency springing response appears in a record when a ship is moving or resting in relatively calm water. In particular, long flexible ships with low natural frequencies as those operating in the Great Lakes do occasionally exhibit such records when operating in calm water or in a low sea state composed mainly of short waves. Under these conditions, a long ship will not respond as a rigid body to the short waves, but the two-node mode frequency of the hull can be sufficiently low to be excited by the energy content of these short waves. Figure 2.29 (from reference [2.36]) shows a measured response spectrum of a large Great Lakes vessel where the response is purely in the two-node mode[5] and higher frequencies with no rigid body response appearing in the spectrum. The figure shows that response at higher modes than the two-node mode can be measured, although small and relatively unimportant in most cases.

Slamming response on the other hand never occurs separately without rigid body response since, obviously, it is a result of the rigid motion of the ship in the waves.
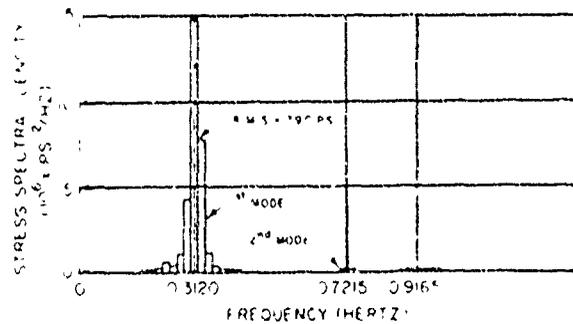
Figure 2.29   Stress response spectrum of a large
Great Lakes vessel. [2.36].

---

5 The two-node mode is labeled in the figure as the first mode.

B. Combining Analytically Determined Response Components

Two main steps should be used in the procedure for combining primary responses of a vessel.

Step 1 To combine the low frequency wave-induced responses (rigid body) with the high-frequency responses (springing or slamming).

Step 2 To add the mean value to the response resulting from Step 1. The mean value consists of the stillwater and the thermal responses.

Step 1:

Consider an input-output system in which the input is common to several components of the system; it is required to determine the sum of the individual outputs. Here, the input represents the waves which can be in the form of a time history if a time-domain analysis is sought, or in the form of a sea spectrum if a frequency-domain evaluation is preferred.
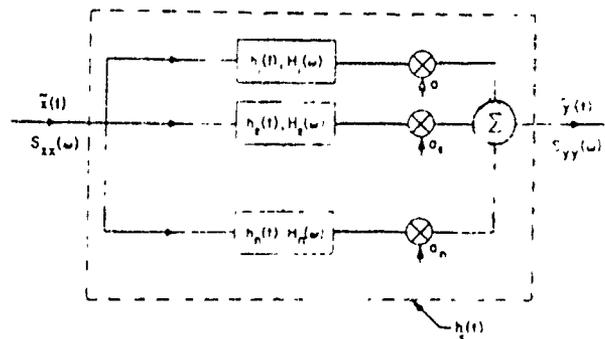
Figure 2.30   Schematic representation of a multiple system with common input.

68

The components of the system represent the components of the load response of the ship to waves, e.g., the low-frequency wave-induced responses which consist of vertical, horizontal and torsional moments, the high frequency responses such as the springing loads . It is required now to determine the sum of these component responses, i.e., to determine the output taking into consideration the proper relations or the appropriate correlation of the response components.

Schematically, the procedure is represented by figure 2.30. In this figure, "n" parallel linear components are considered which have common input $\tilde{x}(t)$ and are summed up at the output to form $\tilde{y}(t)$. The output of each system is multiplied by a constant a_i ($i = 1, 2, ...n$) before summing up all the components at a common node to form $\tilde{y}(t)$. These constants a_i give additional flexibility in the application of the model and can be used to "weigh" the contribution of each linear system to the sum.

In a time domain, the output $\tilde{y}(t)$ is given by the sum of the convolution integral of each system.

$$\tilde{y}(t) = \sum_{i=1}^{n} a_i [\int_0^\infty h_i(\tau)\tilde{x}(t - \tau)d\tau]$$
$$= \int_0^\infty h_c(\tau)\tilde{x}(t - \tau)d\tau$$

(2.76)

where

$$h_c(\tau) = \sum_{i=1}^{n} a_i h_i(\tau)$$

(2.77)

$h_i(\tau)$ is the impulse response function of each linear system, i.e., the response of each linear system to unit excitation multiplied by time (response to the Dirac delta function). $h_c(\tau)$ is a composite impulse response function which sums the responses of the individual components.

It should be noted that the impulse response functions of the individual components "$h_i(\tau)$" may or may not be easy to obtain depending on the complexity of the system. With suitable instrumentation, it is sometimes possible to obtain a good approximation to $h_i(\tau)$ experimentally. For the ship system, $h_i(\tau)$ can be determined for most load components.

In a frequency domain analysis, a similar procedure can be used. In fact, since the system function $H_i(\omega)$ is simply the Fourier transform of $h_i(t)$, i.e.,

$$H_i(\omega) = \int_0^\infty h_i(t) e^{-j\omega t} dt \qquad (2.78)$$

therefore, we can define a composite system function $H_c(\omega)$ as

$$H_c(\omega) = \int_0^\infty h_c(t) e^{-j\omega t} dt$$
$$= \sum_{i=1}^n a_i H_i(\omega) \qquad (2.79)$$

It should be noted that for a single system, the relation between the input spectrum and the output spectrum is given by the usual relation:

$$[S_{yy}(\omega)]_i = S_{xx}(\omega) H^*_i(\omega) H_i(\omega)$$
$$= S_{xx}(\omega) |H_i(\omega)|^2 \qquad (2.80)$$

where $S_{xx}(\omega)$ is the sea spectrum which represents a common input, $[S_{yy}(\omega)]_i$ is a response spectrum of an individual load component , $H^*_i(\omega)$ is the complex conjugate of the system function of a response component.

The modulus of the individual system function $|H_i(\omega)|$ is the response amplitude operator of the individual response components, i..e.,

$$[R.A.O.]_i = [\rho(\omega)]_i = |H_i(\omega)|$$

and, therefore, equation (2.80) represents the familiar relation between the input and the output spectra of a single linear system.

For our composite system, an equation similar to the equation (2.80) can be determined for the n-response components and the "weight" factors "a_i" as follows

$$S_{yy}(\omega) = S_{xx}(\omega) H^*_c(\omega) H_c(\omega)$$

$$= S_{xx}(\omega) \sum_{i=1}^{n} \sum_{j=1}^{n} a_i a_j H_i(\omega) H^*_j(\omega) \qquad (2.81)$$

The double sum in equation (2.81) can be expanded such that a final expression for the total response spectrum $S_{yy}(\omega)$, which combines the individual response spectra, may be written in the form:

$$S_{yy}(\omega) = [\sum_{i=1}^{n} a_i^2 |H_i(\omega)|^2] S_{xx}(\omega)$$

$$+ [\sum_{i=1}^{n} \sum_{\substack{j=1 \\ (i \neq j)}}^{n} a_i a_j H_i(\omega) H^*_j(\omega)] S_{xx}(\omega) \qquad (2.82)$$

It should be noted that the first term in equation (2.82) represents simply the algebraic sum of the individual response spectra, each modified by the factor a_i. The second term, which can be either positive or negative, represents a corrective term which depends on the correlation between the load components as can be seen from the multiplication of $H_i(\omega)$ by the complex conjugate of $H_j(\omega)$.

If the system functions $H_i(\omega)$ do not overlap on a frequency axis (i.e., disjoint systems), that is, it

$$H_i(\omega) H^*_j(\omega) = 0 \qquad (2.83)$$

then the second term in equation (2.82) becomes zero and the load components are uncorrelated. In this case, the total spectrum is simply the algebraic sum of the individual spectra of the load components, modified by the factors a_i . Furthermore, if the wave input is considered to be a normal random process with zero mean, as usually is the case, then the respective output load responses are jointly normal and are independent. Thus, the total response, in this special case, is a zero mean normal process with a mean square value given by:

$$\sigma_y^2 = \int_0^\infty S_{yy}(\omega) d\omega$$

$$= \sum_{i=1}^\infty a_i^2 \int_0^\infty |H_i(\omega)|^2 S_{xx}(\omega) d\omega \qquad (2.84)$$

In the more general (and more realistic) case where some or all of the response components are correlated, the mean square is given by

$$\sigma_y^2 = \int_0^\infty S_{yy}(\omega) d\omega$$

$$= \sum_{i=1}^n a_i^2 \int_0^\infty |H_i(\omega)|^2 S_{xx}(\omega) d\omega$$

$$+ \sum_{\substack{i=1 \\ (i \neq j)}}^n \sum_{j=1}^n a_i a_j \int_0^\infty H_i(\omega) H_j^*(\omega) S_{xx}(\omega) d\omega$$

$$(2.85)$$

It should be noted that in equations (2.84) and (2.85) the mean square is equal to the variance of the combined response since the mean value of the wave responses is usually very small. As noted earlier, the other responses which consist mainly of the stillwater, and the thermal loads will be added later in the second step of the analysis to form a mean value for step 1 combined responses.

In connection with equations (2.84) and (2.85) it should be emphasized that the usual Rayleigh multiplier used to estimate certain average quantities, such as average of the highest one third,one tenth response, etc., are not generally applicable in the case of the combined response, since these multipliers are associated with a narrow-band spectrum for which the amplitudes can be represented by a Rayleigh distribution. It is only in the case where each of the load component responses is narrow-band and each happen to be closely concentrated around a common central frequency "ω_0", that it would be reasonable to conclude the combined response S_{yy} (ω) is, itself, a narrow-band process.

In the more general case, where the combined response spectrum is not a narrow-band spectrum, the various statistical quantities can be determined from a more general distribution (Rice) which includes the Rayleigh distribution as a special case. The general distribution is given by equations (2.37) and (2.38).

Equation (2.85) can be written in a different form which is more convenient to use in applications, and which makes it easier to define the correlation coefficients between the different response components.

$$\sigma_y^2 = \sum_{i=1}^{n} a_i^2 \sigma_i^2 + \sum_{\substack{i=1 \\ (i \neq j)}}^{n} \sum_{j=1}^{n} a_i a_j \rho_{ij} \sigma_i \sigma_j \qquad (2.86)$$

where

$$\sigma_i^2 = \int_0^\infty |H_i(\omega)|^2 S_{xx}(\omega) d\omega = \text{variances}$$

or mean squares of the response spectra of the individual load components.   (2.87)

ρ_{ij} =   correlation coefficients of individual load components defined by,

$$\rho_{ij} = \frac{1}{\sigma_i \sigma_j} \int_0^\infty H_i(\omega) H^*_j(\omega) S_{xx}(\omega) d\omega$$

(2.88)

Equation (2.86) with definitions (2.87) and (2.88) form the basis for combining the step 1 responses of a ship hull girder in a frequency domain analysis taking into consideration the correlation between the response components. If the response components are uncorrelated, i.e., if $\rho_{ij} = 0$, the second term in equation (2.86) drops out and the variance of the combined responses (output) is simply the algebraic sum of the individual variances modified by the factors a_i. As discussed earlier, this occurs when the system function of the various components do not overlap in frequency or overlap in a frequency range where the individual responses are small. On the other hand, if the individual components are perfectly correlated, ρ_{ij} may approach plus or minus unity and the effect of the second term of equation (2.86) on the combined load variance σ^2_y can be substantial.

The physical significance of the correlation coefficient can be further illustrated by considering only two response components for simplicity. If ρ_{12} is large and positive (i.e., approaching +1), the values of the two response components tend to be both large or both small at the same time, whereas if ρ_{12} is large and negative (i.e., approaching -1), the value of one response component tends to be large when the other is small, and vice versa. If ρ_{12} is small or zero, there is little or no relationship between the two response components. Intermediate values of ρ_{12} between 0 and ± 1 depend on how strongly the two responses are related. For example, the correlation coefficient ρ_{12} of the vertical and horizontal bending moments acting on a ship is expected to be higher than of the vertical and springing moments since the overlap of the system functions in the latter case is smaller than in the former case.

In a time domain analysis, the convolution integral represented by equation (2.7b) with the composite impulse response function as

given by equation (2.77) form the basis for determining the combined load response. The question of whether the time or the frequency domain analysis should be used depends primarily on what form the required input data is available. In general, most wave data and practical analysis are done in a frequency domain, although in some cases where slamming loads are a dominant factor, it may be advisable to perform the analysis in time domain.

Step 2:

In this step, the stillwater and the thermal responses should be combined to form the mean value for the rigid body motion and higher frequency responses. The stillwater and thermal responses are weakly time-dependent variables so that in a given design extreme load condition they can be considered constants, say over the duration of a design storm. Therefore, theses two responses can be treated as static cases and can be combined for one or several postulated design conditions without difficulty. Alternately, if statistical data are available for each of these responses, the mean and variances of the combined response can be easily determined.

The stillwater response can be accurately determined for all loading conditions using computer programs such as the Ship Hull Characteristics Program. Several postulated, extreme but realistic, weight distributions can be assumed in the final stages of design, and the corresponding stillwater response can be computed.

If a statistical description of the stillwater bending moment is adopted, data have shown that the general trend assumes a normal distribution for the conventional types of ships. A sample histogram based on actual ship operations data for a containership from reference [2.37] is shown in figure 2.31. A mean value of the stillwater bending moment can be estimated based on this histogram for all voyages, or for a specific route such as inbound or outbound voyages.
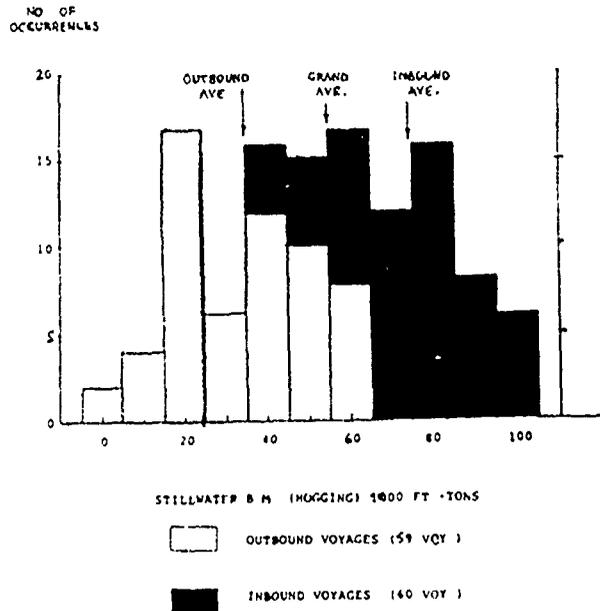
Figure 2.31. Histogram of stillwater bending moment of a containership.
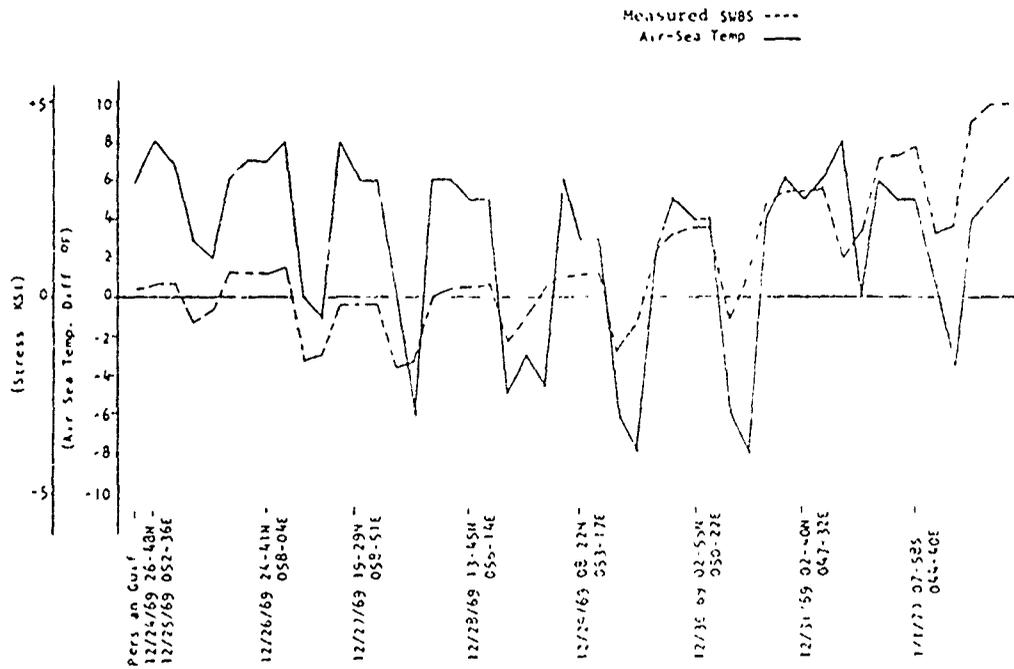
Figure 2.32. Correlation between measured stillwater bending moment and air/sea temperature difference.

These mean values together with a set of standard deviations, which can also be estimated from the histogram, can be utilized to determine the extreme total moment using a statistical approach.

Since the stillwater response, the rigid body motion response, and the higher frequency responses are all functions of the ship weight and its distribution, it is preferred that the combined response be calculated for a group of selected loading conditions (and selected temperature profiles).

Primary thermal response is usually induced by differences in water/air temperatures and by variations in ambient temperatures. A study of full-scale stress data measured on a larger tanker indicates that the diurnal stress variations correlate well, as shown in figure 2.32 with temperature differentials between air and sea.

Taking the North Atlantic route as an example, the average diurnal change of air temperature is about 10 $^\circ$F. The total diurnal change of deck plating temperatures may vary from 10^c to 50° F, depending upon the cloud cover conditions and the color of the deck plating. For estimating the thermal loads on a ship hull, the sea temperature may be assumed as constant. Once the temperature differential along a ship hull is determined, the thermal stresses can be calculated, using either a general purpose finite element computer program or a simplified two-dimensional approach. The maximum thermal response may be then added to the stillwater response for certain postulated design conditions to form the mean value for the low and high frequency dynamic responses.

Although high thermal responses may not happen in high seas, a heavy swell may possibly occur under a clear sky. Therefore, several temperature conditions are to be taken into consideration in determining the combined design response.

Application Examples:

Generally, large tankers travelling in oblique seas may encounter horizontal bending moments of the same order of magnitude of the vertical bending moments. Therefore, the combined effect of the vertical and horizontal moments can be critical under certain conditions. The distribution of the primary stress in the deck as a result of the combined effect becomes non-uniform and assumes a maximum value at one edge. The combined stress at the deck edge, $\tilde{\sigma}_c$ is given by

$$\tilde{\sigma}_c = \frac{\tilde{M}_v(t)}{S_v} + \frac{\tilde{M}_h(t)}{S_h} \qquad (2.89)$$

where,

$\tilde{\sigma}_c$ =   combined edge stress

$\tilde{M}_v(t)$ =   the vertical bending moment component

$\tilde{M}_h(t)$ =   the horizontal bending moment component

S_v, S_h =   the vertical or the horizontal section modulus, respectively.

Defining the combined moment as the combined edge stress multiplied by the vertical section modulus and using equation (2.89), we can write,

$$\tilde{M}_c(t) = \tilde{\sigma}_c(t)S_v = \tilde{M}_v(t) + k\tilde{M}_h(t)$$

$$(2.90)$$

where,

$$K = \frac{S_v}{S_h}$$

Applying equations (2.86), (2.87) and (2.88) and extending the results for the case of a two-dimensional sea spectrum, the mean square value of the combined response σ_{Mc}^2 can be written as (see equation (2.86)):

$$\sigma_{Mc}^2 = \sigma_{Mv}^2 + K^2 \sigma_{Mh}^2 + 2\rho_{vh} K \sigma_{Mv} \sigma_{Mh} \qquad (2.91)$$

where σ_{Mv}^2 and σ_{Mh}^2 are the mean square values of the vertical and horizontal bending moments, respectively, given by equation (2.87) as [6] :

$$\sigma_{Mv}^2 = \int_{-\frac{\pi}{2}}^{+\frac{\pi}{2}} \int_0^\infty S_{xx}(\omega,\mu) \, |H_v(\omega)|^2 \, d\omega d\mu \qquad (2.92)$$

$$\sigma_{Mh}^2 = \int_{-\frac{\pi}{2}}^{+\frac{\pi}{2}} \int_0^\infty S_{xx}(\omega,\mu) \, |H_h(\omega)|^2 \, d\omega d\mu \qquad (2.93)$$

Using equation (2.88) the correlation coefficient is defined as:

$$\rho_{vh} = \frac{1}{\sigma_{Mv} \sigma_{Mh}}$$
$$\cdot \int_{-\frac{\pi}{2}}^{+\frac{\pi}{2}} \int_0^\infty S_{xx}(\omega,\mu) H_v(\omega) H_h^*(\omega) d\omega d\mu$$

$$(2.94)$$

---

6 For simplicity of notation, the dependence of the RAO's $|H_v(\omega)|$ and $|H_h(\omega)|$ on the ship heading with respect to wave components is dropped from the notation.

The Response Amplitude Operators $|H_v(\omega)|$ and $|H_h(\omega)|$ and more generally, the system functions $H_v(\omega)$ and $H_h(\omega)$ can be determined from any typical rigid-body ship motion computer program.

It should be noted that in equation (2.86), the coefficient a_1 was taken as unity and a_2 was taken equal to

$$a_2 = K = \frac{S_v}{S_h}$$

(see equation (2.90)) in determining equation (2.91). It should be also noted that the integrand in equation (2.94) contains the information regarding the phase between the horizontal and vertical moments and that the integration of such information with respect to frequency and the angle μ between a wave component and the prevailing wave system leads to the determination of the correlation coefficient as given by equation (2.94). Finally, the root-mean-square (r.m.s.) of the combined edge stress is given by

$$(\text{rms})_c = \frac{\sigma_{Mc}}{S_v}$$

$$(2.95)$$

where σ_{Mc} is the r.m.s. of the combined moment given by equation (2.91).

The r.m.s. of the combined moment and the correlation coefficient as given by equations (2.91) and (2.94), respectively, were computed in reference [2.38] for a large tanker of DWT 327,000 tons. The r.m.s. values of vertical and horizontal moments were computed using a rigid body ship motion computer program and combined using equation (2.91) to obtain the r.m.s. of the combined moment. The results of the calculations are plotted in figures 2.33 and 2.34 versus the heading angle. Several significant wave heights

were considered in order to examine the general behavior of the responses in low, moderate and high sea states. These results show that the horizontal bending moments is not small compared with the vertical bending moment (see figure 2.34). In severe seas, the maximum response of the combined moment (and the vertical moment) is in head and following seas. Figure 2.35 shows the variation of the combined bending moment with the sea state as obtained by three different methods. The first is based on equation (2.91) with σ_{Mv}, σ_{Mh} and ρ_{vh} given by equations (2.92), (2.93) and (2.94) respectively. The second method is based on equations (2.91), (2.92) and (2.93), also, but with a correlation coefficient ρ_{vh} equal to 0.32 obtained from the 1973 ISSC Proceedings (determined empirically). The third method is based on $\rho_{vh} = 0.53$ as determined by averaging the responses in short crested seas as determined from equation (2.91) for all headings and for the three representative sea states. The mean value of ρ_{vh} obtained in this manner was 0.53, significantly higher than the ISSC value. However, the effect of ρ_{vh} on the r.m.s. combined moment is small, as can be seen from figure 2.35.

As a second application example, the combined vertical and springing moment will be considered next. Using frequency domain analysis and using equations (2.86), (2.87) and (2.88) with $a_1 = a_2 = 1$, we obtained the mean square value of the combined response "σ_{vs}^2" in long-crested seas as

$$\sigma_{vs}^2 = \sigma_v^2 + \sigma_s^2 + 2\rho_{vs}\sigma_v\sigma_s \qquad (2.96)$$

where,

$$\sigma_v^2 = \text{mean square of vertical bending moment}$$

$$= \int_v^\perp S_{xx}(\omega) \mid H_v(\omega) \mid^2 d\omega \qquad (2.97)$$

$$\sigma_s^2 = \text{mean square of the springing moment}$$

81

$$= \int_0^\infty S_{XX}(\omega) \mid H_S(\omega) \mid^2 d\omega \qquad (2.98)$$

$$\rho_{vs} = \text{correlation coefficient}$$

$$= \frac{1}{\sigma_v \sigma_s} \int_0^\infty S_{XX}(\omega) H_V(\omega) H^*_S(\omega) d\omega \qquad (2.99)$$

and $H_V(\omega)$ and $H_S(\omega)$ are the complex system functions of the vertical wave moment and springing moment respectively. The system response functions can be computed using computer programs which take into consideration the effects of ship flexibility in the response, such as the springing-seakeeping program "SPRINGSEA", [2.39]. Applications of equations (2.97), (2.98) and (2.99) to several Great Lakes Vessels where springing is important is given in references [2.38] and [2.39]. These equations together with equations (2.76) and (2.77) for the time-domain analysis have a wide range of applicability to any two or more dynamic random responses including, combining primary and secondary[7] responses [2.38], vertical and torsional moments for ships where torsion is important, high frequency loads with vertical and horizontal moments, etc. In all of the cases, the coefficient a_i must be appropriately determined. When determining the various statistical averages from the combined r.m.s. values, the more general distribution given by Rice for the peaks should be used instead of the usual Rayleigh distribution.

The above procedure for combining loads is not generally applicable for combining slamming with wave induced loads. Reference [2.40] describes a procedure for combining loads on a ship when slamming is involved as one of the loads.

---

7 Such as primary inplane loads on grillages due to overall bending of the hull and secondary lateral pressure arising from the randomly varying water surface.
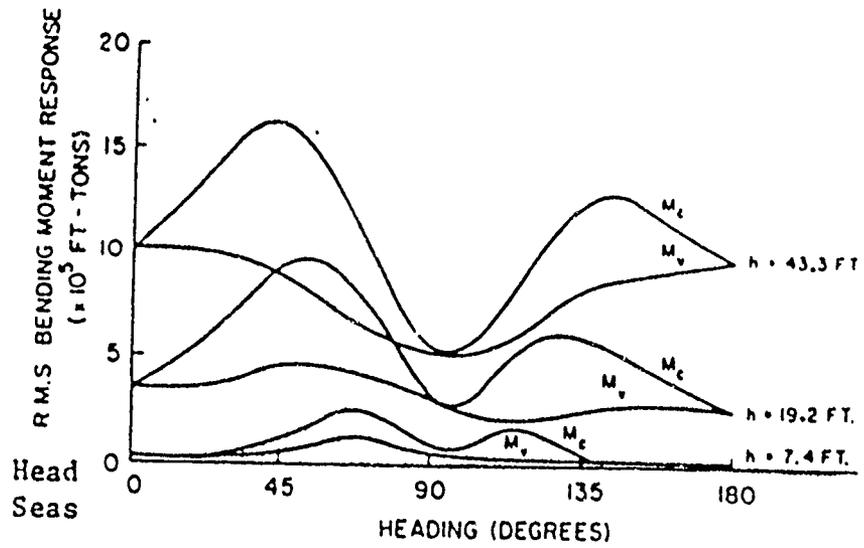
Figure 2.33. Variation of vertical and combined wave bending moments with heading in long-crested seas.
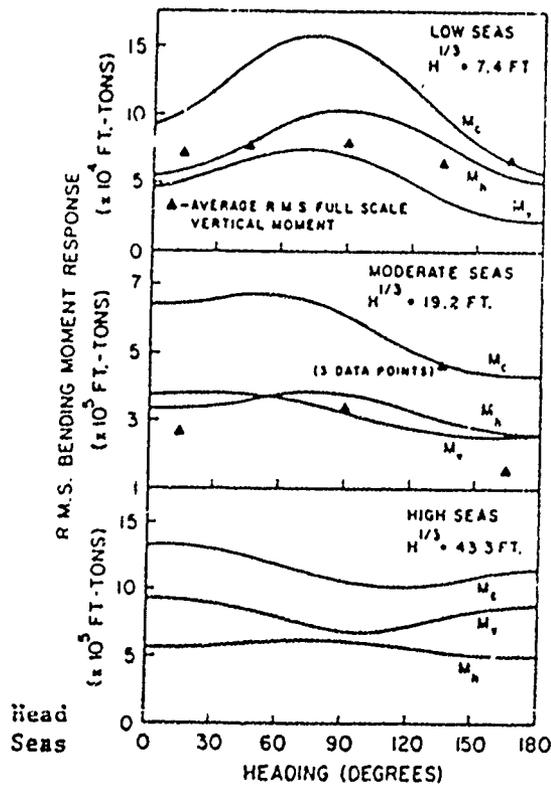
Figure 2.34. Variation of vertical, horizontal and combined moments with heading in short-crested seas.

83
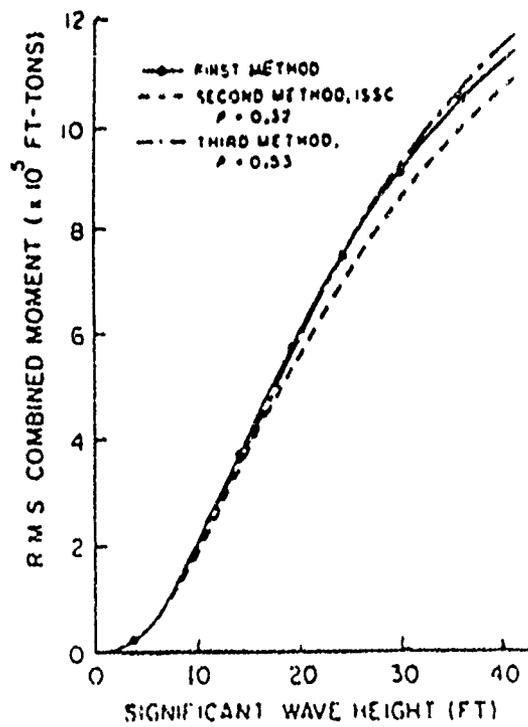
Figure 2.35. Comparison of combined bending moment responses as computed by three methods.

REFERENCES

2.1 Rice, S.O., "Mathematical Analysis of Random Noise," Bell System Technical Journal, Vol. 23, 1944; Vol. 24, 1945. Reprinted in N. Wax, "Selected Papers on Noise and Stochastic Processes," Dover, New York, 1954.

2.2 Crandall, S. and Mark, W., Random Vibration in Mechanical Systems, Academic Press, 1963.

2.3 Davenport, W.B. and Root, W.L., An Introduction to the Theory of Random Signals and Noise, McGraw-Hill, New York, 1958.

2.4 Pierson, W.J. and Moskowitz, L., "A Proposed Spectral Form for Fully Developed Wind Seas Based on the Similarity Theory of S.A. Kitaigorodiskii," Journal of Geophysical Research, Vol. 69, December 1964.

2.5 Bretschneider, C.L., "Wave Variability and Wave Spectra for Wind-Generated Gravity Waves," Beach Erosion Board, U.S. Army Corps of Engineers, Technical Memorandum No. 118, 1952.

2.6 International Ship Structures Congress, Report of Committee 10, Vol. 2, 1967.

2.7 Cartwright, D.E. and Longuet-Higgins, M.S., "The Statistical Distribution of the Maxima of a Random Function, "Proc. R. Soc. of London, Ser. A 237, pp. 212-232, 1956.

2.8 St. Denis and Pierson, "On the Motion of Ships in Confused Seas,"Trans. SNAME, 1955, p. 280.

2.9 Salvesen, N., Tuck, E. and Faltinsen, O., "Ship Motions and Sea Loads," Trans. SNAME, 1970, p.250.

2.10 Abkowitz, M., Stability and Motion Control of Ocean Vehicles, M.I.T. Press, Cambridge, Mass., 1969.

2.11 Korvin-Kronkovsky, B., "Theory of Seakeeping," SNAME, New York, 1961.

2.12 Jacobs, W. "The Analytical Calculation of Ship Bending Moment in Regular Waves," Journal of Ship Research, Vol. 2, No.1, June 1958.

2.13 Tasai, F., "Ship Motions in Beams Seas," Research Institute for Applied Mechanics, Vol. XIII, No. 45, 1965.

2.14 Tasai, F., "On the Swaying, Yawing and Rolling Motions of Ships in Oblique Waves," International Shipbuilding Progress, Vol. 14, No. 153, 1967.

2.15 Smith, W.E., "Computation of Pitch and Heaving Motions for Arbitrary Ship Forms," International Shipbuilding Progress, Vol. 14, No. 155, 1967.

2.16 Raff, A.I., "Program SCORES - Ship Structural Response in Waves." Ship Structures Committee Report SSC-320, 1972.

2.17 "SPRINGSEA II - Springing and Seakeeping (Program)." American Bureau of Shipping, New York. Also see "SPRINGSEA II, Program Listing and User's Manual," Mansour Engineering, Inc., Berkeley, California, 1974.

2.18 Loukakis, T., "Computer-Aided Prediction of Seakeeping Performance in Ship Design." M.I.T. Department of Ocean Engineering, Report No. 70-3, August 1970.

2.19 Meyers, W.G., Sheridan, D.J. and Salvesen, N.. "Manual -NSRDC Ship Motion and Seaload Computer Program." NSRDC Report No. 3376, February 1975.

2.20 Wahab, R., "Amidships Forces and Moments an a $C_B = 0.8$ Series 60 in Waves from Various Directions, "Netherlands Ship Research Center TND Report No. 1065, 1967.

2.21 Dinsenbacher, A. and Andrew, J. "Vertical and Transverse Loads and Motions of a Segmented Model in Regular Waves," NSRDC Report No. 3151, 1969.

2.22 Lewis, E., "Predicting Long-Term Distributions of Wave-Induced Bending Moment on Ship Hulls," Spring Meeting, SNAME, 1967.

2.23 Fukuda, J., "Long-Term Predictions of Wave Bending Moment," Part I and Part II, Journal of the Society of Naval Architects of Japan, Vol. 120, 1966: Vol. 123, 1968.

2.24 Hoffman, D. and Lewis, E., "Analysis and Interpretation of Full Scale Data on Midship Bending Stresses of Dry Cargo Ships," Ship Structure Committee, Report SSC-196, June 1969.

2.25 Bennet, R., "Determination of Wave Bending Moment for Ship Design." Paper presented to the Scandinavian Ship Technical Conference, Finland, 1964.

2.26 Band, E., "Long Term Trends of Hull bending Moments," American Bureau of Shipping, 1966.

2.27 Mansour, A.E., "Extreme Value Distributions of Wave Loads and their Application to Marine Structures." Marine structural Reliability Symposium, Arlington, Virginia, October 1987.

2.28 Ang, H.-S. and Tang, W.H., Probability Concepts in Engineering Planning and Design, Vol. II, John Wiley and Sons, 1984.

2.29 Cramer, H., Mathematical Methods of Statistics. Princeton University Press, 1946.

2.30 Vanmarcke, E.H., "On the Distribution of the First-Passage Time for Normal Stationary Random Process," Journal of Applied Mechanics, Trans. ASME, March 1975, pp. 215-220.

2.31 Gumbel, E., Statistics of Extremes, Columbia University Press, New York, 1958.

2.32 Silveria, W.A. and Brillinger, D.R., "On Maximum Wave Heights of Severe Seas," Proceedings of the Offshore Technology Conference, paper #3232, Houston 1978.

2.33 Mansour, A.E., "A Note on the Extreme Wave Load and the Associated Probability of Failure," Journal of Ship Research, Vol. 30, no. 2, June 1986, pp. 123-126.

2.34 Borgman, L.E., "Extreme Statistics, Risk, and Reliability," Report, University of Wyoming.

2.35 Little, R.S., Lewis, E.V. and Bailey, F.C., "A Statistical Study of Wave Induced Bending Moments on Large Oceangoing Tanker and Bulk Carriers," Trans. SNAME, 1971.

2.36 Critchfield, M., "Evaluation of Hull Vibratory (Springing) Response of Great Lakes Ore Carrier M/V Stewart J. Cort," DTMB Report 4225, Nov. 1973.

2.37 Stiansen, S.G., Mansour, A.E., Jan, H.Y. and Thayamballi, A., "Reliability Methods in Ship Structures," The Naval Architect, Journal of RINA, July 1980.

2.38 Stiansen, S.G., Mansour, A.E., "Ship Primary Strength Based on Statistical Data Analysis," Trans. SNAME, 1975.

2.39 Stiansen, S.G., Mansour, A.E. and Chen, Y.N., "Dynamic Response of Large Great Lakes Carriers to Wave-Excited Loads," Trans. SNAME, 1978.

2.40 Ferro, G. and Mansour, A., "Probabilistic Analysis of the Combined Slamming and Wave-Induced Responses," Journal of Ship Research, Vol. 29, No. 3, Sept. 1985, p.170.

3. STRENGTH INFORMATION REQUIRED FOR RELIABILITY ANALYSIS OF MARINE STRUCTURES:

3.1 Strength Variability and Modelling

Because of limitation on control of properties of steel and other materials used in marine structures and because of limitations on production and fabrication of their components, the strength of apparently identical marine structures will not be, in general, identical. In addition, uncertainties associated with residual stresses arising from welding, the presence of small holes, etc. may affect the strength of the marine structure. These limitations and uncertainties indicate that a certain variability in strength or hull capacity about some mean value will result. This will in turn introduce an element of uncertainty as to what is the actual strength of the marine structure that should be compared with the loads obtained in the previous section.

Additional uncertainties in the strength will arise due to uncertainties associated with the assumptions and methods of analysis used to calculate the strength. Further uncertainties are associated with possible numerical errors in the analysis. These errors may accumulate in one direction or possibly tend to cancel each other. Whatever the case may be, the above uncertainties have to be reflected in any reliability or failure analysis.

Designers and naval architects are aware of the presence of these uncertainties. However, they are usually treated in a qualitative sense and very few attempts have been made to quantify them. The qualitative assessment of the uncertainties does not lend itself to systematic improvement of design procedures based on previous experience. Full advantage of that "experience" can be obtained by attempting to quantify them.

It is convenient to divide and recognize two types of uncertainties (Ang [3.1, 3.2]):

1. Objective uncertainties. These are uncertainties associated with random variables for which statistical data can be collected and examined. They can be quantified by a coefficient of variation derived from available statistical information. The variability in the yield strength of steel is an example.

2. Subjective uncertainties. These are uncertainties associated with the lack of information and knowledge. They can be determined only on the basis of the engineers previous experience and judgment. Examples of these include assumptions of the analysis, error in the design model, and empirical formulas.

Variability in failure load that will cause yielding of a cross section or buckling of plating results from uncertainties in the following factors:

1. Uncertainties associated with the material yield strength and Young's modulus of elasticity of different components of the section such as plates, girders and stiffeners.

2. Uncertainties associated with scantlings of components such as plate thicknesses, stiffeners, girders, and face plate dimensions.

3. Uncertainties associated with the distribution of residual stresses due to welding.

4. Uncertainties associated with major dimensions such as the beam and depth of a cross section.

5. Uncertainties associated with manufacturing imperfections, flaws, plate fairness, etc.

In addition to the above objective uncertainties, the following subjective uncertainties cause a variability in the strength or capacity of the marine structure:

1   Uncertainties associated with the degree of effectiveness of plating due to shear lag effects [3.3, 3.4].

2   Uncertainties associated with the usual Navier hypothesis of plane section remain plane and perpendicular to the neutral axis (modelling assumptions).

3.   Uncertainties related to the presence of small holes and cutouts that may exist in the deck plating.

4.   Uncertainties associated with the residual strength after buckling [3.5] and the effect of initial deformation on the buckling loads [3.6].

As more information and more knowledge is accumulated, some of the factors identified under subjective uncertainties can be classified under objective uncertainties.

Other classification of uncertainties are also possible and will be discussed later.

A physical reasoning may be used in the choice of strength or capacity distribution. Two limiting cases are widely used to represent the strength of a marine structure:

1.   The Gaussian (Normal) Distribution:

The central-limit theorem is often used to justify the use of the normal distribution. It is known that under very general conditions this distribution arises (or is approached asymptotically) in many practical problems. A sufficient condition for this is the possibility of considering the deviation of the given random variable from its mean value as the sum of a large number of independent random variables with different probability laws but none of which has large variance compared with the others. This condition is satisfied in random

quantities such as resistance of materials, weight of materials, and geometric parameters of a section.

Thus in general the strength distribution of any structure whose strength is a linear function of a number of independent random variables may be considered to approach the normal distribution. The rate at which the sum tends to normality depends on the presence of dominant non-normal component [3.7]. The normal strength model will be adopted in this report.

2.   The Lognormal Distribution:

The lognormal distribution arises as a limiting distribution when a random variable is a product of a number of independent and identically distributed random variables. In modelling the strength of a component by lognormal distribution, the advantage of precluding non positive values is obtained. However, the strength or resistance of the member should be regarded as the product of a number of random variables.

3.2 Limit States Associated with Marine Structures:

Several limit states may be defined for a marine structure. These include:

1   Ultimate strength limit state (extreme load)
2.   Fatigue limit state
3.   Serviceability limit state

The ultimate strength limit state can be further decomposed into two modes of failure:

a.   Failure due to spread of plastic deformation, as can be predicted by plastic limit analysis and fully plastic moment for beams (initial yield and shake down moments can be also classified under this category) [3.26].

b. Failure due to instability or buckling of a panel longitudinal stiffeners (flexural or tripping) or overall buckling of transverse and longitudinal stiffeners of a grillage.

Each of the above two modes require separate methods of analysis and are discussed thoroughly in reference [3.25, 3.26 and 3.8] for ships.

The fatigue limit state is associated with the damaging effect of repeated loading which may lead to a loss of a specific function or to ultimate collapse. This particular limit state requires independent type of analysis and is treated in a reliability framework in Chapter 9.

The serviceability limit state is associated with constraints on the marine structure in terms of functional requirements such as maximum deflection of a member or critical buckling loads that cause elastic buckling of a plate.

3.3 Analysis of uncertainty:

As discussed earlier uncertainties can also be classified under objective and subjective uncertainties. They can also be classified under inherent and model uncertainties. The former is associated with physical phenomena that are inherently random such as height of ocean waves. The latter is associated with models for estimation or prediction of reality such as theoretical models for predicting ultimate strength of a marine structure or imperfection of sampling of yield stress tests.

Uncertainties, both inherent and model, can be expressed in terms of a full probability distribution or more simply by coefficient of variation (c.o.v.). The method of quantification depends on the form of available data [3.9].

a. Sample Data Available [3.9].

Consider a set of sample data (x_1, x_2, ..., x_n). The mean $\bar{x}$ and standard deviation σ_x can be estimated from

$$\bar{x} = \frac{1}{n} \sum_{i=1}^{n} x_i$$

and

$$\sigma_x^2 = \frac{1}{n-1} \sum_{i=1}^{n} (x_i - \bar{x})^2$$

thus the inherent uncertainty as given by a c.o.v. is

$$\delta_x = \frac{\sigma_x}{\bar{x}}$$

The estimated mean value may not be totally accurate in comparison to the true mean value because of the sample size n. The sampling or model error in estimating $\bar{x}$ is

$$\sigma_{\bar{x}} = \frac{\sigma_x}{\sqrt{n}}$$

Therefore the uncertainty associated with the sampling (model) error is

$$\Delta_x = \frac{\sigma_{\bar{x}}}{\bar{x}}$$

b. Range of Values Known

In estimating uncertainties that require judgement, it is often convenient and more realistic to express each in the form of a range, i.e., upper and lower bounds (e.g. ultimate strength of a member). Consider now a random variable X with lower and upper bounds x_ℓ and x_u, respectively. The mean and c.o.v. can be determined depending on the assumed distribution. Ang and Tang in reference [3.9] give these values for several representative distributions as follows:

If a uniform distribution is prescribed between x_ℓ and x_u then

$$\bar{x} = \frac{1}{2} \ (\ x_l + x_u \ )$$

and

$$\delta_x = \frac{1}{\sqrt{3}} \ (\ \frac{x_u - x_l}{x_u + x_l} \ )$$
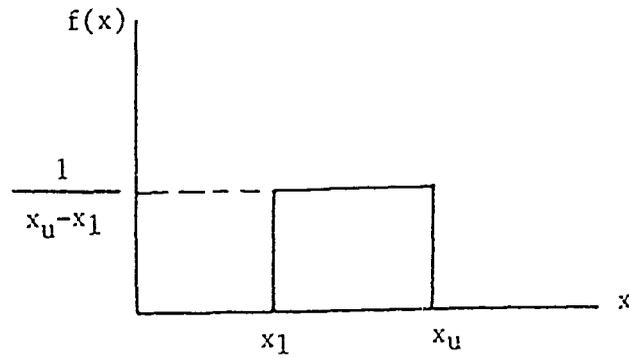
Figure 3.1.   Uniform p.d.f.

If a symmetric triangle distribution is assumed, then

$$\bar{x} = \frac{1}{2} \ (\ x_l + x_u \ )$$

$$\delta_x = \frac{1}{\sqrt{6}} \ (\ \frac{x_u - x_l}{x_u + x_l} \ )$$
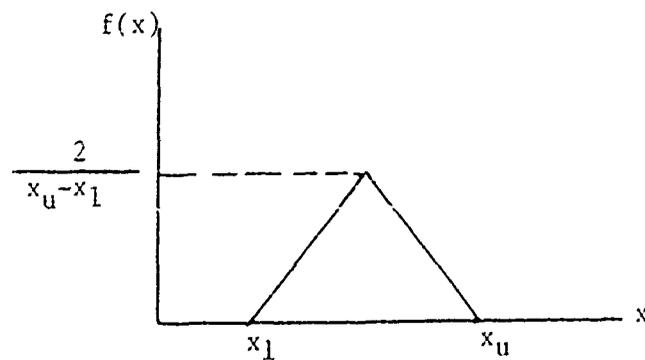
Figure 3.2.   Symmetric Triangular p.d.f.

If there is a bias towards higher values then the upper triangle distribution shown in Fig. 3.3 is more appropriate, and in this case

$$\bar{x} = \frac{1}{3} (x_l + 2x_u)$$

$$\delta_x = \frac{1}{\sqrt{2}} (\frac{x_u - x_l}{2x_u + x_l})$$
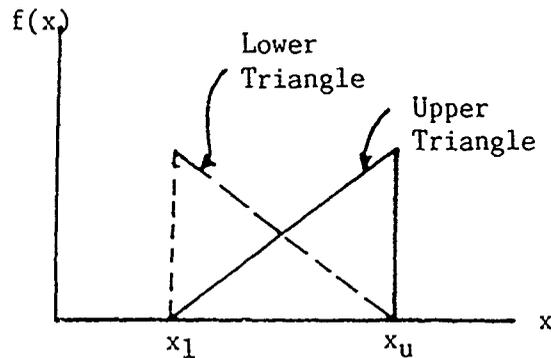
Figure 3.3.   Upper and Lower Triangle p.d.f.

If there is a bias towards the lower range, then a lower triangular distribution may be used (see Fig. 3.3), thus,

$$\bar{x} = \frac{1}{3} (2x_l + x_u)$$

and

$$\delta_x = \frac{1}{\sqrt{2}} (\frac{x_u - x_l}{x_u + 2x_l})$$

If a normal distribution is assumed (Fig. 3.4) with specified limits of $\pm$ k standard deviation, then

$$\bar{x} = \frac{1}{2} (x_l + x_u)$$

and

$$\delta_x = \frac{1}{k} (\frac{x_u - x_l}{x_u + x_l})$$
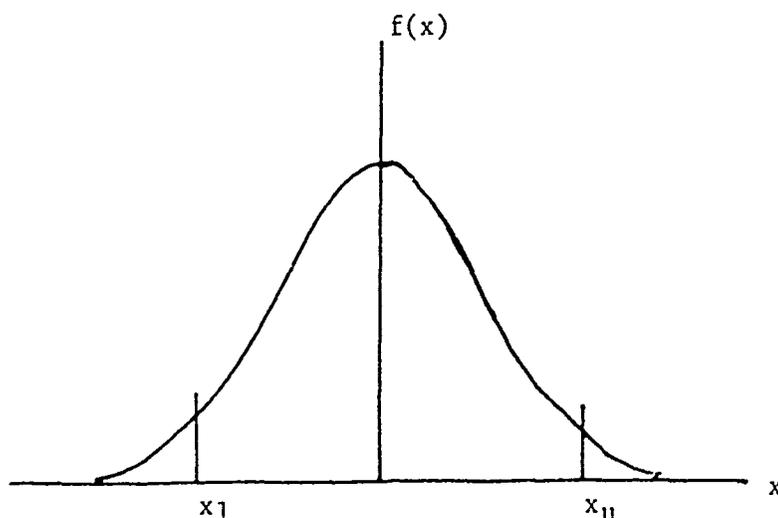
Figure 3.4. Normal Distribution.

3.4 Random Error Analysis:

In the calculation of the strength parameters, use is usually made of the theory of error. This theory can be found in applied statistics books such as [3.10], and its application to ships has been discussed in [3.11] and to other structures [3.12, papers (i), (ii) and (iii)]; therefore, it will not be repeated here. It is shown in references [3.10] and [3.11] that if the strength, S, has a functional relationship with its constituent parts[8] , $\varepsilon_1 , \varepsilon_2 \cdots \varepsilon_n$, in the form

$$S = f(\epsilon_1, \epsilon_2, \ldots \epsilon_n) \tag{3.1}$$

and if ε_i are independent, then, the approximate estimate of the mean μ and variance σ^2 of S are given by[9] :

$$\mu \simeq f(\bar{\epsilon}_1, \bar{\epsilon}_2, \ldots \bar{\epsilon}_n) \tag{3.2}$$

---

8 ε_i are the random variables which affect the strength " S" such as yield stress, plate thickness, stiffeners' dimensions, etc.

9 The random variables, ε_i are assumed to be closely distributed about their mean; S and its derivatives are assumed to be continuous.

$$\sigma^2 \simeq \sum_{i=1}^{n} (\partial S/\partial \epsilon_i)^2 \cdot \sigma_{\epsilon_i}^2$$

$$(3.3)$$

where $\bar{\epsilon}_i$ and $\sigma_{\epsilon_i}^2$ are the mean and the variance of the random variable ϵ_i . The partial derivatives in equation (3.3) are to be evaluated at the mean value $\bar{\epsilon}_i$. Equation (3.3) can be normalized and written in terms of the coefficient of variations (COV):

$$\delta_s^2 = (\sigma/\mu)^2 \cong \sum_{i=1}^{n} \left(\frac{\partial S}{\partial \epsilon_i} \cdot \frac{\bar{\epsilon}_i}{\mu} \right)^2 \cdot \delta_{\epsilon_i}^2$$

$$(3.4)$$

where $\delta_s \equiv \frac{\tilde{\sigma}}{\mu}$ is the strength COV, and $\delta_{\epsilon_i} = \sigma_{\epsilon_i} / \bar{\epsilon}_i$ are the COV of ϵ_i and the partial derivatives are to be evaluated at the mean values.

If the variables ϵ_i are correlated and the correlation coefficients ρ_{ij} between ϵ_i and ϵ_j are known, then equation (3.2) still gives the mean of the strength S in terms of the means of ϵ_i but the c.o.v. of S becomes

$$\delta_s^2 \cong \frac{1}{\mu^2} \sum_i \sum_j \rho_{ij} \left(\frac{\partial S}{\partial \epsilon_i} \right) \left(\frac{\partial S}{\partial \epsilon_j} \right) \sigma_{\epsilon_i} \sigma_{\epsilon_j} \quad (3.5)$$

where the partial derivatives are evaluated at the mean values.

3.5 Uncertainties associated with ship strength:

The strength or a limit state associated with a ship is a function of several variables. In order to determine the mean and c.o.v. of the strength, information must be obtained on those variables affecting it. With that purpose in mind the following variables were evaluated: material yield strength, material ultimate strength,

Young's modulus, ship steel plate thickness, ship steel corrosion rates, residual stresses, and fabrication tolerance.

Computerized on-line periodical searching was used [3.13] to cover efficiently as much ground as possible for three of the variables. Several data bases, available from the DIALOG system and representing several million citations of journal articles, symposia, conference papers and U.S. Government technical reports, were searched. This yielded about 300 citations which were further reviewed for suitability and included as appropriate. The striking result from these broadly based searches was the lack of statistical data on the appropriate variables, even though extensive literature exists on the subjects in general.

Yield strength, ultimate strength, and Young's modulus: The measurement of yield and ultimate strength is the most basic test that can be made in materials research, yet most papers will include only one or two tests to show the relative merits of a new process or alloy. Even when statistics are reported, another difficulty arises, namely, lack of uniformity in the test method and results reported. Under the general category of yielding, there are measurements of proportional limit, elastic limit, yield strength (0.2 percent offset), yield stress level, upper yield point, and lower yield point. Alpsten [3.14] discusses the weakness of each one of these measurements and points out that all of them are affected by the strain rate and or residual stresses in the sample. He recommends use of the 0.2 percent offset measurement because it compares well with static strain tests. Measurement of yield points is particularly sensitive to strain rate, but most of the older data do not report this value.

Table 1 provides a summary of more than 60,000 samples of various steel types and test methods. Galambos [3.15] in reviewing much the same data suggests that any numerical analysis is probably worthless since the measurements are so varied. His judgment is that for rolled shapes the mean yield stress be taken as 1.05 F_y in flanges and 1.10 F_y in webs with COV's of 0.10 and 0.11, respectively.

F_y is the specified yield stress for the steel grade used. The weighted average of the COV's for the data presented in Table 3.1 is 0.089.

The results for ultimate strength are safer to compare since this measurement is not particularly affected by strain rate. Table 3.2 presents results for about 4200 samples but representing several different types of steel. Here the weighted average of the COV's is 0.068.

Finally, Table 3.3 gives the results of 300 samples measuring Young's modulus. Overall, the weighted average of the mean value is 30.07 x 10 ksi and the weighted average of the COV's is 0.031.

<u>Ship steel plate dimensions</u>: A careful literature review revealed only limited statistical data on the thickness of ship steel plate [3.16]. There is an extensive body of literature on the detail of manufacturing plates and how to improve the quality, but no specific numbers as to the variations that typically occur. Informal contacts with one major steel producer tend to confirm that whatever data are collected in the mills are considered proprietary.

In [3.17] Basar did obtain such data from one manufacturer, but he did not report any statistics.

<u>Corrosion</u>: This is another topic where there is a lot of literature, but few statistical data. Only one paper [3.18] giving actual shipboard corrosion rates has been found, but the data are based on observations of a single tanker only. Two other papers were found which have statistics on rates, but they were for unprotected steel samples [3.19. 3.20]. thus any comparisons are of limited value. Table 3.4 presents a summary of this information.

<u>Residual stress</u>: Statistical data on residual stress are extremely difficult to find; in fact, this search revealed very little. While this subject has received considerable study, the testing

method is prohibitively expensive, which precludes gathering statistically significant amounts of data. Alpsten [3.14], for example, reports that surveying a single plate for residual stress took 140 hours, not man-hours, but the time it took a team to collect the data. Two representative papers which give results and empirical methods for predicting residual stress are included in the list of references [3.21, 3.22].

Fabrication tolerances and imperfections While no extensive search was conducted on this subject, it seems safe to say that the literature on the subject is limited. Basar [3.17] in his survey of structural tolerances in the U.S. shipbuilding industry, states that

"The quantity of structural deviations data obtained was rather limited partly due to the fact that the yards did not maintain a statistical record and partly due to the fact that actual measurements proved to be difficult to carry out in that it interfered with the yard's work in progress."

As far as "in service" deviations are concerned, again not enough data were available due to the fact that such data are not being recorded and sometimes not even reported.

This led the International Ship Structures Congress in their 1976 report to recommend for future research the establishment of a comprehensive "Damage Recording System." The report cites the need for all parties concerned-that is, the classification societies, ship owners, and ship repairers-to "take a more liberal view of the subject and to release information of this type for the benefit of the industry."

Two other related papers were located: [3.23], which gives statistical data and distributions for steel-plated highway bridges, and [3.24], which discusses fabrication errors in a Japanese high-rise building.

Table 3.1 Yield strength data

Test	No. of Samples	Mean. psi	COV	Distribution	Remarks
Yield stress		66 000	0.091	assumed lognormal	mill test 1 containment vessel SA537 GrB
Yield stress	.	39 600	0.10	assumed lognormal	mill test 1 containment vessel SA36
Yield stress	9	35 021	0.042	extreme Type I	cold straightened shape HE200B
Yield stress	32	36 583	0.0922	extreme Type I	cold straightened shape HE200B
Yield stress	19 857	40 073	0.103	extreme Type I	mill tests
Yield stress	19 217	43 475	0.099	extreme Type I	mill tests
Yield stress	11 170	57 616	0.057	extreme Type I	mill tests
Yield stress	2447	63 336	0.054	extreme Type I	mill tests
Upper yield point	3974	40 000	0.087	lognormal	mill tests
					implys log normal, refers to Freudenthal, ASCE, Vol. 121, 1956
Yield stress	400	44 000	0.11	...	
Yield stress	33	36 091	0.059	...	1948 tests, ABS Class A plates $^7/_{16}$ and $^1/_2$ in.
Yield point	79	34 782	0.116	...	1948 tests, ABS Class B plates $^9/_{16}$, $^5/_8$, $^{11}/_{16}$, $^3/_4$, $^{13}/_{16}$, $^7/_8$, $^{15}/_{16}$, 1 in.
Yield point	13	33 831	0.081		1948 tests, ABS Class C plates $1^5/_8$, $1^3/_{16}$, $1^1/_4$, $1^3/_8$, $1^1/_2$ in.
Yield strength	39	34 850	0.044	normal	$^3/_4$-in. ABS B Steel
Yield strength	36	35 000	0.069		$1^1/_4$-in. ABS C Steel
Yield point	3124	39 360	0.078	.	ASTM mill tests
Yield point	35	42 900	0.103		mill test ϵ = 1000 μin./in /sec
Yield stress level	35	41 200	0.102		same specimens as above, simulated mill test
Yield stress level	35	34 000	0.121	.	same specimens as above, stub column test, static strain rate
Yield stress 0.2%	50	61 780	0.034	not normal not lognormal	cold-rolled rods
Yield stress 0 2%	38	40 530	0.045	not normal not lognormal	hot-rolled rods
Lower yield	22	30 923	0.110	...	carbon structural $^3/_4$- and 1-in. plate and $^7/_8$-in. angle
Lower yield	20	42 675	0.079	...	low-alloy $^3/_4$- and 1-in. plate
Lower yield	10	50 290	0.068	...	low-alloy $^3/_4$-in. plate
Yield point	120	35 080	0.038	...	ASTM A7-55T WF beams, flanges
Yield point	58	39 079	0.044	...	ASTM A7-55T, WF beams, webs
Yield point	54	38 000	0.0261	...	ASTM A7-55T, WF beams, cover plates
Yield stress		41 800	0.10	lognormal assumed	Mill test, 4 different containment vessels, SA516 GR70
Yield stress			0.066	lognormal assumed	Mill test, 1 containment vessel, SA516 GR70

Table 3.2 Ultimate strength data

Test	No. of Samples	Mean, ksi	COV	Distribution	Remarks
Tension	8	58.291	0.043	.	cold straightened shape
Tension	32	57.909	0.089	.	cold straightened shape
Tension	9	84.039	0.1124	.	annealed, alloy steel
Tension	9	124.9	0.1796	..	quenched, alloy steel
Tension	22	60.405	0.0719	...	nominal maximum stress, various plates, structural steel
Tension	20	73.525	0.074	.	nominal maximum stress, various plates, low-alloy steel
Tension	10	80.39	0.109	..	nominal maximum stress, various plates, low-alloy steel
Tension	120	62.64	0.0226	..	ASTM A7-55T, WF beams, flanges
Tension	58	64.33	0.0341	...	ASTM A7-55T, WF beams, webs
Tension	54	60.64	0.0241	..	ASTM A7-55T, cover plates
Tension	3982	66.27	0.0703	...	mill tests
Tensile strength	33	59.27	0.044	...	1948 tests ABS Class A plates, $^7/_{16}$, $^1/_2$ in.
Tensile strength	79	60.99	0.091	..	1948 tests ABS Class B plates, $^9/_{16}$, $^5/_8$, $^{11}/_{16}$, $^3/_4$, $^{13}/_{16}$, $^7/_8$, $^{15}/_{16}$, 1 in.
Tensile strength	13	60.25	0.051	...	1948 tests ABS Class C plates, $1^1/_{16}$, $1^3/_{16}$, $1^1/_4$, $1^3/_8$, $1^1/_2$ in.
Tension	39	62 57	0.044	normal	$^3/_4$ in. ABS B Steel
Tensile strength	36		0.047	normal	$1^1/_4$ in. ABS C Steel

Table 3.3 Young's modulus data

Test	No. of Samples	Mean, ksi	COV	Distribution	Remarks
Tension	104	30.0×10^3	0.0327	...	structural steel from bridges
Tension	19	28.98×10^3	0.0269	...	various steel alloys, annealed and quenched, and drawn samples
Tension	22	29.50×10^3	0.0072	...	structural steel
Compression	22	29.49×10^3	0.0146	...	structural steel, same samples as above
Tension	20	29.59×10^3	0.0056	...	low alloy
Compression	20	29.64×10^3	0.0070	...	low alloy, same samples as above
Tension	10	29.56×10^3	0.0064	...	low alloy
Compression	10	29.61×10^3	0.01108	...	low alloy, same samples as above
Tension	38	29.42×10^3	0.01565	...	various-size specimens from $1/4$, $1/2$ and 1-in. plate, same test, structural steel
Tension and standard column	94	31.20×10^3	0.060	...	structural steel

Table 3.4 Corrosion rates

(i) Mean corrosion rates for a tanker	[3.10]
Member or Grouping	Corrosion Mean and Standard Deviation mils/year
Internal steel, upper 15 ft	6.5 ± 0.4
Internal steel, lower 30 ft	3.3 ± 0.2
Deck longitudinals	6.5 ± 0.4
Bottom longitudinals	3.3 ± 0.2
Deck plate	11.4 ± 0.7
Shell plate sides	5.4 ± 0.6
Bottom plate, wing tanks	5.4 ± 1.0
Bottom plate, center tanks	17.9 ± 2.9

(ii) Corrosion Rates for Unprotected Steel in Brackish Water [3.2c]	
	Mean and Standard Deviation in mils/year[a]
Maximum pit depth	19.731 ± 2.25
Uniform corrosion	6.83 ± 2.66

(iii) Corrosion Rates for Unprotected Steel in Seawater [5.13]		
Exposure depth	0.5 m	1.5 m
Uniform Corrosion, mil/year[b]	5.5 ± 0.3	5.7 ± 0.2

[a] Originally reported as millimeters of corrosion after 38 months.
[b] Originally reported as g/m^2 weight loss after 16 months

REFERENCES

3.1 Ang, A. H.-S., and Ellingwood, B.R., "Critical Analysis of Reliability Principles Relative to Design," prepared for the conference on applications of statistics and probability to soil and structural engineering, Hong Kong, Sept. 1971

3.2 Ang, A. H.-S., and Amin, M., "Formulation of Wind-resistant Design Based on Acceptable Risk," prepared for the Third International Conference on Wind Effects, Tokyo, Japan, Sept. 1971.

3.3 Schade, H.A., "The Effective Breadth Concept in Ship-Structure Design, "Trans. SNAME, Vol. 61, 1953, pp. 410-430.

3.4 Mansour, A.E., "Effective Flange Breadth of Stiffened Plates Under Axial Tensile Load or Uniform Bending Moment," Journal of Ship Research, Vol. 14, No.1, March 1970.

3.5 Mansour, A.E., "On the Nonlinear Theory of Orthotropic Plates," Journal of Ship Research, Vol. 15, No. 4, Dec. 1971.

3.6 Mansour, A.E., "Post-buckling Behavior of Stiffened Plates with Small Initial Curvature under Combined Loads," International Shipbuilding Progress, Vol. 18, No. 202, June 1971.

3.7 Thoft-Christensen, P. and Baker, M.J., Structural Reliability Theory and its Applications, Springer-Verlag Berlin Heidelberg, New York, 1982.

3.8 Mansour, A.E., "Probability Design Concepts in Ship Structural Safety and Reliability," Trans. SNAME, Vol. 80, 1972.

3.9 Ang, A. H.-S., and Tang, W.H., Probability Concepts in Engineering Planning and Design, Vol. II, John Wiley & Sons, New York, 1984.

3.10 Pardine, C. and Privett, B., Statistical Methods for Technologists, the English University Press, London, 1964.

3.11 Mansour, A.E. and Faulkner, D.,"On Applying the Statistical Approach to Extreme Sea Loads and Ship Strength,:" Trans. RINA, Vol. 115, 1973.

3.12 "A Statistical Method of Design of Building Structures," translation by D.E. Allen of five papers in Russian, National Research Council of Canada, Technical Translation no. 1368, Ottawa, 1969.

3.13 Mansour, A.E. et al, "Implementation of Reliability Methods to Marine Structures," Trans. SNAME, 1984.

3.14 Alpsten, G.A., "Variations in Mechanical and Cross-Sectional Properties of Steel," Tall Building Criteria and Loading, Vol. Ib, Proceedings, International Conference on Planning and Design of Tall Buildings, Lehigh University, Bethlehem, PA, Aug. 1972.

3.15 Galambos, T. and Ravindra, M.,"Properties of Steel for Use in LRFD," Journal of the Structural Division, ASCE, Vol. 104, No. ST9, Sept. 1978, 1459-1468.

3.16 Staugaitis, C.L., "Mill Sampling Techniques for the Quality Determination of Ship Steel Plate," Ship Structure Committee Report No. 141, 1962.

3.17 Basar, N.S. and Stanley, R.F., "Survey of Structural Tolerances in the United States Commercial Shipbuilding Industry," Ship Structure Committee Report No. 273, 1978.

3.18 Purlee, E.L., Leyland, W.A., Jr., and McPherson, W.E., "Economic Analysis of Tank Coatings for Tankers in Clean Service," Marine Technology, Vol. 2, No. 4, Oct. 1965.

3.19 Josefsson, A. and Lounamaa, K., "Comparative Corrosion Tests on Steel Plates Rolled from Continuously Cast Slabs and Rolled from Mold Cast Ingots," Corrosion, Vol. 26, No. 5, May 1981.

3.20 Sabelstrom, S. and Enestrom, L.E., "On the Effect of Casting Method on the Corrosion of Carbon Steel in Water," Scandinavian Journal of Metallurgy, 1976.

3.21 Bjorhoude, R., Brozzetti, J., Alpsten, G.A., and Tall, L., "Residual Stresses in Thick Welded Plates," Welding Journal, Vol. 51, No. 8, Aug. 1972.

3.22 Nagaraja, N.R. and Tall, L., "Residual Stresses in Welded Plates," Welding Journal, Vol. 40, No. 10, Oct. 1961.

3.23 Massonet, C., "Tolerances in Steel Plated Structures," IABSE Surveys, S-14/80, Aug. 1980.

3.24 Tomonaga, K., "Measured Errors on Fabrication of Kasumigaseki Building," Tall Building Criteria and Loading, Vol. Ib, Proceedings, International Conference on Planning and Designing of Tall Buildings, Lehigh University, Bethlehem, PA, Aug. 1972.

3.25 Faulkner, O., "A Review of Effective Plating for Use in the Analysis of Stiffened Plating in Bending and Compression," Journal of Ship Research, March 1975.

3.26 Caldwell, J.B., "Ultimate Longitudinal Strength," Transactions, Royal Institution of Naval Architects, Vol. 107, 1965.

4. BASIC RELIABILITY CONCEPTS BASED ON FULLY PROBABILISTIC METHODS - LEVEL 3:

4.1 Introduction - Reliability Levels:

Structural reliability is currently categorized under three different levels that depend mainly on the degree of sophistication of the analysis and the available input information. Level 3, which sometimes is referred to as the fully probabilistic approach, is the most demanding in terms of the required input information. But even if the input information is available, the analytical or numerical evaluation of the resulting integrals for estimating the probabilities of structural failure is extremely difficult. The basic concept of Level 3 reliability analysis is that a probability of failure of a structure always exists and may be calculated by integrating the joint probability density function (j.p.d.f.) of variable involved in the load and strength of the structure. The domain of integration is over the unsafe region of the variables.

Because of the difficulties in connection with determining the j.p.d.f. of the variables and in evaluating the resulting multiple integration, Level 2 reliability (semi-probabilistic approach) analysis was introduced. In this level, a reliability index, rather than a probability of failure, is introduced to assess the safety of the structure. The reliability index is connected to the probability of failure, and, under certain circumstances, the exact probability of failure may be directly obtained if the safety index is determined. For example, if the design variables are uncorrelated and normally distributed and the performance function[10] is linear, the probability of failure can be determined from the safety index using tables of the standard normal distribution function. If the variables are correlated and not normally distributed, certain transformation

---

10 The performance function is a function that contains the load and strength variables and determines the performance or the state of the structure.

(Rosenblatt transformation (1969)) can be made to obtain equivalent uncorrelated normal variables, thus, approximate probability of failure may be determined. Similarly, certain approximation can be made for nonlinear performance functions.

Originally, the safety index (Level 2) method was based on a simple mean value first order second moment analysis (MVFOSM), see for example [4.1, 4.2, 4.3].

Later Hasofer and Lind [4.4] introduced a more consistent invariant method based on first order reliability which entails expanding the performance function in a Taylor series at the most likely failure point and retaining only the first order terms.

Although Level 2 is easier to apply in practice, it is still of limited use to practitioners. Normally a designer needs factors of safety to apply in the design process such as those applied to the yield strength of the material and to the loads. This need resulted in the introduction of Level 1 reliability analysis. In this level partial safety factors are determined based on Level 2 reliability analysis. If these factors are used in a design, their cumulative effect is such that the resulting design will have a certain reliability level (i.e., a certain safety index). Thus, code developers and classification societies may determine (and specify in their codes) these partial safety factors that ensure that the resulting design will have a specified reliability level.

Level 3 reliability is discussed in this chapter. The following two chapters describe Level 2 and 1, respectively.

4.2 The Basic Problem - Level 3

Level 3 reliability is based on the direct integration of the joint probability density function (j.p.d.f.) of the random variables involved in a design. Therefore it will be called here the "Direct-Integration Method".

The probability of failure or the probability of reaching a specific limit state is determined from:

$$P_f = \int \ldots \int f_{\underline{X}}(x_1, x_2 \ldots x_n) \, dx_1 dx_2 \ldots dx_n \qquad (4.1)$$

where $f_{\underline{X}}(\cdot)$ is the joint p.d.f. of the important design random variables $X_1 \ldots X_n$. The domain of integration is over the unsafe region of a limit state associated with a structure. The limit state function may be represented as $g(x_1, x_2 \ldots x_n)$ and the corresponding unsafe region (integration domain of equation (4.1)) is given by:

$$g(x_1, x_2 \ldots x_n) \leq 0 \qquad (4.2)$$

The above general equations can be simplified for specific cases. In fact, the first basic reliability analysis started with two variables only, the strength of a member "S" and the load acting on it "Z". In this case, instead of the "n" variables described in equation (4.1), we have only two variables $X_1 = S$, $X_2 = Z$. Failure occurs when the load Z exceeds the strength S. The unsafe region is therefore

$$g(x_1, x_2) = g(s, z) = S - Z \leq 0 \qquad (4.3)$$

The probability of failure for statistically independent S and Z is then given by (see equation 1.3):

$$P_f = P[S - Z \leq 0] = \int_0^\infty F_S(z) \, f_Z(z) \, dz \qquad (4.4)$$

$$= \int_0^\infty [1 - F_Z(z)] \, f_S(z) \, dz \qquad (4.5)$$

These two convolution integrals given by equations (4.4) and (4.5) can also be determined from the general formulation for n variables given by equation (4.1). In the case of two variables S and Z, this equation reduces to:

$$P_f = \int\limits_{[(s,z):s-z\leq 0]} \int f_{S,Z}(s,z) \; ds \; dz \qquad (4.6)$$

and if S and Z are independent, then

$$P_f = \int\limits_{[(s,z):s-z\leq 0]} \int f_S(s) \; f_Z(z) \; ds \; dz \qquad (4.7)$$

from which equations (4.4) and (4.5) can be obtained.

Figure 4.1 shows graphically the pdf of S and Z. The overlap of the two curves represents a qualitative measure of the failure probability. This figure shows that a reduction of the probability of failure can be achieved by:

a.   increasing the distance between the means of the two probability density functions $f_S(s)$ and $f_Z(z)$, that is, by increasing the mean of the strength or decreasing the mean of the load.

b.   decreasing the standard deviation (or c.o.v.) of either p.d.f., that is, decreasing the uncertainty.
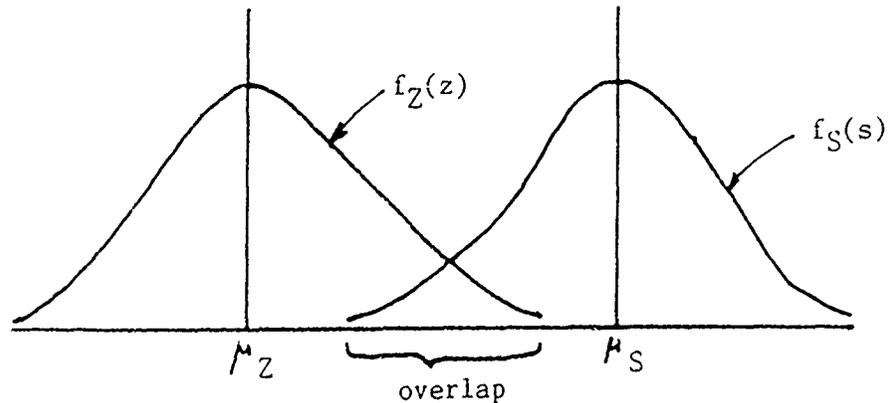
Figure 4.1.   Probability of Failure

The reliability of the structure can be measured by the probability of survival or the non-failure probability given by

$$P_s = 1 - P_f \tag{4.8}$$

4.3 The Normal Tail and Margin of Safety:

The probability of failure can be given also in terms of a margin of safety M defined as the difference between the strength and the load variables, i.e.,

$$M = g(x_1, x_2) = S - Z \tag{4.9}$$

the probability of failure is therefore

$$P_f = P[M<0] = \int_{-\infty}^{0} f_M(m)\, dm = F_M(0) \tag{4.10}$$

This is represented graphically in Fig. 4.2.
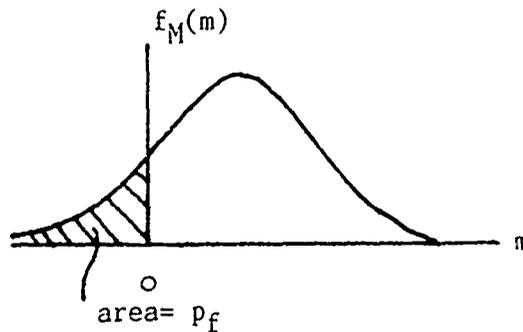
Figure 4.2. P.d.f. of the Safety Margin.

If both S and Z are normally distributed and independent, then M is also normally distributed with a mean μ_M and standard deviation σ_M given by

$$\mu_M = \mu_S - \mu_Z \tag{4.11}$$

and

$$\sigma_M^2 = \sigma_S^2 + \sigma_Z^2 \tag{4.12}$$

The standard distribution of M is obtained by subtracting the mean μ_M and dividing by the standard deviation i.e. $\frac{M - \mu_M}{\sigma_M}$. This standard normal variable has a zero mean and a unit standard deviation, i.e., N(0,1). Equation (4.10) then yields

$$p_f = F_M(0) = \Phi\left(\frac{-\mu_M}{\sigma_M}\right) = 1 - \Phi(\beta) \tag{4.13}$$

where $\quad \beta \equiv \dfrac{\mu_M}{\sigma_M}$

is called the reliability or safety index. Note that the probability of failure decreases as the safety index β increases.

In this particular simple example of independent normally distributed variables the probability of failure can be exactly determined from β and β is given by

$$\beta = \frac{\mu_M}{\sigma_M} = \frac{\mu_S - \mu_Z}{\sqrt{\sigma_S^2 + \sigma_Z^2}} \tag{4.14}$$

and

$$p_f = \Phi(-\beta) = 1 - \Phi(\beta) \tag{4.15}$$

For example, if $\beta = 0$, $p_f = 0.50$; if $\beta = 1$, $p_f = 0.16$ and if $\beta = 3.1$, $p_f = 10^{-3}$

The relations between β and p_f for other distribution of S and Z with a margin given by equation (4.9) are plotted in section A1.2 of Appendix 1.

4.4   Probability of Failure of a Ship Hull Girder

Although level 3 reliability is usually limited in application to actual structures because of the complexity of the analysis, this level of analysis can be still applied to assess ship primary strength when the ship is considered as a beam. In order to determine the probability of failure as described in the previous sections one has first to determine the probability distribution of the total load (in

this case, the total bending moment) acting on the ship. The total bending moment consists of stillwater bending moment and the extreme wave bending moment as developed by one of the methods described earlier.

In principle, the magnitude of the stillwater bending moment is also a random variable since it is a function of the cargo distribution and the shape of the wet envelope which contains a certain amount of randomness. However, the variability in stillwat bending moment due to random factors is expected to be much less than that in the wave moment, and, may for this reason, be considered as a deterministic quantity of a certain maximum value. This maximum value may be determined from the distribution of cargo that gives the maximum permissible stillwater bending moment for the operation of the ship according to classification society rules.

Actual data on stillwater bending moment analyzed by Soares and Moan in reference [4.5] show that the normal distribution fits well the data. In this example we will consider both cases. The stillwater moment is first considered as deterministic quantity with maximum value m_O and then is considered normally distributed with mean m and standard deviation σ_S.

First let $Z_n = m_O + Y_n$ represent the extreme amplitude of the total bending moment in n- encounters, where m_O is the stillwater bending moment considered to be deterministic. Y_n is a random variable representing the extreme wave bending moment using order statistics and based on the Weibull distribution with parameters k and l as the initial distribution.

The probability density function and the distribution function of Z_n are given respectively by [4.6]:

$$\phi_{z_n}(z) = \frac{nl}{k} \left(\frac{z - m_0}{k}\right)^{l-1}$$

$$\cdot e^{-\left(\frac{z-m_0}{k}\right)^l} \cdot \left[1 - e^{-\left(\frac{z-m_0}{k}\right)^l}\right]^{n-1} \qquad z \geq m_0 \quad (4.16)$$

$$= 0 \quad \text{otherwise}$$

$$\Phi_{Z_n}(z) = \left[1 - e^{-\left(\frac{z-m_0}{k}\right)^l} \right]^n \quad z \geq m_0$$
$$= 0 \quad \text{otherwise}$$

(4.17)

The above results are extended to the case when the variability of the stillwater bending moment is not neglected. The stillwater bending moment is considered to follow a normal probability law given by

$$\phi_T(t) = \frac{1}{\sigma_s \sqrt{2\pi}} e^{-\frac{1}{2}\left(\frac{t-m}{\sigma_s}\right)^2}$$

(4.18)

where $\phi_T(t)$ is the probability density function (pdf) of the stillwater bending moment T, σ_s is its standard deviation, and m is the mean.

The extreme total bending moment Z_n is simply the sum of the stillwater bending moment and the extreme wave bending moment

$$Z_n = T + Y_n$$

(4.19)

The distribution function of Z_n is

$$\Phi_n(z) = P\{Y_n + T \leq z\}$$
$$= \iint_{\{(y_n,t) : y_n + t \leq z\}} \phi_{Y_n,T}(y_n,t) dy_n dt$$
$$= \int_0^\infty dy_n \int_{-\infty}^{z-y_n} dt \phi_{Y_n,T}(y_n,t)$$
$$= \int_0^\infty dy_n \int_{-\infty}^{z} dt' \phi_{Y_n,T}(y_n,t' - y_n)$$

(4.20)

where $\phi_{Y_n,T}(\,.\,,\,.\,)$ is the joint probability density function of the random variables Y_n and T; and the domain of integration is overall values of y_n and t such that $y_n + t \leq z$; t' is a dummy variable.

Differentiating the last equation of (4.20) with respect to "z" to get the pdf of Z_n, we get

$$\phi_{Z_n}(z) = \int_0^\infty \phi_{Y_n,T}(y_n, z - y_n) \, dy_n \qquad (4.21)$$

The stillwater bending moment T is assumed to be statistically independent of the wave bending moment Y_n. Therefore equations (4.21) and (4.20) can be written respectively in the form

$$\phi_{Z_n}(z) = \int_0^\infty \phi_{Y_n}(y) \cdot \phi_T(z - y) \, dy \qquad (4.22)$$

$$\Phi_{Z_n}(z) = \int_0^\infty dy \int_{-\infty}^z \phi_{Y_n}(y) \cdot \phi_T(t - y) \, dt \qquad (4.23)$$

where the dummy variable y_n is changed to y and t' to t for simplicity of notation.

Using the Weibull distribution as an initial distribution for Y_n and equation (4.18) in (4.22) and (4.23), we obtain

$$\phi_{Z_n}(z) = \frac{nl}{k} \cdot \frac{1}{\sigma_t \sqrt{2\pi}} \int_0^\infty (y/k)^{l-1} \cdot e^{-(y/k)^l - \frac{1}{2}\left(\frac{z-y-m}{\sigma_t}\right)^2}$$
$$\cdot [1 - e^{-(y/k)^l}]^{n-1} dy \qquad (4.24)$$

and

$$\Phi_{Z_n}(z) = \frac{nl}{k} \cdot \frac{1}{\sigma_t \sqrt{2\pi}} \int_0^\infty (y/k)^{l-1} \cdot e^{-(y/k)^l}$$
$$\cdot [1 - e^{-(y/k)^l}]^{n-1} \cdot \int_{-\infty}^z e^{-\frac{1}{2}\left(\frac{t-y-m}{\sigma_t}\right)^2} dt\, dy \qquad (4.25)$$

The safety R is represented by the ratio of the strength to the extreme bending moment, $R = S/Z_n$. The probability law of R can be determined from the probability laws of both S and Z_n. If statistical independence is assumed between the extreme total bending moment Z_n and the strength S, then the probability density and distribution functions of R are given respectively by

$$f_R(r) = \int_0^{+\infty} \phi_{Z_n}(z) \cdot f_S(rz) z \, dz \qquad (4.26)$$

116

$$F_R(r) = \int_0^{+\infty} \phi_{z_n}(z) \cdot F_S(rz) dz \qquad (4.27)$$

Integrating equation (4.27) by parts and noticing that the probability of failure p_f is

$$p_f = P[R \leq 1] = F_R(1) \qquad (4.28)$$

p_f can be written either in the form (see also equations (4.4) and (4.5))

$$p_f = \int_0^{+\infty} \phi_{z_n}(z) F_S(z) dz \qquad (4.29)$$

or

$$p_f = 1 - \int_0^{+\infty} \Phi_{z_n}(z) f_S(z) dz \qquad (4.30)$$

The strength S is assumed to be normally distributed with mean $= \mu$ and standard deviation $= \sigma$. Its probability density function is given by

$$f_S(s) = \frac{1}{\sigma\sqrt{2\pi}} {}^{-\frac{1}{2}\left(\frac{s-\mu}{\sigma}\right)^2} \qquad (4.31)$$

and the corresponding distribution function is

$$F_S(s) = \int_{-\infty}^{+s} f_S(s) ds = \Psi_S\left(\frac{s-\mu}{\sigma}\right) \qquad (4.32)$$

where Ψ_S (.) is the standard normal function tabulated in many statistics books.

Two cases will be considered next. First, the case when the stillwater bending moment is regarded to be deterministic of value m_o. Using equation (4.17) for $\Phi_{z_n}(z)$ and equation (4.31) for $f_S(z)$ in equation (4.30), and noticing that $z \geq m_0$, the probability of failure can be written in the form

117

$$p_f = 1 - \frac{1}{\sigma\sqrt{2\pi}} \int_{m_0}^{\infty} [1 - e^{-(z-m_0/k)^l}]^n \cdot e^{-\frac{1}{2}\left(\frac{z-\mu}{\sigma}\right)^2} dz \qquad (4.33)$$

Equation (4.33) is a function of n; i.e., the probability of failure is dependent on the number of encounters or the length of time the ship is underway (see Fig. 4.3). It should be noticed that as n → ∞,

$$[1 - e^{-(z-m_0/k)^l}]^n \to 0 \text{ and } p_f \to 1$$

that is to say, as the ship encounters wave loads for an infinitely long time, failure will eventually occur with probability equal to 1.
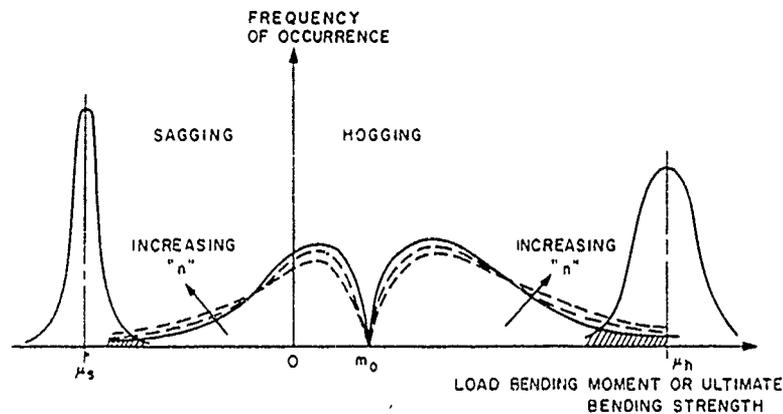
Figure 4.3.   Probability of failure under extreme bending moment

A closed-form solution of equation (4.33) in its general form is not possible. It is best at this point to specialize in the short- and long-term analyses individually.

For short term, (Rayleigh initial distribution) $l = 2$ and $k = \sqrt{E}$, [11] and assuming, for the moment, $n = 1$, equation (4.33) becomes

$$p_f|_{n-1} = \left[1 - \Psi\left(\frac{\mu - m_0}{\sigma}\right)\right] + \frac{1}{\sqrt{2(\sigma/\sqrt{E})^2 + 1}}$$

$$\cdot e^{-\frac{[(\mu - m_0)/\sqrt{E}]^2}{2(\sigma/\sqrt{E})^2 + 1}} \cdot \Psi\left(\frac{\mu - m_0}{\sigma\sqrt{2(\sigma/\sqrt{E})^2 + 1}}\right) \qquad (4.34)$$

$$= p_f^{st} + p_f^{w} \simeq p_f^{w}$$

---

[11] $E = 2E = 2 \times \text{mean square of the process.}$

For long term exponential distribution, $\ell = 1$ and $k = \hat{\lambda}$, and letting $n = 1$, equation (4.33) becomes

$$p_f\big|_{n=1} = \left[1 - \Psi\left(\frac{\mu - m_0}{\sigma}\right)\right]$$
$$+ e^{-\frac{\mu - m_0}{\lambda} + \frac{\sigma^2}{2\lambda^2}} \cdot \Psi\left(\frac{\mu - m_0}{\sigma} - \frac{\sigma}{\lambda}\right) \qquad (4.35)$$
$$= p_f{}^{\prime\prime} + p_f{}^{\prime\prime\prime} \simeq p_f{}^{\prime\prime\prime}$$

where $\Psi(\;\cdot\;)$ indicates the standard normal distribution function of $(\cdot)$.

We now return to the second case where the stillwater bending moment is assumed to be a random variable that follows a normal distribution with mean m and standard deviation σ_s. Substituting in equation (4.29) for ϕ_{Z_n} from equation (4.24) and $F_S(z)$ from equation (4.32), the probability of failure in this case is given by

$$p_f = \frac{nl}{k} \cdot \frac{1}{\sigma_s \sqrt{2\pi}} \int_0^{+\infty} \int_0^{+\infty} (y/k)^{l-1}$$
$$\cdot e^{-(y/k)^l - \frac{1}{2}\left(\frac{z - y - m}{\sigma_s}\right)^2} \cdot [1 - e^{-(y/k)}]^{n-1} dy$$
$$\cdot \Psi[(z - \mu)/\sigma] dz$$
$$(4.36)$$

For short term, $\ell = 2$ and $k = \sqrt{E}$, and letting $n = 1$, equation (4.36) reduces to

$$p_f\big|_{n=1} = (1/\sigma_s)\sqrt{2/\pi E} \int_0^\infty \int_0^\infty \Psi[(z - \mu)/\sigma] \cdot (y/\sqrt{E})$$
$$\cdot e^{-(y/\sqrt{E})^2 - \frac{1}{2}\left(\frac{z - y - m}{\sigma_s}\right)^2} dy\, dz \qquad (4.37)$$

For long term, $\ell = 1$ and $k = \hat{\lambda}$, and letting $n = 1$, equation (4.36) becomes

$$p_f|_{n=1} = (1/\lambda)e^{(\sigma_s^2+2\lambda m)/2\lambda^2}\int_0^\infty e^{-z/\lambda}$$

$$\cdot \Psi\left(\frac{z-m}{\sigma_s} - \frac{\sigma_s}{\lambda}\right)\cdot\Psi\left(\frac{z-\mu}{\sigma}\right) dz \qquad (4.38)$$

where equation (4.38) can be further reduced by letting $\sigma_S = 0$ and equating it to equation (4.35) with $m_0 = m$. If the first term in (4.35) representing the probability of failure under stillwater bending moment is neglected, then

$$\int_0^\infty e^{-z/\lambda}\Psi\left(\frac{z-\mu}{\sigma}\right)\cdot\Psi\left(\frac{z-m}{\sigma_s} - \frac{\sigma_s}{\lambda}\right) dz$$

$$= \lambda e^{-\frac{\mu}{\lambda}+\frac{\sigma^2}{2\lambda^2}}\cdot\Psi\left(\frac{\mu-m}{\sigma} - \frac{\sigma}{\lambda}\right) \qquad (4.39)$$

The equality in equation (4.39) holds if

$$\Psi\left(\frac{z-m}{\sigma_s} - \frac{\sigma_s}{\lambda}\right) \simeq 1.0$$

in the relevant range of z. This leads to the condition

$$\mu - m \geq \frac{\sigma_s^2}{\lambda} + 4.0(\sigma_s + \sigma) \qquad (4.40)$$

Using equation (4.39) in equation (4.38) yields

$$p_f|_{n=1} \simeq \Psi\left(\frac{\mu-m}{\sigma} - \frac{\sigma}{\lambda}\right)e^{\frac{\sigma_s^2+2\lambda m+\sigma^2}{2\lambda^2}-\frac{\mu}{\lambda}} \qquad (4.41)$$

For the more general case when n >1, Bernoulli trials may be assumed, and the total probability of failure, p_f, can be written in the form

$$P_f = 1 - [\ 1 - P_f|_{n=1}\ ]^n \qquad (4.42)$$

Equation (4.42) is applicable for both short and long terms, and also for deterministic and random stillwater bending moment.

It should be noted that several values may be assumed, in the case of deterministic stillwater moment, m_o , over different periods of the life of the ship, if a long-term analysis is considered. The corresponding values of n and the probabilities of failure during these periods can then be calculated. Since different values of m_0 correspond to mutually exclusive events, the total probability of failure is equal to the sum of probabilities of failure. In this way an allowance can be made for discrete variation of m_0 .

Although the derivation of the probability of failure for a ship as given above seems to be complicated, the final results are not. Equations (4.34) and (4.35) for a deterministic stillwater moment are simple algebraic equations that can be easily used to calculate p_f for a given set of values for the variables. For the case of a random stillwater bending moment, equation (4.41) for the long- term analysis gives a simple means for calculating p_f . Equation (4.37) which gives p_f for a random stillwater moment under stationary condition (short- term) is not simplified further since these conditions are unrealistic from a practical point of view. In the short-term analysis (e.g. a storm condition) it is more appropriate to consider a deterministic constant value of the stillwater moment rather than a random one, therefore, equation (4.34) is more appropriate to use. Finally, equation (4.42) may be used to calculate p_f for values of n larger than one. It should be noted that this equation may give large errors if n is very large, and, in this case numerical integration may be necessary. Numerical examples of the use of the derived equations for p_f will be given later (Chapter 10).

Notice that, in principle, the hull girder may fail in hogging or sagging mode (see figure 4.3). Since these two events are mutually exclusive events, i.e., the hull can be either in a sagging or a hogging mode, then the total probability of failure is the sum of the two

individual failure probabilities provided that the distributions are determined separately. In practical application, however, the total probability of failure is controlled by the direction of the stillwater bending moment (just as in the deterministic approach). Thus if the stillwater bending moment is a hogging moment, the total probability of failure is simply equal to the probability of failure in that mode since the probability of failure in the sagging mode will generally be very small. Some naval vessels however, may deviate from this rule.

REFERENCES

4.1 Cornell, C.A., "A Probability-based Structural Code," ACI Journal, Dec. 1969.

4.2 Mansour, A.E., "Approximate Probabilistic Method of Calculating Ship Longitudinal Strength," Journal of Ship Research SNAME, Vol. 18, No. 3, Sept. 1974, p. 203.

4.3 Ang, A. H.-S. and Cornell, C.A., "Reliability Bases of Structural Safety and Design," Journal of Structural Division, ASCE, Vol. 100, No. ST9, Nov. 1974.

4.4 Hasofer, A.M. and Lind, N.C., "Exact and Invariant Second Moment Code Format," Journal of the Engineering Mechanics Division, ASCE, Vol. 100, No. EMI, Feb. 1974, p. 111.

4.5 Soares, C.G. and Moan, T., "Statistical Analysis of Stillwater Bending Moments and Shear Forces in Tankers, Ore and Bulk Carriers," Proceedings, Third Iberoamerican Congress of Naval Engineering, Madrid, 1982.

4.6 Mansour, A.E., "Methods of Computing the Probability of Failure under Extreme Values of Bending Moment," Journal of Ship Research, Vol. 16, No. 2, June 1972.

5. LEVEL 2 RELIABILITY ANALYSIS

As mentioned in Chapter IV, Level 3 reliability analysis can be very difficult to apply in practice. The two main reasons for this is the lack of information to determine the joint probability density function of the design variables and the difficulty associated with the evaluation of the resulting multiple integrals. For these reasons, Level 2 reliability was developed. In Level 2, the safety index concept which was first introduced by Cornell [5.1] in 1969, was further developed by several researchers. In the next few sections, the development of Level 2 reliability will be presented starting with the simple safety index concept, followed by several improvements of the concept.

5.1 The Mean-Value First-Order Second-Moment (MVFOSM) Method :

If Z is a random variable representing the load and S is a random variable representing the strength, then the safety margin as defined previously is:

$$M = S - Z \qquad (5.1)$$

Failure occurs when the total applied load Z exceeds the ultimate capacity S, that is, when the margin M is negative. Therefore, the probability of failure pf is

$$pf \quad = \quad P[M \leq 0] \quad = \quad F_M(0) \qquad (5.2)$$

For statistically independent load Z and strength S, the mean μ_m and variance σ_m^2 of the margin are given by

$$\mu_m = \mu_s - \mu_z$$
$$\sigma_m^2 = \sigma_s^2 + \sigma_z^2 \qquad (5.3)$$

The standardized margin G, which has a zero mean and a unit standard deviation, can be written as

$$G = \frac{M - \mu_m}{\sigma_m} \qquad (5.4)$$

Failure occurs (or a limit state is reached) when $M \leq 0$ so that equation (5.2) can be written as

$$P_f = F_M (0) = F_G \left(\frac{-\mu_m}{\sigma_m} \right) = F_G (-\beta) \qquad (5.5)$$

where $\beta = \mu_m/\sigma_m =$ safety index, which is the inverse of the coefficient of variation of the safety margin.

If the distribution function $F_G (.)$ is known, then the exact probability of failure associated with the safety index can be determined.[12] But even for unknown or unspecified distribution function $F_G (.)$, there will be a corresponding though unspecified probability of failure for each value of β. Thus β may be taken as a safety measure as is the case in the MVFOSM method.

The foregoing results can be generalized as follows. Define a limit state (or performance) function $g(.)$ as

$$M = g (x_1, x_2 \cdots x_n) \qquad (5.6)$$

where x_i are the applied and strength parameters considered as random variables, and the limit state function $g(.)$ is a function that relates these variables for the limit state of interest (serviceability or ultimate state). The limit state is reached when:

$$M = g (x_1, x_2 \cdots x_n) \leq 0 \qquad (5.7)$$

Notice that the above equation is the same as the integration domain in the Level 3 reliability (see equation (4.2)). The limit state function can be expanded using Taylor's series, and if only the first order terms are retained, we get

$$
\begin{aligned}
g(x_1, x_2, \ldots x_n) &\simeq g(x_1^*, x_2^* \ldots x_n^*) \\
&+ \sum_i (x_i - x_i^*) \left(\frac{\partial g}{\partial x_i} \right)_{x^*}
\end{aligned}
\qquad (5.8)
$$

---

[12] See section A1.2 of Appendix 1 for the relationship between ß and the probability of failure for several distributions.

where x_i^* is the linearization point, and the partial derivatives are evaluated at that point. In the MVFOSM method the linearization point is set at the mean values ($\bar{x}_1, \bar{x}_2 \cdots \cdots \bar{x}_n$).

The mean and variance of M are then approximated by

$$\mu_m \simeq g(\bar{x}_1, \bar{x}_2, \dots \bar{x}_n) \tag{5.9}$$

$$\sigma_m^2 \simeq \sum_i \sum_j \left(\frac{\partial g}{\partial x_i}\right)_{\bar{x}_i} \left(\frac{\partial g}{\partial x_j}\right)_{\bar{x}_j} \rho_{x_i x_j} \sigma_{x_i} \sigma_{x_j} \tag{5.10}$$

where $\rho_{x_i x_j}$ is the correlation coefficient and the subscripts $\bar{x}_i$ and $\bar{x}_j$ denote evaluation of the partial derivatives at the mean point.

The accuracy of equations (5.9) and (5.10) depends on the effect of neglecting the higher-order terms in equation (5.8).

If the variables x_i are statistically uncorrelated, then (5.9) remains unchanged but (5.10) becomes

$$\sigma_m^2 \simeq \sum_i \left(\frac{\partial g}{\partial x_i}\right)_{\bar{x}_i}^2 \sigma_{x_i}^2 \tag{5.11}$$

As an example, if the margin M is represented by the variables S an Z only, that is

$$M = g(x_1, x_2) = g(S, Z) = S - Z$$

then applying equation (5.9) and (5.11) for determining the mean and variance, one immediately obtains identical results as given by equations (5.3). Equations (5.2) and (5.5) follow accordingly. This method is called the MVFOSM method because the linearization of the limit state function takes place at the mean value (MV); only the first-order (FO) terms are retained in Taylor series expansion, and up to the second moment (SM) of the random variables (means and

126

variances) are used in the reliability measure rather than their full probability distributions.

A geometric interpretation of the safety margin M = S - Z will be useful particularly for the discussio.: of the Hasofer Lind reliability index which will be presented later. First we notice that M $>$ 0 represents a safe state or region, M $<$ 0 represents failure state and M = 0 represents a limit state or failure surface (or line in the case of two variables). The standard or "reduced" variates of S and Z can be written as

$$S' = \frac{S - \mu_S}{\sigma_S} \quad ; \quad Z' = \frac{Z - \mu_Z}{\sigma_Z}$$

Therefore, the limit state function M = 0 can be written in the space of reduced variates as:

$$M = \sigma_S S' - \sigma_Z Z' + \mu_S - \mu_Z = 0$$

which is a straight line shown in Fig. (5.1).
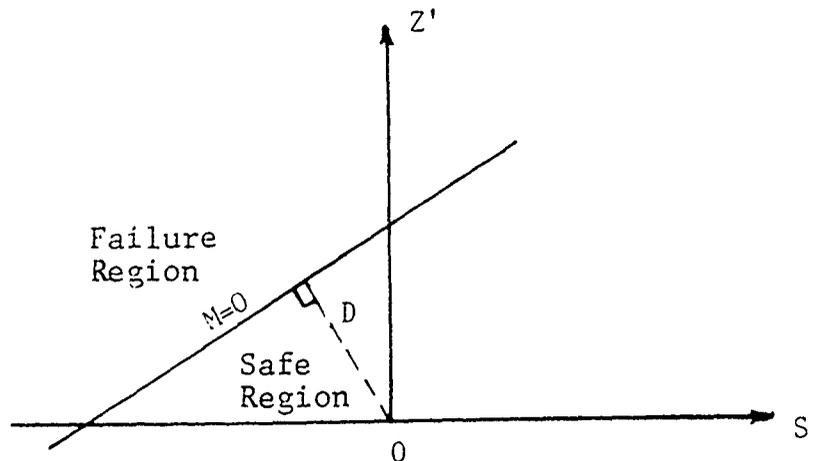
Figure 5.1. Limit State Function in the Space of Reduced Variates

The region on one side of the straight line which contains the origin "0" represents the safe state (M $>$ 0) and the other region represents the failure state (M $<$ 0). Thus the distance from the origin to the line M = 0 can be used as a measure of reliability. In

127

fact, from geometry, the minimum distance "D" shown on Figure 5.1 is given by

$$D = \frac{\mu_s - \mu_z}{\sqrt{\sigma_s^2 + \sigma_z^2}}$$

Notice that D is equal to the safety index β for the case of the normal variates and linear limit state function discussed earlier, i.e., for this case

$$\beta = D = \frac{\mu_m}{\sigma_m} = \frac{\mu_s - \mu_z}{\sqrt{\sigma_s^2 + \sigma_z^2}}$$

and the probability of failure is thus

$$p_f = \Phi(-D)$$

5.2 Improvements to the Mean Value First Order Second Moment Reliability Index:

The MVFOSM method described previously has three basic shortcomings:

First, if g(.) is nonlinear and the linearization takes place at the mean values of $\mathcal{X}_i$, errors may be introduced at increasing distance from the linearization points by neglecting higher-order terms.

Second, the method fails to be invariant to different equivalent formulations of the same problem. In effect this means that the safety index β depends on how the limit state equation is formulated. For example if the M is set to be a nonlinear function of S and Z such as

$$M = S^2 - Z^2$$

128

then $P_f = F_M(0)$, still given as before by equation (5.5); however, when μ_m and σ_m are computed from (5.9) and (5.11) and substituted in

$$\beta = \frac{\mu_m}{\sigma_m} \qquad (5.12)$$

the following β is obtained

$$\beta = \frac{\mu_s^2 - \mu_z^2}{\left[4\mu_s^2 \sigma_s^2 + 4\mu_z^2 \sigma_z^2 \right]^{0.5}} \qquad (5.13)$$

which is different from the β obtained when M is taken as M = S - Z, even though the criterion of failure is still given by equation (5.5).

Third, in the MVFOSM method the safety index β can be related to a probability of failure in cases when the variables x_i are normally distributed [and when the function g(.) is linear in x_i]. It is known that wave bending moments in ships follow a Weibull or exponential distribution. Thus, one of the improvements in an advanced method over the MVFOSM method would be to include such distribution information   (see section 5.2.2).

5.2.1 The Hasofer/Lind Index:

The first two shortcomings discussed previously are avoided by using a procedure usually attributed to Hasofer and Lind [5.2]. Instead of expanding Taylor's series about the mean value point, which causes the invariance problem, the linearization point is taken at some point on the failure surface. On the failure surface, the limit state function g(.) and its derivatives are independent of how the problem is formulated.

In the Hasofer/Lind procedure, the load and resistance variables, x_i, are transformed to reduced (standardized) variables with zero mean and unit variance by

129

$$y_i = \frac{x_i - \bar{x}_i}{\sigma_{x_i}} \qquad (5.14)$$

The Hasofer/Lind reliability index is defined as the shortest distance from the origin to the failure surface in the reduced space. This point is found by solving the following set of equations

$$G(y_1^*, y_2^*, \dots y_n^*) = 0 \qquad (5.15)$$

$$y_i^* = -\alpha_i^* \beta \qquad (5.16)$$

$$\alpha_i^* = \frac{\left(\frac{\partial G}{\partial y_i}\right)_{y_i^*}}{\sqrt{\sum_i \left(\frac{\partial G}{\partial y_i}\right)^2_{y_i^*}}} \qquad (5.17)$$

G(.) is the failure surface in the reduced space, and y_i^* are coordinates of the point closest to the origin in the reduced space (the checking point). All partial derivatives are evaluated at the checking point. In effect, this procedure is equivalent to linearizing the limit state function in the reduced variables space at the checking point and computing β associated with that point.

In the original space, the checking point or the most likely failure point is obtained from

$$\begin{aligned} x_i^* &= \bar{x}_i + \sigma_{x_i} y_i^* \\ &= \bar{x}_i - \sigma_{x_i} \alpha_i \beta \end{aligned} \qquad (5.18)$$

In general, for a linear limit state function, the Hasofer/Lind method will yield the same result for β as the MVFOSM method. For nonlinear limit state functions, this method yields a safety index β which is invariant to the formulation of the performance function. To illustrate this point, the following example is considered (see ref. [5.11]).

130

<u>Example:</u>

Suppose that a simple beam is subjected to random loading that produces a maximum stress with a mean value μ_z = 20,000 p.s.i. and a standard deviation σ_2 = 2,500 p.s.i. The beam is made of material of mean yield strength μ_s = 30,000 p.s.i. and a standard deviation σ_s = 3,000 p.s.i.

The following three limit state functions are considered. They all represent failure of the beam and, therefore, should yield the same value of the safety index if the method used to determine the safety index is consistent (i.e., invariant to the formulation of the limit state function). The three limit state functions are:

$$M_1 = S - Z \tag{5.19}$$

$$M_2 = S^2 - Z^2 \tag{5.20}$$

$$M_3 = \alpha S - \alpha Z \tag{5.21}$$

The strength S and the load Z are independent; S is normally distributed and Z follows a Weibull distribution. The safety index β will be computed for each of these three limit state functions using, first, the mean value first order second moment method (MVFOSM) then the Hasofar-Lind method. Notice that the first limit state function (5.19) is linear; the other two are non-linear.

<u>a. The Mean Value First Order Second Moment Method</u>

In this method the safety index β is defined as (see equation 5.12)

$$\beta = \frac{\mu_m}{\sigma_m} \tag{5.22}$$

Where the margin means μ_m and its standard deviation σ_m are computed for each limit state function using equations (5.9) and (5.11), respectively. The resulting β's for the three limit state equations (5.19) to (5.21) are:

131

$$\beta_1 = \frac{\mu_s - \mu_z}{(\sigma_s^2 + \sigma_z^2)^{1/2}} \qquad (5.23)$$

$$\beta_2 = \frac{\mu_s^2 - \mu_z^2}{(4\mu_s^2 \sigma_s^2 + 4\mu_z^2 \sigma_z^2)^{1/2}} \qquad (5.24)$$

$$\beta_3 = \frac{\log \mu_s - \log \mu_z}{(\sigma_s^2/\mu_s^2 + \sigma_z^2/\mu_z^2)^{1/2}} \qquad (5.25)$$

Substituting in the above equations the values of μ_s, μ_z, σ_s and σ_z, one obtains the following results:

$$\beta_1 = 2.5607 \qquad \beta_2 = 2.4282 \qquad \beta_3 = 2.5329$$

The values of β's are not the same indicating that the MVFOSM method is not invariant to mechanically equivalent formulation of the same problem. Notice that we have not made use of the distribution information (S: Normal and Z: Weibull) in the calculation of the β values.

If the probability of failure for each limit state is to computed from $p_{f_i} = \Phi(-\beta_i)$, an error will result since this equation is valid only if all the random variables are normally distributed and the limit state function is linear. Let us, however, use this equation in order to compare the results with those obtained by a more accurate method described in the next section entitled "Inclusion of Distribution Information". Using,

$$p_{f_i} = \Phi(-\beta_i) \qquad (5.26)$$

the following values are obtained:

$$p_{f_1} = 0.005223 \qquad p_{f_2} = 0.007574 \qquad p_{f_3} = 0.005655$$

b.   The Hasofar/Lind Method

Equations (5.15) to (5.17) are applied to determine the β value for each limit state function according to this method. For the non-linear limit state functions, these equations must be solved iteratively since the evaluation of the derivatives required for calculating β will depend on the coordinates of the most likely failure point which are unknown. An iterative procedure would be simply to assume values for the most likely failure point (e.g. mean values of the variables) and to evaluate the derivatives of the limit state function at that point as required by equation (5.17). Equation (5.17) is then substituted in (5.16) to obtain a set of coordinates y_i^* which will be a function of the unknown β. These coordinates are substituted in (5.15) and the resulting equation is solved for β. The obtained β is then used in (5.16) to obtain a new set of coordinates of the most likely failure point. The procedure is repeated until convergence is obtained. The procedure will be described in more detail in Chapter 6.

The procedure was applied to the limit state equations given by (5.19) to (5.21). The linear limit state function (5.19) did not require any iteration; the second limit state function given by (5.20) required five iterations and the last one (5.21) required seven. The following results were obtained:

$$\beta_1 = 2.5607 \qquad \beta_2 = 2.5607 \qquad \beta_3 = 2.5607$$

These results indicate that the value of β is invariant to the formulation of the problem. They also show that the MVFOSM method gives identical result to the Hasofar/Lind method if the limit state function is linear (see β_1 obtained using the MVFOSM method).

The probability of failure calculated from equation (5.26) for all β values according to Hasofar/Lind method is 0.005223. Here again no use is made of the distribution information given in the problem. Therefore, unless all variables are normally distributed (which is not the case in this problem), the probability of failure computed using equation (5.26) will be in error. More accurate values of the probability of failure will be given for this example after the next section.

5.2.2 Inclusion of Distribution Information:

The third and final refinement of the advanced method over the MVFOSM method is that the information about the variable distributions (if known) can be incorporated in the computation of the safety index and the corresponding probability of failure. In the MVFOSM method the index β can be related to the probability of failure in cases when the variables x_i are normally distributed [and when g(.) is linear in x_i]. This relation is given by [see equation (5.5)]

$$P_f = \Phi (-\beta) \tag{5.27}$$

where Φ is the standard normal distribution function. In order to be able to use equation (5.18), approximately, in the case of non-normal variables, a transformation of these variables into equivalent normal variables is necessary prior to each iteration in the solution of equations (5.15) to (5.17).

The tail of the distribution is usually the location where most of the contribution to the probability of failure comes from. It is, therefore, better to fit the normal distribution to the tail of the non-normal distribution at the linearization point x_i^*, which is where failure is most likely to occur (that is, minimum β). This is the basic idea of the Rackwitz/Fiessler method as given in [5.3].

By requiring that the cumulative distributions and the probability density functions of both the actual distribution and the normal distribution be equal at the linearization point, one can determine the mean μ'_x and standard deviation σ'_x of the equivalent normal variable, that is

$$F_x(x^*) = \Phi \left(\frac{x^* - \mu'_x}{\sigma'_x} \right) \tag{5.28}$$

and

$$f_x(x^*) = \frac{1}{\sqrt{2\pi}\,\sigma_x'} \exp\left[-\frac{1}{2}\left(\frac{x^* - \mu_x'}{\sigma_x'}\right)^2\right]$$

$$= \frac{1}{\sigma_x'}\,\varphi\{\Phi^{-1}[F_x(x^*)]\} \qquad (5.29)$$

where $\varphi(.)$ is the standard normal probability density.

Since we are concerned with finding μ_x' and σ_x', the parameters of the equivalent normal distribution once fitted at the linearization point, we can solve for them as follows:

$$\sigma_x' = \frac{\varphi\{\Phi^{-1}[F_x(x^*)]\}}{f_x(x^*)} \qquad (5.30)$$

$$\mu_x' = x^* - \Phi^{-1}[F_x(x^*)]\sigma_x' \qquad (5.31)$$

This process is illustrated in Fig. 5.2.

Since the linearization point x_i^*, changes with each iteration, σ_{x_i}' and μ_{x_i}' must be calculated for each iteration also. These values are then used in equations (5.15) through (5.17) as before. Note that if the iteration is performed in reduced space, then distribution transformation into reduced space has to be performed in each step.
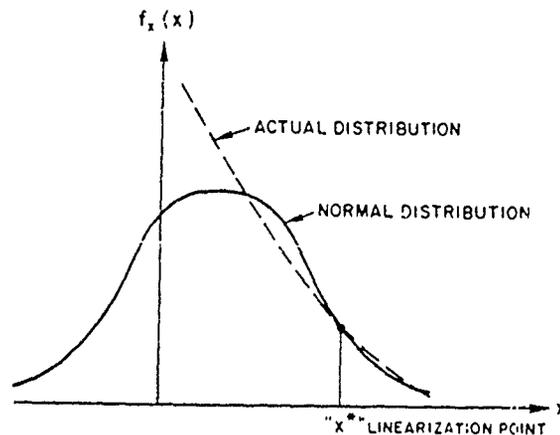
Figure 5.2. Equivalent Normal Distribution at Linearization Point

In our simple beam example discussed earlier, the load follows a Weibull distribution while the strength was assumed to be normal. An equivalent normal distribution can be determined for the load using the procedure described above. The three limit state functions describing the failure of the beam are given by equations (5.19) to (5.21). If one uses Hasofar/Lind method, then one must determine the parameters of the equivalent normal distribution in each step of the iteration procedure for the nonlinear limit state functions (equations 5.20 and 5.21). The results for the β values including the distribution information are [5.11]:

$$\beta_1 = 2.6690 \qquad \beta_2 = 2.6690 \qquad \beta_3 = 2.6690$$

and the corresponding probability of failure is $p_f = \Phi(-\beta) = 0.003802$.

The results indicate that the β values are invariant to the problem formulation since $\beta_1 = \beta_2 = \beta_3$. They also show that, in this case, inclusion of the distribution information increased the β value from 2.5607 to 2.6690 and decreased the corresponding probablity of failure from 0.005223 to 0.003802. The values of β and p_f determined including the distribution information are more accurate. It should be emphasized that inclusion of the distribution information does not always yield larger safety index.

5.3   Correlated Random Variables

So far, the random variables X_i have been assumed to be uncorrelated.   If the variables are normal and correlated through a correlation matrix [C], a transformation to a set of uncorrelated variables Y_i is possible.   The new uncorrelated set can be then used in the procedure developed earlier for computing the safety index β .

The set of uncorrelated variables Y_i can be determined from the reduced variables X_i' using the orthogonal transformation

$$\underline{Y} = \underline{T}^t \underline{X}' \tag{5.32}$$

where $\underline{T}$ is an orthogonal transformation matrix and the superscript t indicates the transpose.   The transformation matrix $\underline{T}$ is such that

$$\underline{T}^t \left[C' \right] \underline{T} = \left[\lambda \right] \tag{5.33}$$

where $[C']$ is the covariance matrix of $\underline{X}$ and $[\lambda]$ is a diagonal matrix of the eigen values of $[C']$.   The covariance matrix of $\underline{X}'$ is to be related to the covariances of the original variables $\underline{X}$ through

$$[C'] = \begin{bmatrix} 1 & \rho_{12} & \rho_{13} & \text{-----} & \rho_{1n} \\ \rho_{21} & 1 & \rho_{23} & \text{-----} & \rho_{2n} \\ \rho_{31} & \rho_{32} & 1 & \text{-------} & \rho_{3n} \\ \text{-----} & \text{-----} & \text{-----} & \text{-----} & \text{-----} \\ \rho_{n1} & \rho_{n2} & \rho_{n3} & \text{------} & 1 \end{bmatrix} \qquad (5.34)$$

where

$$\rho_{ij} = \frac{\text{cov}\left(x_i, x_j\right)}{\sigma_{x_i}\, \sigma_{x_j}} \qquad (5.35)$$

The safety index β can be then calculated from equations (5.15 to 5.17) for the new uncorrelated set $\underline{Y}$ or more directly from (see reference [5.4]):

$$\beta = \frac{-\,\underline{G}^{*t}\,\underline{X}'^{*}}{\sqrt{\underline{G}^{*t}\left[C'\right]\underline{G}^{*}}} \qquad (5.36)$$

where $\underline{G}^{*}$ is a gradient vector evaluated at the linearization point (most likely failure point), i.e.,

$$\underline{G}^{*t} = \left(\begin{array}{ccccc} \dfrac{\partial g}{\partial x'_1} & \dfrac{\partial g}{\partial x'_2} & \cdots\cdots & \dfrac{\partial g}{\partial x'_n} \end{array}\right) * \qquad (5.37)$$

Notice that since $\underline{T}$ is orthogonal, $\left(\underline{T}^{-1} = \underline{T}^{t}\right)$ and from (5.32):

$$\underline{X}' = \underline{T}\,\underline{Y} \qquad (5.38)$$

and

$$\underline{X} = \left[\sigma_x\right]\underline{X}' + \underline{\mu}_x \qquad (5.39)$$

where

$$\left[\sigma_x\right] = \begin{bmatrix} \sigma_{x_1} & & & 0 \\ & \sigma_{x_2} & & \\ & & \ddots & \\ 0 & & & \sigma_{x_n} \end{bmatrix}$$

138

$$
\text{and} \quad \underline{\mu}_x = \left\{ \begin{array}{c} \mu_{x_1} \\ \mu_{x_2} \\ \vdots \\ \mu_{x_n} \end{array} \right\}
$$

It can be shown (see reference [5.5]) that the eigen values $[\lambda]$ are also the variances of the variables Y_i .

For linear performance function g(x) represented by

$$
g(\underline{X}) = a_0 + \sum_i a_i X_i \tag{5.40}
$$

equation (5.36) for calculating β is reduced to:

$$
\beta = \frac{a_0 + \sum_{i=1}^{n} a_i \mu_{x_i}}{\sqrt{\sum_{i=1}^{n} \sum_{j=1}^{n} a_i a_j \rho_{ij} \sigma_{x_i} \sigma_{x_j}}}
$$

where ρ_{ij} is given by (5.35).

The above procedure is valid for transforming a set of correlated normal variables to a set of uncorrelated normal variables. If the variables are non-normal, then as an approximation, equivalent normal variables can be determined as described previously under "Inclusion of the distribution information". A more exact procedure would be to use Rosenblatt transformation [5.6] which requires information on the joint probability density function of $\underline{X}$. The degree of approximation is illustrated through a numerical example given in [5.5] and is usually small.

5.4   Trend of the Reliability Index for Eighteen Ships

First order reliability was used to calculate the safety indices for eighteen existing ships. A linear performance function was used, therefore the MVFOSM method yields the same results as the Hasofer/Lind method. The margin "M" or performance function for the primary strength is simply given by:

$$M = S - Z$$

where S is the hull resistance given in terms of moment capacity and Z is the total applied bending moment which consists of stillwater and wave moments. A worldwide mission profile was chosen for sixteen of the ships as indicated in figure 5.3. The remaining two ships have mission profiles shown in references [5.7, 5.8]. Three of the eighteen ships are large tankers (190,000 dwt or larger), nine are small to medium-size tankers (26,500 to 75,500 dwt), and the rest are cargo and bulk carriers. Table 5.1 shows the general characteristics of the eighteen ships. A strip theory program was used in conjunction with Pierson-Moskowitz spectra [5.9] in order to determine the root mean square and the mean values of the wave bending moment in different sea conditions specified by their significant wave heights. Figures 5.4, 5.5 and 5.6 show these results for sixteen ships. The required results for the remaining two ships, a Mariner and a tanker, were obtained from references [5.7] and [5.8], respectively. Reference [5.10] was used in order to determine the frequency of occurrence of the different sea conditions. The mean value of the wave bending moment was then obtained from the mean values in the different sea conditions and the frequency of occurrence of these sea conditions. A typical procedure is illustrated in detail in references [5.7, 5.8]. The variance of the wave bending moment was determined using the equation:

Variance   =   Mean square - square of mean value

In the computation, the following assumptions regarding the sea description were made in order to reduce the computer cost:

(a)   Pierson-Moskowitz spectra were used (fully developed seas)

(b)   Long-crested head seas were assumed.
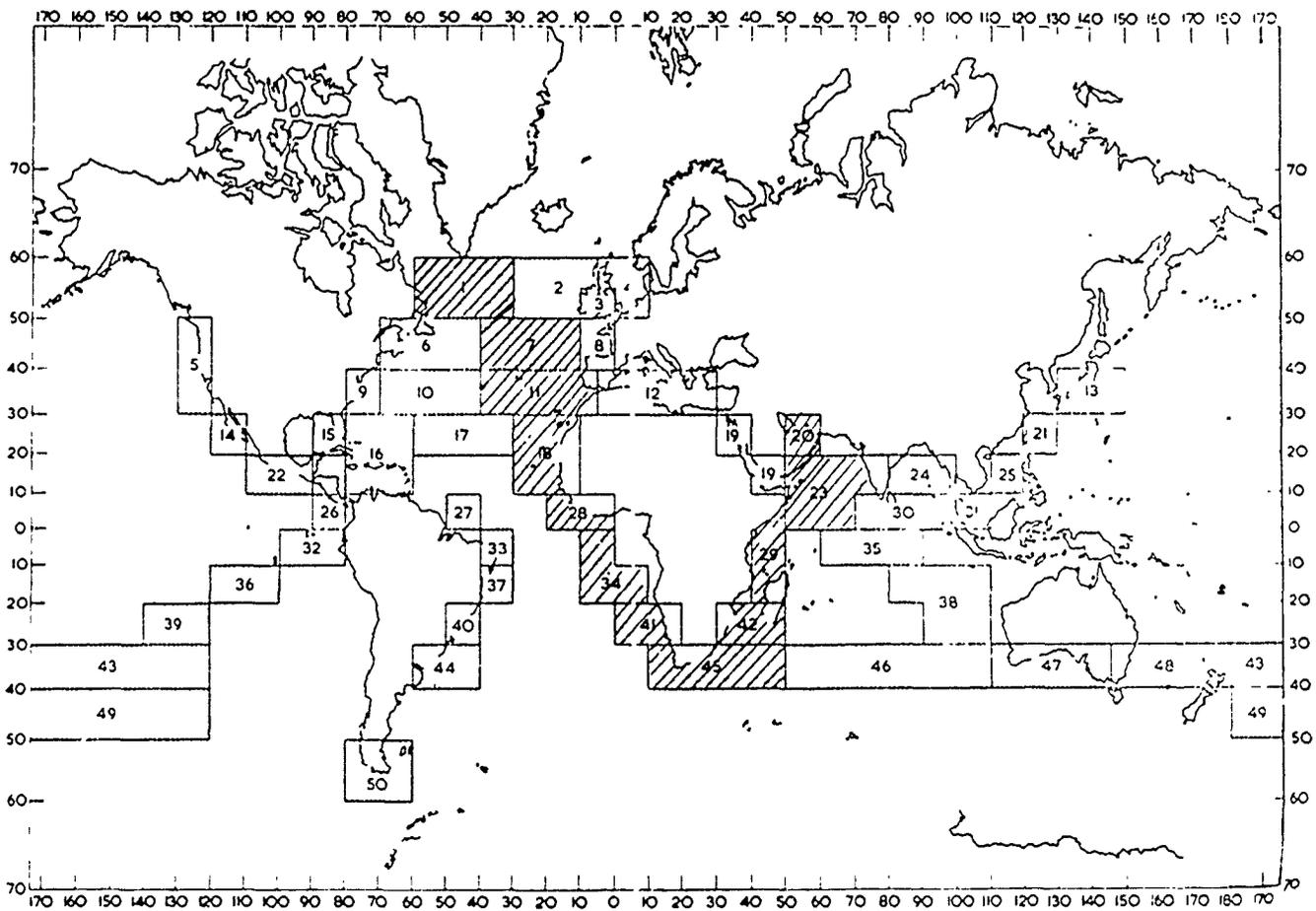
Figure 5.3.   Assumed ships' route (Figure without the indicated route
was obtained from reference [5.10])

Table 5.1. General Characteristics of Eighteen Ships.

SHIP	LBP (ft)	B (ft)	d (ft)	C_b	dwt (approx.)
Tanker No 1	1076.00	174 87	81.40	0.86	326,600
Tanker No. 2	1069.25	163.25	58.05	0.83	206,100
Tanker No. 3	1000.00	154.76	60.45	0.83	190,800
Tanker No. 4	763.00	115.99	42.01	0.77	67,900
Tanker No. 5	754.70	104.46	44.40	0.82	66,500
Tanker No. 6	754.70	105.65	44.74	0.809	63,300
Tanker No. 7	754.69	105.65	44.74	0.804	62,000
Tanker No. 9	719.10	82.50	39.15	0.786	40,970
Tanker No. 10	620.81	85.96	35.72	0.784	31,500
Tanker No. 11	594.00	74.00	33.48	0.800	26,580
Tanker No. 12*	775.00	105.50	47.00	0.831	75,500
Oil-ore carrier No. 13	700.65	98.43	40.70	0.774	45,100
Cargo ship No. 14	528.50	75.99	29.88	0.615	13,400
Cargo ship No. 15	520.00	75.00	31.42	0.573	12,750
Cargo ship No. 16*	528.00	76.00	29.80	0.6098	13,400
Bulk carrier No. 17	800 00	106.00	44.55	0.840	74,200
Bulk carrier No. 18	656.20	93.80	42 63	0.793	48,550
Tanker No. 8	693.75	97.00	39.17	0.775	46,650

* Tanker and mariner ships from references[5.7]and[5.8]respectively
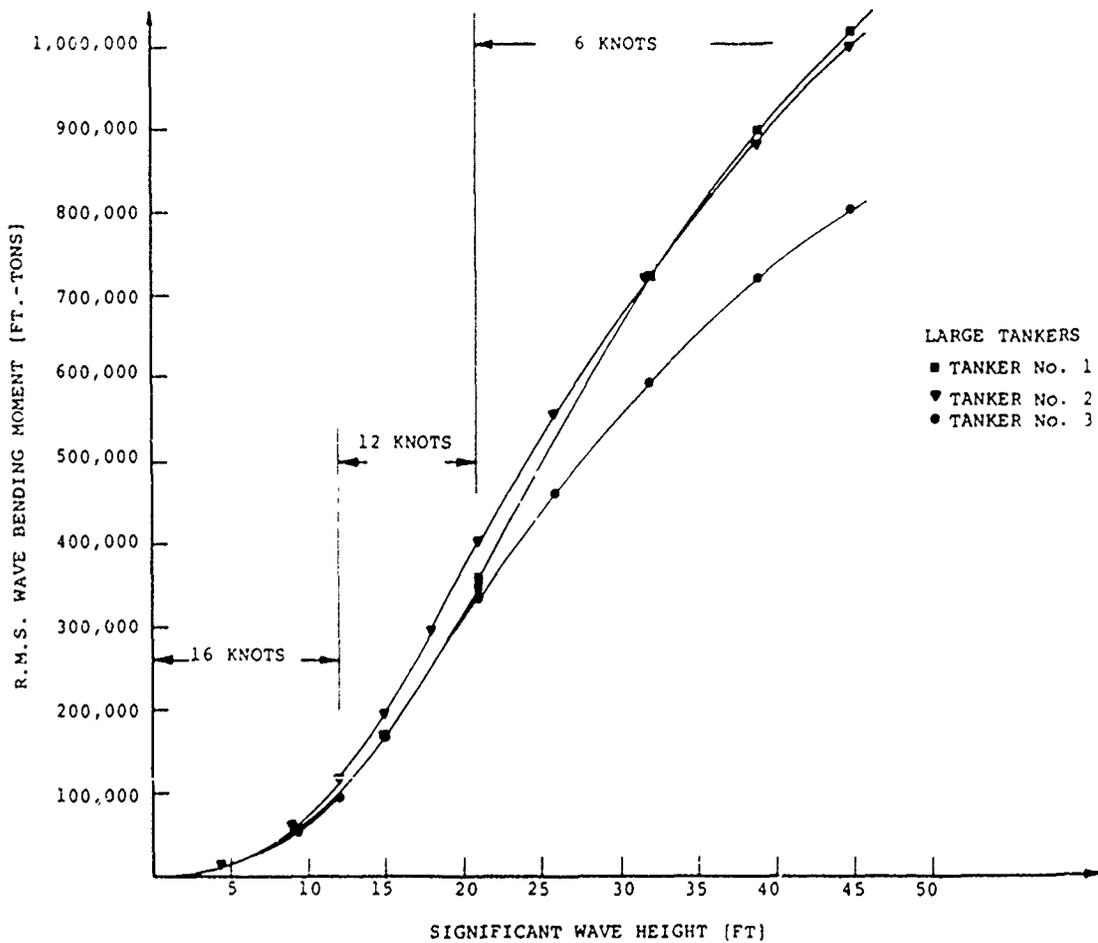
Figure 5.4. Rms of Wave Bending Moment for Three Large Tankers

142
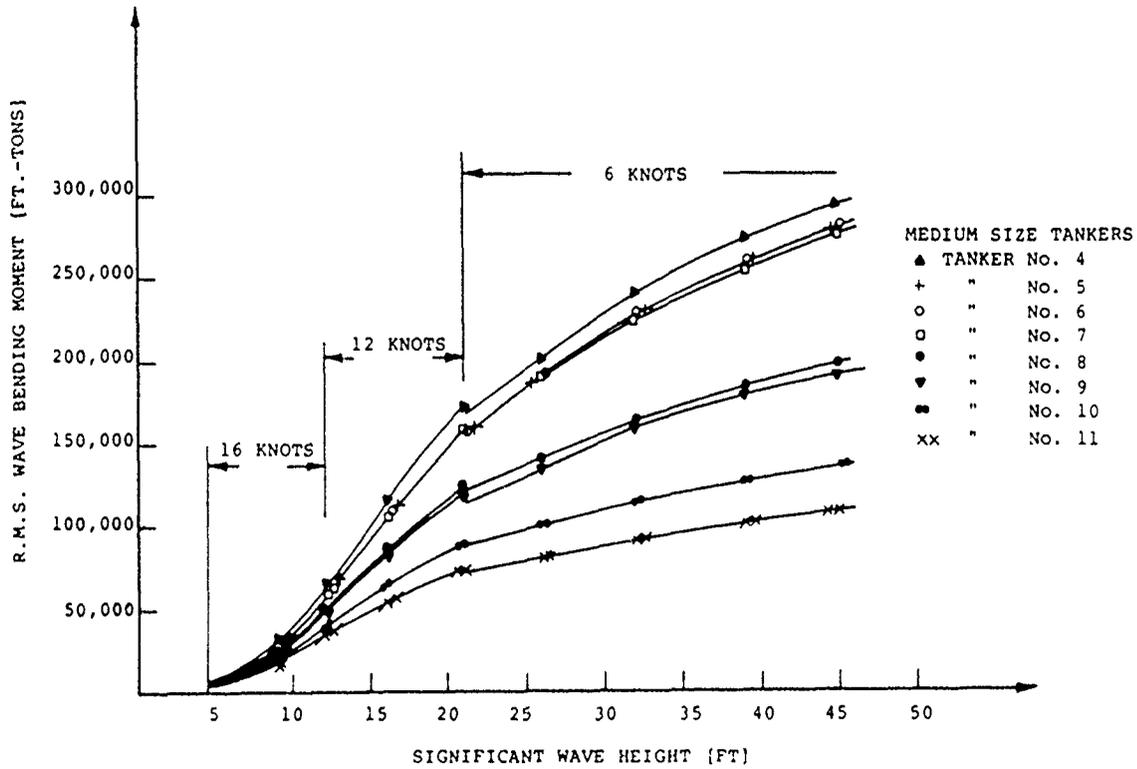
Figure 5.5. Rms of Wave Bending Moment for Eight Medium-Size Tankers
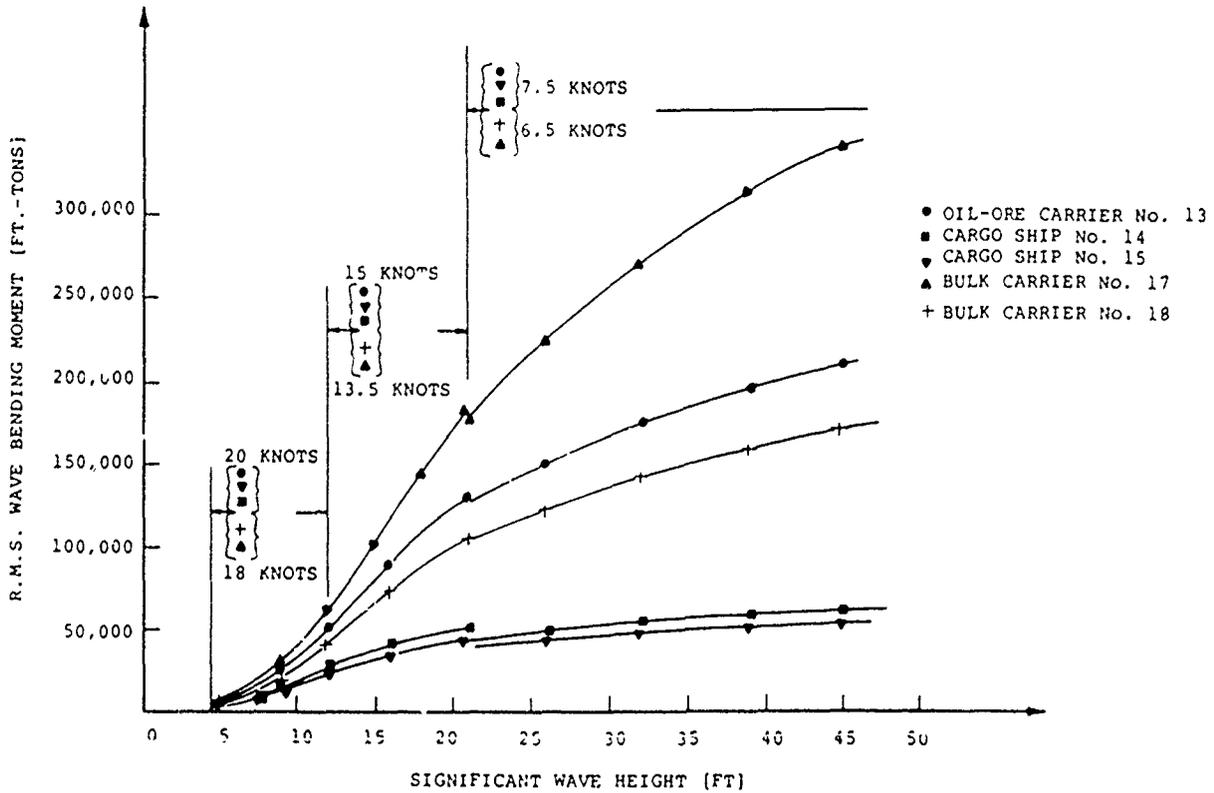
Figure 5.6. Rms of Wave Bending Moment for Cargo and Bulk Carriers

143

The strength coefficient of variation V_S was investigated next. A detailed procedure for determining this coefficient is described and applied to three ships (tanker, cargo, and frigate) in references [5.7, 5.8]. The strength coefficients of variation of these three ships were in the range of 7 to 11.3 percent. These figures include the estimated subjective and the computed objective uncertainties. The eighteen ships under consideration were assumed to have a strength coefficient of variation = 13 percent. This is rather pessimistic and is on the conservative side. The mean values of the strength, m_S were considered to be equal to the section modulus of the ship multiplied by the yield strength, taken = 30 k/sq in.

Obviously, the foregoing parameters for the eighteen ships were determined in an approximate manner. More accurate procedures can be used. However, the main objective was to provide a preliminary investigation of the order of the magnitude of the safety index β for as many ships as possible.

With these parameters determined for all the ships, the safety index is computed from the equation:

$$\beta = \frac{\theta - 1}{\sqrt{\theta^2 V_s^2 + V_z^2}}$$

where $\theta = m_s / m_z$ and V_s and V_z are c.o.v. of the strength and load, respectively.

Figure 5.7 shows the computed values of the safety index β of these ships plotted versus the length between perpendiculars. These results show a wide variation of the safety level, with β ranging from about 4 to about 6.5. There seems to be a general tendency for higher longitudinal strength safety, that is, higher β , with increased ship size.

The safety index β was also plotted versus several other parameters. Figure 5.8 shows β plotted versus the parameter

$M_S = \rho g L^2 B d$, which is proportional to the static bending moment. Only 15 ships are shown in this figure as the three large tankers 1, 2, and 3 have very large M_S values (470×10^6, 310×10^6, and 267×10^6, respectively) and would change the abscissa scale considerably. They do however follow the same general trend of the data, which is higher safety β for higher M_S. The physical significance of this figure is that designing ships on the basis of the static bending moment M_S would lead, in general, to higher safety for larger ships; that is, the static bending moment seems to overestimate the load on large ships.
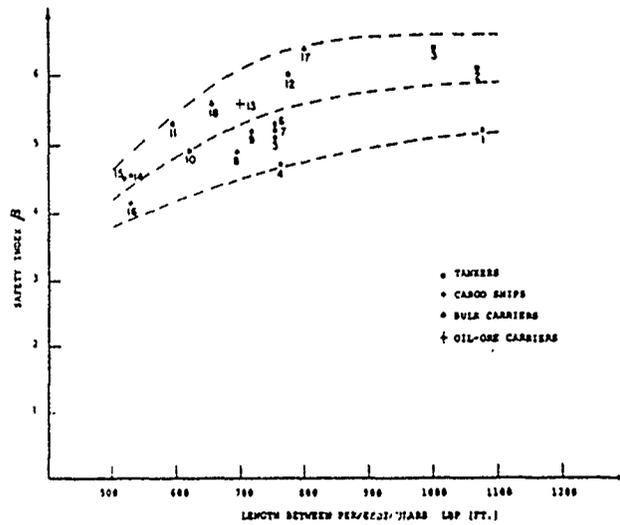
Figure 5.7. Safety index β for Eighteen Ships
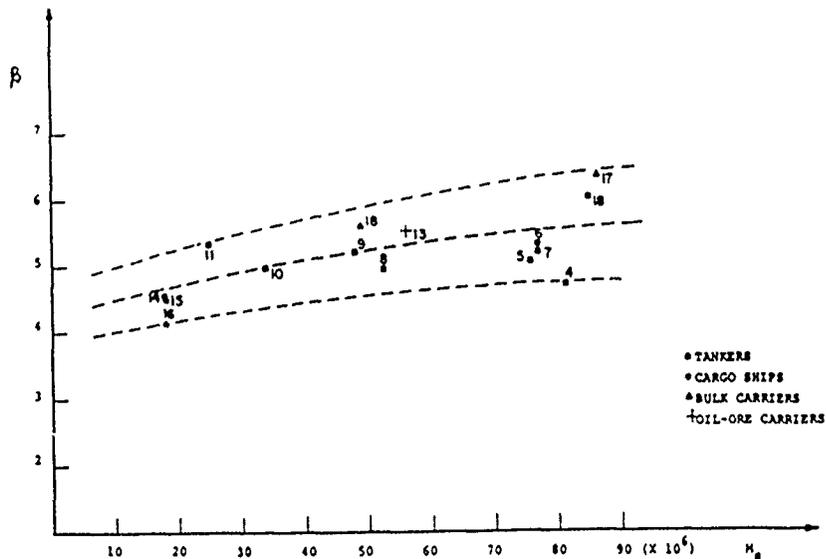
Figure 5.8. Safety Index β for Fifteen Ships

Figure 5.9 shows the computed safety index β plotted versus the parameter

$$F_s = \frac{(SM)\ \sigma_y}{\rho g\ L^2\ Bd}$$

Where (SM) is the elastic section modulus, σ_y is the yield strength, ρg is the water weight density and L, B and d are the length, beam and draft, respectively. The parameter F_s is proportional to a conventional factor of safety defined by dividing the ship strength by the static bending moment. The figure shows that some of the eighteen ships may have actually a lower safety β than the others even though F_s may indicate the opposite. This, and the scatter in the data, suggest the inadequacy of the parameter F_s as a measure of the real safety of ships. The same result was pointed out in reference [5.8] for a more specific case.
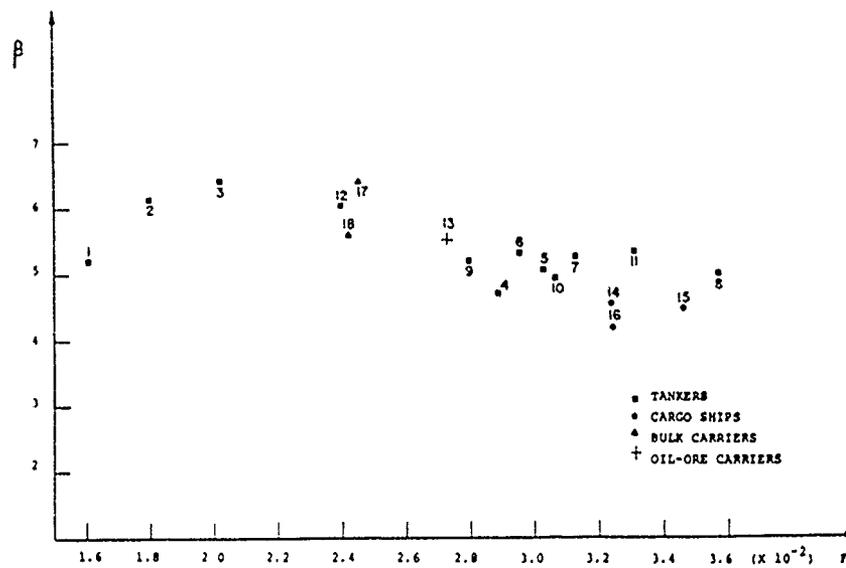
Figure 5.9. Safety Index β for Eighteen Ships

In general, the wide range of the safety level of the eighteen ships indicated by β as shown in figures 5.7, 5.8 and 5.9 could be due to several reasons. The lack of allowance, or at least the lack of uniform measure for the allowance of the uncertainties in the

146

bending moment and the strength in the traditional design procedures is a possible reason. Another reason is the possibility of inadequacy in the prediction of the wave bending moment when using the traditional static balance procedures. A third reason may be due to the slightly different rules of the different classification societies used for determining the section moduli of the ships. In addition, the variation of the actual values of the section moduli of the ships with respect to those specified by the rules is also a contributing factor. Finally, a more exact procedure for determining the parameters used in this application may lead to a slightly different range of level of safety.

5.5   Ship Safety Index Based on Non-Linear Limit State Function:

The following analysis is presented to illustrate the use of Hasofar/Lind procedure and the method of including the distribution information in calculating the safety index for a ship. The following limit state function is considered

$$g(\underline{x}) = (SM) f_y - M_{sw} - M_w \tag{5.41}$$

where

(SM)	=	minimum section modulus
f_y	=	yield strength of the material
M_{sw}	=	stillwater bending moment
M_w	=	wave bending moment

Notice that the product in the first term of (5.41) makes the limit state equation nonlinear. The limit state equation in the reduced space is

$$g(\underline{x}') = (\mu_{sm} + \sigma_{sm} (SM')) (\mu_{fy} + \sigma_{fy} f'_y) - (\mu_{sw} + \sigma_{sw} M'_{sw})$$
$$- (\mu_w + \sigma_w M'_w) = 0 \tag{5.42}$$

where the prime superscript indicates a reduced variable and μ and σ indicate the mean and standard deviation, respectively.

The derivatives required in evaluating the direction cosines (equation 5.17) are:

$$\frac{\delta g}{\delta (SM)'} \quad = \quad \sigma_{sm} (\mu_{f_y} + \sigma_{f_y} f'_y) = \sigma_{sm} f_y \qquad (5.43)$$

$$\frac{\delta g}{\delta f'_y} \quad = \quad \sigma_{f_y} (SM) \qquad (5.44)$$

$$\frac{\delta g}{\delta M'_{sw}} \quad = \quad \sigma_{sw} \qquad (5.45)$$

$$\frac{\delta g}{\delta M'_w} \quad = \quad -\sigma_w \qquad (5.46)$$

The direction cosines α_i can then be calculated from (5.17). Using these, the coordinates of the most likely failure point are calculated from (5.16) and substitute in the limit state equation in the reduced space (equation 5.15) to yield the following result:

$$(\mu_{sm} - \sigma_{sm} \alpha^*_{sm} \beta) \ (\mu_{f_y} - \sigma_{f_y} \alpha^*_{f_y} \beta) -$$
$$(\mu_{sw} - \sigma_{sw} \alpha^*_{sw} \beta) - (\mu_w - \sigma_w \alpha^*_w \beta) \ = \ 0 \qquad (5.47)$$

Equation (5.47) is to be solved for β. Notice that the α^*_i are to be evaluated at the most likely failure point, i.e., f_y and (SM) values at that point must be inserted in equations (5.43) and (5.44), respectively, when evaluating α^*_i given by equation (5.17). Since these coordinates are unknown apriori, the mean values of these variables can be used as initial values in an iterative procedure. After solving for β from (5.47), a new set of coordinates can be determined from (5.16) and used to determine a new set of α^*_i. The procedure is repeated until convergence is achieved.

The above procedure is accurate if all the random variables in the limit state function (equation 5.41) are normally distributed. However, as discussed earlier, the wave bending moment M_w follows a Weibull or an exponential distribution. In this case, the mean and standard deviation of an equivalent normal distribution must be determined in each iteration step according to equations (5.30) and (5.31) and used in equation (5.47) prior to solving for β. This

transformation will produce additional non-linearity in the limit state equation in the reduced space.

For an exponential distribution with a parameter λ, the equivalent parameters (σ^n and μ^n) of the normal distribution for the wave bending moment can be calculated from equations (5.30) and (5.31) which yield:

$$\sigma^n_{m_w} = \lambda\, e^{\frac{m^*_w}{\lambda}}\, \varphi\{\Phi^{-1}[1 - e^{-\frac{m^*_w}{\lambda}}]\} \tag{5.48}$$

and

$$\mu^n_{m_w} = m^*_w - \Phi^{-1}[1 - e^{\frac{-m^*_w}{\lambda}}]\, \sigma^n_{m_w} \tag{5.49}$$

This procedure is further illustrated by the following numerical example.

Numerical Example:

Consider a Tanker of the following characteristics:

Length = 763 ft	Beam = 125 ft	Depth = 54.5 ft
Draft = 41.33 ft	Block Coefficient = 0.805	
Displacement = 90,650 L.ton		DTW = 75,650 L.ton

The values the means (μ) and coefficients of variation (δ) of the variable in the limit state equation were determined as:

μ_{sm} = 150,441 in^2-ft	δ_{sm} = 0.09
μ_{f_y} = 18.16 t/in^2	δ_{f_y} = 0.10
μ_{sw} = 425,000 ft-ton	δ_{sw} = 0.35
$\mu_w = \lambda$ = 150,500 ft-ton	δ_w = 1.0

For the first iteration in the procedure described above the mean values were taken as the most likely failure point. The parameters for the equivalent

normal distribution for the wave bending moment can be calculated directly from (5.48) and (5.49). The derivatives and direction cosines are then calculated from equation (5.43 to 5.46) and (5.17), respectively. The resulting direction cosines are substituted in (5.47) yielding an equation in β. The first iteration solution for β is 5.95. Using the determined value of β a new set of coordinates of the most likely failure point is determined according to (5.16). The procedure is repeated and the second iteration results in a β value of 5.04. More iterations should be performed until convergence is achieved. For comparison, if the information on the wave bending moment distribution was not included, the resulting β values are 5.83 and 5.73 for the first and second iterations, respectively.

REFERENCES

5.1 Cornell, C.A., "A Probability-based Structural Code," ACI Journal, Dec. 1969.

5.2 Hasofer, A.M. and Lind, N.C., "Exact and Invariant Second Moment Format," Journal of the Engineering Mechanics Division, ASCE, Vol. 100, No. EMI, Feb. 1974, pp. 111-121.

5.3 Rackwitz, R. and Fiessler, B., "Structural Reliability under Combined Random Load Sequences," Computers and Structures, Vol. 9, 1978.

5.4 Shinozuka, M., "Basic Analysis of Structural Safety," J. of Structural Division, ASCE, Vol. 3, No. 109, March 1983.

5.5 Ang, A. H.-S. and Tang, W. H., Probability Concepts in Engineering Planning and Design, Vol. II, John Wiley & Sons, New York, 1984.

5.6 Rosenblatt, M., "Remarks on a Multivariate Transformation," Annals of Math. Stat., Vol. 23, No. 3, September 1952, pp. 470-472.

5.7 Mansour, A.E., "Probability Design Concepts in Ship Structural Safety and Reliability," Trans. SNAME, 1972.

5.8 Mansour, A.E. and Faulkner, D., "On Applying the Statistical Approach to Extreme Sea Loads and Ship Hull Strength," Trans. RINA, Vol. 115, 1973.

5.9 Pierson, W. and Moskowitz, L., "A Proposed Spectral Form for Fully Developed Wind Seas Based on the Similarity Theory of S.A. Kitaigorodskii," Journal of Geophysical Research, Vol. 69, Dec. 1964.

5.10 Hogben, N. and Lumb, F., Ocean Wave Statistics, National Physical Laboratory, Ministry of Technology, London 1967.

5.11 Skjolds, M., "An Evaluation of Different Formulations of the Reliability Index", Report for NA240B, Dept. of Naval Architecture and Offshore Engineering, University of California, Berkeley, May 6, 1988.

6. LEVEL 1 RELIABILITY ANALYSIS:

Although Level 2 is easier to apply in practice, it is still of limited use to practitioners. Normally a designer needs factors of safety to apply in the design process such as those applied to the yield strength of the material and to the loads. This need resulted in the introduction of Level 1 reliability analysis. In this level partial safety factors are determined based on Level 2 reliability analysis. If these factors are used in a design, their cumulative effect is such that the resulting design will have a certain reliability level (i.e., a certain safety index). Thus, code developers and classification societies may determine (and specify in their codes) these partial safety factors that ensure that the resulting design will have a specified reliability level. The method of determining these partial safety factors for a given safety index is discussed next:

6.1 Derivation of Partial Safety Factors from Level 2 Method:

The partial safety factors (psf) or load and resistance factors LRF are simply safety factors that are multiplied by the basic design variables in order to assure a specified reliability level β . They are usually applied to the mean values of the design variables, thus, we may write the limit state function as:

$$g \left(\Delta_1 \mu_{X_1} , \Delta_2 \mu_{X_2} , \ldots \ldots \Delta_n \mu_{X_n} \right) = 0 \tag{6.1}$$

where Δ_i are psf and μ_{x_i} are the mean values of the variables. Since equation (6.1) represents the failure surface, $\Delta_i \mu_{x_i}$ must fall on the surface, preferably, the most probable failure point, i.e.,

$$\Delta_i = \frac{x_i^*}{\mu_{x_i}} \tag{6.2}$$

In the normalized variate space (see equation (5.16)) we may write

$$x_i' {}^{*} = - \alpha_i^{*} \beta \qquad \text{where} \qquad \alpha_i^{*} = \frac{\left(\frac{\partial g}{\partial x_i'} \right)_{*}}{\sqrt{\sum_i \left[\frac{\partial g}{\partial x_i'} \right]_{*}^{2}}}$$

Thus the original variate is

$$x_i^{*} = \mu_{x_i} + \sigma_{x_i} x_i' {}^{*} = \mu_{x_i} - \alpha_i^{*} \beta \sigma_{x_i}$$

$$= \mu_{x_i} (1 - \alpha_i^{*} \beta v_{x_i}) \tag{6.3}$$

Comparing equations (6.2) and (6.3) we conclude that

$$\Delta_i = 1 - \alpha_i^{*} \beta v_{x_i} \tag{6.4}$$

Evaluation of the psf Δ_i requires evaluation of the direction cosines α_i at the design point, i.e., the most probable failure point x_i^{*}. For non-linear limit state functions, the determination of x_i^{*} requires an iterative solution. The following simple procedure may be used [6.1]:

1. Assume x_i^{*} and determine $x_i' {}^{*} = \dfrac{x_i^{*} - \mu_{x_i}}{\sigma_{x_i}}$

2. Evaluate $\left(\dfrac{\partial g}{\partial x_i'} \right)_{*}$ and α_i^{*}

3. Determine $x_i^{*} = \mu_{x_i} + \sigma_{x_i} x_i' {}^{*} = \mu_{x_i} - \alpha_i^{*} \beta \sigma_{x_i}$

4. Use the new values of x_i^{*} from step 3 again in 1 until convergence is achieved.

5. Calculate the psf from $\Delta_i = 1 - \alpha_i^{*} \beta v_{x_i}$ for a given β .

Notice that if β is not prescribed but is to be determined, then the above procedure can be modified as follows. After Step 3, follow the following steps:

4. Substitute x_i^{*} determined in Step 3 into $g(x_1^{*}, \cdots x_n^{*}) = 0$ and solve for β .

5. Using β obtained in "4" above, reevaluate $x'^{*}_{i} = - \alpha^{*}_{i} \, \beta \cdot$

6. Repeat Steps 2 to 5 until convergence is obtained.

6.1.1 Linear Performance Functions:

In this case the psf are such that

$$g \, (\, \Delta_1 \mu_{x_1}, \, \ldots \ldots \, \Delta_n \mu_{x_n} \,) = 0$$

and

$$g \, (\, \underline{x} \,) = a_0 + \sum_{i=1}^{n} a_i \, x_i$$

or

$$a_0 + \sum_{i=1}^{n} a_i \, \Delta_i \, \mu_{x_i} = 0$$

Because of linearity the partial derivatives $\dfrac{\partial g}{\partial x'_i}$ are independent of x_i, that is

$$\frac{\partial g}{\partial x'_i} = a_i \, \sigma_{x_i}$$

(since $\qquad x_i = \sigma_{x_i} x'_i + \mu_{x_i} \qquad$)

Therefore from (6.4), the psf are

$$\Delta_i = 1 - \frac{a_i \, \sigma_{x_i}}{\left[\, \sum_{i} (\, a_i \sigma_{x_i})^{2} \, \right]^{\frac{1}{2}}} \, \beta \, v_{x_i} \tag{6.5}$$

6.1.2 Example

Consider the simple linear performance function

$$M = g \, (x_1, x_2) = S - Z$$

where S represents strength and Z represents load.

In order to determine the psf for a given value of β, we first write the reduced variables as

155

$$S' = \frac{S - \mu_s}{\sigma_s} \qquad ; \qquad Z' = \frac{Z - \mu_z}{\sigma_z}$$

therefore $\quad M = S - Z = \sigma_s S' + \mu_s - \sigma_z Z' - \mu_z$

and $\qquad \dfrac{\partial M}{\partial S'} = \sigma_s \qquad ; \qquad \dfrac{\partial M}{\partial Z'} = -\sigma_z$

therefore $\quad \alpha_s = \dfrac{\sigma_s}{\left(\sigma_s^2 + \sigma_z^2 \right)^{\frac{1}{2}}}$ and $\quad \alpha_z = -\dfrac{\sigma_z}{\left(\sigma_s^2 + \sigma_z^2 \right)^{\frac{1}{2}}}$

The psf are thus:

$$\Delta_s = 1 - \alpha_s \beta v_s = 1 - \beta v_s \dfrac{\sigma_s}{\left(\sigma_s^2 + \sigma_z^2 \right)^{\frac{1}{2}}}$$

and

$$\Delta_z = 1 - \alpha_z \beta v_z = 1 + \beta v_z \dfrac{\sigma_z}{\left(\sigma_s^2 + \sigma_z^2 \right)^{\frac{1}{2}}}$$

Notice that $\Delta_s < 1$ and $\Delta_z > 1$, as expected. The determination of psf's for eighteen ships will be given in Chapter 10 of this report.

6.2 Recently Developed Reliability-Based Codes:

The procedure described above for the derivation of psf may be used to develop safety factors for use in codes. This necessitates a change in code format as well. Changing from a working stress design code to a reliability-based code is not an easy task. Complicating the procedure is the fact that there is no set method for introducing reliability into a code. The implementation of reliability theory in design codes changes from organization to organization. Even when two organizations use the same reliability-based design format, the details differ as it must for different types of structures.

It is the objective of this section to review and assess the implementation methods and use of reliability analysis in certain design codes. Specifically, work attributed to or sponsored by the American Petroleum Institute, the National Bureau of Standards, and Comite Euro-International du Beton are examined in some detail. Codes of several other organizations are also discussed and compared.

Proposed American Petroleum Institute Code Format

The work reviewed in this subsection is the proposed revision to the "API Recommended Practice for Planning, Designing and Constructing Fixed Offshore Platforms" (RP2A) which is issued by the American Petroleum Institute (API) [6.2]. API is currently sponsoring research aimed at changing the code format of RP2A from working stress design (WSD) to load and resistance factor design (LRFD), with the release of an LRFD-based RP2A for industry review and comment envisioned in the near future. Much of the information reviewed here that pertains to the proposed LRFD RP2A was obtained from references [6.3, 6.4, 6.5, 6.6].

In the currently used working stress approach, the maximum or yield stress is divided by a safety factor to obtain an allowable stress. Designs are then limited so that the maximum calculated stress under extreme operating loads does not exceed this allowable value. The basic safety checking format is of the form:

$$\frac{R}{SF} \geq D + L + W + \text{other load effects} \qquad (6.6)$$

where

R	=	nominal component strength
SF	=	safety factor
D	=	nominal gravity load effects on components
L	=	nominal live load effects on components
W	=	nominal environmental load effects on components

Presently, nominal loads are all combined with factors of 1.0, and constant safety factors of 1.67 and 1.25 are used for operating and extreme loading, respectively. Note that there is a probabilistic statement implicit in the given safety factors, in that since extreme events are by nature, rare, the associated safety factor can be reduced.

Design based on the WSD format has provided structures with high reliability without explicitly considering uncertainties and probabilistic safety descriptions. The WSD format, however, does not provide for structures with uniform reliability. The problem with WSD is that the one safety factor in equation (6.6) cannot possibly account for uncertainties in all variables, including those arising from the theories and analysis methods employed.

In the LRFD format, individual partial safety factors are calibrated according to the different component strength and loading uncertainties. The advantage of LRFD with its multiple factors is that proper weight is given to the degree of accuracy with which the various loads and resistances can be determined, resulting in a more rational procedure and a greater uniformity or reliability [6.7]. The LRFD format recommended [6.3, 6.4, 6.6] for API RP2A has the form

$$\phi_{R_i} R_i > r_D D + r_L L + r_W W + \ldots \ldots \qquad (6.7)$$

where

R_i	=	nominal strength or resistance of component i
ϕ_{R_i}	=	partial resistance factor for component i
D	=	nominal gravity or dead load effect
γ_D	=	load factor for dead load
L	=	nominal live load effect
γ_L	=	load factor for live load
W	=	nominal environmental force effects with prescribed return period (usually 100 years)
γ_W	=	load factor for environmental load

158

Each resistance factor ϕ_{R_i} is calculated as the product of two terms representing component strength uncertainty (ϕ_i) and system consequence (ϕ_s), that is

$$\phi_{R_i} = \phi_i \times \phi_s \qquad (6.8)$$

The component resistance factor ϕ_i takes into account variations in material properties, strengths of fabricated components, and errors in mathematical predictions of strengths (due to underlying assumptions and approximations).

The system consequence factor reflects the relative consequence on the entire structure of the failure of a component. This, in turn, depends on whether the component was redundant or not, brittle or ductile, main or secondary, etc. In addition, the system consequence factor covers any other social and economic impacts of platform failure.

The load factors γ are also calculated as the product of two terms. These terms correspond to uncertainty in the load intensity (γ_i) and uncertainty in the analysis required to calculate the load effects (γ_A). We then have,

$$\gamma \text{ Load effects } = (\gamma \text{ intensity}) \times (\gamma \text{ analysis}) = \gamma_i \wedge \gamma_A \qquad (6.9)$$

In an actual design, the ϕ - and γ-values would be tabulated, and the design equation would be checked for all specified load combinations. Actual derivations of load and resistance factors for proposed use in API RP2A are explained in [6.8, 6.6].

Comite Euro-International Du Beton Code Format

The code discussed in this section is a joint effort of the Comite Euro- International Du Beton (CEB), sometimes referred to as the European Committee for Concrete, and the International Federation

for Prestressing (FIP). The design code is entitled "CEB-FIP Model Code for Concrete Structures" [6.9]. Information explaining the use of probability in the CEB Model Code can be found in references [6.9, 6.10]. It should be mentioned that CEB has been studying structural reliability for many years and, for this reason, is considered a leader in the field of such code development.

The CEB design checking equation has the general form

$$R_d \geq S_d \qquad (6.10)$$

where R_d is design resistance and S_d the design load effect.

The CEB code is a Level-I code, meaning appropriate levels of structural reliability and provided by the specification of a number of partial safety factors. The code development uses the Level-II method whenever possible to assess appropriate values for the safety factors used in the code. The code considers both ultimate and serviceability limit states.

The format used for defining the design load effects, following CEB notation, is

$$S_d = S\left\{\gamma_g G + \gamma_p P + \gamma_q\left[Q_{1k} + \sum_{i>1}(\psi_{0i}Q_{ik})\right]\right\} \qquad (6.11)$$

where

S_d	=	design (factored) load effects
$S\{\ldots\}$	=	refers to load effects due to all loads in brackets (that is, it is not a numerical operator)
G	=	nominal dead load
P	=	a representative value of prestressing force
Q_{1k}	=	characteristic value of principal variable load
Q_{ik}	=	characteristic value of other less important variable loads

$\gamma_g, \gamma_p, \gamma_q =$ partial safety coefficients

$\psi_{oi} =$ load combination factor

The CEB Model Code uses, in general, two types of partial safety factors, γ_m and γ_f, related to the strength and the loads [as in equation (6.11)], respectively.

γf is the partial safety factor which is multiplied by the characteristic action (load) value, F_k, to obtain the design load effect, that is

$$\text{Design action} = \gamma_f \, F_K \qquad (6.12)$$

γ_f is a function of three factors: γ_{f_1}, γ_{f_2}, and γ_{f_3}.

γ_{f_1} accounts for variations in load magnitude from the specified characteristic (that is, nominal) value. It is analogous to the γ_i factor used by API.

γ_{f_2} reflects the reduced probability of combinations of loads all acting at their respective characteristic values. γ_{f_2} is referred to as a load combination factor. [γ_{f_2} is written as ψ_{oi} in equation (6.11).]

γ_{f_3} accounts for the structural response to loads and the possibility of redistribution of the load effects. γ_{f_3} reflects inaccuracies in predicting load effects, and is a function of the construction material, design and construction process, and the limit state under consideration. In equation (6.11), γ_f -values are written as γ_g, γ_p, and γ_q since the γ_f -value differs for each load. Also in the CEB nomenclature, F refers to a load in general while Q refers to a variable load.

γ_m, the second type of partial safety factor, is used in the structural analysis by dividing the characteristic strength of a section (f_K) by γ_m to obtain the design strength of the section, that is

$$\text{design strength} = f_k / \gamma_m \quad (6.13)$$

γ_m, accounts for any uncertainties in the predicted strength of the materials used to build the structure. Specifically, it reflects any variation in the strength of materials from the specified characteristic value; any variation in the strength of the materials from that predicted by control test specimens; possible flaws in the structural material due to either the construction process or the material itself; dimensional inaccuracies of the material; and the effect on the predicted structural resistance of inaccurate values of material strengths. The γ_m partial safety factor is the CEB version of a resistance factor such as ϕ_{Ri} used by the API.

There is an additional factor in the CEB code - the modifying factor γ_n. This factor takes account of the inherent structural behavior, that is, of parts of the structure which can fail without warning, and the consequences corresponding to this failure. γ_n is broken down into two factors:

γ_{n1} reflects the type of failure (ductile or brittle)

γ_{n2} accounts for the consequences of failure

γ_n is not used explicitly, but only modify γ_m or γ_f-values. In [6.8, 6.6], actual values of some of these factors are presented.

National Bureau of Standards Code Format

The design code referred to in this section is American National Standard A58, Building Code Requirements for Minimum Design Loads in Buildings and Other Structures, published by the National Bureau of Standards (NBS). Much of the information dealing with the use of reliability in this Code was obtained from "Development of a Probability Based Load Criterion for American National Standards A58"[6.11].

The format recommended for use in the A58 Standard is a combination of the CEB-FIP format described previously, and the load and resistance factor design format proposed by Ravindra and Galambos [6.12]. Since the CEB format has already been described , The LRFD format of Ravindra and Galambos is explained together with how the two formats are combined in an optimum way. Information concerning the LRFD method of Ravindra and Galambos can be found accompanying reference [6.12] in the September 1978 Journal of the Structural Division of the American Society of Civil Engineers.

The LRFD criterion can be expressed as

$$\phi R_n \geq \gamma_E(\gamma_D C_D D_m + \gamma_L C_L L_m + \gamma_W C_W W_m + . .) \tag{6.14}$$

where

ϕ =   resistance factor

R_n =   nominal resistance

$\gamma_{E,D,L,W}$ =   partial safety coefficients

$C_{D,L,W}$ =   deterministic influence coefficients

D_m, L_m, W_m =   mean dead, live, wind loads, etc.

The terms representing the load effects (that is, the right-hand side of equation (6.14) are defined as follows:

C_D, C_L, C_W are deterministic influence coefficients that transform the load intensities to load effects.

γ_E is partial safety factor representing the uncertainties in structural analysis. It accounts for approximations and assumptions in the underlying theory and is somewhat analogous to the γ_A load analysis factor used by API.

$\gamma_D, \gamma_L, \gamma_W$ account for the degree of uncertainty inherent in the determinations of the loads D_m, L_m and W_m.

163

The major difference between the CEB and the Ravindra and Galambos load representations is that the live load is a separate case with its own load factor in equation (6.14), but is a multiple of the maximum load $\psi_{0i} Q_{iK}$ in equation (6.11). NBS believes that the computational simplification realized by expressing the arbitrary-point-in-time load as per equation (6.11) will outweigh certain advantages due to the increased accuracy of having a separate loading case in equation (6.14).

The CEB format is not considered advantageous in other ways, however. If the methodology of the CEB format was applied to a situation combining dead, live, wind, and snow loads, a total of 32 loading combinations is possible [6.11]. On the other hand, the LRFD method has only four combinations to be considered. Since it is desired to explicitly state just a small number of fundamental load combinations for simplification in design, the LRFD method is the optimum choice in this regard.

The NBS format for load factors is therefore a combination of the best features of two methods. However, the NBS format for load factors follows LRFD much more closely than it follows the CEB format. The CEB method is used such as in the case of factored arbitrary-point-in-time loads, mentioned earlier when comparing the two methods. The design equations for load effects take the LRFD form, however, as it is simpler to use in the design process. Also, from now on, the NBS format will be referred to as LRFD.

In the case of resistance factors, ϕ , the LRFD method is used and not the CEB concept of using material partial safety factors, γ_m . This factor is closely analogous to the factor used by API. The resistance factor, always less than unity, accounts for variability in member strengths due to assumptions used in determining the resistance equations, variability of material properties, variability of dimensions, uncertainties in fabrication, and importance of the component to the structure.

In summary, the format recommended by NBS is

$$\phi R_n \geq \sum_{i=1}^{n} \gamma_i Q_i \qquad (6.15)$$

NBS has tabulated many γ-values for various materials and loading combinations, and has outlined a procedure to determine values consistent with an organization's objectives. These values of γ and the ϕ determination procedure are discussed in references [6.8, 6.6].

Code Formats of Other Organizations

The American Institute of Steel Construction (AISC) released, in September 1983, a proposed design code entitled, "LRFD Specification for Structural Steel Buildings," for the purpose of industry trial and review. The code is based directly upon the LRFD method of Ravindra and Galambos which represents a prototype for a new generation of structural design codes. The implications of the proposed change of the AISC code to the LRFD format will be felt by other organizations which use this code in some way. The American Petroleum Institute is one such organization as the current working stress based API RP2A adopts several of its design provisions through explicit reference to the AISC Code.

Another organization which uses an LRFD procedure is the American Concrete Institute (ACI). In fact, ACI introduced split load factors to North American design codes back in 1963. The history of the use of reliability in the ACI Code is presented by MacGregor [6.10]. In [6.8], the ACI method of deriving partial safety factors is discussed.

The National Building Code of Canada [6.13] uses the following split load factor format for load effects:

Load effects $= S\{\gamma_D D + \psi(\gamma_L L + \gamma_w W + \gamma_T T)\}$ (6.16)

165

where

$S\{...\}$ =   load effects due to all loads in the brackets (that is, it is not a numerical operator)

$\gamma_D, \gamma_L, ...$ =   load factors

$D, L, ...$ =   are the loads (dead, live, . . .)

ψ =   load combination probability factor equal to 1.0, 0.7, or 0.6 depending upon whether one, two, or three loads are included within the brackets

γ_D =   1.25 if D acts in the same way as the loads in the brackets and is 0.85 if D acts in the opposite way.

The load factors account for variations in the load effects due to model errors and uncertainties in the structural analysis. The ψ term reflects the reduced probability of maximum dead, live, wind, etc., loads acting simultaneously. Note that if both live and wind loads were present, equation (6.16) would design using the entire wind effect (depending, of course, upon the chosen load factor). The LRFD procedure and the CEB method are both considered more flexible than the format of equation (6.16).

Another organization which uses a split load and resistance factor format in a design code is Det norske Veritas (DnV) in their "Rules for the Design, Construction, and Inspection of Offshore Structures" [6.14], although the partial factors are not reliability based. The format is somewhat similar to other European codes such as CEB. The general format for ultimate limit state design is

$$\frac{R_k}{\gamma_m} \frac{1}{K} \geq S\{\sum F_i \gamma_{fi}\} \qquad (6.17)$$

where

R_k =   characteristic resistance (strength)

$$\gamma_m \quad = \quad \text{material factor}$$
$$R_k/\gamma_m \quad = \quad \text{design resistance}$$
$$K \quad = \quad \text{factor depending on type of resistance}$$
$$S\left\{\sum F_i \gamma_{fi}\right\} = \quad \text{design loading effect}$$
$$F_i \quad = \quad \text{characteristic load}$$
$$\gamma_{fi} \quad = \quad \text{load factor}$$

The material presented in the foregoing subsections gives a description of the major reliability-based code formats. There are, of course, other formats, but these are generally variations of the formats given herein. The format used more widely than any other, at least in North America, is the load and resistance factor design method. Whether it be the procedure proposed by Ravindra and Galambos, or a variation thereof, LRFD seems to be a good practical way of incorporating reliability into a design code. Most importantly, an LRFD-based code is the simplest to use in practice, and this may be a major consideration.

Deciding upon a design code format which allows for the implementation of reliability methods is a complicated process. However, once an organization has chosen a reliability-based code format, the work is by no means over. A load and resistance factor design code format may look quite impressive, but is of very little use without the corresponding load and resistance factors.

Generally, the first step in deriving partial load and resistance factors for use in the LRFD format is to calibrate these factors based on the reliability level inherent in the current design criteria. From this inherent reliability, a corresponding target reliability level β is established. Using this target value, load and resistance partial safety factors are determined for the new format such that they minimize the deviation of the calculated reliability from the target level over the range of design applications. Although the target reliability level cannot be reached for all design conditions, it should be achieved on the average. Reference [6.8] gives more detailed

information on this procedure as well as some typical values of the load and resistance factors corresponding to code formats developed by the various organizations discussed previously. Examples and additional information can be found in [6.8, 6.6, 6.3, 6.9, 6.11, 6.15].

REFERENCES

6.1 Ang, A. H.-S. and Tang, W.H., Probability Concepts in Engineering Planning and Design, Vol. II, John Wiley & Sons, New York, 1984.

6.2 API Recommended Practice for Planning, Designing and Constructing Fixed Offshore Platforms, API RP2A, American Petroleum Institute, 12th ed., Dallas, Texas, 1981.

6.3 Moses, F., "Guidelines for Calibrating API RP2A for Reliability-Based Design," API Prac. Project 80-22, American Petroleum Institute, Oct. 1981.

6.4 Moses, F. and Russel, L., "Applicability of Reliability Analysis in Offshore Design Practice," API Prac. Project 79-22, American Petroleum Institute, June 1980.

6.5 Anzari, T. and Bryant, L.M., "Comparison of a Limit State Design Code with API RP2A," Proceedings, 14th Annual Offshore Technology Conference, Reprint OTC 4191, Houston, TX, May 1982, pp. 291-306.

6.6 Moses, F., "Utilizing a Reliability-based API RP2A Format," Final Report, API Prac. Project 82-22, American Petroleum Institute, Nov. 1983.

6.7 Galambos, T.V. and Ravindra, M.K., "Tentative Load and Resistance Factor Design Criteria for Steel Beam Columns," Research Report No. 32, Civil Engineering Department, Washington University, St. Louis, MO, Feb. 1976.

6.8 Mansour, A.E., Harding, S. and Ziegelman, C., "Implementation of Reliability Methods to Marine Structures," First Annual Report ABS, University of California, Berkeley, Jan. 1983.

6.9 Common Unified Rules for Different Types of Construction and Material, Bulletin D'Information No. 124E, Comite Euro-International du Beton, Paris, April 1978.

6.10 First Order Reliability Concepts for Design Codes, Bulletin D'Information No. 112, Comite Euro-International du Beton, Munich, July 1976.

6.11 Ellingwood, B., Galambos, T., MacGregor, J. and Cornell, C., "Development of a Probability Based Load Criterion for American National Standard A58," NBS Special Publication SP-577, National Bureau of Standards, Washington, DC, June 1980.

6.12 Ravindra, M. and Galambos, T., "Load and Resistance Factor Design for Steel," Journal of the Structural Division, ASCE, Vol. 104, No. ST9, Sept. 1978, pp. 1355-1370.

6.13 National Building Code of Canada, National Research Council of Canada, Ottawa, 1977.

6.14 Rules for the Design, Construction and Inspection of Offshore Structures, Det norske Veritas, Oslo, 1977 (and Appendices).

6.15 Yura, J., Galambos, T. and Ravindra, M., "The Bending Resistance of Steel Beams," Journal of the Structural Division, ASCE, Vol. 104, No. ST9, Sept. 1978, pp. 1355-1370.

(THIS PAGE INTENTIONALLY LEFT BLANK)

7. SIMULATION AND THE MONTE CARLO METHOD:

7.1 General Concept

In general, simulation is a technique for conducting experiments in a laboratory or on a digital computer in order to model the behavior of a system. Usually simulation models result in "simulated" data that must be treated statistically in order to predict the future behavior of the system. In this broad sense, simulation has been used as a predictive tool for economic systems, business environment, war games and management games.

The name "Monte Carlo method" was introduced in 1944 by von Newmann and Ulam as a code name for their secret work on neutron diffusion problems at the Los Alamos Laboratory [7.1]. The name was chosen apparently because of the association of the town "Monte Carlo" with roulette which is one of the simplest tools that can be used for generating random numbers.

Monte Carlo simulation is usually used for problems involving random variables of known or assumed probability distributions [7.2]. Using statistical sampling techniques, a set of values of the random variables are generated in accordance with the corresponding probability distributions. These values are treated similar to a sample of experimental observations and are used to obtain a "sample" solution. By repeating the process and generating several sets of sample data, many sample solutions can be determined. Statistical analysis of the sample solutions is then performed.

The Monte Carlo method thus consists of the three basic steps:

a. Simulation of the random variables and generation of several sample data using statistical sampling techniques

b. Solutions using the sampled data

c. Statistical analysis of the results

170

Since the results from the Monte Carlo technique depend on the number of samples used, they are not exact and are subject to sampling errors. Generally the accuracy increases as the sample size increases.

Sampling from a particular probability distribution involves the use of random numbers as will be discussed later. Random numbers are essentially random variables uniformly distributed over the unit interval [0,1]. Many codes are available for computers for generating sequence of "pseudo" random digits where each digit occurs with approximately equal probability. The generation of such random numbers plays a central role in the generation of a set of values (or realizations) of a random variable that has a probability distribution other than the uniform probability law.

The Monte Carlo method is considered now as one of the most powerful techniques for analyzing complex problems. Since its chief constraint is computer capability, it is expected to become even more commonly used in the future as computer capabilities increase and become less expensive to use.

7.2   Use of Monte Carlo Method in Structural Reliability Analysis

As was discussed in Chapters 1, 4 and 5, the reliability of a structure can be characterized by a limit state function $g(\underline{x}) = g(x_1, x_2 \ldots x_n)$, where x_i are random variables representing the basic design variables. The inequality $g(\underline{x}) \leq 0$ corresponds to failure while $g(\underline{x}) > 0$ represents the safe region. In the Monte Carlo approach a random sample values x_i for the basic design variables is generated numerically according to their probability distributions using a random number generator (see the following section). The generated sample values are then substituted in the limit state function whose value is then computed to see if it is negative or positive, i.e., failure or no failure. Repeating this process many times, it is possible to simulate the probability distribution of $g(\underline{x})$. This will require a very large number of samples. The probability of failure can then be estimated from either of the following methods:

a.   The probability of failure is given by

$$p_f = P[g(\underline{x}) \le 0] = \lim_{N \to \infty} \frac{n}{N} \qquad (7.1)$$

where N is the total number of trials or simulations and n is the number of trials in which $g(\underline{x}) \le 0$.

The ratio n/N is usually very small and the estimated probability of failure is subjected to considerable uncertainty. In particular the variance of n/N depends on the total number of trials N, decreasing as N increases. That is, the uncertainty in estimating p_f decreases as N increases. Statistical rules can be used to establish the necessary number of trials which depends on the magnitude of p_f. Many variance reduction techniques have been developed to decrease the variance of n/N with smaller number of trials than would have been necessary otherwise.

b.   In the second method, the probability of failure is estimated by, first fitting an appropriate probability distribution for $g(\underline{x})$ using the trial values described earlier [7.3]. The moment or any other established statistical method may be used in the fitting process. Elderton and Johnson [7.4] suggested some distributions that are suitable for fitting the $g(\underline{x})$ data. The probability of failure is then determined from

$$p_f \approx \int_{-\infty}^{0} f_M(m) \, dm \qquad (7.2)$$

where $M = g(\underline{x})$ is a random variable representing the margin and $f_M(m)$ is its probability density function as estimated from the fitting process.

7.3   Generation of Random Numbers For a Random Variable With a Prescribed Continuous Probability Distribution:

As mentioned earlier the process of generating random numbers with a specified probability distribution may be accomplished by first generating uniformly distributed random number between 0 and 1. Through appropriate transformation, one may then obtain a corresponding random number with a

specified probability distribution. Therefore, in this section we will first discuss how to generate uniformly distributed random numbers then how to obtain the corresponding random numbers with a specified probability distribution.

7.3.1 Random Numbers With Uniform Distributions:

Special devices may be used to generate uniformly distributed random numbers within a given range. For example, by equally subdividing the circumference of a wheel into a number of intervals equal to the given range and spinning the wheel, the desired uniformly distributed random number can be generated. Uniformly distributed random numbers are also tabulated and are available in the literature for pencil-and-paper Monte Carlo simulations.

In computer simulation, methods for generating uniformly distributed random numbers are generally based on recursive calculations which, because of cyclic effects, do not generate truly random numbers. The generated set eventually repeats itself after a very long cycle and, therefore, referred to as pseudo-random or quasi-random. An example of a recursive calculation of the residues of modulus "m" that produce such a set of pseudo-random numbers is

$$x_i = a\,x_{i-1} + b \,(\text{mod } m) \tag{7.3}$$

where a, b and m are nonnegative integers and the quotients x_i/m constitute the sequence of pseudo-random numbers [7.1, 7.2]. Such a sequence repeats itself after almost m steps, i.e., cyclic. For this reason m must be set very large e.g. 10^8 or larger.

7.3.2 Random Numbers with Prescribed Distribution:

Based on a generated set of uniformly distributed random numbers between 0 and 1, one may obtain the corresponding random numbers with a specified probability distribution. This can be done using a method known as the "inverse-function" method. The method is suitable if the inverse of the prescribed cumulative distribution function "C.D.F." of the random variable can be expressed analytically. The method is illustrated as follows.

Suppose that a set of random numbers are to be generated for a random variable Y which follows a prescribed distribution with C.D.F. $F_Y(y)$. The value of Y at $F_Y(y) = x$ is

$$y = F_Y^{-1}(x) \tag{7.4}$$

where $F_Y^{-1}(x)$ is the inverse of the C.D.F. at "x". If X is a uniformly distributed random variable "r.v." between 0 and 1, then

$$F_X(x) = x \qquad 0 \le x < 1$$

Thus if x is an outcome of the r.v. X, the corresponding value of Y obtained from (7.4) will satisfy the following equations.

$$P[Y \le y] = P[F_Y^{-1}(X) \le y] = P[X \le F_Y(y)] = F_X[F_Y(y)] = F_Y(y)$$

This means that if $(x_1, x_2 \ldots x_n)$ is a set of numbers of the r.v. X, the corresponding number obtained from equation (7.4), i.e.,

$$y_i = F_Y^{-1}(x_i) \qquad i = 1, 2, \ldots n \tag{7.5}$$

will have the C.D.F. $F_Y(y)$ as required. As an example consider the r.v. Y to have a Weibull distribution with C.D.F. given by

$$F_Y(y) = 1 - e^{-(y/k)^\ell} \qquad y \ge 0 \tag{7.6}$$

The inverse function is

$$y = F_y^{-1}(x) = k[-\ln(1-x)]^{1/\ell} = k[-\ln x]^{1/\ell} \tag{7.7}$$

since x and (1-x) have identical distributions, i.e., uniform distribution. Thus one can generate the random numbers y_i, i = 1, 2, ... n corresponding to uniformly distributed random numbers x_i according to (7.7) from:

$$y_i = k[-\ln x_i]^{1/\ell} \tag{7.8}$$

The Weibull distribution can be reduced to the Rayleigh and the exponential distributions as discussed earlier. If the Weibull parameters k and ℓ are equal to $\sqrt{2E}$ and 2, respectively, the Weibull distribution reduces to the Rayleigh distribution. If k and ℓ are equal to λ and 1, it reduces to the exponential distribution. Thus, substitution for k and ℓ in equation (7.8) will lead to a set of random numbers for these two special distributions as well.

7.4   Sample Size and Variance Reduction Techniques

As mentioned earlier, the simulated data according to Monte Carlo method should be treated as a sample of experimental observation, and therefore, is subjected to sampling error. If the probability of structural failure is to be computed from the simulated data the underlying error becomes an important consideration since the sought probability of failure is usually small. Shooman [7.5] developed the following expression for estimating the error in the estimated probability of failure:

$$\text{error} = 2\left(\frac{1 - p_f}{N \, p_f}\right)^{1/2} \qquad (7.9)$$

where N is the total number of simulations (sample size) and p_f is the probability of failure. There is a 95% chance that the actual error in the estimated probability is less than that given by equation (7.9). It is seen that the error is dependent on the number of simulations N and the probability of failure p_f; it decreases by increasing N or p_f. Therefore, if the estimated probability p_f is small which is usually the case, N should be large enough to decrease the error.

There are techniques, however, which may reduce the error (or variance) without increasing the sample size. These techniques are known as variance reduction techniques, and the one that is used often in structural failure problems is called "Antithetic Variates".

7.4.1   Antithetic Variates

Let Y_1 and Y_2 be two unbiased estimates of Y as determined from two separate sets of samples or simulation cycles. The average of these two unbiased

175

estimations $Y_a = 1/2 (Y_1 + Y_2)$ is also an unbiased estimator since its expected value $E [Y_a]$ is equal to Y. The variance "σ_{ya}^2" of the new estimator Y_a is determined from the individual variances "σ_{y1}^2" and "σ_{y2}^2" as:

$$\sigma_{ya}^2 = 1/4 [\sigma_{y1}^2 + \sigma_{y2}^2 + 2 \text{ cov} (Y_1, Y_2)] \qquad (7.10)$$

If Y_1 and Y_2 are negatively correlated, i.e., the cov. $(Y_1, Y_2) < 0$, it is seen from equation (7.10) that the third term becomes negative and

$$\sigma_{ya}^2 < 1/4 (\sigma_{y1}^2 + \sigma_{y2}^2) \qquad (7.11)$$

That is, the accuracy of the estimator Y_a can be improved (or its variance can be reduced) if Y_1 and Y_2 are negatively correlated estimators. The antithetic variates method is thus a procedure that ensures a negative correlation between Y_1 and Y_2. This can be accomplished in structural reliability problems as follows.

If X is a random variable uniformly distributed between 0 and 1, then 1-X is also a uniformly distributed random variable between 0 and 1 and the two random variables X and 1-X are negatively correlated. Each of these random variables can be then used to generate the basic random variables Y_i which have prescribed probability distributions as described earlier. This results in a pair of negatively correlated basic random variables. The procedure is repeated for all the random variables Y_i in the limit state equation. The limits state equation is then solved for each negatively correlated set of random variables separately and the results are averaged to estimate the population mean. Note that the error (or variance) of the result is reduced because of the negative correlation between the generated variables according to equation (7.11).

7.5   Application Examples:

7.5.1 Comparison of Analytical and Simulated Evaluations of a Random Function

The purpose of this example is to compare numerically simulated results obtained using a "standard" random number generator with exact analytical values. For this purpose, the random process $x^{(i)}(t)$ was examined in ref. [7.6]

$$x^{(i)}(t) = A \sin (\sigma t + \theta^{(i)}) \tag{7.12}$$

where A and σ are fixed (deterministic) constants and $\theta^{(i)}$ is a random phase angle with uniform distribution shown in Figure 7.1.

Analytical Results

The analytical result for the first order and joint probability density functions (jpdf) of x given that θ is uniformly distributed can be derived by standard statistical methods. These are given by:

$$f(x) = 1/[\pi\sqrt{A^2 - x^2}] \qquad -A < x < A$$

and
$$\qquad\qquad = \emptyset \qquad\qquad\qquad otherwise$$

$$f(x1,x2) = 1/[2\pi\sqrt{A^2 - x1^2}] * \qquad -A < (x1,x2) < A$$
$$[\ \delta(x2 - x1\cos\sigma\tau + \sqrt{A^2 - x1^2} \ \sin\sigma\tau)$$
$$\quad \delta(x2 - x1\cos\sigma\tau - \sqrt{A^2 - x1^2} \ \sin\sigma\tau)] \tag{7.13}$$
$$\qquad = \emptyset \qquad\qquad\qquad otherwise$$

where $\tau = t_2 - t_1$.

The first order pdf of x is shown is figure 7.2. In general, the jpdf is difficult to represent graphically. It is three-dimensional with spikes when the argument of either of the two delta functions is equal to zero. The occurrence of these spikes will depend on the values of A, σ and τ as well as the current values of x_1 and x_2. The factor in front of the delta functions modifies their sum so that the total area underneath the jpdf will equal one.

Numerical Results

First Order Pdf: For given values of A, σ and τ, a data file of N random phase angles and the corresponding values of the x was created. The values of x were generated by simply substituting the random values of θ into equation (7.12).

BASIC language was used to create the data file, because it contains a random number generator. A separate routine was written in FORTRAN to compute the pdf of either the random phase angle or the random x's. This routine divides the range from 0 to 2π for θ, or from -A to A for x, into n intervals of size $\Delta\theta$ or Δx. Then the number of θ's or x's in each interval was counted. The value of the pdf at the center of each interval is given by,

$$f(\cdot) = (\text{\# of occurrences per interval}) / [(\Delta\theta \text{ or } \Delta x) * N]$$

where N is the total number of samples (simulations).

The probability density function of theta compares well with the expected uniform distribution, see figure 7.3. The pdf of x was computed for the case of

A	=	1 magnitude unit
σ	=	1 rad / (time unit)
t	=	1 time unit
N	=	100000 samples

The numerically computed points compare extremely well with the analytical curve, see figure 7.4. There is, however, disagreement between the computed values and the analytical curve at the singularities, $x = \pm 1$.

Second Order PDF: The numerical procedure used to calculate the jpdf was very similar to that for the first order pdf.

Some easily visualized cases of the jpdf were investigated. Consider the case when $t_1 = t_2$ so that $\sigma\tau = 0$. Since $\sin(0) = 0$ and $\cos(0) = 1$, the argument of both delta functions in the analytically derived result (equation 7.13) simplify to $(x_1 - x_2)$. This implies that the jpdf will consist of spikes along the line, $x_1 = x_2$. The numerical results for this case with

A	=	1 magnitude unit
N	=	100000 samples
$\Delta x1, \Delta x2$	=	0.05 magnitude units

178

is given in figure 7.5.

Another interesting case is when $\sigma = 1$ rad / (time unit), $t_1 = 1$ time unit and $t_2 = 2.57$ time units, then $\sigma\tau = \pi/2$. Since $\sin(\pi/2) = 1$ and $\cos(\pi/2) = 0$, the argument of both delta functions will equal zero when $x_1^2 + x_1^2 = A^2$. This means that the jpdf will be a series of spikes along a circle centered at $(x_1, x_2) = (0, 0)$ and of radius A. The numerically computed jpdf evaluated under this condition is shown in figure 7.6 and 't inde d appears as expected.

Effect of Number of Samples and Size of Increment: The analytical derivation of the probability density function assumes an infinite number of samples and infinite resolution of x. In a numerical computation, however, both N and Δx are finite values. On the average, the number of samples per interval will equal the total number of samples divided by the numbers of increments, i.e.,

$$\# \text{ samples per interval} = N / [\ 2A/\Delta x\ ].$$

The trend shown in figure 7.7, as well as, in figure 7.8, shows that as N increases for a constant Δx, the numerical values converge to the analytical result for the pdf. In addition, comparing figure 7.7 to figure 7.8 for a constant N, shows that decreasing the size of the interval Δx appears to increase the spread of the numerical data. Therefore, in order to get an accurate numerical representation of the probability density function, not only the total number of samples and the size of the increments are important, but mainly their relationship in determining the number of samples per interval is important.

179

Probability Density Function of Theta
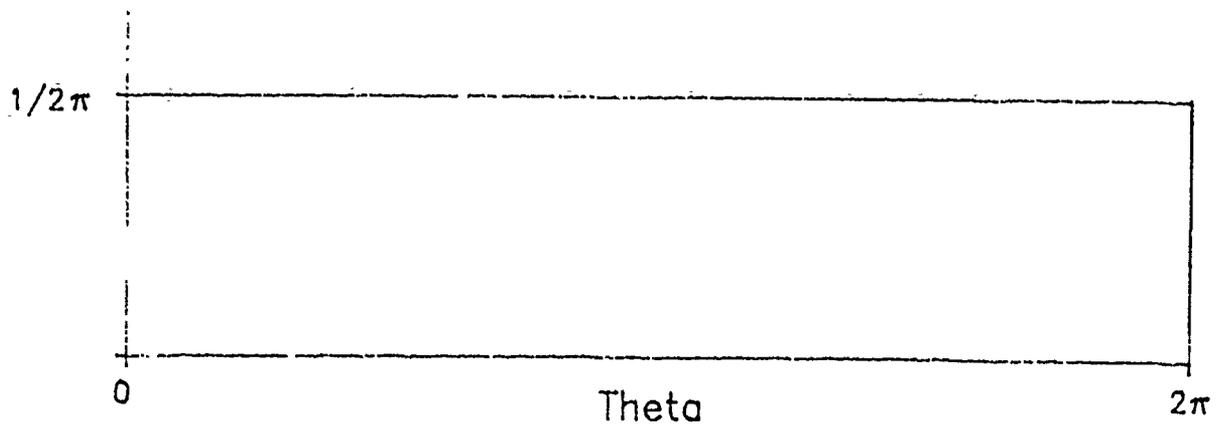
Figure 7.1. Analytically Derived PDF of Theta

Probability Density Function of X

$$X^{(i)} = A(\sin \sigma t + \Theta^{(i)})$$
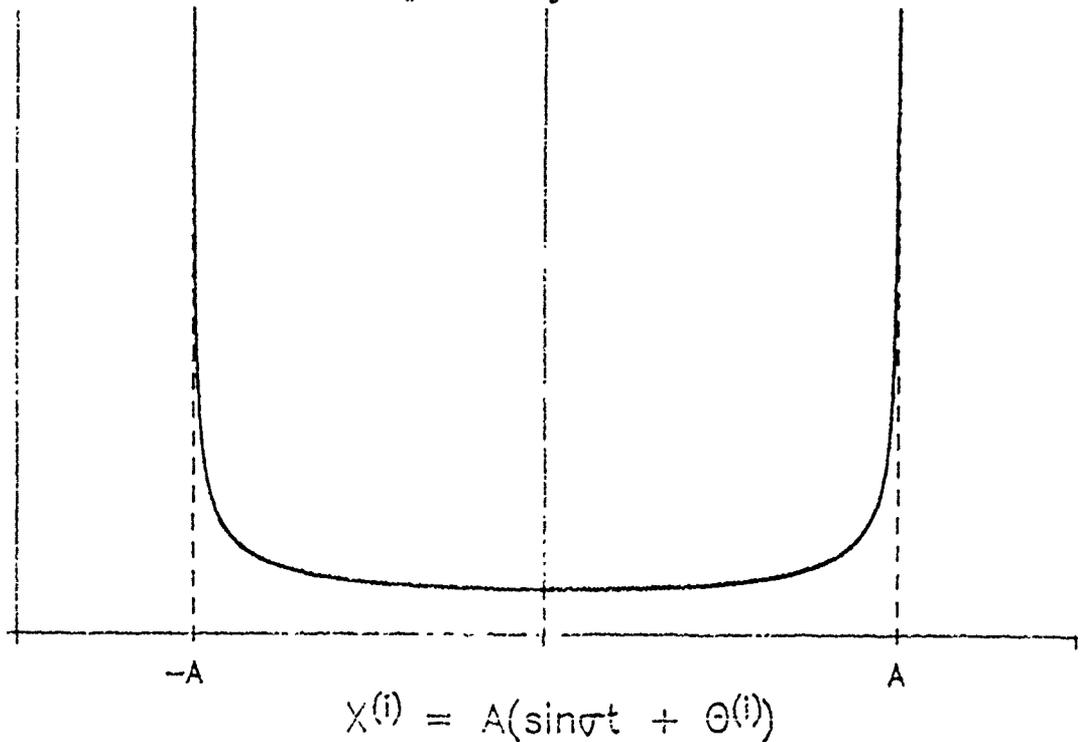
Figure 7.2. Analytically Derived PDF of X

Probability Density Function of Theta

100000 Samples.　　　$\Delta\theta = 0.01$
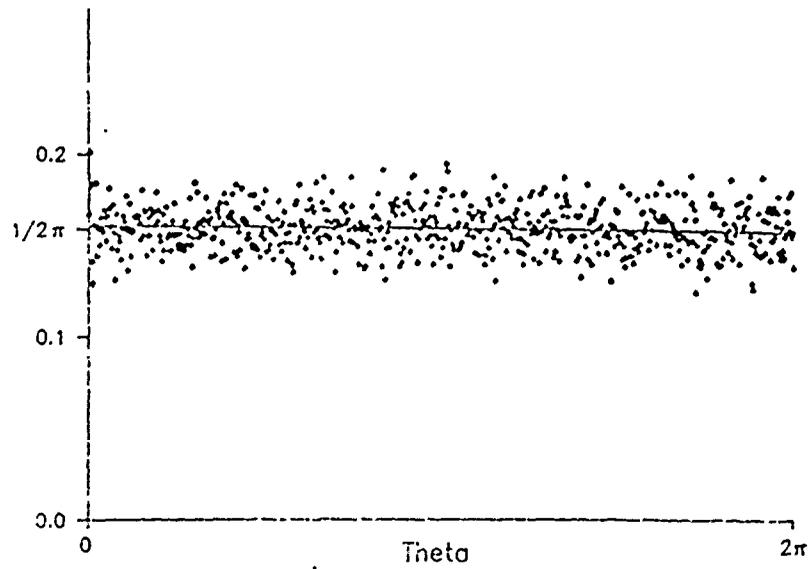
Probability Density Function of Theta

100000 Samples.　　　$\Delta\theta = 0.1$
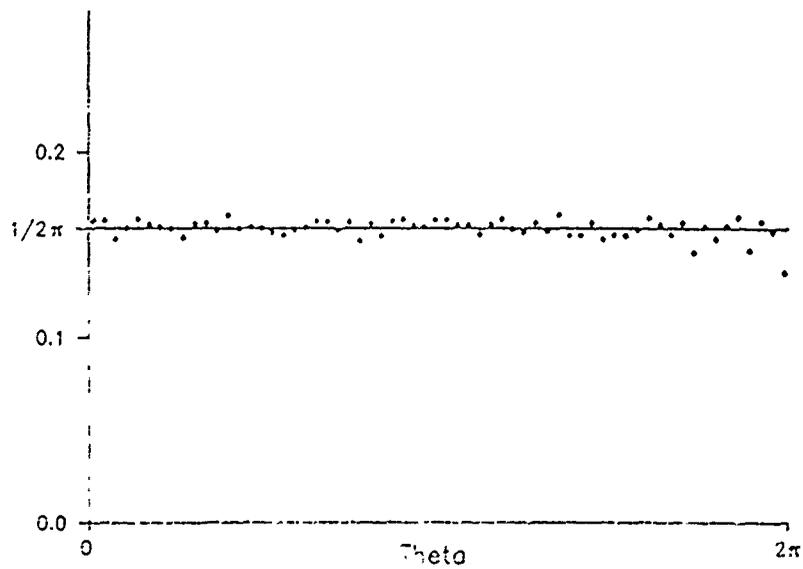
Figure 7.3. Numerically Computed PDF's of Theta
$\Delta\theta = 0.01$ and $\Delta\theta = 0.1$

Probability Density Function of x

$(A, \sigma, t) = (1, 1, 1)$

100000 Samples $\Delta x = 0.01$

$X^{(i)} = A\sin(\sigma t + \Theta^{(i)})$
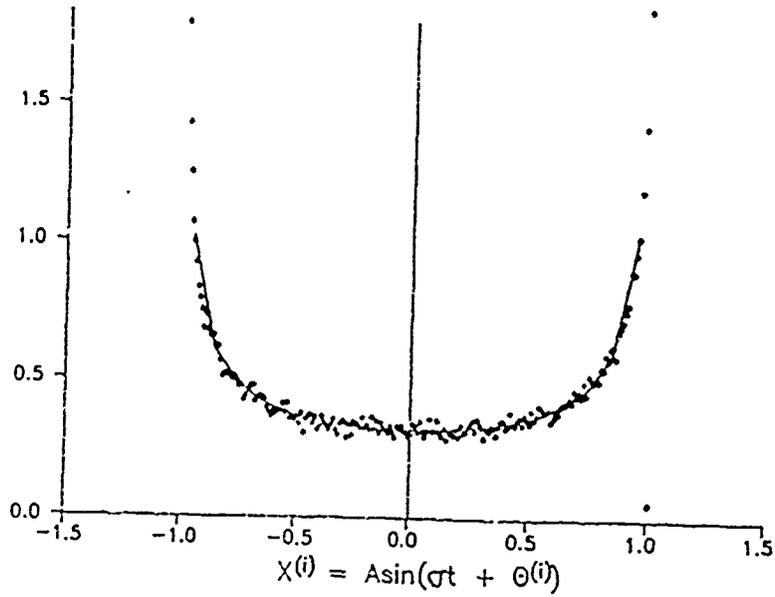
Probability Density Function of x

$(A, \sigma, t) = (1, 1, 1)$

100000 Samples $\Delta x = 0.1$

$X^{(i)} = A\sin(\sigma t + \Theta^{(i)})$
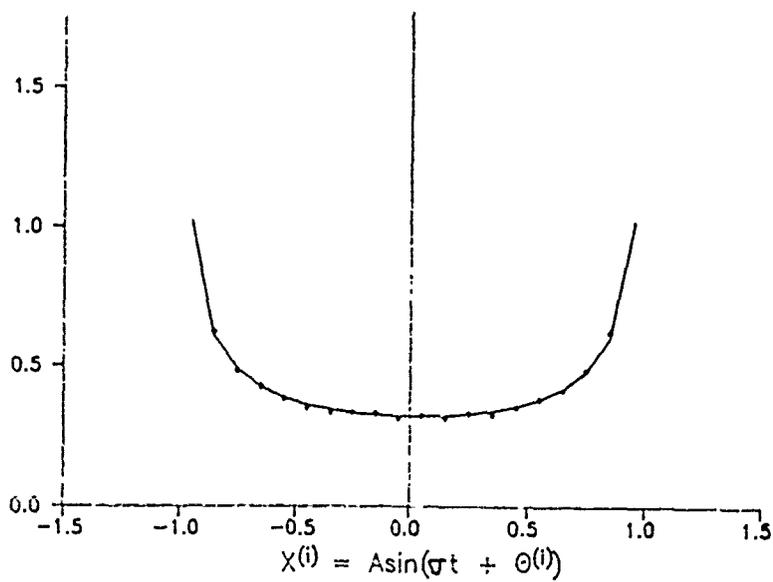
Figure 7.4. Numerically Computed PDF's of x
$\Delta x = 0.01$ and $\Delta x = 0.1$
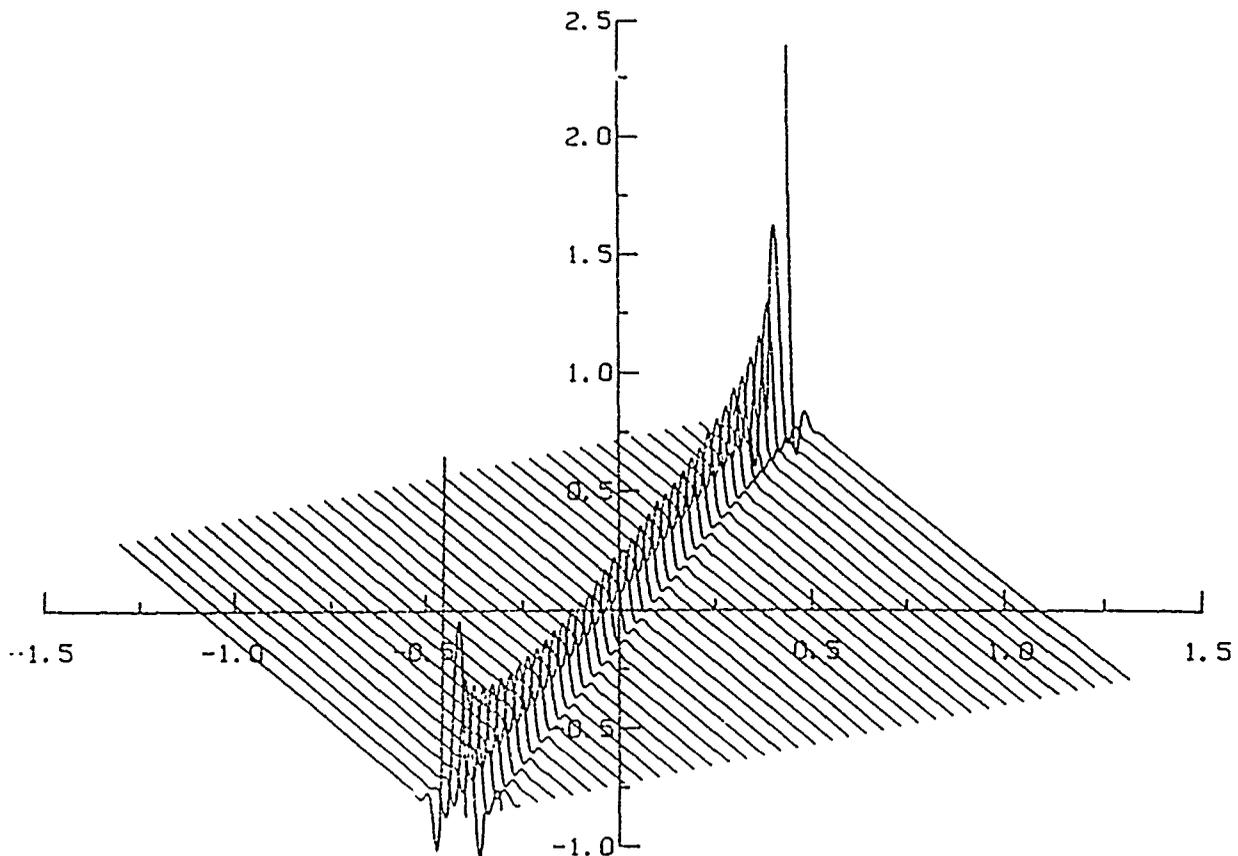
Figure 7.5. Joint Probability Density Function
$(A, \sigma, t_1, t_2) = (1, 1, 1, 1)$
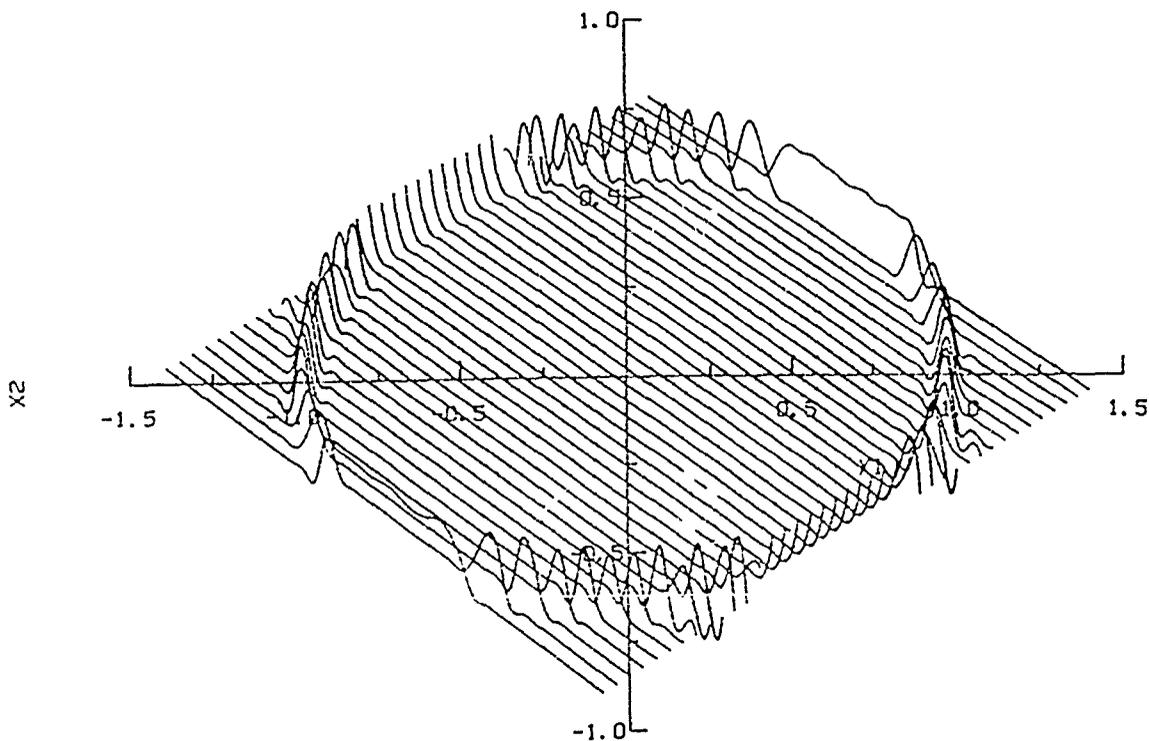
Figure 7.6. Joint Probability Density Function
$(A, \sigma, t_1, t_2) = (1, 1, 1, 2.57)$

Figure 7.7. $\Delta x = 0.01$

184
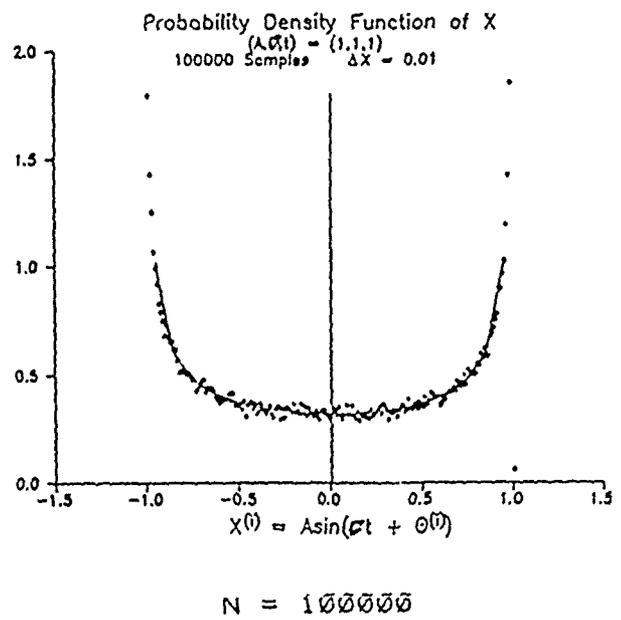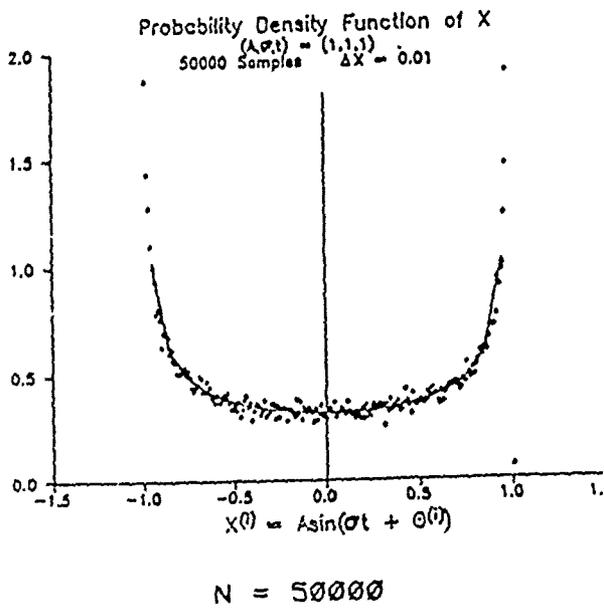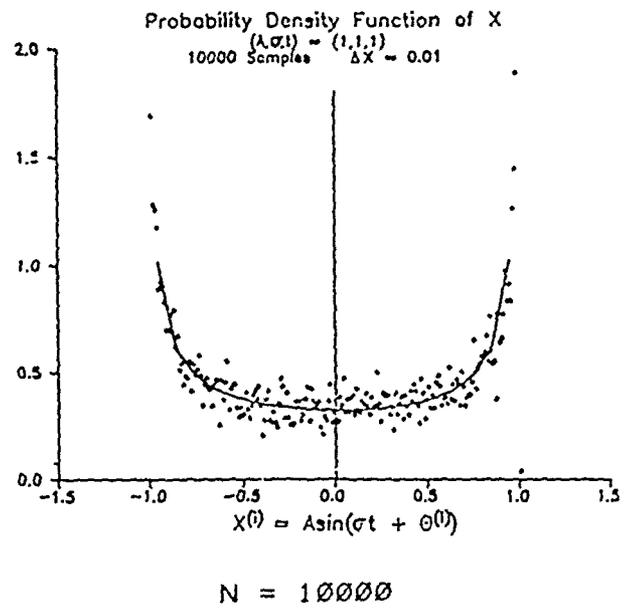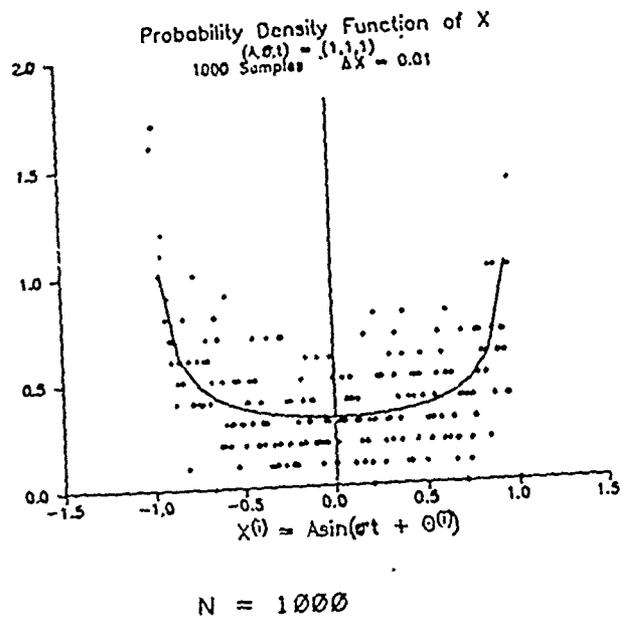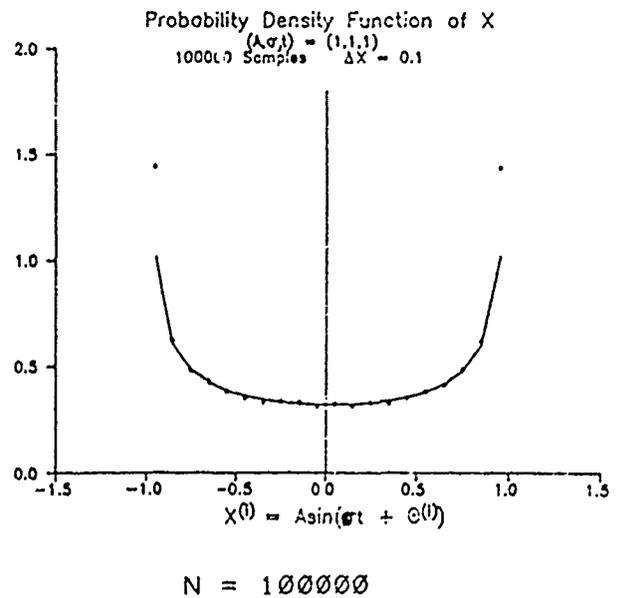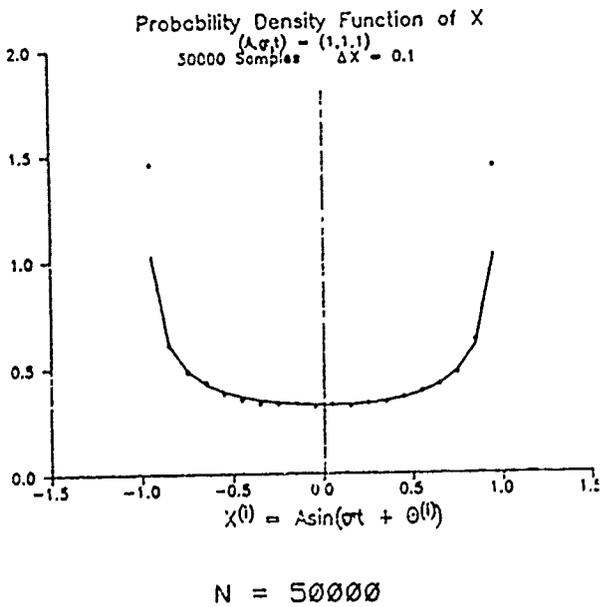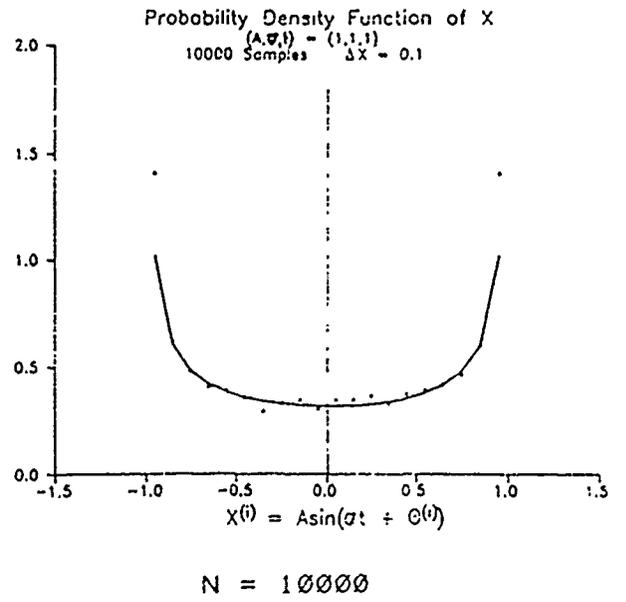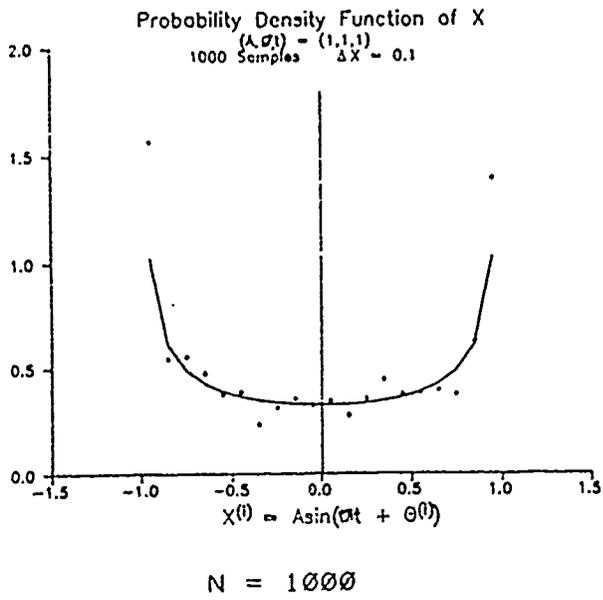
Figure 7.8. $\Delta x = 0.1$

7.5.2 Application of Monte Carlo Method to Reliability of Ship Structures
(excerpted from White and Ayyub [7.7]):

In order to compare results of the Monte Carlo simulation method with the other reliability methods discussed earlier in Chapters 4 and 5 an example problem is solved using each method. The problem chosen is to determine probability of ductile yielding of a vessel's deck under extreme bending moments. Any of the other possible modes of failure could have been chosen, for example, plastic collapse or buckling, but the availability of data on this problem facilitated comparison of methods. The vessel chosen for the analysis is a naval frigate, the same one used by Mansour and Faulkner [7.8]. The principal dimensions are given in Table 7.1 and the midship section is shown in Figure 7.9.

The problem is essentially a simple beam in bending and can be written as:

$$M_u = CY \tag{7.14}$$

where M_u is the ultimate bending moment; C is the section modulus of the vessel; Y is the tensile yields stress of the vessel material.

In order to see the effect of different, but mechanically equivalent formulations on each method two limit-state equations will be used. The first limit-state equation has a simple linear form:

$$Z = R - Q \tag{7.15}$$

where R is the resistance, given in tons/in^2 and is equal to Y in Equation (7.14); Q is the total load in tons/in^2 .

Next a more complicated non-linear form is used. This form separates the wave and still water bending moments, M_w and M_0 respectively; and Z is expressed in units of bending moment:

$$Z = YC - M_0 - M_w \tag{7.16}$$

186

The basic variables for each form are shown in Table 7.2 along with their respective statistical properties.

First Order Reliability Method (Level 2): The method described in Chapter 5 was applied in [7.7] to the linear and non-linear limit state functions given by equations (7.15) and (7.16), respectively. In both cases the distribution information was included in the analysis. The results for the safety index "β" and the corresponding probability of failure "p_f" are given in column 2 of Table 7.3.

Direct Integration Method (Level 3): The method described in Chapter 4 was applied in reference [7.8] using the linear limit state equation only (equation 7.15) and assuming the stillwater bending moment to be deterministic. In reference [7.8], the probability of failure was computed for ship operation period of twenty one years (n=3). To be consistent with the results given in this example, the value given in [7.8] must be divided by 3 and the corresponding resulting value for p_f is 1.3×10^{-6} which is shown in Table 7.3.

Monte Carlo Simulation Method: In reference [7.7] the same problem (equations 7.15 and 7.16) was solved using Monte Carlo simulation technique described in this chapter. Use was made of Antithetic Variate reduction method and conditional expectation in order to reduce the number of simulation cycles. The primary steps involved in the solution according to reference [7.7] are:

Step 1. Identify the basic variable with the most variability in the limit state equation.

Step 2. Condition the variable in Step 1 with respect to all the remaining variables in the limit state equation.

Step 3. Generate a uniformly distributed random deviate for each of the conditional variables.

Step 4. Generate a second uniformly distributed random deviate which is negatively correlated to the one from Step 3.

Step 5. Using the inverse transform method produce a random variable for each deviate from Step 4.

Step 6. Calculate the probability of failure using the probabilistic characteristics of the variable identified in Step 1 for each set of random variables.

Step 7.   Find the average probability of failure for the two p_f's in Step 6.

Step 8.   Repeat Steps 3 to 7 N times.

Step 9.   Calculate the statistics of the N number of probabilities of failure thus generated.

The results are shown in Table 7.3 for 2000 simulations cycles. Figures 7.10 and 7.11 from reference [7.7] show the simulation scheme converges on a solution with increasing N.
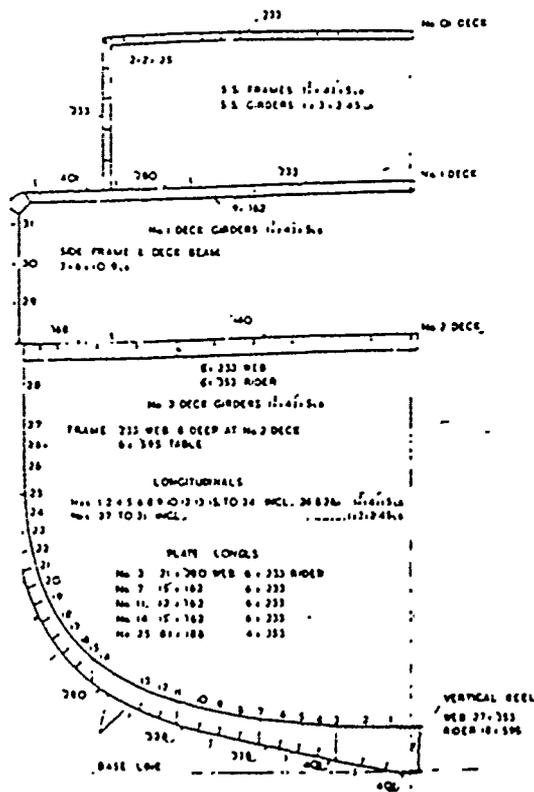
Midship Section of Frigate of 360 ft LBP [7.8]

189
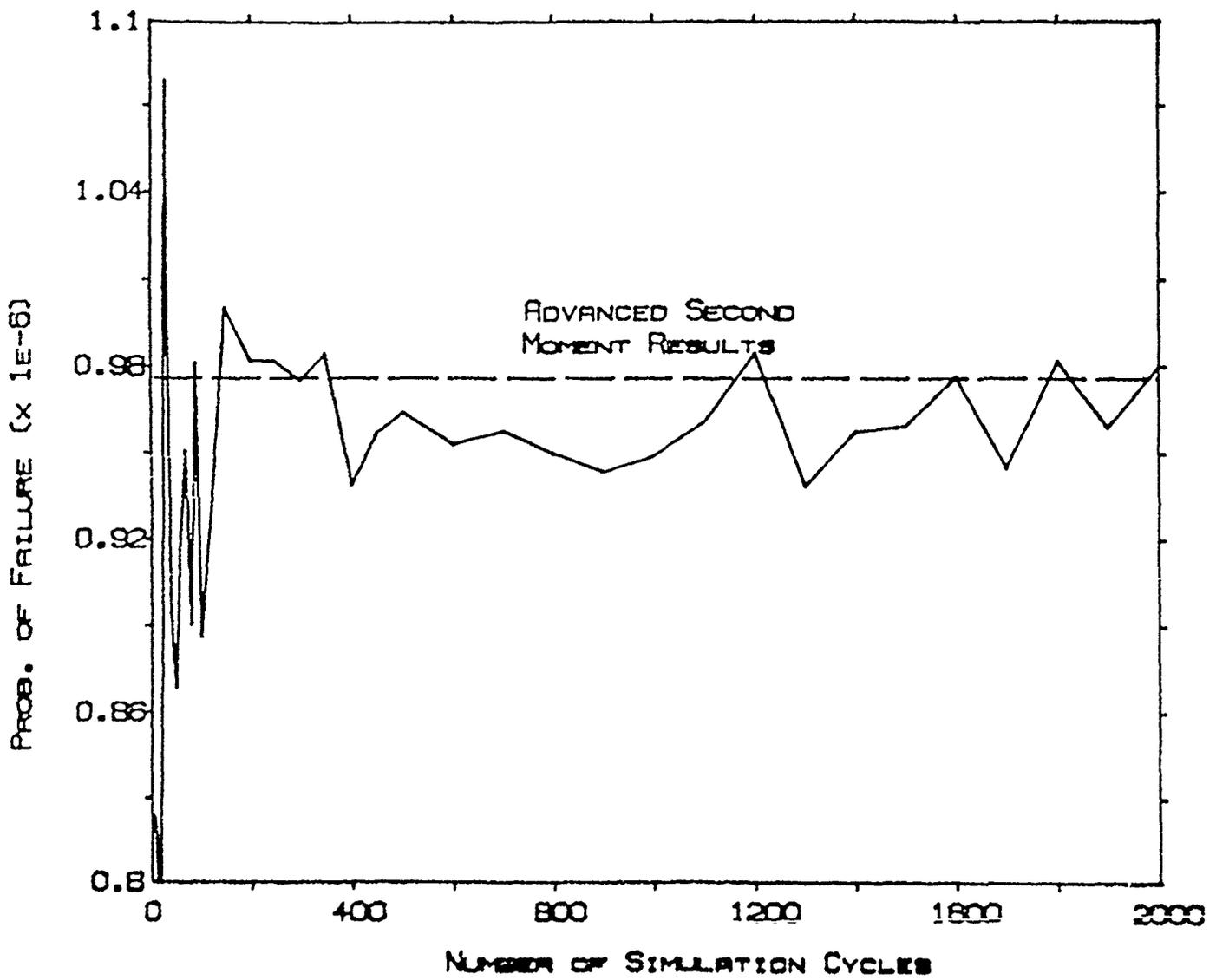
Figure 7.10. Probability of Failure vs. Number of Simulations
Using Variance Reduction Techniques

190
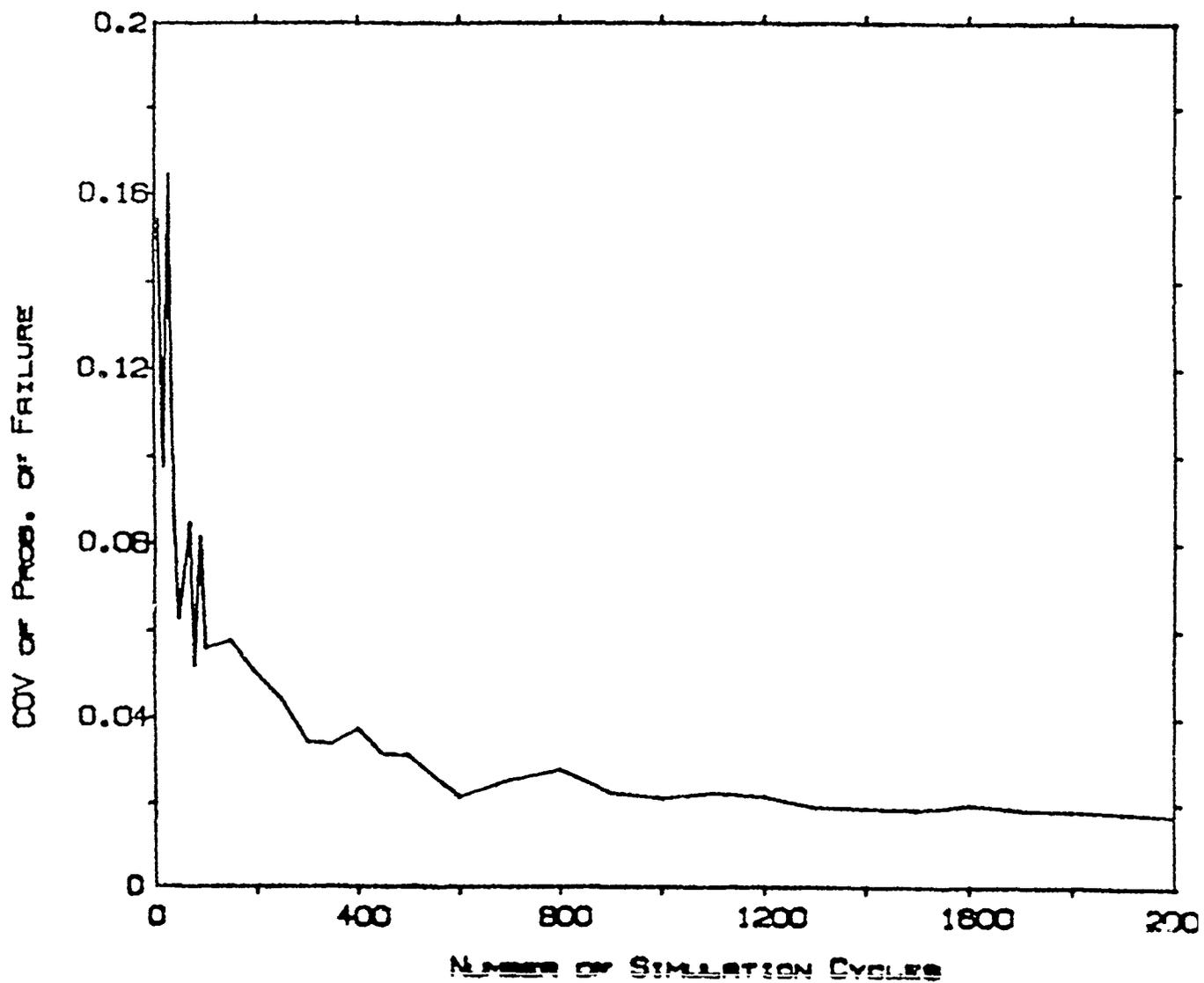
Figure 7.11. COV of Probability of Failure vs. Number of
Simulations Using Variance Reduction Techniques

Table 7.1. Vessel Characteristics

Length Between Perpendiculars	360.0 ft	(110.00 m)
Beam (molded)	41.0 ft	(12.50 m)
Depth	28.9 ft	(8.78 m)
Draft	12.0 ft	(3.66 m)
Displacement	2800.0 tons	(2845.00 tonnes)
Section Modulus (at deck)	5700.0 in^2 ft	(1.12 m^3)

Table 7.2. Probabilistic Characteristics of Basic Variables

Basic Variable	Mean	COV	Distribution
Linear Formulation			
R	22.20 tons/in^2	.0710	Normal
Q	2.70 tons/in^2	.5390	Weibul
Non-Linear Formulation			
Y	22.20 tons/in^2	.0610	Normal
C	5700.00 in^2 ft	.0379	Log-Normal
M_0	7080.00 ft-tons	---	Deterministic
M_w	8290.00 ft-tons	1.0000	Weibul (k=1)

Table 7.3. Example Problem Results

	First Order Method	Direct Integration Method	Monte Carlo Method
Linear Limit State Equation (7.15)	$\beta = 4.75$ $p_f \approx 0.97 \times 10^{-6}$	$p_f \approx 1.33 \times 10^{-6}$	$p_f = 0.98 \times 10^{-6}$ (C.O.V. = 0.0192)
Non-Linear Limit State Equation (7.16)	$\beta = 4.75$ $p_f \approx 0.976 \times 10^{-6}$	---	$p_f = 0.98 \times 10^{-6}$ (C.O.V. = 0.0174)

REFERENCES

[7.1] Elishakoff, I., <u>Probabilistic Methods in the Theory of Structures</u>, John Wiley and Sons, 1983.

[7.2] Ang, A. H.-S. and Tang, W. H., Probability Concepts in Engineering Planning and Design, Risk and Reliability, John Wiley and Sons, New York, 1984.

[7.3] Thoft-Christensen, P. and Baker, M., Structural Reliability Theory and Its Application, Springer-Verlag, Berlin, 1982.

[7.4] Elderton, W. P. and Johnson, N. L., Systems of Frequency Curves, Cambridge University Press, 1969.

[7.5] Shooman, M. L., Probabilistic Reliability: An Engineering Approach, McGraw-Hill Book Co., New York, 1968.

[7.6] Ochs, J., "Comparison of Analytical and Numerical Evaluation of the Random Function $x^{(i)} = A \sin(\sigma\tau + \theta)$," Report for NA 240B, University of California, Berkeley, May 1988.

[7.7] White, G. J. and Ayyub, B. M., "Reliability Methods for Ship Structures," Naval Engineers Journal, Vol. 91, No. 4, May 1985.

[7.8] Mansour, A. and Faulkner, D., "On Applying the Statistical Approach to Extreme Sea Loads and Ship Hull Strength," Trans., Royal Institute of Naval Architects, Vol. 115, 1973.

8. SYSTEM RELIABILITY

8.1. Introduction

The reliability analysis discussed in Chapter 4, 5 and 6 has been mainly concerned with a single failure mode (or a limit state) defined by a single limit state equation. Marine structures, however, involve several modes of failure, i.e., there is a possibility that a structure may fail in one or more of several possible failure scenarios. The subject of system reliability deals specifically with the methods of combining the probabilities of failure associated with these modes in order to determine the total reliability of the structure as a system.

Two main sources of "system effects" are identified. The first is due to possible multiplicity of failure modes of a component or a structural member. For example, a beam under bending and axial loads may fail in buckling, flexure or shear. Each one of theses modes can be defined by one limit state equation. Even though in this case, we are dealing with a single member (beam), system reliability methods must be used in order to combine the possible failure modes and to obtain an assessment of the total risk of failure of the beam. The probability of failure of one mode may be larger than the others, but the fact that there is a possibility that the others may occur indicates that they must be included and combined to obtain the total probability of failure of the beam.

Another example of multiplicity of failure modes is the primary behavior of a ship hull. In the primary behavior, one treats the ship as a single beam subjected to weight, buoyancy and wave loads which induce sagging and hogging bending moments. The hull may fail (or reach a limit state) in one of several possible modes, e.g., buckling of deck or bottom panels or grillages, yielding of deck or bottom plating, etc. Here again, system reliability methods must be used to combine these different modes of failure and to obtain a total probability of failure.

Multiple modes of failure of a member are usually modelled in system reliability analysis as a series system. A series system is one that is composed of links connected in series such that the failure of any one or more of these links constitute a failure of the system, i.e., "weakest link" system. In the case of the

primary behavior of a ship hull, for example, <u>any one</u> of the failure modes discussed earlier will constitute failure of the hull (or a limit state to be prevented) and therefore can be considered as a series system. Series systems will be discussed in more detail in a later section of this chapter.

The second source of "system effects" is due to redundancy in multi-component engineering structures. In such structures, the failure of one member or component does not constitute failure of the entire system. Usually several members must fail to form a "failure path" before the entire structure fails. The failure of each member is defined by at least one limit state equation and a corresponding probability of failure. These individual member probabilities of failure must be combined to get the probability of failure of the system for a particular "failure path". Thus, system reliability methods must be used to determine the reliability of a redundant structure. An example of a multi-component redundant structure in which system effects are important is a fixed offshore platform. For such a platform to fail, several members must fail to form a failure path. The probability of failure of the system in this case is usually modelled as a <u>parallel system</u> in which <u>all links</u> along the failure path of the system must fail for the entire structure to fail. More over, there will be several possible paths of failure any of which will constitute failure of the entire platform. Therefore each failure path and the associated probability of failure can be considered as a link in a series system since failure of any link constitute a failure of the system in the series model. The total offshore platform can be thus modelled as several parallel subsystems each of which represents a failure path connected together in series since any of them constitutes failure of the platform. Parallel systems and general systems consisting of series and parallel subsystems will be discussed in later sections of this chapter.

8.2.   General Formulation

The exact system reliability problem taken into consideration possible time-dependent random variables is an outcrossing problem. If the time-dependant loads or response of the structure exceeds (outcrosses) one or more of several possible failure modes (surfaces), failure of the structure occurs. The problem formulated in terms of stochastic processes however is difficult to solve. Only a few cases of very simply structures with certain load history models can be

evaluated in this manner and the reliability of the structure at any time during its life can be calculated. For a single time varying load it is possible to treat the peaks as a random variable and its extreme-value distribution may be formulated to perform the reliability calculation.

At the present, the general problem is formulated as a time-independent problem which is sufficient only for the evaluation of an instantaneous reliability. As such, the form of the equation to evaluate the system reliability is the same as that of component reliability (equations 4.1 and 4.2) except that, now, the multiple integration is carried out over all possible limit state functions corresponding to the potential modes of failure. For k modes of failure, and n random variables, the system probability of failure can be written as:

$$p_f = \int \cdots \int f_X(x_1, x_2, \ldots x_n) \, dx_1 \ldots dx_n \qquad (8.1)$$

$$g_i(\underline{x}) \leq 0$$
$$i = 1, 2, \ldots k$$

where $f_{\underline{X}}(x_1, x_2 \ldots x_n)$ is the joint probability density function of the n random variables and $g_i(\underline{x})$ are the k limit state functions. The domain of integration in equation (8.1) is over the entire space where each of the "k" limit state function is negative or zero.

The same difficulties encountered in the level 3 computation of component reliability will be encountered in determining system reliability from equation (8.1), namely, the determination of the joint density function and the evaluation of the multiple integration. In addition, the domain of integration over all possible modes of failure in equation (8.1) will present additional numerical difficulties. For these reasons this general exact formulation is not used, and instead of determining the combined total probability of failure of the system as given by (8.1) only an upper and lower bounds on that system probability are determined. These upper and lower bounds are usually determined by considering the structure to be a series system or a parallel system or a combination of both (general system).

It should be noted that, in principle, simulation methods and the Monte Carlo technique can be used to solve equation (8.1) in basically the same manner discussed in Chapter 7. In this case numerical simulation of the random variables is performed according to their prescribed joint distribution and all limit state equations are checked to see if failure occurs. The ratio of failure realizations to total number of simulations gives an estimate of the probability of system failure. Reduced variate techniques and other methods for improving convergence may be used here. Usually, for realistic structures the number of simulations required for a reliable estimate of the system probability of failure is still high, but these methods have potential for application in system reliability.

8.3. Bounds on the Probability of Failure of a Series System

A series system is one which fails if any one or more of its components fails. Such a system has no redundancy and is also known as "weakest link" system. Schematically a series system is represented as in figure 8.1
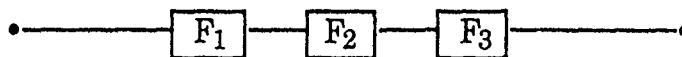
Figure 8.1. Schematic Representation of a Series System

A typical example of a series system is a statically determinate structure where a failure of any member constitutes failure of the structure. Another example of a series system is a beam or an element which may fail in any of several possible modes of failure each of which may depend on the loading condition of the beam. A ship hull girder in its "primary behavior" is such a system with the additional complication that failure may occur in hogging or sagging condition. Each condition includes several modes of failure. A third example of a series system arise when combining the probabilities of failure of several possible failure paths in an offshore platform, any of which constitutes failure of the platform.

If F_i denotes the ith event of failure, i.e., the event that $[g_i (\underline{x}) \leq 0]$, and S_i represents the corresponding safe event, i.e., $[g_i (\underline{x}) > 0]$, then the combined

system failure event F_S is determined as the union "U" of all individual failure events F_i as

$$F_S = \underset{i}{U}\ F_i \qquad\qquad i = 1, 2, \ldots k$$

The corresponding probability of system failure is

$$P(F_S) = P\left(\underset{i}{U}\ F_i\right) = 1 - P\left(\underset{i}{\cap}\ S_i\right) \qquad\qquad (8.2)$$

where $\cap$ represents the intersection or mutual occurrence of events.

The calculation of the probability of systems failure for a series system using equation (8.2) is generally difficult and requires information on correlation of all failure events. Approximations are therefore necessary and upper and lower bounds on the system probability of failure are constructed instead of evaluating the exact value. Two types of bounds can be constructed; first and second order bounds.

First Order Bounds:

These are bounds on the probability of system failure which require no information on the correlation between the events of failure. In other words, the user of such bounds does not need any information on the correlation between the events of failure which, in many cases, are not available. They are constructed as follows (see reference 8.1).

If the events of failure of a series system are assumed to be perfectly correlated, the probability of system failure is simply the maximum of the individual probabilities of failure. For positively correlated failure events, this assumption leads to the lower non-conservative bound on the actual system probability, i.e.,

$$\underset{j}{\max.}\quad P(F_i) \leq P(F_S) \qquad\qquad (8.3)$$

On the other hand, if the events of failure are assumed to be statistically independent, an upper bound (conservative) can be determined. In this case, for independent failure events of a series system, the right hand side of equation (8.2) reduces to

$$1 - P\left(\bigcap_i S_i\right) = 1 - \prod_{i=1}^{k} P(S_i) = 1 - \prod_{i=1}^{k} [1 - P(F_i)] \tag{8.4}$$

where $\displaystyle\prod_{i=1}^{k} P(S_i)$ represents the product of the probabilities of survival. The result given by equation (8.4) represents an upper bound on the true probability of system failure, i.e.,

$$P(F_s) \le 1 - \prod_{i=1}^{k} [1 - P(F_i)] \tag{8.5}$$

Combining equations (8.3) and (8.5), one obtains an upper and lower bounds, i.e.,

$$\max_i \; P(F_i) \le P(F_s) \le 1 - \prod_{i=1}^{k} [1 - P(F_i)] \tag{8.6}$$

Although the upper bound in equation (8.6) is not difficult to evaluate, it can be further simplified by noticing that

$$1 - \prod_{i=1}^{k} [1 - P(F_i)] \le \sum_{i=1}^{k} P(F_i) \tag{8.7}$$

therefore, equation (8.6) can be written as

$$\max_i \; P(F_i) \le P(F_s) \le \sum_{i=1}^{k} P(F_i) \tag{8.8}$$

Equation (8.8) gives the final result for the bounds of a series system and states the obvious conclusion that the actual probability of system failure lies between the maximum of the individual probabilities and the sum of all individual probabilities. These bounds are narrow if one mode of failure is dominant, i.e., if one of the individual probabilities of failure is much larger than the others. If not, these bounds may be too wide to be useful. In such cases a more narrow set of bounds should be considered (second order bounds).

Second Order Bounds:

These bounds were developed in references [8.2, 8.3, 8.4 and 8.5] and are given in terms of pair-wise dependence between failure events, therefore, are called second order bounds. The original bounds for k potential modes of failure are given as [8.2, 8.3]:

$$P(F_1) + \sum_{i=2}^{k} \max \left\{ \left[P(F_i) - \sum_{j=1}^{i-1} P(F_i F_j) \right]; 0 \right\} \le P(F_s) \le$$

$$\sum_{i=1}^{k} P(F_i) - \sum_{i=2}^{k} \max_{j<i} P(F_i F_j) \qquad (8.9)$$

where $P(F_1)$ is the maximum of the individual probabilities of failure and $P(F_i F_j)$ is the probability of intersection (mutual occurrence) of two events of failure, F_i and F_j.

The bounds given by equation (8.9) depend on the ordering of the failure modes and different ordering may correspond to wider or narrower bounds. Therefore, bounds corresponding to different ordering may have to be evaluated to determine the narrowest bounds.

The evaluation of the joint probability $P(F_i F_j)$ required in equation (8.9) remains difficult. A weakened version of the of these bounds (more relaxed bounds) was proposed by Ditlevsen in [8.4] as follows.

In the lower bound of equation (8.9), $P(F_i F_j)$ is replaced by [8.5]

$$P(F_i\,F_j) \;=\; P(A) + P(B) \tag{8.10}$$

whereas, in the upper bound, the same term is replaced by

$$P(F_i\,F_j) \;=\; \max\,[\,P(A),\,P(B)\,] \tag{8.11}$$

where

$$P(A) \;=\; \Phi\,(-\beta i)\ \ \Phi\!\left(-\frac{\beta_j - \rho\beta_i}{\sqrt{1-\rho^2}}\right) \tag{8.12}$$

$$P(B) \;=\; \Phi\,(-\beta j)\ \ \Phi\!\left(-\frac{\beta_i - \rho\beta_j}{\sqrt{1-\rho^2}}\right) \tag{8.13}$$

and $\Phi(\cdot)$ is the standard normal cumulative distribution function and β_i are the individual safety indices (Hasofar-Lind) as discussed in Chapter 5. ρ is the correlation coefficient between two failure events (or modes). Such a correlation coefficient between the failure events $(F_i) = (g_i\,(\underline{x}) \le 0)$ and $(F_j) = (g_j\,(\underline{x}) \le 0)$ can be evaluated from [8.4]:

$$\rho_{g_i,\,g_j} \;=\; \frac{\text{cov}\,(g_i,\,g_j)}{\sigma_{g_i}\ \sigma_{g_j}} \tag{8.14}$$

where

$$\text{cov}\,(g_i,\,g_j) \;=\; \sum_{m=1}^{n}\ \left[\frac{\delta g_i}{\delta X'_m}\right]_*\ \left[\frac{\delta g_j}{\delta X'_m}\right]_* \tag{8.15}$$

and

$$\sigma_{g_i} \;=\; \left[\sum_{m=1}^{n}\ \left(\frac{\delta g_i}{\delta X'_m}\right)^2_*\right]^{1/2} \tag{8.16}$$

$$\sigma_{g_j} \;=\; \left[\sum_{m=1}^{n}\ \left(\frac{\delta g_j}{\delta X'_m}\right)^2_*\right]^{1/2} \tag{8.17}$$

In equations (8.14) to (8.17), X_1', X_2' ... X_n' are the reduced random variables and the derivatives are evaluated at the most likely failure points as discussed in Chapter 5. The proposed bound by Ditlevsen [8.4] apply only for normally distributed random variables.

Narrower bounds than the second order bounds can be constructed, but, they involve intersection of more than two failure events and are much more complicated.

8.4   Bounds on the Probability of Failure of a Parallel System:

A parallel system is one which fails only if all its components fail, i.e., failure of one component only will not necessarily constitute failure of the system. Schematically, such a system can be represented as shown in Figure 8.2
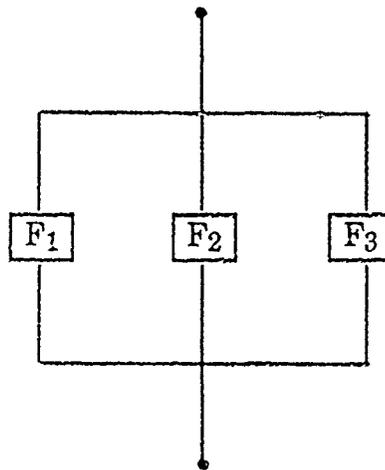
Figure 8.2. Schematic Representation of a Parallel System.

A typical example of a parallel system is a statically indeterminate structure where, because of redundancy, failure of several members along a "failure path" must take place for the entire structure to fail. The behavior of such a structure depends also on whether the members are brittle or ductile.

Generally, brittle failure implies that the member looses completely its load-carrying capacity while in ductile failure, the member maintains a certain level of load-carrying capacity after failure.

If F_i denotes again the $i\underline{th}$ event of failure and S_i the corresponding safe event, then the system failure event of a parallel system F_P of k components (i.e., failure events) is the intersection or mutual occurrence of all failure events, i.e.,

$$F_P = \bigcap_i F_i \qquad\qquad i = 1, 2, \ldots k \qquad\qquad (8.18)$$

The corresponding probability of system failure is

$$P(F_P) = P\left(\bigcap_i F_i\right) = 1 - P\left(\bigcup_i S_i\right) \qquad\qquad (8.19)$$

Equation (8.19) for failure of a parallel system should be compared with equation (8.2) for failure of a series system. It is clear that the failure of a series system is the union (any) of the component failures, whereas, the failure of a parallel system is the intersection (all) of the component failures.

Just as in a series system, the evaluation of equation (8.19) for determining the exact system failure of a parallel system is generally difficult, and, approximation by constructing bounds is usually necessary.

Simple first order lower and upper bounds can be constructed using similar arguments as for the series system. Now however, perfect correlation between all failure events ($\rho = 1.0$) corresponds to the upper bound and no correlation between any pair corresponds to the lower bound. Thus, for positively correlated failure events, these bounds are:

$$\prod_{i=1}^{k} P(F_i) \leq P(F_P) \leq \min_i P(F_i) \qquad\qquad (8.20)$$

Unfortunately, the bounds given by equation (8.20) on the probability of failure of a parallel system are wide and no second order bounds are available. In

some special cases, however, the "exact" system failure can be evaluated. For example, Thoft-Christensen and Baker (see reference [8.7]) evaluated the probability of parallel system failure under deterministic loading and other restrictive conditions.

8.5   General Systems.

A general system is one that consists of a combination of series and parallel subsystems. A useful general system from an application point of view, is one that consists of parallel subsystems connected together in a series. An example of application for such a general system is an offshore platform (or, in general a statically indeterminate structure) where each failure path can be modelled as a parallel subsystem and all possible failure paths (parallel subsystems) are connected together in a series since any of them constitute failure of the platform. This representation is called "minimal cut set" since no component failure event in the parallel subsystem (a failure path) can be excluded without changing the state of the structure from failure to safe. A schematic representation of parallel subsystems connected together in a series is shown in figure (8.3).
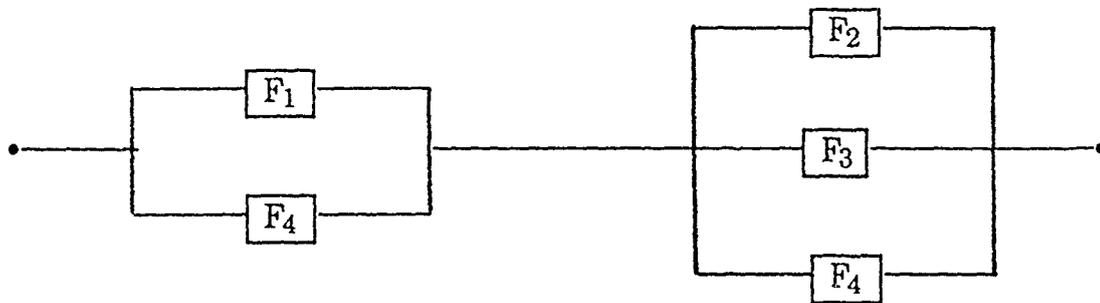
Figure 8.3. Schematic Representation of Parallel Subsystems
Connected in a Series (Minimal Cut Set)

A general system may also consist of a series of subsystems connected together in parallel (minimal link set). Such systems, however, have less potential for application to structural reliability and therefore will not be discussed further.

The failure event "F_g" of a general system consisting of parallel subsystems connected together in a series (minimal cut set) is given by the union (series) of intersection (parallel) of individual failure events, i.e.,

$$F_g = \bigcup_j \bigcap_i (F_{ij}) \qquad (8.21)$$

where (F_{ij}) is the ith component failure in the jth failure path. The probability of failure of such a system is thus determined from

$$P(F_g) = P\left[\bigcup_j \bigcap_i (F_{ij}) \right] \qquad (8.22)$$

Exact evaluation of (8.22) is difficult and requires information of the joint dependence of failure events. Similarly bounds on the probability of failure given by (8.22) are not available in general. If however, one is able to determine the probability of failure of each parallel subsystem (for example, under restrictive conditions), then first or second order bounds can be determined using equations (8.8) or (8.9) for the remaining series system.

8.6   The Probabilistic Network Evaluation Technique (PNET):

The PNET is an approximate method for estimating a single value of the system probability of failure rather than bounding it [8.5]. The motivation behind the method is that the bounds given by equations (8.8) or (8.9) for a series system can be wide if none of the events or modes of failure is dominant, i.e., if none of the probabilities of failure is much larger than the others. The same problem is encountered if the series system consists of parallel subsystems (failure paths) none of which is a dominant failure mode.

The PNET method is based on the fact that perfectly correlated (or, as approximation, highly correlated) events of failure in a series system have a system probability given by the lower bound of equation (8.6) or (8.8), whereas, independent failure events have a system probability given by the upper bound. Therefore, one may select a threshold value for the correlation coefficient and

206

assumes that failure events with correlation coefficient ρ_{1j} above or equal to the threshold value to be perfectly correlated, thus can be represented by a "representative event" which is the event among them that gives the maximum probability of failure, say $P(F_r)$ (see lower bound of equation 8.8). If a set of n failure events (modes) F_i where $i = 1, \ldots n$ is arranged in a decreasing order then the failure probability of the representative event is $P(F_1)$. The remaining, events with $\rho_{1j} < \rho_o$ are again rearranged in a decreasing order of their failure probabilities. Let these be $F_2', F_3', \ldots F_k'$ and the pair-wise correlation are $\rho_{23}', \rho_{24}', \ldots \rho_{2k}'$. Those events with $\rho_{2j}' \geq 0$ are represented by F_2'. The remaining ones are rearranged in a decreasing order and the procedure is repeated to search for other representative events (modes) of failure. The mutual correlation between the representative events will be low therefore, they may be assumed independent. Thus, the probability of system failure may be approximated by (see upper bound of equation 8.6)

$$P(F) \approx 1 - \prod_r [1 - P(F_r)]$$
(8.23)

8.7   Fault Tree and Event Tree

Fault tree is a systematic and effective method of identifying various possible failure events and their interaction that lead to a main failure event called "top event". It is usually represented by a "fault tree diagram" which starts with basic events whose probabilities of occurrence may be readily estimated and describes the various possible combinations (unions and intersections) of such events that lead to the top event or failure of the system. Its value becomes more important in complex systems where some possible modes of failure may be overlooked.

Fault tree analysis finds many applications in the design and operation of nuclear power plants. It can also be applied to complex structural system such as offshore platforms. In such analysis the fault tree diagram will help in identifying in a systematic manner the various component failures that form a "failure path" and the different possible failure paths that will lead to the top event, the failure of the entire structure. In addition to identifying all potential

failure paths, the fault tree analysis may single out the critical events that contribute significantly to the likelihood of failure of the structure.

The probability of top event (main failure) in a fault tree analysis is calculated through unions and intersections of subevents which are expressed in terms of basic events (component failure) for which the failure probabilities can be estimated. Although fault tree analysis provides the logic leading to the top event, it does not eliminate the difficulties in computing the probabilities of unions and intersections of correlated events. Approximations and bounds may still have to be used if a quantitative assessment is to be made of the probability of occurrence of the top event.

Qualitative evaluation of a fault tree can provide also valuable information to designers. Without knowing accurately the probabilities of failure of events and subevents, the fault tree analysis may point out the critical basic events and the critical paths that contribute significantly to the occurrence of the top event. With this knowledge a designer may then take the appropriate steps to reduce the probability of occurrence of such critical basic events.

Event tree analysis on the other hand starts with the top event (main failure) and examines in a logical manner all possible consequences resulting from the occurrence of such an event (for example loss of life, pollution, explosion, fire, etc). The consequences of the top event (now called the initiating event) may or may not be series depending on the possible occurrence of other adverse events following the initiating event. The identification of all possible subsequences and scenarios is best accomplished through an event tree diagram. Each "path" in the event tree represents a sequence of subsequent events leading to a particular consequence. The probability of occurrence of a specific consequence depends on the probabilities of the subsequent events and is simply the product of conditional probabilities of all events along that path.

8.8   Reliability Bounds for Ship Primary Strength:

Reliability bounds for ship primary strength were developed in 1972 in reference [8.6]. In the primary behavior, the ship hull is considered as free-free non-uniform beam supported by water pressure. Wave loads (bending moment)

208

are calculated using the equations of motion of the ship if dynamic effects are to be included otherwise by balancing the vessel on a wave configuration. The loads on the vessel alternate from hogging which produce compression in the bottom plating to sagging which induce compression in the deck. This hog/sag variation must be considered in the hull reliability analysis.

In each hog/sag condition there will be several possible modes of failure eg., plate and panel buckling, tensile yield, etc. If F^h and F^s represent hogging and sagging events of failure, respectively, then the combined event of failure F^c is given by the union of the two events, i.e.,

$$(F^c) = (F^h) U (F^s) \tag{8.24}$$

Since hogging and sagging are mutually exclusive events, i.e., the vessel can be either in hogging or in sagging condition (but not both at the same time), then the union of the two events given in (8.24) is simply their sum. The probability of combined event of failure is thus

$$P(F^c) = P(F^h) + P(F^s) \tag{8.25}$$

As mentioned earlier, each of the hogging and sagging conditions will have several possible modes of failure (or limit states). In each case these modes can be modelled as a series system since any of them constitute a failure of the hull (or a limit state to be prevented). Thus bounds on the probability of failure in hogging condition $P(F^h)$ and in sagging condition $P(F^s)$ can be constructed using equation (8.8) or (8.9) for first or second order bounds, respectively. The bounds on the combined probability $P(F^c)$ are simply the sum of the bounds on each condition as implied by equation (8.25).

Experience indicated that in many cases either hogging or sagging condition is governing in the reliability analysis depending on whether the stillwater bending moment is hogging or sagging (in much the same manner as in the usual deterministic analysis). In some cases, however, both conditions must be included otherwise the estimated reliability will be unconservative.

8.8.1 Numerical Example:

In reference [8.6], the probabilities of failure (or reaching a limit state) were calculated for a Mariner class vessel in hogging and sagging conditions using level 3 reliability method. The stillwater moment for the Mariner is a hogging moment. Several modes were considered in each condition and the results are as follows:

a. Hogging Condition

i) Tensile yield of deck plating: $p_f = 6.16 \times 10^{-7}$

ii) Compressive post-buckling yield of inner bottom plating: $p_f = 4.03 \times 10^{-5}$

iii) Compressive post-buckling yield of bottom plating under lateral and inplane loads: $p_f = 62.99 \times 10^{-5}$

iv) Compressive grillage failure of bottom shell under combined loads: $p_f = 1.47 \times 10^{-5}$

The first order bound on the probability of failure in hogging condition p_f^h were thus obtained (see equation 8.8) as

$$\max (6.16 \times 10^{-7}, 4.03 \times 10^{-5}, 62.99 \times 10^{-5}, 1.47 \times 10^{-5}) \leq p_f^h$$

$$\leq 6.16 \times 10^{-7} + 4.03 \times 10^{-5} + 62.99 \times 10^{-5} + 1.47 \times 10^{-5}$$

or

$$6.3 \times 10^{-4} \leq p_f^h \leq 6.8 \times 10^{-4} \tag{8.26}$$

Notice that these bounds are tight since one mode of failure is dominant (post-buckling yield of bottom plating). There is no need to consider second order bounds.

b. Sagging Condition

i) Tensile yield of bottom plating: $p_f = 1.55 \times 10^{-14}$

ii) Inelastic buckling of deck plates between stiffeners: $p_f = 2.29 \times 10^{-11}$

iii) Grillage instability of deck: $p_f = 2.18 \times 10^{-7}$

Bounds on the probability of failure in sagging condition $p_f{}^s$ can be constructed in a similar manner as those for the hogging condition. The sum of the two sets of bounds would then give the bounds on the combined probability of failure. It is clear, however, that in this case the bounds on the failure modes in sagging are of the order $\sim 10^{-7}$, much smaller than those given by equation (8.26) for the hogging condition. The latter bounds, therefore, can be considered as bounds on the combined probability of failure.

REFERENCES

8.1 Cornell, C. A., "Bounds on the Reliability of Structural Systems," Journal of Structural Division, ASCE, Vol. 93, No. ST1, February 1967.

8.2 Kounias, E. G., "Bounds for the Probability of a Union with Applications," Annals of Math. Stat., Vol. 39, No. 6, 1968.

8.3 Hunter, D., "An Upper Bound for the Probability of a Union," Journal of Applied Probability, Vol. 3, No. 3, 1976, pp. 597-603.

8.4 Ditlevsen, O., "Narrow Reliability Bounds for Structural Systems," Journal of Structural Mechanics, Vol. 7, No. 4, 1979, pp. 453-472.

8.5 Ang, A. H.-S. and Tang, W. H., Probabili y Concepts in Engineering Planning and Design, Vol. II, John Wiley and Sons, Inc., New York, 1984.

8.6 Mansour, A., "Probabilistic Design Concepts in Ship Structural Safety and Reliability," Trans. SNAME, Vol. 80, 1972, pp. 64-97.

8.7 Thoft-Christensen, P. and Baker, M., Structural Reliability Theory and Its Application, Springer-Verlag, Berlin, 1982.

9. FATIGUE RELIABILITY

9.1 INTRODUCTION

Fatigue is the degradation in material, element, and system strength and stiffness as a result of cyclic straining-stressing.

Materials in marine structures can consist of steels, concretes, synthetic fibers, and soils (foundation). Elements can range from bulkheads to hatch cover openings, from cylindrical braces to mooring lines, and from deep (piles) to shallow (anchors, mats) foundations. Systems represent assemblages of elements, and can range from cargo ships to fixed and floating platforms.

Cyclic straining can develop from a wide variety of environmental (thermal, wind, wave, current, ice, earthquake), construction (installation transport, launch), and operational (slamming, equipment, cargo) causes. The relentless cyclic forces are perhaps one of the most distinguishing characteristics of the marine structures' environment.

Design for fatigue reliability has four principal lines of defense:

1. Minimize stress-strain risers (stress concentrations) and cyclic straining-stressing through good engineering of the structural system and its details. This requires a high level of engineering quality assurance (QA) at the concept-development-design stage.

2. Minimize flaws (misalignments, poor materials, porosity-voids, etc.) through good, practical material and fabrication

specifications and practices. This requires a high level of QA during the development of plans and specifications and during construction (involving materials selection, fabrication, transportation and installation). Further, there is a similar QA program required during operations to properly maintain the system.

3. <u>Minimize</u> <u>degradation</u> <u>at</u> <u>the</u> <u>local</u> <u>element</u> through selection of good materials and fabrication practices, and good engineering designs (e.g. crack stoppers, damage, localizer, and repairable elements). This requires a recognition that when (not if) fatigue degradation occurs, all reasonable precautions are taken to restrict its development and effects. Note, again QA plays a key role, particularly during operations to disclose the presence of fatigue degradation (early warning).

4. <u>Minimize</u> <u>degradation</u> <u>at</u> <u>the</u> <u>system</u> <u>level</u> so that when (not if) local fatigue degradation occurs, there are no significant effects on the system's ability to perform satisfactorily. Here good fatigue design requires system robustness (redundancy, ductility, capacity) and system QA. Inspections and monitoring to disclose global system degradation are another strategy to minimize potential fatigue effects.

The purpose of this discussion has been to outline the major factors and the complex interplay of these factors in determining fatigue reliability. Cyclic strains, material characteristics, engineering design, specifications, and life-cycle QA (inspections, monitoring) are all parts of the fatigue equation. This is the engineering equation of "fail safe design" -- fatigue may occur, but the structure can continue

to function until the fatigue symptoms are detected and repairs are made. The alternative is "safe life design" - no significant degradation will occur and no repairs will be necessary. Safe life designs are difficult to realize in many long-life marine structures or elements of these structures.

Uncertainties and variabilities are present in each of the parts, and thus, reliability methods can play an important role in assisting the engineer to achieve fatigue reliable-durable structural systems.

9.2 FATIGUE ANALYSIS

A fatigue analysis can be organized into five basic components:

1. Characterize the life-cycle (short term and long term) cyclic conditions.

2. Determine the cyclic forces imposed on or induced in the structure (system).

3. Evaluate the cyclic strains-stresses developed in the element (detail) of concern.

4. Determine the degradation in strength and stiffness (damage of the element (detail) caused by the cyclic strains-stresses).

5. Given the fatigue damage, evaluate the acceptability of the element (detail) performance.

In development of the following simplified fatigue design procedures [9.1], it will be assumed that waves are the source of cyclic forces. It will be assumed that the long-term (e.g. T = 100 years) wave height distribution can be represented by Weibull distribution (Figure 9.1).

For storms, the cumulative distribution function [CDF = $F_X(X)$] of wave heights (h) is:

$$F_H(h) = 1 - \exp\left[-\left(\frac{h}{H_i}\right)^{\epsilon_i} \ln N_i\right] \qquad (9.1)$$
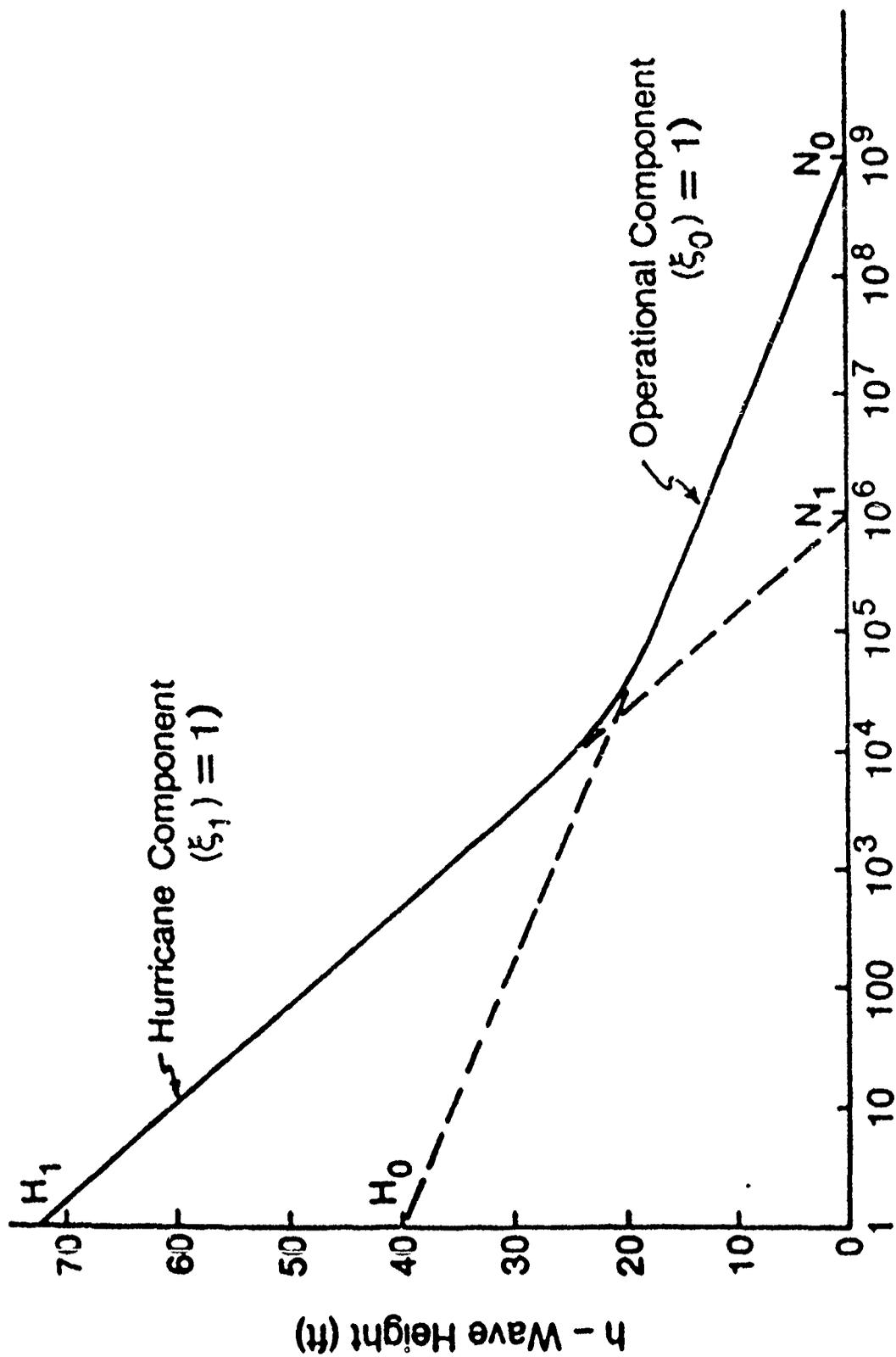
FIG. 9.1 **TWO-COMPONENT WAVE HEIGHT DISTRIBUTION**

217

For non-storm conditions, the CDF is:

$$F_H(h) = 1 - \exp\left[-\left(\frac{h}{H_o}\right)^{\epsilon_o} \ln N_o \right]$$

(9.2)

The structural detail fatigue stress range (peak to peak) (S_f) will be taken to be a function of the wave height:

$$S_f = CH^a$$

(9.3)

Next, the number of cycles to "failure" (N) of the detail subjected to a cyclic stress range (S_f) will be taken as (Figure 9.2)* [9.2]:

$$N = KS_f^{-m}$$

(9.4)

Accumulation of fatigue damage (D) will be assumed to be described by a linear damage accumulation rule (Palmgren-Miner):

$$D = \sum_i \frac{n(S_{fi})}{N(S_{fi})}$$

(9.5)

---

*Footnote:

Log N = Log K - m Leg S_f

and,   Sf = (K/N)$^{1/m}$

and,   N = K S_f^{-m}

m = negative slope of S-N curve

Log K = life intercept of S-N curve

218

FIG. 9.2 API DESIGN STRESS RANGE (S$_{cD}$) AND NUMBER OF CYCLES TO FAILURE (N)

219
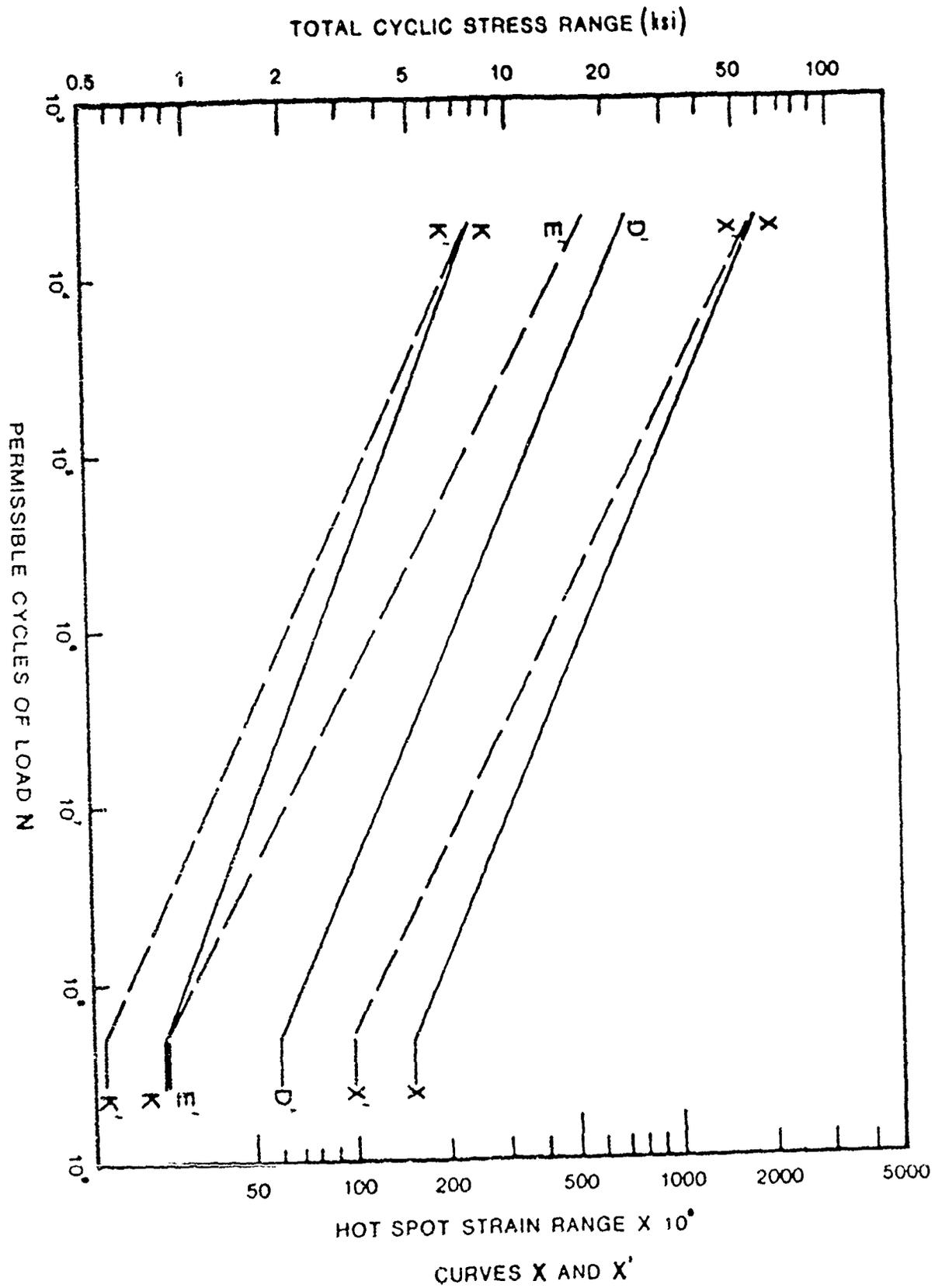
Where

$n(S_{fi})$ = number of stress cycles at stress fi

$N(S_{fi})$ = number of cycles to failure at stress fi.

The summation is overall stresses, S_{fi}, experienced by the structural detail. When $D = 1$, failure is presumed to occur.

Fatigue damage (D_L) accumulated over the life (T) of the detail can be computed from the following equation [9.1]:

$$D_L = \frac{TC^m}{K}(Y_0 + Y_1) \tag{9.6}$$

Where

$$Y_0 = \frac{N_0}{T}H_0^{\alpha_m}(\ln N_0)^{\frac{-\alpha_m}{\epsilon_0}}\Gamma\left(1 + \frac{\alpha_m}{\epsilon_0}\right) \tag{9.7}$$

$$Y_1 = \frac{N_1}{T}H_1^{\alpha_m}(\ln N_1)^{\frac{-\alpha_m}{\epsilon_1}}\Gamma\left(1 + \frac{\alpha_m}{\epsilon_1}\right) \tag{9.8}$$

$\Gamma(\cdot)$ = Gamma function

Now, let the design accumulated damage be limited to a fraction of the life damage:

$$D_D = \frac{D_L}{F_{sf}} \qquad\qquad (9.9)$$

or the design service life (T_S) be:

$$T_s = (F_{sf}) \cdot T \qquad\qquad (9.10)$$

where

F_{sf} = fatigue life or damage Factor of Safety (commonly in the range of 2 to 3).

The fatigue design stress (S_{fD}) will be related to the fatigue design wave height (H_{fD}) as before:

$$S_{fD} = CH^{\alpha}_{fD} \qquad\qquad (9.11)$$

Thus,

$$S_{fD} = \left[\frac{KH^{\alpha m}_{fD}}{T_s(Y_0 + Y_1)} \right]^{\frac{1}{m}} \qquad\qquad (9.12)$$

Based on an H_{fD} = 70 feet,* the long-term wave height distribution in Figure 9.1, and the API-X S-N curve (weld without profile control, Figure 9.2), S_{fD} can be computed as functions of T_S and α (Figure 9.3) [9.1].

Note:

Use an H_{fD} close to extreme condition design wave height, e.g. 100-year height.
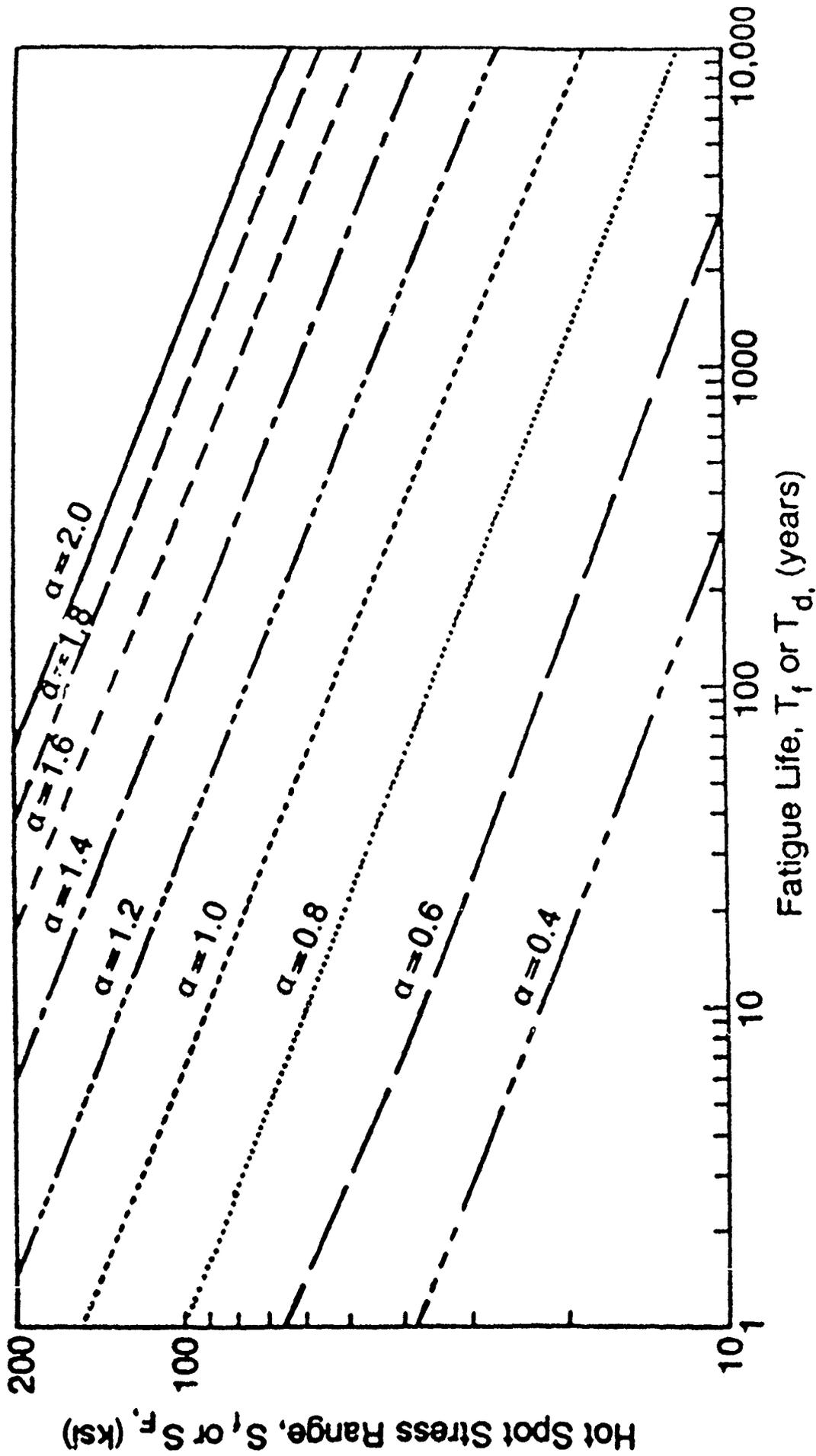
FIG. 9 .3   STRESS RANGE VS. FATIGUE LIFE FOR RANGE OF α

222

For example, for a detail life of 25 years and a factor-of-safety of 2
(T_S = 50 years), and a wave height exponent (α) of 1.0, the design stress
range is indicated to be 65 ksi. For a detail stress concentration
factor (SCF) of 3, this would equate to a nominal allowable design stress
of 22 ksi (based on API X S-BN curves, Figure 9.2). For an α = 1.5, the
design stress range would increase to 150 ksi. For an SCF = 3, the
nominal stress range would be 50 ksi.

In design practice, it is often useful to state the design stress range,
S_{fD}, as a peak stress value, S_{PD}. This can be accomplished by defining a
stress ratio, R, that is the ratio of the minimum stress, S_{min}, to the
maximum stress, S_{max} for the design wave height, H_{fD}. Thus:

$$S_{PD} = \frac{S_{fD}}{(1-R)} \tag{9.13}$$

The values of R will be structure dependent. For conventional
template-type, shallow water platforms, R is typically close to -0.33.

9.3 RELIABILITY MODELS

Based on a fatigue analysis as outlined in the previous section, the principal sources of uncertainty can be organized as follows:

1. S-N relationship (Eq. 9.4, Figure 9.2)
2. D-N relationship (Eq. 9.5)
3. S-H relationship (Eq. 9.3)
4. H-N relationship (Eqs. 9.1, 9.2)
5. S-SCF relationship
6. D_D-D_L (or L_D-L) relationship (Eqs. 9.9, 9.10)
7. Other factors such as corrosion and cathodic protection

Additional details on these sources of uncertainty are given in Table 9.1 [9.3]. There are many sources of complexly interrelated uncertainties and variabilities. It is the primary purpose of a fatigue reliability analysis to logically organize these sources, and then to quantitatively evaluate them to determine what factors-of-safety (e.g. Eqs. 9.9 and 9.10) (alternatively, levels of reliability) should be employed in a given design-analysis framework.

Wirsching [9.3, 9.4] has made extensive fatigue reliability studies for fixed offshore structures. Munse [9.5] has made similar studies for ship structures. Recently, Wirsching and Chen [9.6] have summarized and contrasted results of these two studies. The following discussion will be based on these developments.

Alternative methods for computing fatigue damage are summarized in Figure 9.4 [9.3]. Table 9.2 [9.3] summarizes the alternative analytical expression for computing fatigue damage at a joint (detail).

TABLE 9.1

A SUMMARY OF FACTORS AND CONSIDERATIONS
RELATED TO FATIGUE IN WELDED JOINTS OF OFFSHORE PLATFORMS

FATIGUE BEHAVIOR OF WELDED JOINTS

- Definition of fatigue failure in S-N data
- Size effect in S-N data
- Effect of weld profile
- Effect of corrosion and cathodic protection
- Assumption of a linear model and lognormal distribution for N
- Classification of joint on the basis of geometry rather than load pattern
- Relationship between stress at joint and stress used to obtain S-N curve
- Ignoring possible stress endurance in S-N curve
- Compatibility of determination of hot spot stress with S-N curve

---

MANUFACTURING CONSIDERATIONS

- Fabrication uncertainties '
- Requirements on weld contours not met

DEFINITION OF THE ENVIRONMENT

- Use of full scatter diagram of H_s - T_D
- Variations in T_D
- % occurrence estimates
- Wave directionality
- Interaction of Waves and Currents
- Theoretical model used for ocean waves

HYDRODYNAMIC LOADS ON STRUCTURE

- Inertia and Drag Coefficient
- Directional wave spectra which accounts for wave spreading
- Marine growth
- Sheltering effects

STRUCTURAL RESPONSE TO HYDRODYNAMIC LOADS

- Assumptions made in spectral analysis

   a. linear response during transfer function development
   b. linearization of drag term
   c. at joints, i. No flexibility
                  ii. effect of can
                  iii. center to center coordinates
   d. Soil stiffness in Dynamic Model
   e. Damping effects in structural response
   f. Dynamic response not accounted for in analysis

FATIGUE STRESSES AT JOINT

- Method of analysis to evaluate stress concentration factors (SCF)
- Parametric equations used for SCF
- Point at intersection where failure occurs

FATIGUE DAMAGE EQUATIONS

- Assumption of Miner's Rule
- Assumption of narrow band damage equation in spectral approach
- Assumption of Weibull distribution for stress ranges in stress distribution approach

---

OTHER CONSIDERATIONS

- Errors by designers
- Bad judgement during towing and installation
- In service loads

FIG. 9.4 CLASSIFICATION OF FOUR BASIC METHODS OF COMPUTING FATIGUE DAMAGE

Seastate Definition

Wave Height History

Wave Exceedance Histogram (sometimes called the "deterministic" method). This technique used by Lloyd's. Damage computed from wave exceedance diagram

Wave distribution method; stress assumed proportional to wave height, and wave height distribution described by lognormal, Weibull, etc. Nolte-Hansford methdo assumes Weibull distribution.

Stress Range History

Stress Range Distribution Method; stress range modelled theoretically, usually Weibull. Stress range distribution can be derived from spectral method, wave distribution method, etc.

Spectral Analysis (Based on a full scatter diagram defining the long term seastate)

Spectral Method (sometimes called the "probabilistic" method). Damage computed from each seastate in scatter diagram, in which stress is considered a stationary random process

The Equivalent Weibull Method: This method used by DnV. An equivant Weibull distribution of long term stress ranges is derived using spectral analysis

226

TABLE 9.2

A SUMMARY OF EXPRESSIONS FOR FATIGUE DAMAGE JOINT

FATIGUE DAMAGE AT TIME T,

$$D = TB^m \Omega / K$$

m, K = parameters from S-N curve

B = factor to account for uncertainties in estimating fatigue stresses from oceanographic data

Ω = stress parameter

STRESS PARAMETER USING VARIOUS APPROACHES TO THE STRESS DISTRIBUTION

Wave Exceedance Diagram (Deterministic Method)

$$\Omega = f_0 \sum_i \zeta_i S_i^m$$

f_0 = average frequency of stresses

S_i = stress range

ζ_i = fraction of total stress ranges that S_i is acting

Spectral Method (Probabilistic Method)

$$\Omega = \lambda(m)(2\sqrt{2})^m \Gamma(\frac{m}{2} + 1) \sum_i \gamma_i f_i \sigma_i^m$$

$\lambda(m)$ = rainflow correction

$\Gamma(\cdot)$ = gamma function

γ_i = fraction of time in i^{th} seastate

f_i = frequency of wave loading in the ith seastate

σ_i = RMS of stress process in the ith seastate

Weibull Model for Stress Ranges

$$\Omega = \lambda(m) f_0 S_m^m [\ln N_T]^{-m/\xi} \Gamma(\frac{m}{\xi} + 1)$$

S_m = largest "once in a lifetime: stress range

ξ = stress range parameter

N_T = total number of stress ranges in design life

Note: Let $\lambda(m) = 1$ unless the Rayleigh assumption was made in the analysis.

227

Wirsching's reliability analysis has been cast in a lognormal format in which the random variables are assumed to have lognormal distributions. The time for fatigue failure (T) is expressed as a function of the accumulated damage (D = Δ), the S-N curve parameters (K, m, Eq. 9.4), a stress range model error parameter (B = actual/computed stress range), and a stress range parameter (Ω, Table 9.2):

$$T = \frac{\Delta K}{B^m \Omega} \tag{9.14}$$

The probability of a fatigue failure (P_f) is taken as:

$$P_f = P\left[T \leq T_s\right] \tag{9.15}$$

where P[·] is the CDF of T, and T_S is the service life.

$$P_f = \Phi(-\beta) \tag{9.16}$$

where $\Phi(\cdot)$ = standard Normal distribution function and β is the Safety Index:

$$\beta = \frac{\ln \overline{T}/T_s}{\sigma_{\ln T}} \tag{9.17}$$

where

$$T^{\overline{x}*} = \text{median value of T, and}$$

*Note: $\overline{x}$ will be taken as the median (50th percentile) value of the parameter x.

228

$$T = \frac{\overline{\Delta K}}{\overline{B}^m \Omega} \qquad (9.18)$$

$$\sigma_{\ln T} = \left[\ln \left(1 + C_{\Delta}^2 \right) \left(1 + C_K^2 \right) \left(1 + C_B^2 \right)^{m^2} \right]^{1/2} \qquad (9.19)$$

in which the C's are the Coefficients of Variation (COV = C) of each variable.

Uncertainty in the stress ranges (S) is expressed through the stress range model error parameter (B). The errors are attributed to:

1. Fabrication and assembly (B_M)

2. Seastate characterization (B_S)

3. Wave load predictions (B_F)

4. Determination of member loads (B_N)

5. Estimation of stress concentration factors (B_H)

Thus,

$$B = B_M \cdot B_S \cdot B_F \cdot B_N \cdot B_H \qquad (9.20)$$

and

$$C_B = \left[\prod_i \left(1 + C_i \right) - 1 \right]^{1/2} \qquad (9.21)$$

for i = M, S, F, N, H.

229

Tables 9.3 and 9.4 summarize the statistical estimates on the B components and K, B and Δ random variables, respectively. At the bottom of Table 4, note the range of Safety Index implied by API's RP 2A design wave peak stress rule (limits nominal brace stress to 60 ksi).

Munse's fatigue reliability analysis [9.5, 9.7] has been based on a two parameter Weibull distribution of stresses (S) and cycles (N) (Figure 9.5).

$$F_s(s) = P(S \le s) = 1 - \exp\left[-\left(\frac{s}{\delta}\right)^\epsilon\right] \qquad (9.22)$$

where

ϵ = Weibull distribution shape parameter

δ = Weibull distribution scale parameter

Defining a design stress (S_m) such that this value is exceeded on an average once every N_T times:

$$\delta = S_m\left[\ln N_T\right]^{-\frac{1}{\epsilon}} \qquad (9.23)$$

N_T* is the total number of cycles in the service life T. Thus,

$$F_s(s) = 1 - \exp\left[-\left(\frac{s}{S_m}\right)^\epsilon \ln N_T\right] \qquad (9.24)$$

---

*Note: $N_T = T_s f_0$ = Service Life x Average Stress Frequency

TABLE 9.3

SUMMARY OF BIAS AND COEFFICIENT
OF VARIATION OF COMPONENTS OF B

Random variables representing sources of uncertainty in fatigue stress estimates (1)	Bias[a] (2)	COV[b] (3)
B_M	0.90–1.30[g]	0.10–0.30[g]
B_S	0.60[c]–1.20	0.40[d]–0.60[e]
B_F	0.60[f]–1.10	0.10–0.30
B_N	0.80–1.10	0.20–0.40[g]
B_H	0.80[g]–1.20	0.10–0.50[g]

[a]Bias = actual load or stress/load or stress estimated by current analysis procedure; for each B_i, the bias can be interpreted as the median value $\bar{B}_i$.

[b]COV $= \sqrt{\exp(\sigma^2) - 1}$, in which $\sigma = \ln(X_U/X_L)/6$; and X_U and X_L = upper and lower limits of X.

[c]$\bar{B}_S = \bar{B}_P \cdot \bar{B}_D = (0.9)(0.7) \cong 0.60$ in which P = percent occurrence of each seastate; and D = directionality.

[d]This relatively large figure, which dominates C_s, is due to the sensitivity of the dynamic response to small variations in T_D. The figure of 0.40 is due to this effect only.

[e]This figure was obtained by Eq. 7.18 by assuming "maximum" COV's of 0.4 for dynamic response, and 0.3 each for directionality and percent occurrence effects. The resulting figure of 0.60 is considered to be the largest reasonable value.

[f]This bias occurs when wave spreading is not considered in the development of the response spectra.

[g]These extreme values should be used only when supporting evidence exists.

TABLE 9.4

EVALUATION OF SAFETY INDEX, β

IMPLIED BY API RP2A DESIGN WAVE PEAK STRESS RULE

USING DIFFERENT DATA SETS

Design factors (1)		Data Set					
		A (2)	B (3)	C (4)	D (5)	E (6)	F (7)
S-N curve, in kips	m	4.38[a]	4.38[a]	4.42[b]	3.00[c]	3.22[d]	3.00[i]
per square inch	$\bar{K}$	4.6E12	4.6E12	1.55F12	5.25E10	1.29E11	1.46E10
units	C_K	0.73	0.73	1.35	0.73	1.25	0.67
Rainflow correction	λ	0.79	0.79	0.79	0.86	0.85	0.86
Damage ratio	Δ	1.00	1.00	1.00	1.00	1.00	1.00
	C_Δ	0.30	0.30	0.30	0.30	0.30	0.30
Stress modeling	$\bar{B}$	0.80[e]	0.70[f]	0.70[f]	0.70[f]	0.70[f]	0.70[f]
error	C_B	0.17	0.50	0.50	0.50	0.50	0.50
Average frequency, f_0, in hertz		0.25	0.25	0.25	0.25	0.25	0.25
Safety index implied by[g] RP2A design wave peak stress rule (60 ksi rule), β		5.34[h]	2.78	2.09	2.62	2.57	1.83

[a]Data from Commentary of API RP2A, p. 81, Fig. C2.5.3-2.

[b]AWS-X data, elastic range only.

[c]T and K joint data provided by member of Technical Advisory Committee

[d]T and K joint data: an "improved" version of data set D.

[e]Values provided by member of Technical Advisory Committee. Value of C_B now thought to be low.

[f]Values provided by member of Technical Advisory Committee. Numbers are now considered reasonable for "worst case" analysis in which wave spreading and wave directionality are not considered.

[g]As computed by solving for β_0 in Eq. 7.16

[h]Relatively high value due to small value of C_B. See superscript e above.

[i]The "T-curve" from UK DOE RULES

Note: For a 20-year life, $S_R = 53.2$ ksi; $\xi = 0.69$ for 20 year-wave. (Same structure would have $S_R = 100$ ksi and $\xi = 0.57$ for 100-year wave climate.)

232

Figure 9.5 [9.3] shows this distribution for $N_T = 10^8$ cycles. Figure 9.6 [9.7] shows measured long term, low frequency, wave-induced ship hull girder stresses. Shape parameters (ϵ) in the range of 0.7 to 1.3 model these data well.

The Weibull shape parameter (ϵ) will depend on a large number of factors such as wave conditions, type of structure, dynamic response of structure, position of fatigue detail in the structure. ϵ characterizes the severity of the fatigue stresses relative to the extreme design stress. $\epsilon = 1$ yields a straight line on a semi-log plot (Figure 9.1), and $\epsilon = 2$ results in the Rayleigh distribution.

Guidelines for ϵ for platforms in the Gulf of Mexico are given in Figure 9.7 [9.8]. Waterline braces and floating marine structures may have ϵ in excess of 1.0. Munse reports [9.5] ϵ's in the range of 0.7 to 1.3 for hull girder stresses in tankers and cargo ships.

Munse's fatigue reliability model addresses the uncertainty of fatigue life (expressed as COV = C_N) as a function of uncertainties in stress evaluation (C_S), workmanship in fabrication of the details (C_C), and fatigue assessment (C_F):

$$C_N = \left[C_F^2 + m^2 C_s^2 + C_c^2 \right]^{1/2} \tag{9.25}$$

where

$$C_F = \left[S_{SN}^2 + C_{mR}^2 \right] \tag{9.26}$$

233
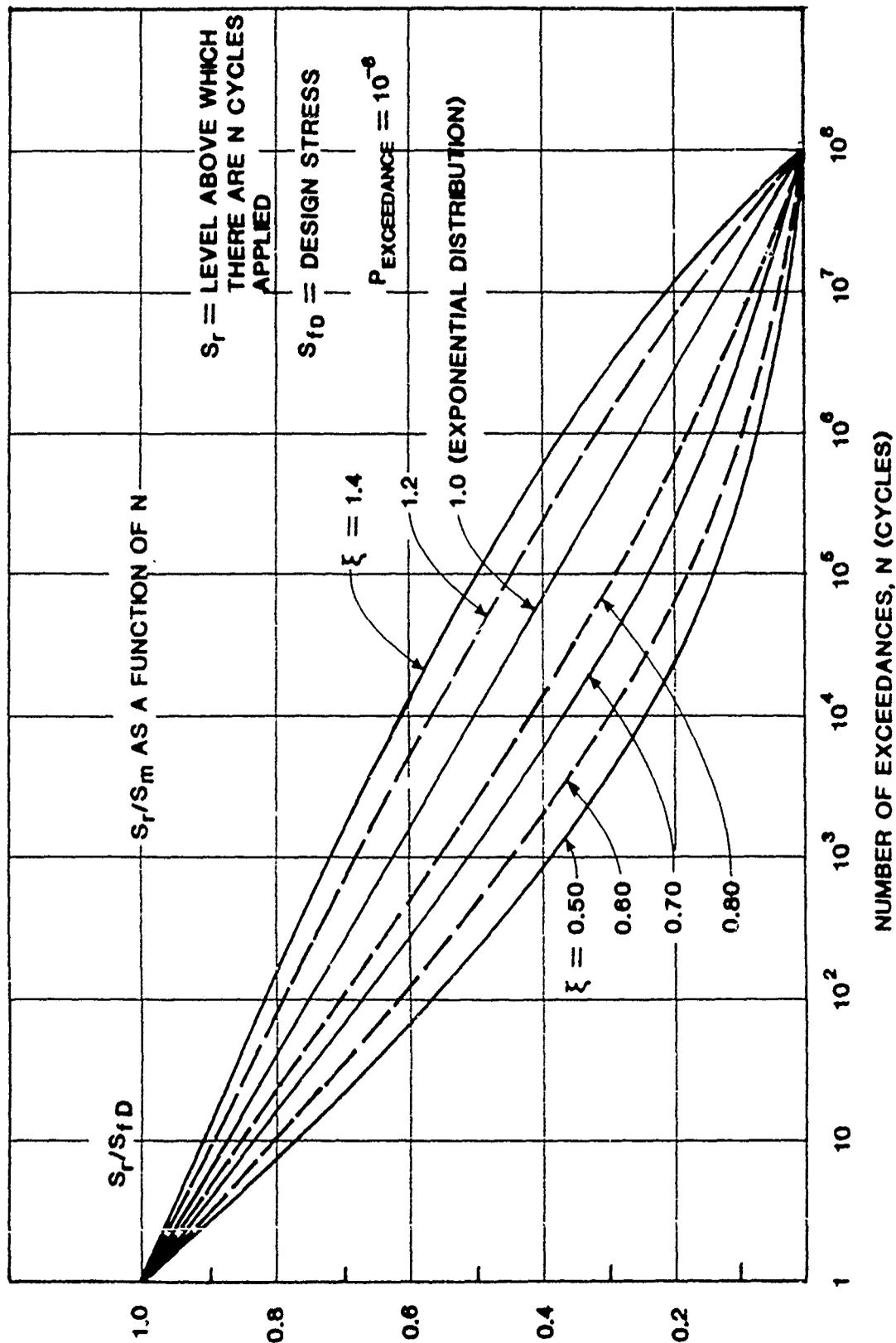
FIG. 9.5   WEIBULL LONG TERM DISTRIBUTION OF STRESS RANGE

234
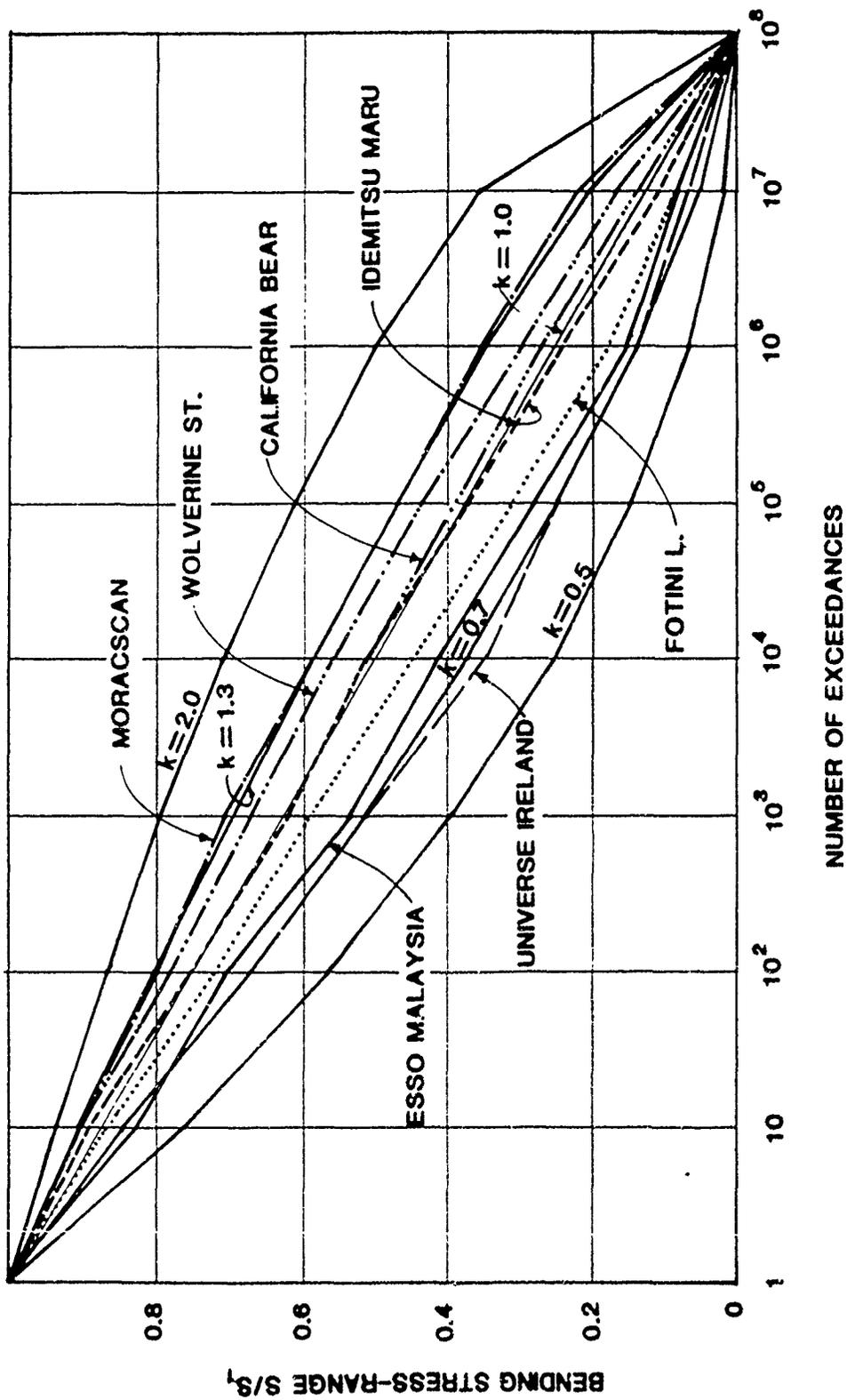
FIG. 9.6 **LOADING HISTORIES OF LARGE TANKERS, BULK CARRIERS AND DRY CARGO VESSELS COMPARED WITH WEIBULL**

235

DEPENDS ON
SHOALING
(SHELF PROFILE)

DEPENDS ON
NAT. PERIOD

VERY NARROW

BROAD

GULF OF MEXICO

(A) WATER DEPTH
GULF OF MEXICO

HOMOGENEOUS
WAVE CLIMATE

GULF OF
MEXICO

WATER DEPTH $\geq$ 100 FT.

(B) POSITION IN STRUCTURE
FEET BELOW MSL

HOMOGENEOUS
WAVE CLIMATE

INERTIA
DOMINATED

GULF OF MEXICO

DRAG
DOMINATED

WATER DEPTH $\geq$ 100 FT.

(C) NATURAL PERIOD-
SECONDS

AFTER REF. 9.8
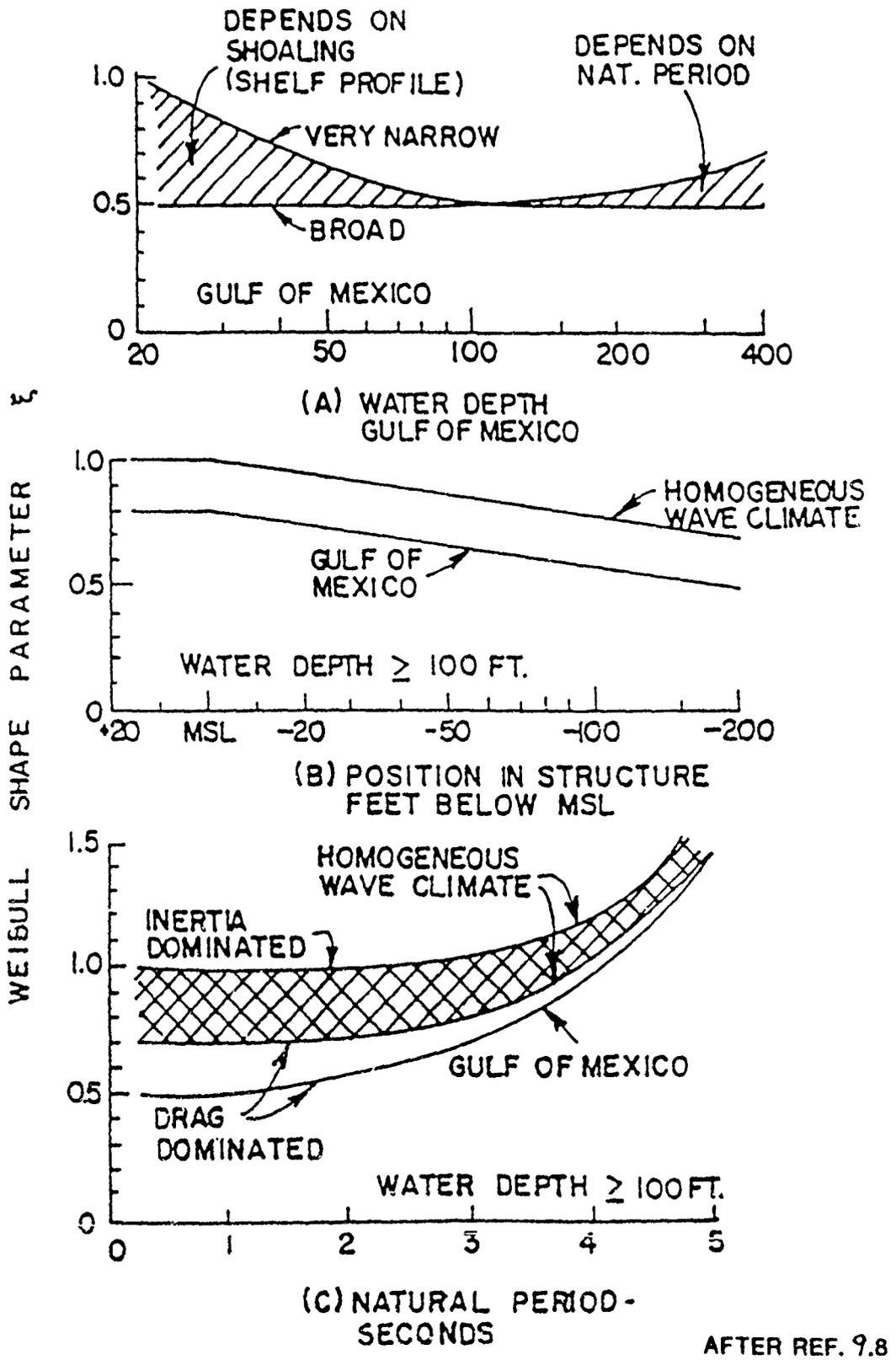
FIG. 9.7   SUMMARY DESCRIPTION OF ξ FOR GULF OF MEXICO
FIXED PLATFORMS

236

and

C_{SN} = COV associated with S-N data

C_{mR} = COV associated with Miner's rule

m = slope of N-N curve

Based on available fatigue data [9.7], Munse estimates the following
coefficients of variation:

- C_{SN} = 0.62
- C_{MR} = 0.15
- C_{S} = 0.10
- C_{C} = 0.40
- C_{N} = 0.96

These estimates do not include any effects due to corrosion. Munse [9.7]
recommends use of a total uncertainty (C_N) of 0.80 until letter values
can be established. Munse's C_N can be directly compared with Wirsching's
C_K (0.73 to 1.35, Tables 9.1 and 9.4).

Again, assuming Miner's rule and that $D = 1$,

$$E\left(S^m\right) = \frac{K}{\bar{N}} \tag{9.27}$$

where $\bar{N}$ is the mean life, and $E(S^m)$ is the mean or expected value of S^m,
gives the probability of failure (P_f) at the service life (N_S) as:

$$P_f = \left[\frac{T_s E(S^m) \Gamma\left(1 + C_N^{-1.08}\right)}{K}\right]^{C_N^{-1.08}} \tag{9.28}$$

where

$$E(S^m) = \lambda(m) S^m \Gamma\left(\frac{m}{\epsilon} + 1\right) \tag{9.29}$$

Note that the Weibull shape parameter ϵ has been approximated as:

$$\epsilon = C_N^{-1.08} \tag{9.30}$$

and the scale parameter δ determined as:

$$\delta = \frac{\tilde{N}}{\Gamma\left(\frac{1}{\epsilon} + 1\right)} \tag{9.31}$$

where

$\tilde{N}$ = mean life to failure obtained from a least squares analysis of fatigue data.

As noted in Table 9.2, a correction factor, identified as the rainflow correction factor λ_m [9.9] should be applied to the stress parameter when the Weibull parameters (ϵ, δ) are based on an analysis which uses the assumption of a narrow-band process (Rayleigh) used to describe short term distributions of wave heights in each of the stationary seastates composing the long-term distribution. For S-N curve slopes ranging between m = 3 and m = 4, and short-term seastate spectral widths greater than 0.5, λ_m = 0.86 to λ = 0.80 [9.3].

9.4 DESIGN APPLICATIONS - DETAILS

Reliability evaluations of the fatigue design of a structural detail (joint) can be developed from either the Wirsching lognormal based distribution of N (Eqs. 9.16 to 9.19) or the Munse Weibull based distribution of N (Eqs. 9.25 to 9.29).

Using these two approaches, an allowable/design stress range, S_{fD}, can be defined based on a Weibull distribution of stresses as [9.5, 9.6]:

$$S_{fD} = S_f \psi R_F \qquad (9.32)$$

where

$$S_f = \left(\frac{K}{N}\right)^{1/m} = \text{mean stress range for failure at N cycles} \qquad (9.33)$$

$$\psi = \ln N^{\frac{1}{\epsilon}} \left\{ \Gamma\left(1 + \frac{m}{\epsilon}\right)\right\}^{-\frac{1}{m}} \qquad (9.34)$$

$$= \text{random load factor}$$

$$R_{Fm} = \left[\frac{P_{fD} C_N^{-1.08}}{\Gamma(1 + C_N^{1.08})}\right]^{\frac{1}{m}} \qquad (9.35)$$

$$= \text{Munse Reliability Factor [9.7]}$$

$$R_{Fw} = \frac{1}{B}\left[\frac{\Delta}{\exp(\beta_D \sigma_{\ln T})}\right]^{\frac{1}{m}} \qquad (9.36)$$

$$= \text{Wirsching Reliability Factor [9.6]}$$

239

where P_{fd} and β_0 are the design probability of failure and safety index, respectively.

Ideally, P_{fd} and β_0 should be based on considerations of the design details' influence on capacity of the structural system, inspectability, and repairability. Life cycle operations, reliability, and costs should be optimized.

Munse's fatigue design process proceeds through six steps:

Step 1 - Establish the expected loading history for the detail to be designed. This is equivalent to choosing a Weibull distribution shape parameter, ϵ (Figure 9.5). ϵ commonly ranges from 0.7 to 1.3 [9.7].

Step 2 - Identify the type of detail to be designed. An extensive summary of typical ship details is given in reference [9.7].

Step 3 - Obtain the mean fatigue stress ranges and slope of the S-N curve based on the type of details and the design number of cycles (N_T). Based on laboratory tests of typical ship details, reference [9.7] summarizes S_f and m data.

Step 4 - Compute the random load factor ψ from Eq. 9.34 based on N_T, ϵ and m.

Step 5 - Compute an appropriate reliability factor, R_{Fm}, from Eq. 9.35 based on an estimate of the COV of fatigue life (e.g. $C_N = 0.8$) and desired probability of failure (e.g., $P_{fD} = 10^{-2}$).

Step 6 - Determine the design fatigue stress range from Eq. 9.32.

Wirsching's [9.3, 9.4] procedure for a fatigue design check proceeds through six steps:

Step 1 - Define an appropriate value of of the Weibull stress range shapes parameter ϵ (e.g. Figure 9.7) for the environment, type of structure, and detail location.

Step 2 - Define an appropriate stress ratio ($R = S_{min}/S_{max}$, Eq. 9.13) for the detail.

Step 3 - Define an appropriate S-N curve slope, m (e.g. Figure 9.2) and then use Figure 9.8 to establish the design stress range, $S_{fD} = S_R$, for the desired service life, T_S.

Step 4 - The peak stress value for the detail is computed as $S_{PD} = S_{fD}/(1-R)$ (Eq. 9.13).

Step 5 - The fatigue strength can be stated in terms of a nominal stress by using an appropriate stress concentration factor (SCF) or $S_{PDN} = S_{PD}/SCF$.

Step 6 - The detail (joint) is taken as satisfactory if $S_m \leq S_{PD}$, where S_m is the hot spot stress corresponding to the "design wave" (assumed to be the 100-year wave). Alternatively, $S_{mN} \leq S_{PDN}$, where S_{mN} is the nominal (brace) stress.

Wirsching's procedure is based on a "code calibration" approach to define the fatigue design safety index (β_D) [9.3, 9.4]. Table 9.5 summarizes the data and method used to construct the design stress range curves of Figure 9.8.

241

TABLE 9.5

SUMMARY OF THE DATA USED TO ESTABLISH THE
DESIGN STRESS RANGE CURVES OF FIGURE 9.8

	Figure 9.8(a)	Figure 9.8(b)
m	4.38	3.00
k	4.6E12	5.25E10
c_K	.73	0.73
λ	.79	.86
$\tilde{\Delta}$	1.00	1.0
C_Δ	.3	.3
B	.7	0.7
c_B	.5	0.5
F_0 (Hz)	0.25	0.25
β_0	2.78	2.62

Method for constructing curves: Consider Data Set B for which the target
safety index is $\beta_* = 2.78$. S_R for $T_S = 100$ years is computed directly using
Eq. (a) with $\beta = 2.78$. The 20-year curve we know must pass through the
reference. From Eq. (a), $\beta = 1.63$ for the 100-year wave condition. Using
this β, the 20-year curve is establish from Eq. (a). For $\beta_0 = 2.78$ for a
$T_S = 40$ years, Eq. (a) fixed $S_R = 52.4$ ksi. This value is scaled to $S_R = 78.7$
ksi for the 100-year wave. Then corresponding to $\xi = 0.57$, Eq. (a) gives $\beta =
2.11$ for the 100-year wave. This value of β in Eq. (a) is used to construct
the 40-year curve; a $\beta = 2.11$ for 100 years ensures $\beta = 2.78$ for 40 years.
Eq. (a) is:

$$ S_R \left(\text{or} \, S_{/D} \right) = \left[\ln \left(f_0 T_s \right) \right]^{\frac{1}{\epsilon}} \left[\frac{\Delta K}{\lambda f_0 T_s B^m \exp \left(\beta_0 \sigma_{\ln T} \right) \Gamma \left(\frac{m}{\epsilon} + 1 \right)} \right] $$

242

(a) m=4.38

(b) m=3.00

DESIGN STRESS RANGE, S_R (ξ,100) (ksi)
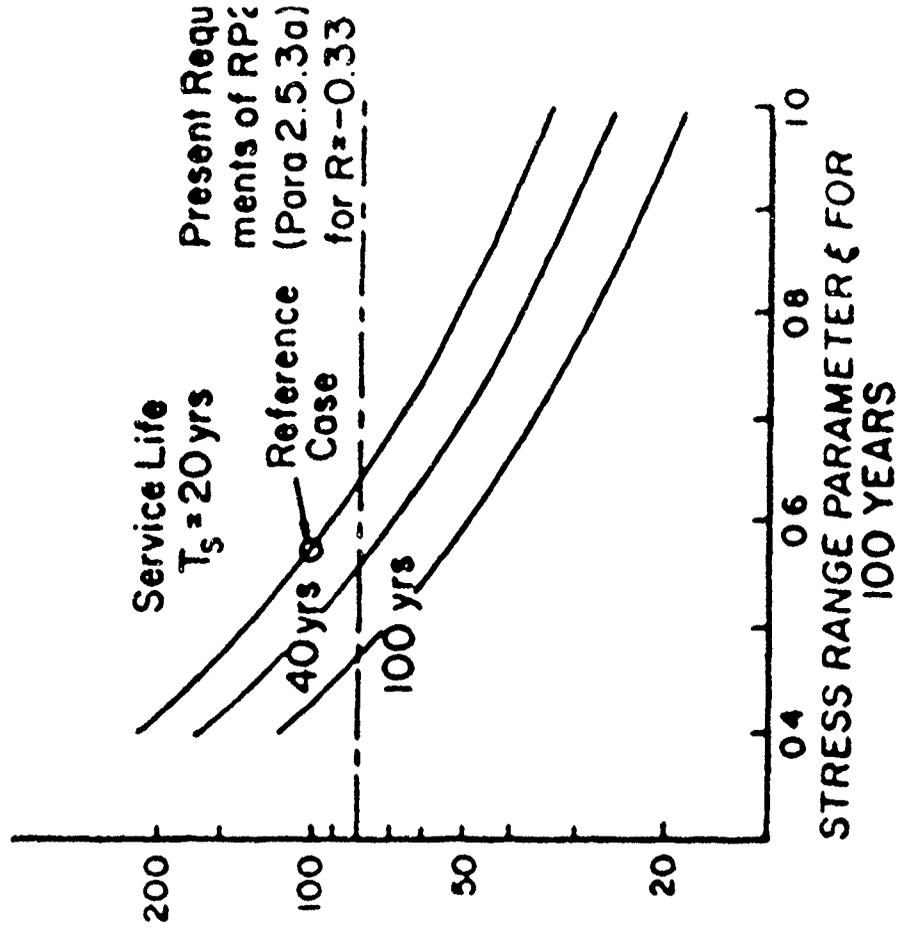
FIG. 9.8   DESIGN STRESS RANGE VERSUS STRESS RANGE PARAMETER

Based on the fatigue analysis process outlined in Eqs. 9.1 through 9.13, Geyer and Stahl [9.1] have developed a very useful simplified fatigue design procedure. The key to this procedure is the use of a uniform fatigue life criterion (Eqs. 9.9, 9.10).

Based on the API X S-N curve (Figure 9.2, m = 4.38), a deepwater Gulf of Mexico wave height distribution (Figure 9.1), a design wave height of 70 feet, and a 20-year service life (T) with a factor of safety of 2 (T_S = 40-year design fatigue life), they developed the design fatigue stress range curves shown in Figure 9.9 as a function of the stress-wave height exponent, α (Eq. 9.11). For details and structures in which $\alpha \leq$ 1.2, the low-cycle fatigue stresses developed by hurricanes has an insignificant effect. However, for $\alpha \geq$ 1.2, the low cycle hurricane stresses can have a major influence on damage.

As an alternative to a design stress range, Wirsching and Chen [9.6] have formulated the fatigue design as a design damage ratio (Eq. 9.5), Δ_D:

$$\Delta_D = \frac{\gamma \bar{\Delta}}{B^m \exp\left(\beta_D \sigma_{lnT}\right)} \tag{9.37}$$

The safety check on the computed damage D_0 is:

$$D_o \leq \Delta_D \tag{9.38}$$

where

$$D_o = \frac{T_s \Omega}{K} \tag{9.39}$$

244
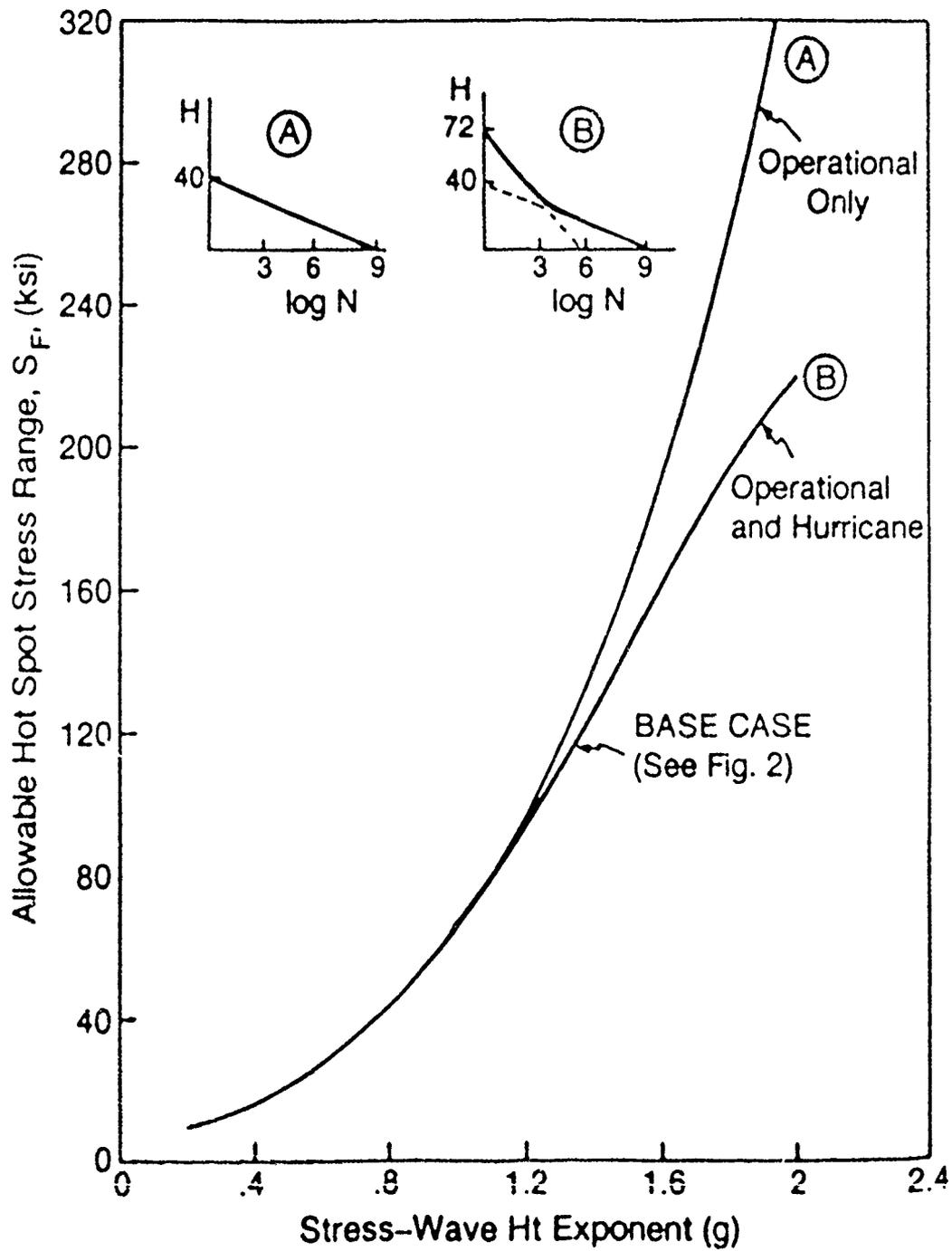
FIG. 9.9 **SENSITIVITY TO WAVE HEIGHT DISTRIBUTION**

Using reasonable fatigue reference data for calculation of Δ_D as a function of β_d, Wirsching and Chen developed Figure 9.10. Then, β_d's were chosen depending upon the levels of importance, inspectability, and repairability of the design details.

It should be realized that in the foregoing design applications, the design reliability (Safety Index, β_D or probability of failure, P_{fD}) has been targeted to a service life, T_S. For the lognormal formulation (Eq. 9.17), the safety index, β_t, for any exposure period, (t) can be expressed in terms of the design safety index, β_D for a service life as:

$$\beta_t = \beta_D - \frac{\ln(t/T_s)}{\sigma_{\ln T}} \tag{9.40}$$

For $t < T_S$, the safety index is much larger than β_D (Figure 9.11). This explains why there is a very low probability of finding fatigue failures early in the life of a structure (if all has gone well).

This equation also points out how inspections and repairs might be utilized to maintain the safety index above some value (Figure 9.12). Inspections can be used to reduce the uncertainties that contribute to $\sigma_{\ln T}$ (Eq. 9.17), and thus increase β_t. Repairs (if effective and well done) can increase β_t by erasing all or a large portion of the cyclic damage.

The optimum inspection and repair strategy will be a function of the element's (detail's) importance to the capacity and serviceability of the system, inspectability, repairability, and costs. The reader is referred to reference [9.10] for additional details on the roles of quality assurance and inspections in maintaining fatigue reliability.

Design Life, T_D, for a Service Life, T_S, of 20 Yrs.
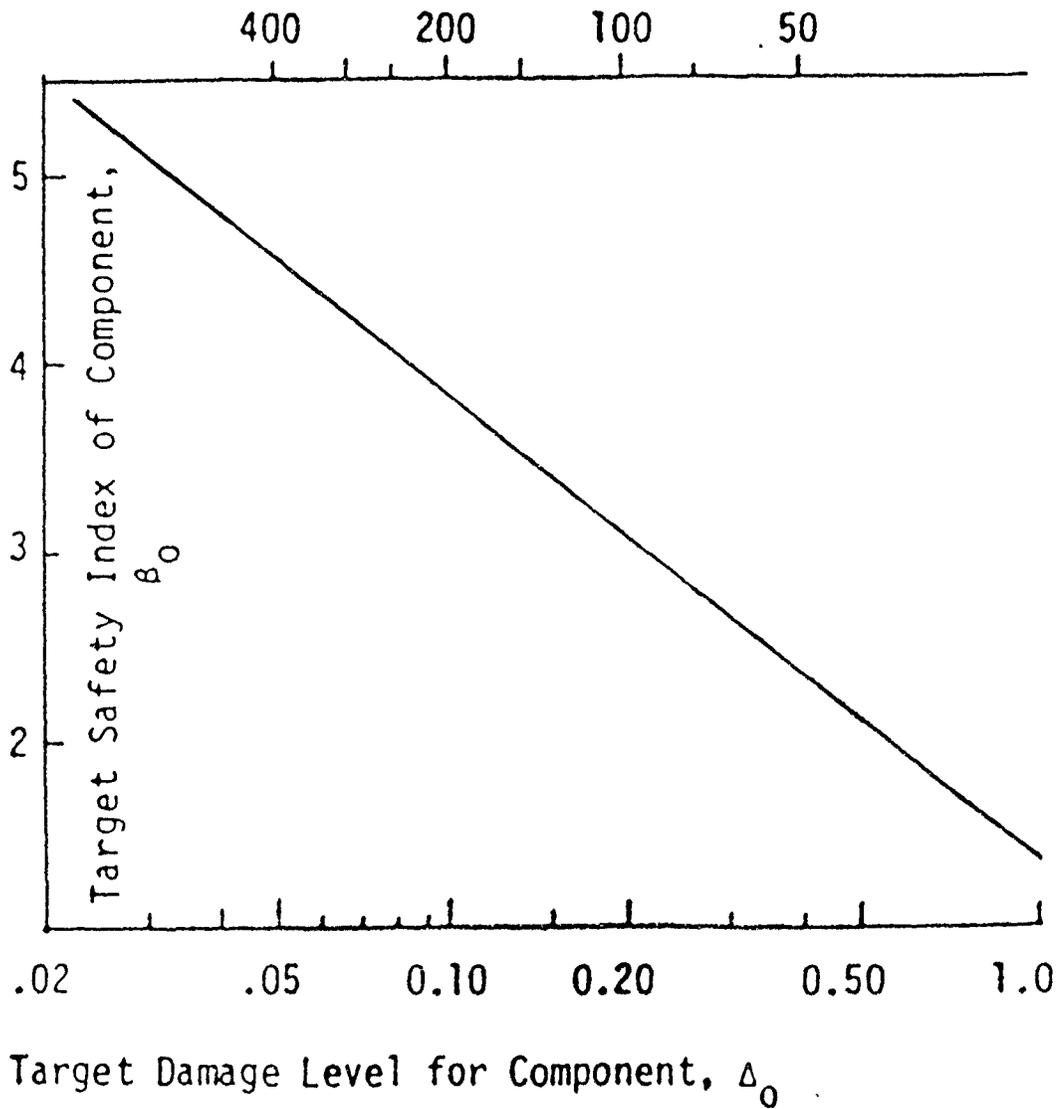
FIG. 9.10 **EXAMPLE: THE TARGET SAFETY INDEX AS A FUNCTION OF THE TARGET DAMAGE LEVEL FOR A COMPONENT**

247

FIG. 9.11

FIG. 9.12

249
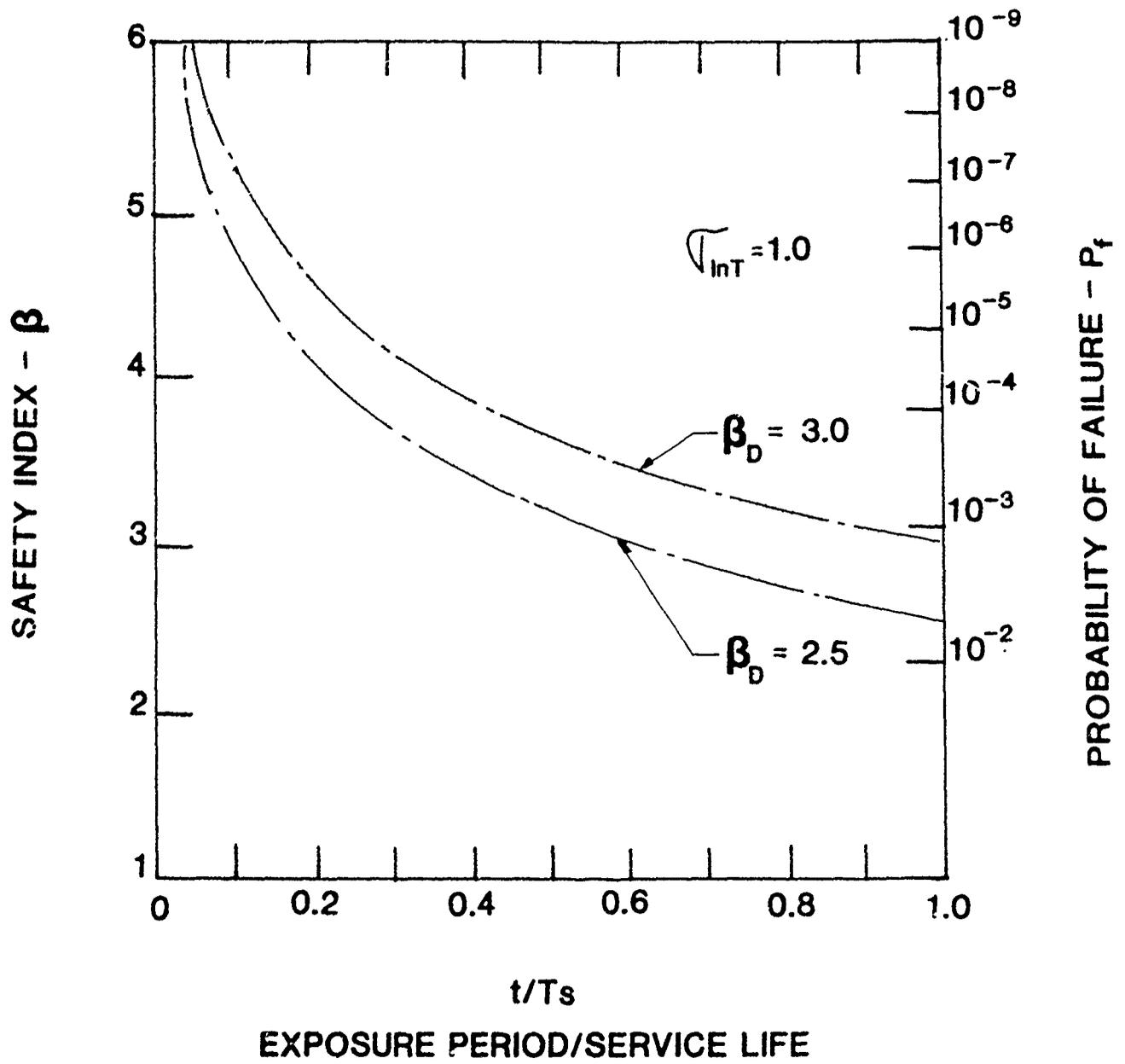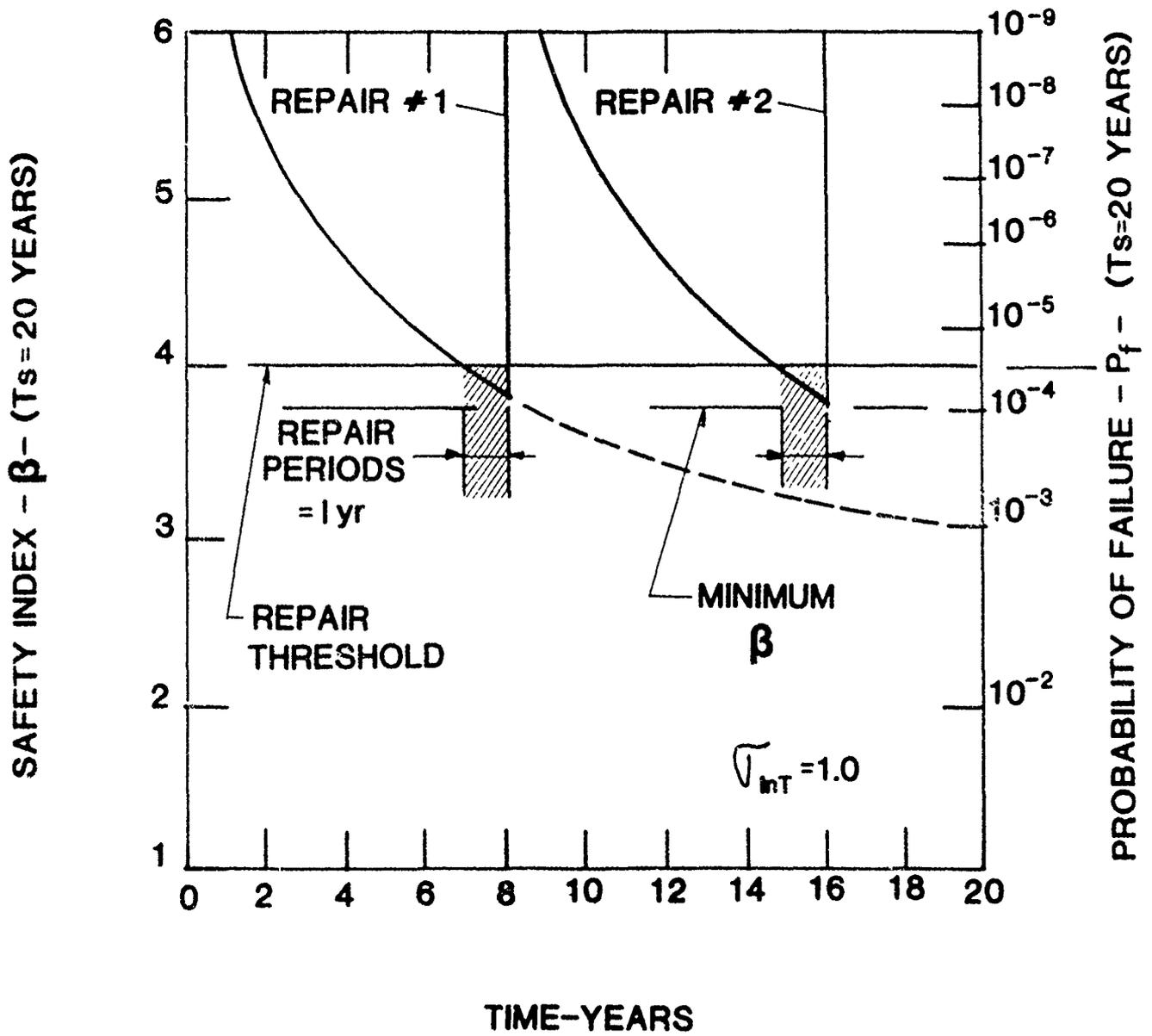
9.5   FATIGUE RELIABILITY - SYSTEMS

Fatigue failure of a detail in a "fail-safe" engineered structure does not constitute failure of the system (recalling the Introduction to this Section). Thus, in addition to design of details for fatigue, consideration must be given to fatigue reliability of the structural system. The reader is referred to Section VIII for a discussion of system reliability.

For a system of N identical and independent elements in series (a chain system), the probability of failure of the system, P_{fs}, is related to the element probability of failure, P_{fe} as:

$$P_{fs} = \left[1 - \left(1 - P_{fe} \right)^{N} \right] \tag{9.41}$$

or approximately,

$$F_{fs} \cong N P_{fe} \tag{9.42}$$

If because of materials, construction, design, or loading, there is a very high degree of correlation of the strengths of the elements, then for perfectly correlated (dependent) elements:

$$P_{fs} = P_{fe} \tag{9.43}$$

Thus in a series system, correlation in element strengths has the effect of reducing the probability of failure.

Correlation expresses the degree of dependence (or independence) between random variables (refer to Section II for a discussion of correlation). Zero correlation implies independence. Unity correlation implies perfect dependence.

Correlation is generally expressed by. a correlation coefficient, ρUV:

$$\rho UV = \frac{COV(U,V)}{\sigma_U,\sigma_V} \tag{9.44}$$

where U and V are two random variables and the σ's are the standard deviations of these variables. The covariance of U and V, COV(U, V), is:

$$COV(U,V) = E\left[\left(U - \mu_u\right)\left(V - \mu_V\right)\right]$$

where the μ's are the expected values, E[·], of the variables. The two random variables are said to be uncorrelated if $\rho = 0$ (independent), and to be perfectly correlated if $\rho = \pm1$ (dependent).

Cornell [9.11] has suggested a useful approximation for the correlation coefficient between the probabilities of failure of the system's components as:

$$\rho = \frac{V_S^2}{V_R^2 + V_S^2} \tag{9.45}$$

where V_S^2 and V_R^2 are the squared coefficients of variation of the load(s) and resistance (R), respectively.

If the resistance is the dominant uncertainty, then ρ tends toward unity (dependence).

Figure 9.13 [9.12] shows the Safety Indices for series systems, β_s, as a function of the correlation coefficient, the number of elements (N), and the element safety index β_e (assuming normal distributed strengths and equally correlated elements). For the high reliability elements ($\beta_e = 3$), the system safety index is approximately equal to the value based on zero correlation (Eqs. 9.41 and 9.42) for $\rho < 0.8$. For high degrees of correlation ($\rho > 0.8$), there is a small correction to the element safety index to determine the system safety index.

For the fatigue reliability of a series system, the design probability of failure of the N elements which compose the system (P_{feD}) can be reasonably and realistically related to the system design probability of failure (P_{fsD}) as:

$$P_{feD} = \frac{P_{fsD}}{N} \tag{9.46}$$

Such an approach has been used in developing fatigue design criteria for the connector elements of a tendon system for a Tension Leg Platform (TLP) [9.13].

In the case of a parallel member system, the problem is much more complex. Martindale and Wirsching [9.14] and Stahl and Geyer [9.15] have studied the progressive fatigue characteristics of such systems. Typical results for a system comprising parallel brittle members ($\beta_e = 3.0$) (2 joints per member) and a correlation in element fatigue lives of 32 percent is shown in Figure 9.14. The three curves are for:

252
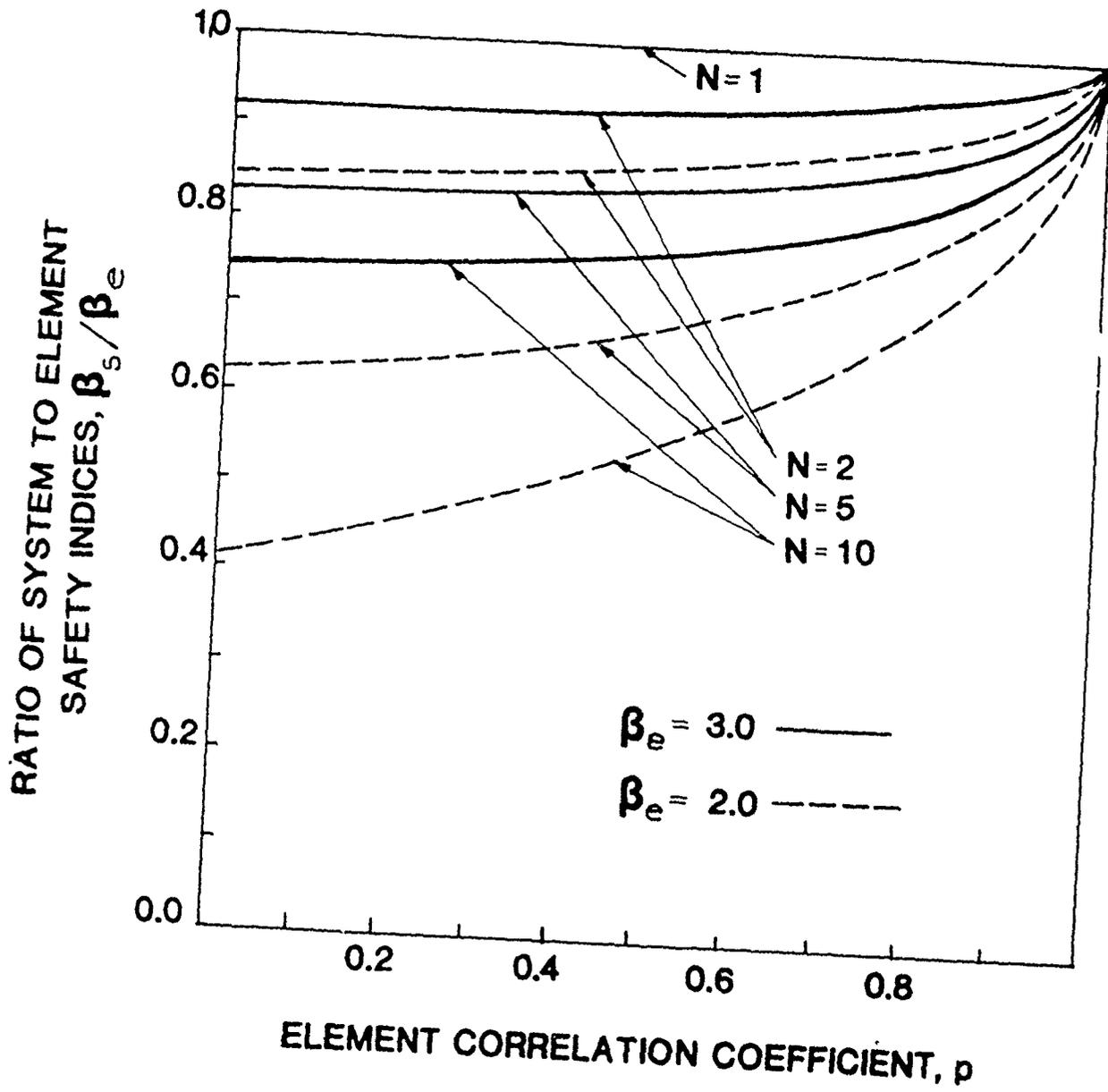
FIG. 9.13 SAFETY INDICES FOR SERIES SYSTEM OF N ELEMENTS
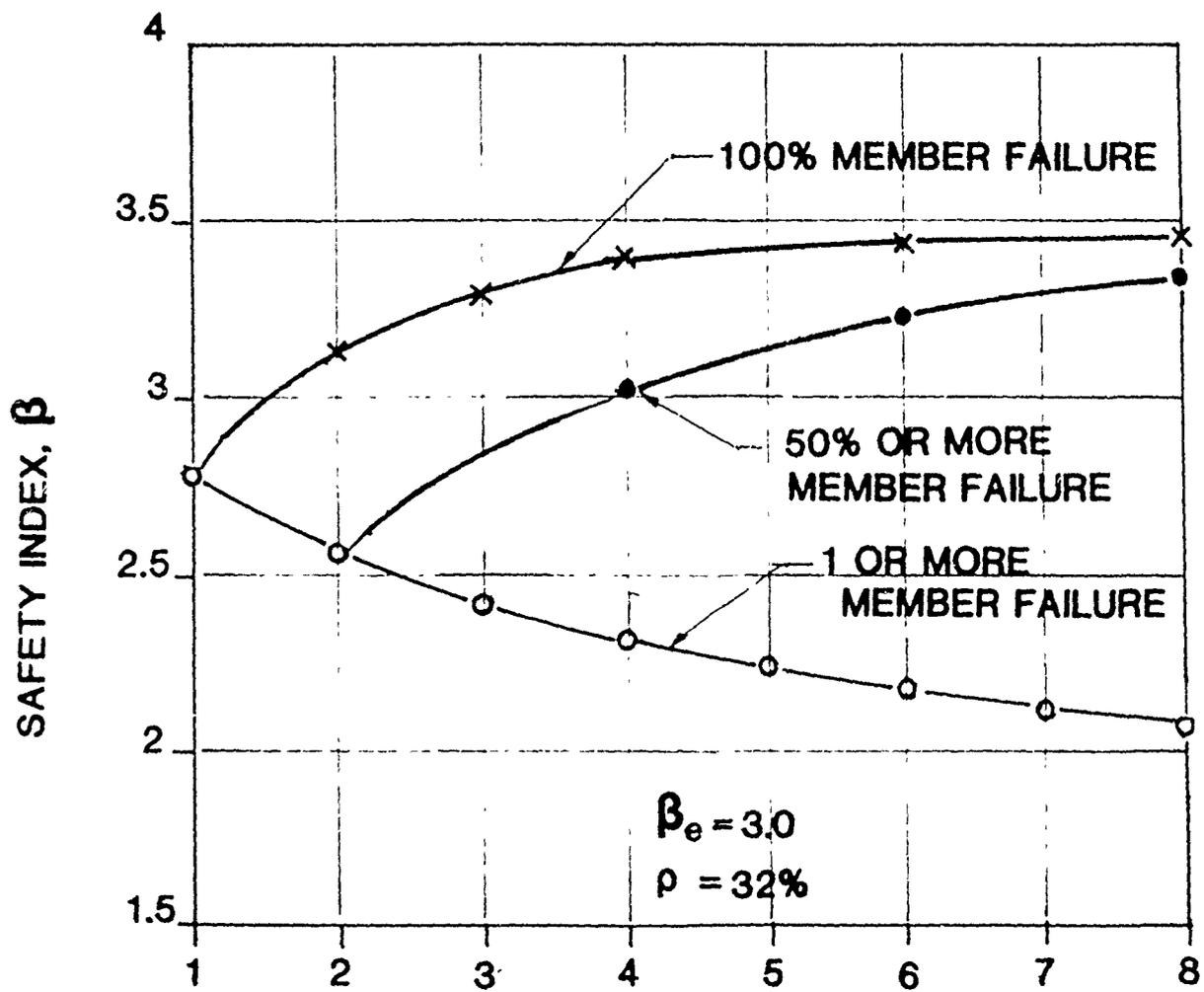
NUMBER OF PARALLEL MEMBERS (2 JOINTS PER MEMBER)

FIG. 9.14 SAFETY INDEX VERSUS NUMBER OF MEMBERS, COMPARISON TO PROGRESSIVE COLLAPSE MODEL $\beta_0 = 3.0$, $\rho = 32\%$

254

a. First member failure

b. 50 percent member failure (50 percent loss in capacity)

c. 100 percent member failure (100 percent loss in capacity).

Only in the case of >50 percent member failure is there a beneficial influence from adding parallel elements.

The effect of adding joints to the parallel elements for the condition of 100 percent member failure is summarized in Figure 9.15 (based on results from [9.15]). The ratio of system to element safety indices (β_s/β_*) is for correlations of 30 to 60 percent, 1 to 4 parallel elements, and 2 to 16 joints per parallel members. Adding joints to the parallel members swamps out much of the beneficial effects of redundancy, and the system behaves much more like a series system (Figure 9.15). For example, for an element correlation of 50 percent, Figure 9.15 indicates that for a system of 10 elements (joints) in series, the β_s/β_* ratio is 0.5 and 0.75 for $\beta_* = 2$ and 3, respectively. Referring to Figure 9.13 for the same number of joints per member, $\beta_s/\beta_* = 0.5$ to 0.6 and 0.75 to 0.80 for $\beta_* = 2$ and 3, respectively.

Given a target reliability for design of the system (β_{sD}), Figures 9.13 and 9.15 could be used to define the target reliability for the individual elements (β_{*D}).

Reliability based methods for analyses of complex structural systems are being developed [9.11, 9.16], and these methods are being extended to considerations of inspections and repairs [9.16, 9.17, 9.18]. The reader is referred to the cited references for these research developments.
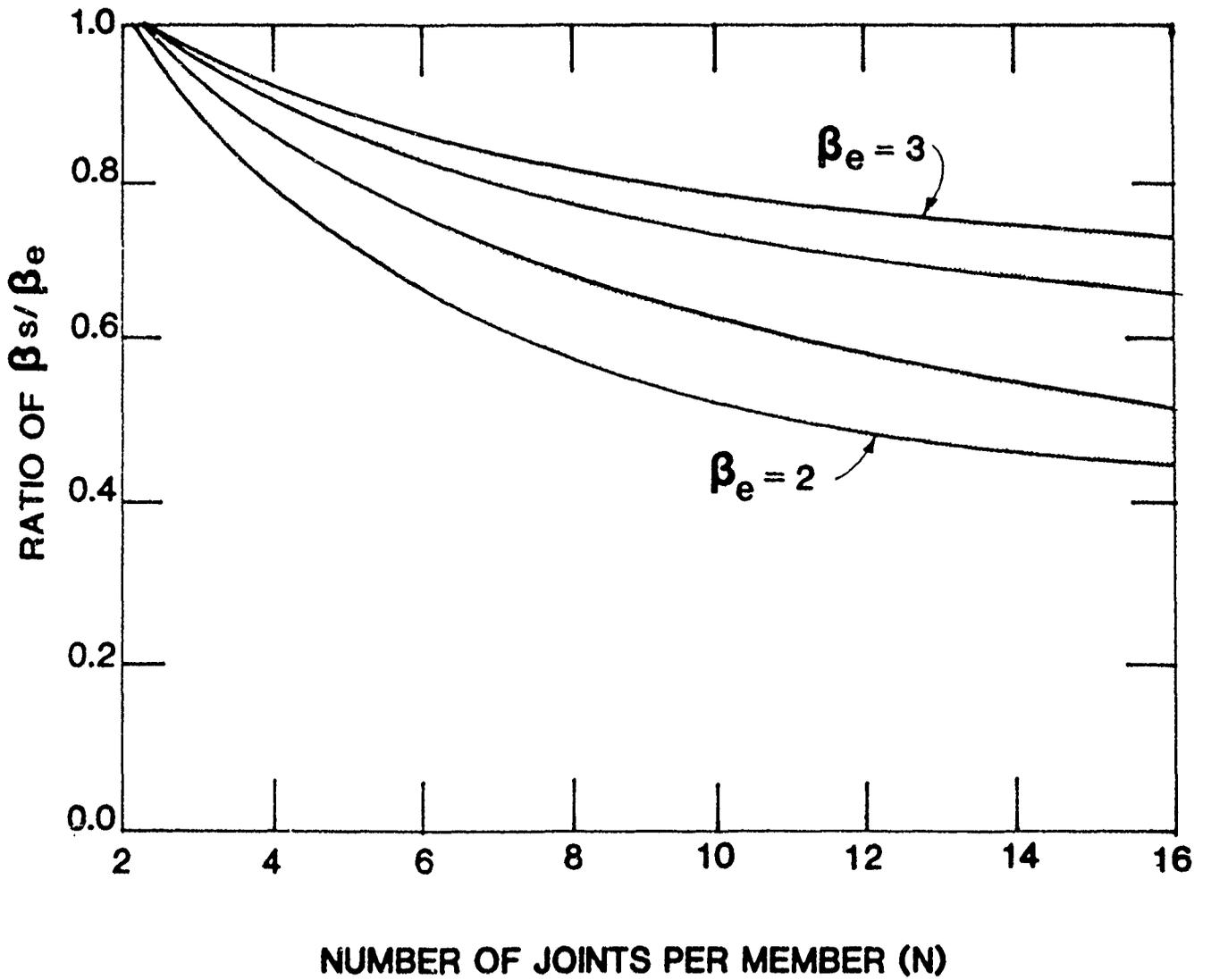
FIG. 9.15

REFERENCES

9.1   Geyer, J. F. and Stahl, B., "Simplified Fatigue Design Procedure for Offshore Structures," Offshore Technology Conference, OTC Paper 5331, Houston, Texas, May 5-8, 1986.

9.2   American Petroleum Institute, "Recommended Practice for Planning, Designing and Constructing Fixed Offshore Platforms," API Recommended Practice 2A (RP2A), Sixteenth Edition, April 2, 1986.

9.3   Wirsching, P. H., "Probability-Based Fatigue Design Criteria for Offshore Structures," API-PRAC Project #81-15, Prepared for American Petroleum Insttiute, Dallas, Texas, January 1983.

9.4   Wirsching, P. H., "Fatigue Reliability for Offshore Structures," ASCE Journal of Structural Engineering, Paper No. 19235, Vol. 110, No. 10, October 1984.

9.5   Munse, W. H., "Fatigue Criteria for Ship Structure Details," Extreme Loads Response Symposium, Arlington, VA, October 19-20, 1981.

9.6   Wirsching, P. H. and Chew, Y.-N., "Considerations fo Probability-Based Fatigue Design for Marine Structures," Marine Structural Reliability Symposium, Sheraton National Hotel, Arlington, Virginia, October 5-6, 1987.

9.7   Munse, W. H. et al., "Fatigue Characterization of Fabricated Ship Details for Design," SSC-318, U.S. Coast Guard, Aug. 1982.

9.8   Marshall, P. W. and Luyties, W. H., "Allowable Stress for Fatigue Design," BOSS '82, Boston, Mass., August 1982.

9.9   Wirsching, P. H. and Light, M. C., "Fatigue Under Wide Band Random Stress," ASCE Journal of the Structural Division, Vol. 106, No. ST7, July, 1980.

9.10   Committee on Fatigue and Fracture Reliability of the Committee on Structural Safety and Reliability of the Structural Division, "Fatigue Reliability: Quality Assurance and Maintainability," Journal of the Structural Division, ASCE, Vol. 108, No. ST1, January, 1982.

9.11   Nordal, H., Cornell, C. A., and Karamchandani, A., "A Structural
       System Reliability Care Study of an Eight-leg Steel Jacket
       Offshore Production Platform, Marine Structural Reliability
       Symposium, Society of Naval Architects and Marine Engineers,
       Arlington, Virginia, October 5-6, 1987.

9.12   Grigoriu, Mircea and Turkstra, Carl, "Safety of Structural
       Systems with Correlated Resistances," Applied Mathematical
       Modelling, Vol. 3, April 1979.

9.13   Chen, Y. N., and Wirsching, P. H., "Probability Based Fatigue
       Design Criteria for TLP Tendons," Proceedings of the Fifth
       International Offshore Mechanics and Arctic Engineering (OMAE)
       Symposium, The American Society of Mechanical Engineers, Vol. 1,
       Tokyo, Japan, April 13-18, 1986.

9.14   Martindale, Scott G. and Wirsching, Paul H., "Reliability-Based
       Progressive Fatigue Collapse," Journal of Structural
       Engineeering, Vol. 109, No. 8, August, 1983.

9.15   Stahl, Bernhard, and Geyer, John F., "Fatigue Reliability of
       Parallel Member Systems, Journal of Structural Engineering, Vol.
       110, No. 10, October, 1984.

9.16   Paliou, C., Shinozuka, and Chen, Y. N.,"Reliability and
       Durability of Marine Structures," Journal of Structural
       Engineering, Vol. 113, No. 6, June, 1987.

9.17   Carr. P., Clayton, M., Busby, P. L, and Dobson, J., "A
       Probabilistic Strategy for Subsea Inspection of Steel
       Structures,", Proceedings of Society of Petroleum Engineers
       European Petroleum Conference, SPE 15868, London, 20-22 October,
       1986.

9.18   Madsen, H. O., Skjong, R. K., Tallin, A. G., and Kirkemo, F.,
       "Probabilistic Fatigue Crack Growth Analysis of Offshore
       Structures, with Reliability Updating Through Inspections,"
       Proceedings of the Marine Structural Reliability Symposium,
       Society of Naval Architects and Marine Engineers, Arlington,
       Virginia, October 5-6, 1987.

10. APPLICATIONS TO SHIPS AND MARINE STRUCTURES

10.1 Long- and Short-Term Procedures:

Two types of analyses may be used for assessing a vessel strength under extreme load; short-term and long-term analyses. At the design stage, if one knows the route of the ship and and if that route is more or less permanent, then the probability of failure can be predicted using long-term analysis. If on the other hand the route of the ship is not defined, then the short-term analysis can be used to obtain the probability of failure under one or more conditions that are considered to be the severest the ship may encounter during its lifetime. An example of this situation are the design conditions checked in the ASR catamaran by Lankford [10.1]:

(a) "One year of continuous service in average North Atlantic weather."

(b) "Six months at a position in the North Atlantic where the worst weather for this period of time would normally be expected."

(c) "Two months on station in the worst area and the worst season in the North Atlantic."

A more simple short-term analysis criterion is to consider the single most severe sea condition (or a sea condition with a specified return period) and subject the vessel to this condition for a specified period of time.

These two methods, short- and long-term analyses, will naturally produce different final results for the safety margins and therefore care must be taken when comparing safety margins of different ships, i.e., the method and criterion used in predicting the loads acting on the ship will have a considerable impact on the resulting safety index.

To further amplify on this point, the long-term distribution of the wave loads acting on a ship may be determined by tracing the expected route of the ship during its lifetime. Based on ocean wave statistics along that route, the long-term wave load probability distribution (usually taken as Weibull or exponential distribution) for the entire history may be determined. Any lack or deficiency of data on wave statistics over a period of time covering the ship life should be corrected for. In the short-term analysis, a distribution of the extreme load is predicted on the basis of criteria such as one occurrence in a lifetime, one extreme sea storm of a specific duration or a short-term operation in a specific location under severe sea conditions. For that purpose, one of the extreme wave load distributions discussed under "Prediction of Extreme Wave Loads" in Chapter II is used.

It should be noted that there is a fundamental difference between computed results based on these two avenues. In the short-term analysis, the computed probabilities of failure are conditional probabilities given the occurrence of an extreme wave load per a selected criterion. Care must be taken in this case in determining the response of the ship to this extreme load since non-linearities may play an important role. In the long-term analysis, however, the resulting probabilities of failure are associated with the entire history of the expected load acting on a ship during its lifetime.

A.   Procedure for long-term analysis

The following procedure may be used for calculating the probability of failure during the ship's operational lifetime.

1.   Define the mission profile for the ship that includes estimates of
   a.   ship route
   b.   expected total years of service

c. Number of days per year the ship is expected to be at port and underway

d. Nominal cruising speed and maximum speed and the corresponding fraction of time during operation.

2. From the ship route and available wave statistics such as in reference [10.2], obtain the frequency of occurrence of different sea conditions the ship will encounter in each of the geographic areas[11].

3. From step 2 above and the mission profile of the ship (more specifically from expected number of days in each geographic area), determine the total frequency of encountering different sea conditions.

4. Determine the root-mean-square value $\sqrt{E}$ (rms) of the wave bending moment in each sea condition. First, the response amplitude operator, RAO, has to be determined either from available strip-theory (seakeeping) program or from model experiment. The rms values can then be obtained using the determined RAO in conjunction with existing sea spectra such as Pierson-Moskowitz [10.3]. These programs usually give the value of the stillwater bending moment also.

5. From the total frequency of encountering different sea conditions (step 3) and the rms values of the wave bending moment in each sea condition, determine the average wave bending moment λ.

---

11 In almost all the main areas where ships operate, statistical data concerning wave heights and periods have been observed and tabulated. The surface of the earth is divided into a grid of ten-degree squares known as Marsden squares. These squares are arranged into geographic areas over which wave conditions are fairly uniform. The areas are given a code number; see, for example reference [10.2].

6.   Estimate the strength parameters (mean μ and standard deviation σ or the coefficient of variation)   including the objective and subjective uncertainties.   Each failure mode will have its corresponding μ and σ.

7.   Calculate the probabilities of failure in the different modes[12]   (that is, yielding or buckling at different locations) in sagging and in hogging.   Combine to get the total probability of failure.

A block diagram of the foregoing procedure is given in Figure 9.1.

B.   Procedure for short-term analysis

The following procedure may be applied in the   short-term analysis.

1.   From the assumed design criteria and ocean   wave statistics, calculate the frequency of operation in different sea conditions.

2.   Calculate the rms value of the wave bending moment in each sea condition using either strip-theory approach [10.4,10.7] or towing tank experiment results in conjunction with available sea spectra.   Calculate also the stillwater bending moment.

3.   Estimate the strength parameters (μ and σ) for each failure mode.

---

12 The probability of failure in the different modes can be calculated using equation (4.35) if the stillwater bending moment is considered deterministic or from equation (4.38 or 4.41), if it is considered as a random variable.   In the former case, if desired, different values of the stillwater bending moment could be used with an estimate of the corresponding fraction of time.

4. Calculate the probabilities of failure in each sea condition, i.e.,

$$P [R \leq 1/\text{ith sea condition}]$$

5. The total probability of failure is thus

$$P_f = \sum_i P [R \leq 1 / \text{ith sea condition}] \, p(i)$$

where $p(i)$ = probability of operation in the ith sea condition as determined from step 1.

A block diagram of the above procedure is given in Figure 10.2.

If only one storm condition (with a certain return period) is specified in the short-term analysis, then only the probability of failure in that condition needs to be calculated. This probability is thus a conditional probability given that the vessel encounters the specified sea condition, and, is expected to be larger than the long-term or life probability of failure.

In general, long-term analysis requires much more information and computational effort than the short-term analysis. Long-term analysis is, however, necessary if fatigue failure is considered since the entire history of loading should be included. On the other hand, failure under an extreme load can be more easily estimated using short-term analysis.

10.2 Application Examples:

10.2.1. Short-term analysis - Level 3 Reliability

In this example, we will evaluate the probability of exceeding any limit state of a ship during a specified storm condition. The limit state can be an initial yield limit state, an initial buckling limit state, the ultimate strength limit state, or any other condition desired to be

evaluated. The duration of the presence of the ship in the storm is limited by the stationarity condition to a short period of time.

Consider now a tanker of length = 763 ft, breadth =125 ft, and depth = 54.5 ft. We will evaluate the probabilities of exceeding the
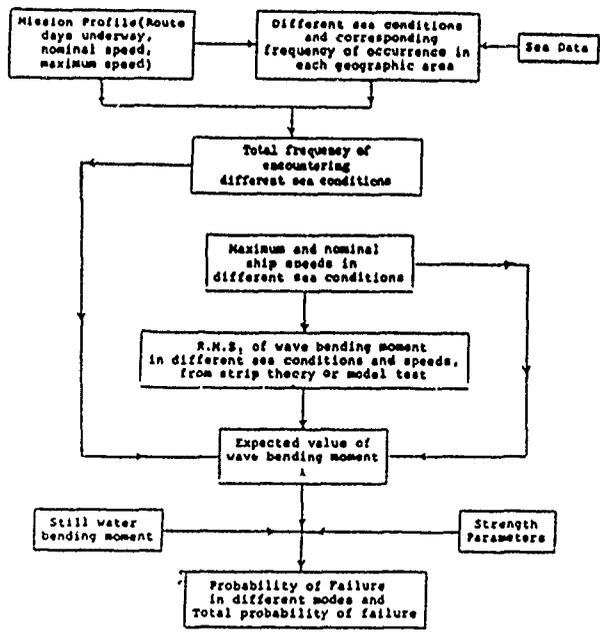
Figure 10.1. Long-Term Procedure
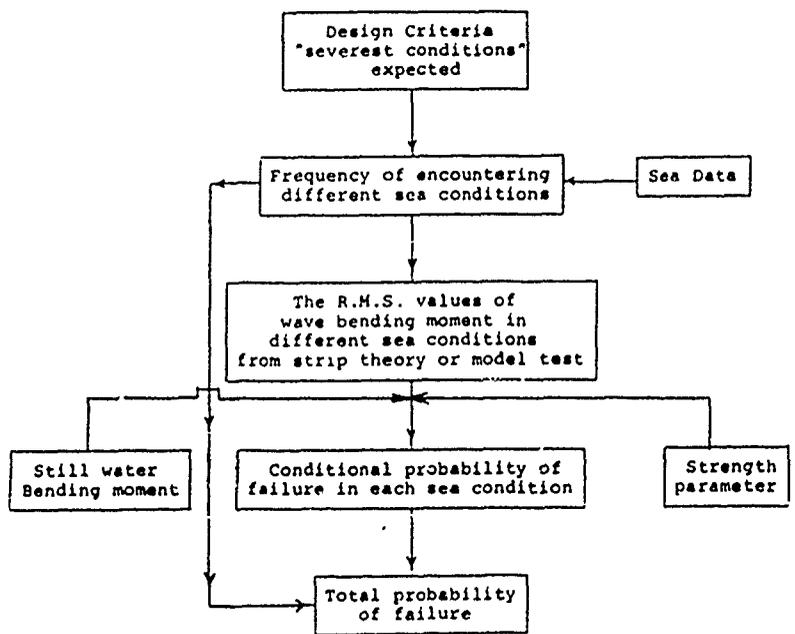
Figure 10.2. Short-Term Procedure.

initial yield limit state and the ultimate strength limit state in a storm condition specified by a significant wave height of 29.0 ft and an average wave period of 10.1 sec. The storm is assumed to be stationary under these conditions for a period of one hour. The following parameters were computed for the tanker using a typical ship motion program:

Stillwater moment (full load) m_S = 669,037 ft-ton
(considered deterministic)
Rms of the wave moment $\sqrt{m_0}$ = 216,450 ft-ton
Average wave moment period = 12.1 sec
Bandwidth parameter of wave moment spectral density ε = 0.337

Number of moment peaks (in one hour) $N = \dfrac{60 \times 60}{12.1} = 297.5$

The mean and standard deviation of the initial yield limit state were computed to be μ_r = 2,420,488 ft-ton and σ_r = 314,663 ft-ton, respectively. The corresponding values for the ultimate limit state were computed to be μ_r = 2,804,760 ft-ton and σ_r = 392,666 ft-ton. The mean of the initial yield limit state was simply computed as the minimum section modulus of the hull amidship multiplied by the average yield stress. The mean of the ultimate strength was computed using "USAS," an elaborate nonlinear finite-element program (see [105]).

Using order statistics and the determined values of $\sqrt{m_0}$, ε, and N, the expected maximum wave bending moment in N peaks is computed from equation (2.57), to be 763,859 ft-ton. If one assumes an ideal narrow-band case, such as ε = 0 instead of 0.337, one obtains, using equation (2.57) again, the slightly more conservative value of 767,543 ft-ton. That is, the error due to the assumption of ε = 0 is less than 0.5 percent.

Equation (2.58) may be used to compute the extreme wave bending moment with probability of exceedence α. For example, the

265

value of the extreme wave moment with a probability of exceedence $\alpha = 0.0001$ in the given storm condition is computed to be 1,086,685 ft-ton.

A semiprobabilistic factor of safety may be defined as the resistance mean μ_r divided by the sum of the stillwater bending moment and the maximum expected wave bending moment as given by (2.57). The computed values of this factor of safety in the given storm condition are 1.69 and 1.96 with respect to the initial yield and ultimate strength, respectively.

Finally, the probability of exceeding a limit state pf, which combines all the given information on the ship and the storm condition, is computed using the basic reliability equation for a normally distributed strength (see equation (4.5)).

$$p_f = 1 - \frac{1}{\sigma_r \sqrt{2\pi}} \int_{-\infty}^{\infty} F_{Z_N}(z) \; e^{-\frac{1}{2}\left[\frac{z - \mu_r}{\sigma_r}\right]^2} \; dz \quad (10.1)$$

where $F_{Z_N}(z)$ is the extreme total bending moment (stillwater plus extreme wave bending moment). Several distributions can be used for F_{Z_N} as discussed earlier in the section entitled "Prediction of Extreme Wave Load" in Chapter II. We will use $F_{Z_N}(z)$ as predicted from order statistics given by equation (2.54) with Rice distribution given by equation (2.38) as the initial distribution. In the latter equation, m_s, the stillwater moment is added. Substitution of these equations in (10.1) and carrying out the integration numerically we obtain the following values for the initial yield and ultimate strength limit states:

pf (initial yield) = 1.19×10^{-3}
pf (ultimate strength) = 3.13×10^{-4}

In order to examine the effect of the sea state on these probabilities, a storm condition characterized by significant wave height of 38.75 ft. and average wave period of 11.5 sec is considered

next. The ship motion program computed values for the rms wave moment $\sqrt{m_0}$, the bandwidth parameter ε, and the average period of the wave moment are, respectively, 2.863×10^5 ft-tons, 0.364, and 13.0 sec. It should be noted that the rms value of the moment is on the conservative side because of the linearity assumption. The number of wave moment peaks in one hour is thus 276.9. Based on these values and the resistance parameters given previously, the following probabilities of exceeding the limit states where determined:

$$p_f \text{ (initial yield)} = 1.23 \times 10^{-2}$$
$$p_f \text{ (ultimate strength)} = 2.73 \times 10^{-3}$$

It is interesting to note that when p_f for the ultimate strength case was recomputed using equation (2.60), which is based on asymptotic distribution instead of order statistics distribution, a value of $p_f = 3.14 \times 10^{-3}$ was determined (compared with 2.73×10^{-3} based on order statistics distribution). As expected, equation (2.60) gives an upper bound on p_f and its accuracy should increase as $N \to \infty$.

It should be noted that the computed probabilities given in this example are conditional probabilities given that the ship encounters a specified storm for a specified length of time. They are fundamentally different from those calculated by constructing the long-term distribution of the wave moment along the ship route during its lifetime (see [10.6]). The elaborate procedure in this latter case produced unconditional lifetime probabilities of failure.

The main advantage, however, of the presented storm-based procedure is its simplicity and consistency. From the environmental data along the ship route (or structure location), a design storm condition can be postulated and the probabilities of exceedence can be immediately determined from the simple results given previously.

The procedure can be used to determine the average probability of failure (or exceedence of a limit state) during the entire duration of a storm rather than just the severest one-hour period of the storm. In this case, a simulation of the storm condition during successive short intervals of time (say one hour each) is necessary. During each interval, the waves are assumed to be stationary and may be represented by a pair of significant wave heights and average wave periods. The rms values $\sqrt{m_0}$ of the wave bending moment can be calculated for each pair and the corresponding probabilities p_f are determined from (10.1). The average probability of exceeding a limit state during the entire storm duration is then

$$P_f = \sum_{i=1}^{n} p_f^i \cdot f_i \quad ; \quad \sum_{i=1}^{n} f_i = 1$$

where f_i is the frequency of occurrence of the ith pair of significant wave heights and average wave periods, and n is the number of stationary short intervals during the storm.

The important high-frequency moments which may increase the bandwidth parameter are due to either springing or slamming. It is unlikely that springing moment is of any appreciable value in high sea states where wave periods are typically large. Therefore any increase in the wave moment rms value $\sqrt{m_0}$ will be negligibly small. Slamming, however, may have some effect on the rms value of the wave moment for small ships. It may be combined with the wave moment to obtain a total rms value using, for example, a procedure developed in [10.8]. It should be noted, however, that the underlying combined process of the wave and slamming moments is not general Gaussian except in one limiting case when slamming decay rates are negligible in comparison with the mean slamming rate.

Equation (10.1) which gives the probability of failure has been plotted as a function of non-dimensional variables for the case of FZ_N (z) estimated from order statistics with Raleigh distribution as the initial distribution (i.e., Rice distribution with $\varepsilon = 0$). This approximation leads to conservative estimates of the probability of failure as discussed earlier. Figure 10.3, 10.4, 10.5, 10.6 and 10.7 show the value of pf as a function of $\sigma^* = \dfrac{\sigma}{\sqrt{m_0}}$, N and $\mu^* = \dfrac{\mu_r - m_s}{\sqrt{m_c}}$.

As an example of the approximation involved, the probability of failure computed from these figures for the initial yield limit state and the second storm condition (significant wave height 38.75 ft.) of the above example (with $\varepsilon = 0$) is 1.40×10^{-2} compared to pf = 1.23×10^{-2} obtained earlier. These figures thus will give slightly more conservative values for pf but eliminate the necessity of numerical integration.
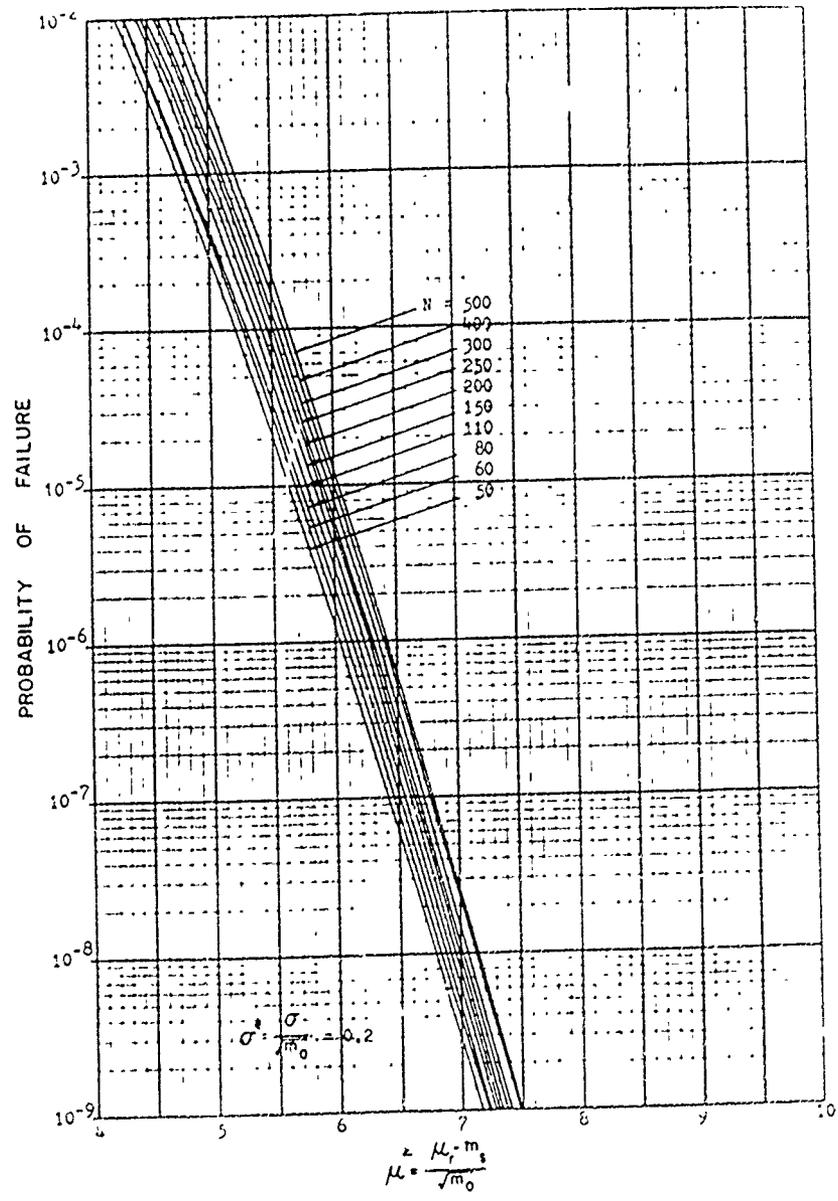
Figure 10.3.   Probability of Failure.

270
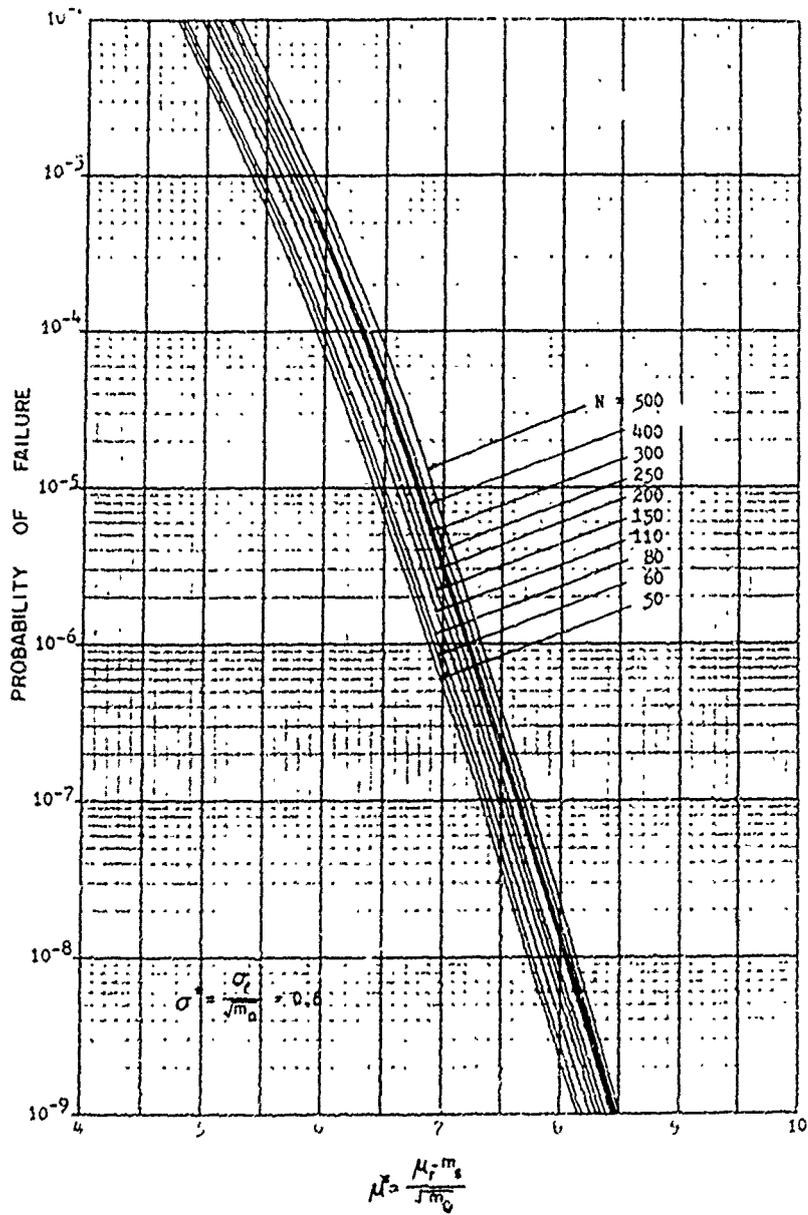
Figure 10.4.   Probability of Failure.

271
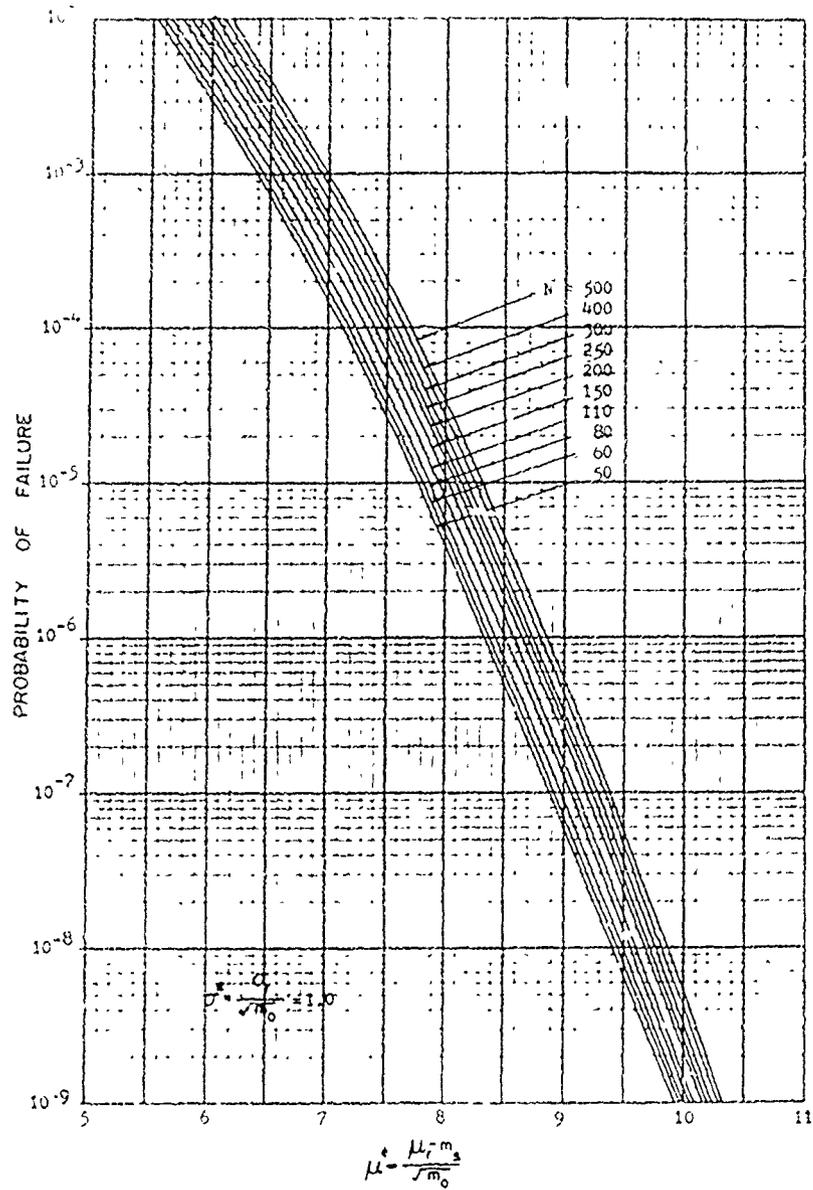
Figure 10.5.　Probability of Failure.

272
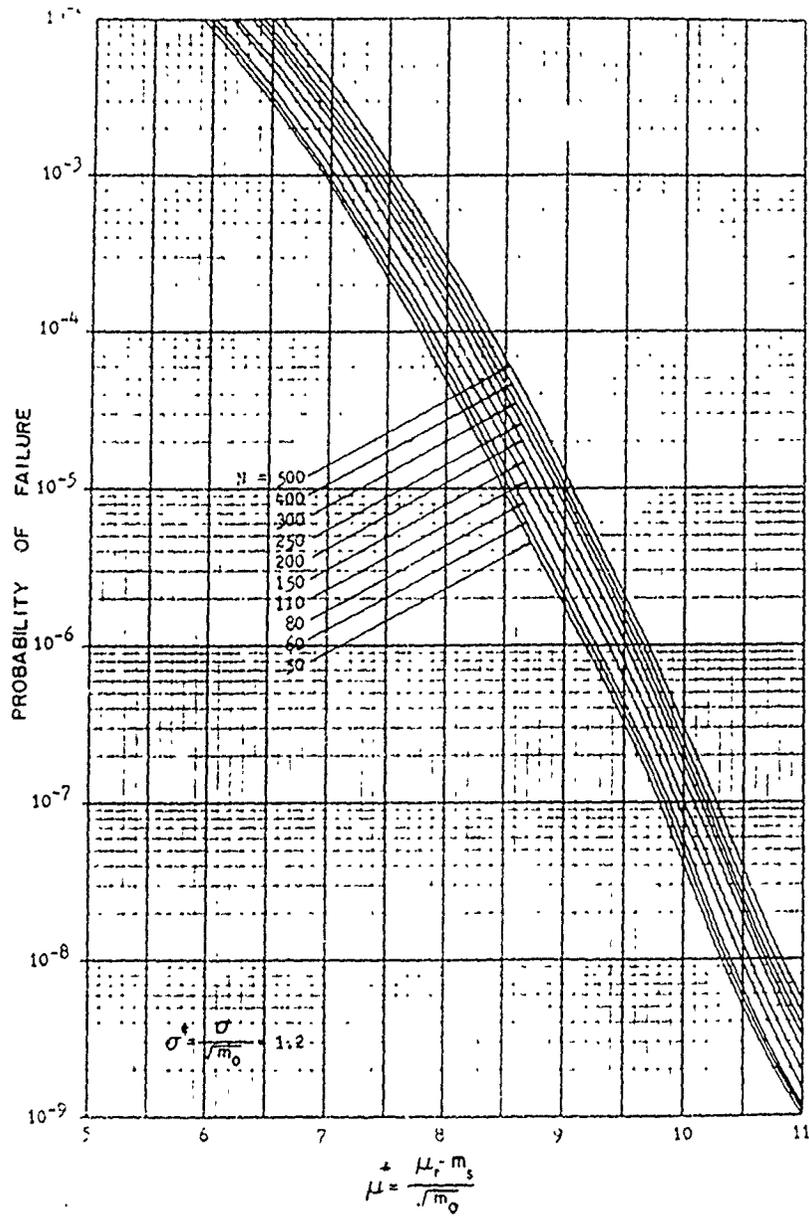
Figure 10.6. Probability of Failure.

273
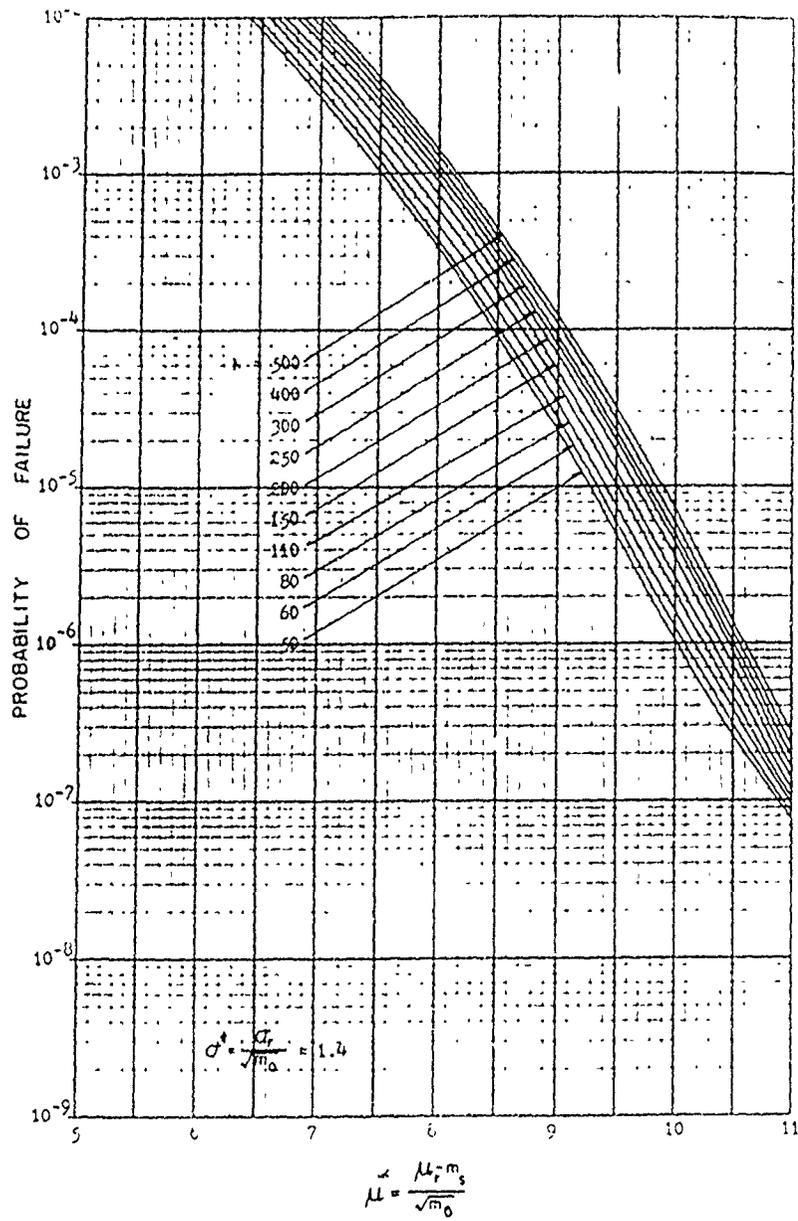
Figure10.7.   Probability of Failure.

274

10.2.2. -- Level 3 Reliability Based on Four Different Extreme Distributions.

Short-term Analysis:

The impact on the probability of failure of the different extreme value distributions of wave bending moment discussed earlier in Chapter 2 will be examined in this example. The distribution function F_{Z_N} (z) in equation (10.1) will be substituted for, using equations (2.56) ; (2.60); (2.70) and (2.71) in order to obtain p_f based on order statistics, type I asymptotic distribution, upcrossing analysis and a two state description of the random process. The tanker cited in example 1 is used again with bending moment parameters (the second storm condition) given by:

$$m_s = 669{,}037 \text{ ft-tons} \; ; \; \sqrt{m_o} = 286{,}300 \text{ ft-tons}$$

$$N = 276.9 \qquad ; \quad q = 0.35$$

The ultimate limit state was considered (μr = 2,804,760 ft-tons and σr = 392,666 ft-tons). The results of the probability of failure are shown in figure 10.8 and table 10.1. As expected the probability of failure based on the asymptotic distribution is higher than the rest and, in general, the agreement between the other three distributions is very good.
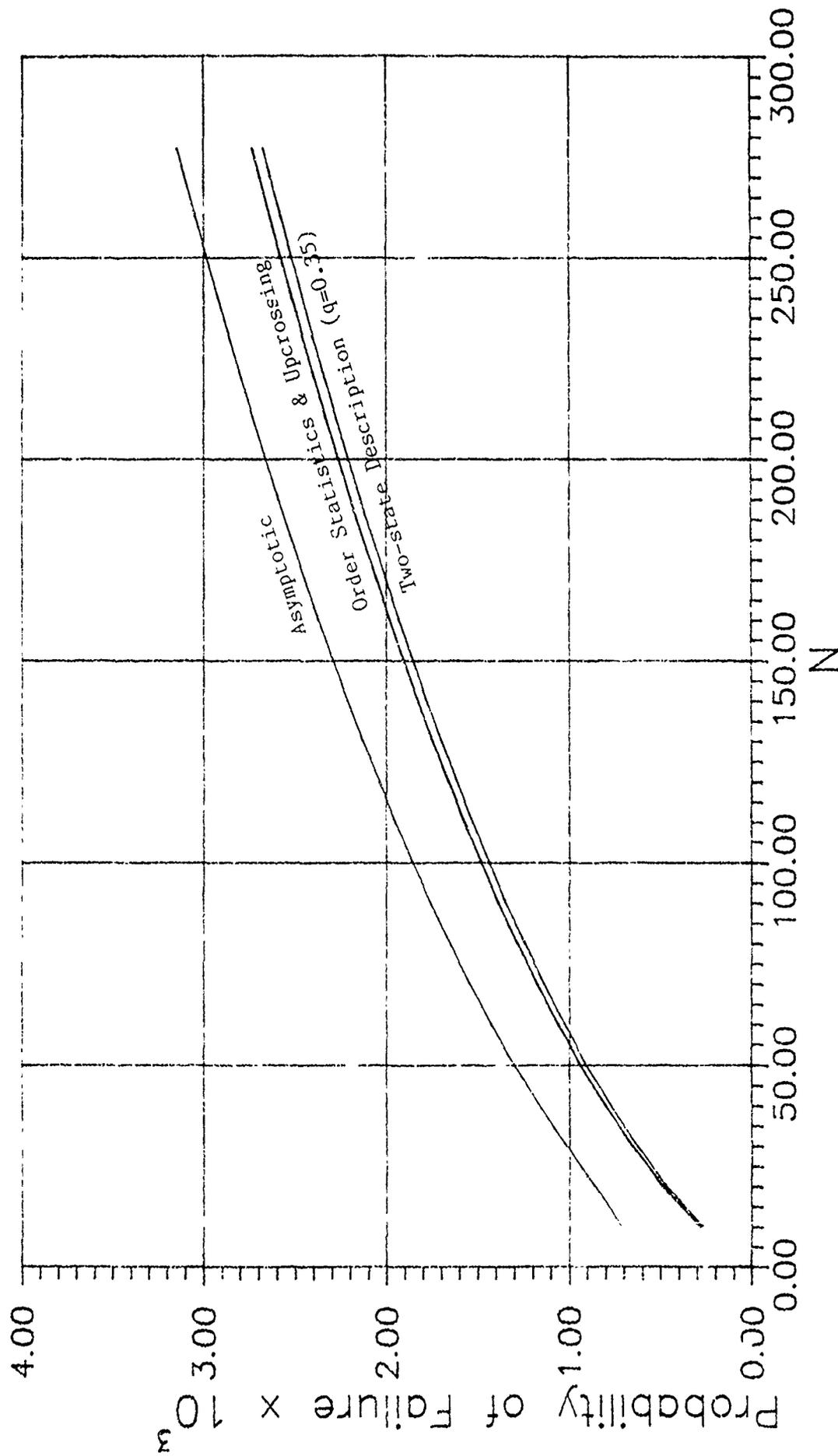
Figure 10.8   Probability of Failure According
to Four Different Extreme
Distributions

276

TABLE 10.1 PROBABILITY OF FAILURE ACCORDING TO FOUR DISTRIBUTIONS

N	Order Statistics	Asymptotic Dist. Type 1	Up-crossing Analysis	Two-State Description (q=0.35)
10	0.284183×10^{-3}	0.711313×10^{-3}	0.280864×10^{-3}	0.268484×10^{-3}
20	0.486767×10^{-3}	0.856830×10^{-3}	0.483547×10^{-3}	0.463786×10^{-3}
30	0.655854×10^{-3}	0.101578×10^{-2}	0.652819×10^{-3}	0.627937×10^{-3}
40	0.804382×10^{-3}	0.116312×10^{-2}	0.801514×10^{-3}	0.772696×10^{-3}
50	0.938461×10^{-3}	0.129867×10^{-2}	0.935738×10^{-3}	0.903715×10^{-3}
60	0.106161×10^{-2}	0.142424×10^{-2}	0.105901×10^{-2}	0.102428×10^{-2}
70	0.117608×10^{-2}	0.154149×10^{-2}	0.117359×10^{-2}	0.113652×10^{-2}
80	0.128344×10^{-2}	0.165174×10^{-2}	0.128105×10^{-2}	0.124191×10^{-2}
90	0.138483×10^{-2}	0.175600×10^{-2}	0.138252×10^{-2}	0.134154×10^{-2}
100	0.148109×10^{-2}	0.185508×10^{-2}	0.147887×10^{-2}	0.143621×10^{-2}
110	0.157291×10^{-2}	0.194963×10^{-2}	0.157075×10^{-2}	0.152656×10^{-2}
120	0.166080×10^{-2}	0.204017×10^{-2}	0.165871×10^{-2}	0.161312×10^{-2}
130	0.174522×10^{-2}	0.212713×10^{-2}	0.174318×10^{-2}	0.169629×10^{-2}
140	0.182651×10^{-2}	0.221087×10^{-2}	0.182452×10^{-2}	0.177642×10^{-2}
150	0.190496×10^{-2}	0.229169×10^{-2}	0.190303×10^{-2}	0.185380×10^{-2}
160	0.198085×10^{-2}	0.236985×10^{-2}	0.197897×10^{-2}	0.192867×10^{-2}
170	0.205438×10^{-2}	0.244558×10^{-2}	0.205254×10^{-2}	0.200124×10^{-2}
180	0.212576×10^{-2}	0.251906×10^{-2}	0.212395×10^{-2}	0.207170×10^{-2}
190	0.219513×10^{-2}	0.259047×10^{-2}	0.219336×10^{-2}	0.214021×10^{-2}
200	0.226264×10^{-2}	0.265996×10^{-2}	0.226092×10^{-2}	0.220691×10^{-2}
210	0.232844×10^{-2}	0.272766×10^{-2}	0.232674×10^{-2}	0.227192×10^{-2}
220	0.239262×10^{-2}	0.279369×10^{-2}	0.239096×10^{-2}	0.233536×10^{-2}
230	0.245529×10^{-2}	0.285815×10^{-2}	0.245366×10^{-2}	0.239731×10^{-2}
240	0.251654×10^{-2}	0.292114×10^{-2}	0.251494×10^{-2}	0.245788×10^{-2}
250	0.257646×10^{-2}	0.298274×10^{-2}	0.257488×10^{-2}	0.251714×10^{-2}
260	0.263512×10^{-2}	0.304304×10^{-2}	0.263357×10^{-2}	0.257516×10^{-2}
270	0.269258×10^{-2}	0.310209×10^{-2}	0.269106×10^{-2}	0.263201×10^{-2}
277	0.273214×10^{-2}	0.314273×10^{-2}	0.273063×10^{-2}	0.267115×10^{-2}

10.2.3. — Comparison of Level 2 and Level 3 - Effect of Correlation Between Wave and Stillwater Bending Moments.

Long-Term Analysis:

This example consists of two parts. In the first part we will discuss a long-term procedure applied to the ship used in the previous example. A comparison will be made between Level 3 (exact) and Level 2 (approx.) methods of reliability analysis. In the second part of the example we will examine the effect of correlations between the stillwater and wave bending moments on the probability of failure using again a long-term analysis.

The ship is assumed to have the following mission profile,

a)   ship life   =   20 years
b)   ship in port 65 days/yr. and underway 300 days/hr.
c)   ship route: Marsden square numbers, 1, 2, 4, 12, 21, 23, 25, 30, 31 (see Figure 5.3)
d)   time proportions in Marsden squares: 2, 2, 1, 1, 1, 1, 1, 1, 1

The frequency of occurrence of different sea conditions specified by the significant wave height is calculated in each geographic area. For the ship, frequency of encountering the different sea states during the operational lifetime is obtained using such information in conjunction with (a), (b), (c) and (d), and is shown in Table 10.2.

To calculate the number of wave bending moment (or, wave peaks (N)) the ship will encounter throughout her life, at different sea states, first we calculate the average wave period at different sea states from wave data (Ref.10.2) as shown in Table 10.2. The ratio of number of days the ship spends in a particular sea state and average period of waves in that sea state gives the number of peaks. Such results are also shown in the same table.

The root mean square of the WBM ($\sqrt{m_0}$) in each sea state are calculated from standard sea-keeping program and are shown in Table 10.3. In the same table the scale and location parameters α_{N_i} and U_{N_i} of the asymptotic distribution as calculated from equations (2.65) and (2.64) are shown ($\varepsilon = 0$).

The SWBM is assumed deterministic and all variables are assumed independent. The complete problem reduces to calculation of β (or, pf) for the performance function

$$g(\underline{x}) = R - M_S - M_W$$

R $\sim$ Normal (2420488,314663) ft-ton (strength)

M_S $\sim$ Deterministic $=$ 669037 ft-ton (stillwater)

M_W $\sim$ Extreme Value 1 (α_{N_i}, u_{N_i})(wave)

In the exact method the probabilities of failure p_i for each sea state 'i' are calculated by numerical integration of the equation:

$$p_i = 1 - \frac{1}{\sigma_r \sqrt{2\pi}} \int_{-\infty}^{+\infty} \exp\{-e^{-\alpha_{N_i}(m-M_s-u_{N_i})} - \frac{1}{2}\left(\frac{m-\mu_r}{\sigma_r}\right)\} \, dm$$

The results are shown in Table 10.3. Similar calculations were done by the advanced Level 2 method and are also shown in the same table. The lifetime probability of failure (exceedence of the initial yield limit state) can now be calculated from,

$$p_f = \sum_i p_i \, f_i \qquad (10.2)$$

where f_i is the frequency of occurrence of such sea state. In our application example, the results are,

$$pf \text{ exact} = 5.2268 \times 10^{-3} \quad \text{(Level 3)}$$
$$pf \text{ approx.} = 4.7851 \times 10^{-3} \quad \text{(Level 2)}$$

In the second part of this example the SWBM is assumed to be non-deterministic and correlated to the WBM. Only Level 2 method was used to find β (or, pf), where,

$$R \sim \text{Normal} \ (2420488,314663) \ \text{ft-ton}$$
$$M_S \sim \text{Normal} \ (403520,161408) \quad \text{ft-ton}$$
$$M_W \sim \text{Extreme Value 1} \ (\alpha_{N_i}, U_{N_i})$$

The correlation matrix is:

$$\bar{R} = \begin{bmatrix} 1 & 0 & 1 \\ 0 & 1 & \rho_{23} \\ 0 & \rho_{32} & 1 \end{bmatrix}$$

To show the effect of such correlation we calculated failure probabilities for $\rho_{23} = \rho_{3\lambda} = \ 0\cdot0, \ 0\cdot1, \ 0\cdot3, \ 0\cdot5, \ 0\cdot7, \ 0\cdot9$. The results are presented in Table10.4 and Figure10.9.

A comparison of results in Table 10.3 reveals that in our example, the Level 2 method yielded lower values of failure probabilities than those obtained from the exact method. The extent and direction of difference in results between approximate and exact method depends on the nature and shape of the nonlinear transformed failure surface. As an example, let us consider the failure surface in sea state 10 in the first part of our application example. For the linear failure surface $R - M_S - M_W = 0$ in the original space, one obtains, by transformation, the nonlinear failure surface in the standard space as,

$$(\mu_r + Y_r \sigma_r) - M_s - \{ u_{\tilde{N}} - \frac{1}{\alpha_N} \ln \ln [\ \frac{1}{\Phi(Y_{mw})} \ ]\} = 0$$

$$(10.3)$$

where Y_r and Y_{m_W} are standard uncorrelated variables of R and Mw respectively and are expressed as,

$$Y_r = \frac{r - \mu_r}{\sigma_r}$$

(10.4)

$$Y_{m_W} = \phi^{-1} \left[\exp \left\{ -e^{-\alpha(m_W - u_W)} \right\} \right]$$

(10.5)

Substituting the appropriate values in equation (10.3), the failure surface is obtained as shown in Figure 10.10. The area of the single shaded region in this figure represents exact failure probability. On the other hand, area of the double shaded zone on the failure side of the linearizing tangent line represents the approximate failure probability according to Level 2. Since the area of the double shaded zone is less than that of the single shaded region, the approximate method is seen to give lower values of pf. Instead of being concave, if the failure surface is convex, such linearization would have yielded higher values of pf.

While it is attractive to use approximate methods for ease in calculations, one must have an idea of the failure surface for the problem under consideration. The extent of approximation is well understood by having this surface drawn. If this surface is highly nonlinear, first order approximation analysis may yield gross error. However, for most practical cases, the problem is not very acute and the approximate method of level 2 would suffice. Also, if the surface is highly nonlinear, one may use a few linearization points and express the actual failure probability in terms of bounds.

Results in Table 10.4 and Figure 10.9 show the effect of correlation between M_W and M_S. As expected, as the extent of positive correlation grows, failure probability, too, increases. From zero correlation to almost full correlation (ρ = 0.9), failure

probability increases by about 25%. Such an increase in the probability of failure is not considered to be significant and, in fact, in terms of β, it would be very small. The results indicate, therefore, that the correlation between the stillwater and wave bending moments is not important and may be neglected in future analysis.

Sea State (i)	Sig. Wave Height (ft.)	Sea State Frequency	Number of days	Avg. Wave Period (Secs.)	Number of Peaks (N)
0	7.15	0.0737246	537.40	5.721	8115952
1	7.80	0.1019174	743.00	5.897	10886078
2	9.15	0.1808501	1318.40	6.031	18887375
3	10.49	0.1592058	1160.60	6.555	15289703
4	11.84	0.0970026	707.20	6.987	8745109
5	13.18	0.0710068	517.60	7.253	6165813
6	14.53	0.0449062	327.40	7.484	3779711
7	15.88	0.0318023	231.80	7.641	2621060
8	17.22	0.0196168	143.00	7.783	1587459
9	18.56	0.0182419	133.00	7.847	1464407
10	19.90	0.0032569	23.80	7.831	262587
11	21.24	0.0035286	25.80	7.951	280357
12	22.58	0.0050191	36.60	8.067	391997
13	23.93	0.0040398	29.40	8.069	314883
14	25.27	0.0017686	12.80	8.023	137847
15	26.61	0.0019604	14.20	8.102	151429
16	27.95	0.0020007	14.60	8.239	153106
17	29.29	0.0008293	6.00	8.453	61125
18	30.63	0.0008039	5.80	8.287	60471
19	31.98	0.0015291	11.20	8.481	114100
91	36.00	0.0000232	1.65	8.771	16254
92	38.68	0.0000389	0.29	8.609	2910
94	44.05	0.0000059	0.05	7.420	582
95	46.73	0.0000149	0.11	8.273	1149
port	–	0.1780822	1300.00	–	–

Table 10.2. Estimation of Number of Wave Peaks the Ship Faces at each Sea State, During Operational Lifetime.

Sea State (i)	R.M.S. of WBM (m) (ft-ton)	Scale Parameter (α_{N_i})	Location Parameter (u_{N_i})	Exact Failure Probability $(p_i)_{exact}$	Approx. Failure Probability $(p_i)_{approx}$
00	21650	2.6055e-04	1.2212e05	3.2187e-06	1.1515e-07
01	26700	2.1321e-04	1.5199e05	3.2187e-06	1.9185e-07
02	40415	1.4323e-04	2.3395e05	3.2187e-06	7.4390e-07
03	55570	1.0351e-04	3.1964e05	3.5167e-06	2.8659e-06
04	76500	7.3909e-05	4.3253e05	1.6212e-05	1.5214e-05
05	100315	5.5743e-05	5.6095e05	9.2506e-05	8.7141e-05
06	129905	4.2367e-05	7.1495e05	6.1077e-04	5.7095e-04
07	155885	3.4877e-05	8.4751e05	2.5651e-03	2.3866e-03
08	180420	2.9618e-05	9.6411e05	7.8703e-03	7.3035e-03
09	199185	2.6752e-05	1.0614e06	1.7956e-02	1.6695e-02
10	221560	2.2548e-05	1.1068e06	2.6627e-02	2.4546e-02
11	241045	2.0779e-05	1.2073e06	5.3888e-02	4.9997e-02
12	262695	1.9320e-05	1.3332e06	1.1368e-01	1.0663e-01
13	278570	1.8063e-05	1.4017e06	1.6216e-01	1.5281e-01
14	294450	1.6522e-05	1.4325e06	1.9008e-01	1.7899e-01
15	308880	1.5813e-05	1.5086e06	2.9189e-01	2.4856e-01
16	324040	1.5080e-05	1.5834e06	3.4412e-01	3.2866e-01
17	338470	1.3871e-05	1.5891e06	3.5483e-01	3.3817e-01
18	350740	1.3379e-05	1.6459e06	4.2291e-01	4.0512e-01
19	363730	1.3268e-05	1.7553e06	5.5559e-01	4.6154e-01
91	398370	1.1054e-05	1.7543e06	5.6263e-01	4.5673e-01
92	418580	9.5417e-06	1.6718e06	4.7341e-01	4.5091e-01
94	453940	7.8608e-06	1.6198e06	4.2787e-01	4.0343e-01
95	469100	1.5610e-05	3.4350e06	8.9814e-01	8.6712e-01
$\sum_i p_i f_i$	–	–	–	5.2268e-03	4.7851e-03

(Note that e-03 = 10^{-3})

Table 10.3. Comparison of Exact and Approximate Failure Probabilities.

Sea State (i)	p_i for $\rho_{ij}=0.0$	p_i for $\rho_{ij}=0.1$	p_i for $\rho_{ij}=0.3$	p_i for $\rho_{ij}=0.5$	p_i for $\rho_{ij}=0.7$	p_i for $\rho_{ij}=0.9$
00	4.31e-08	4.39e-08	4.58e-08	4.83e-08	5.14e-08	5.52e-08
01	6.89e-08	7.05e-08	7.42e-08	7.88e-08	8.48e-08	9.24e-08
02	2.41e-07	2.49e-07	2.67e-07	2.89e-07	3.19e-07	3.57e-07
03	8.46e-07	8.80e-07	9.61e-07	1.06e-06	1.20e-06	1.37e-06
04	4.07e-06	4.27e-06	4.75e-06	5.38e-06	6.19e-06	7.25e-06
05	2.15e-05	2.27e-05	2.56e-05	2.93e-05	3.41e-05	4.02e-05
06	1.34e-04	1.42e-04	1.61e-04	1.84e-04	2.14e-04	2.51e-04
07	5.55e-04	5.88e-04	6.64e-04	7.57e-04	8.70e-04	1.00e-03
08	1.74e-03	1.84e-03	2.06e-03	2.33e-03	2.64e-03	2.99e-03
09	4.13e-03	4.34e-03	4.82e-03	5.37e-03	5.99e-03	6.68e-03
10	6.25e-03	6.60e-03	7.37e-03	8.25e-03	9.23e-03	1.03e-02
11	1.36e-02	1.42e-02	1.57e-02	1.72e-02	1.89e-02	2.06e-02
12	3.21e-02	3.33e-02	3.58e-02	3.84e-02	4.11e-02	4.39e-02
13	4.92e-02	5.08e-02	5.40e-02	5.74e-02	6.08e-02	6.43e-02
14	5.98e-02	6.17e-02	6.55e-02	6.94e-02	7.34e-02	7.74e-02
15	9.00e-02	9.23e-02	9.68e-02	1.01e-01	1.06e-01	1.10e-01
16	1.30e-01	1.32e-01	1.37e-01	1.42e-01	1.47e-01	1.52e-01
17	1.35e-01	1.38e-01	1.43e-01	1.49e-01	1.54e-01	1.59e-01
18	1.73e-01	1.76e-01	1.81e-01	1.87e-01	1.92e-01	1.97e-01
19	2.61e-01	2.63e-01	2.68e-01	2.72e-01	2.76e-01	2.80e-01
91	2.67e-01	2.70e-01	2.75e-01	2.80e-01	2.85e-01	2.89e-01
92	2.07e-01	2.11e-01	2.18e-01	2.24e-01	2.30e-01	2.36e-01
94	1.82e-01	1.87e-01	1.95e-01	2.03e-01	2.10e-01	2.17e-01
95	4.13e-01	4.14e-01	4.17e-01	4.20e-01	4.24e-01	4.29e-01
$\sum_i p_i * f_i$	1.78e-03	1.83e-03	1.91e-03	2.02e-03	2.12e-03	2.22e-03

(Note that e-03 = 10^{-3})

Table 10.4. Comparison of Failure Probabilities for Different Correlation Co-efficients (ρ_{ij}) between M_S and M_W.
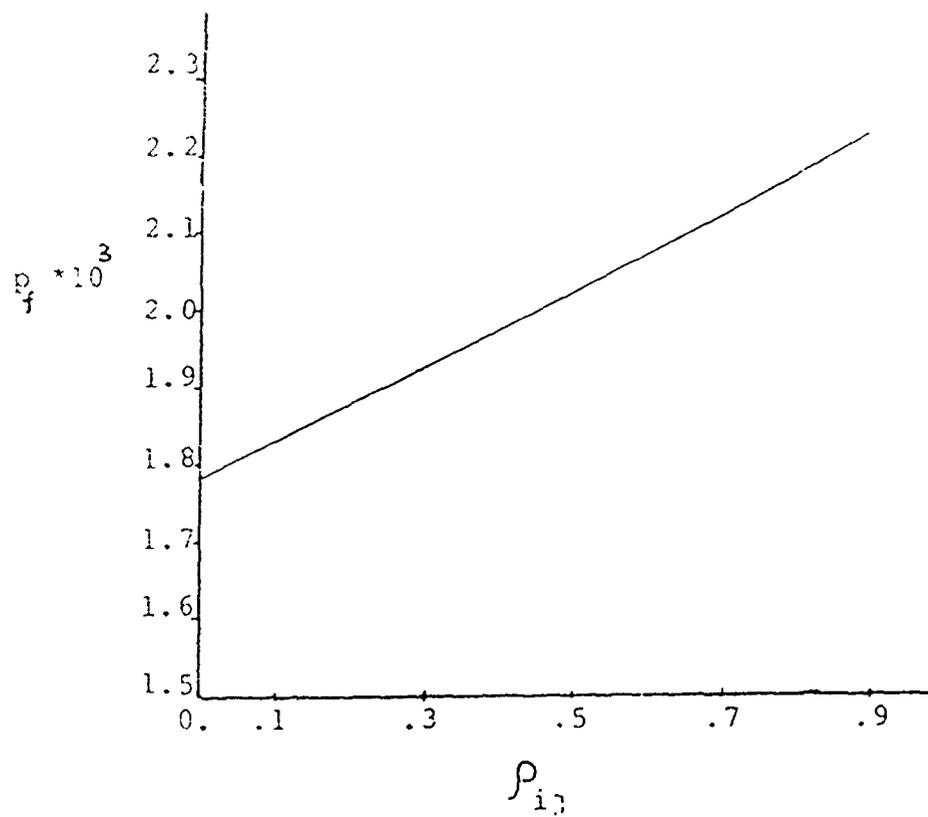
Figure 10.9. Effect of Correlation (ρ_{ij}) between M_S and M_W on Lifetime Failure Probability (p_f).

285
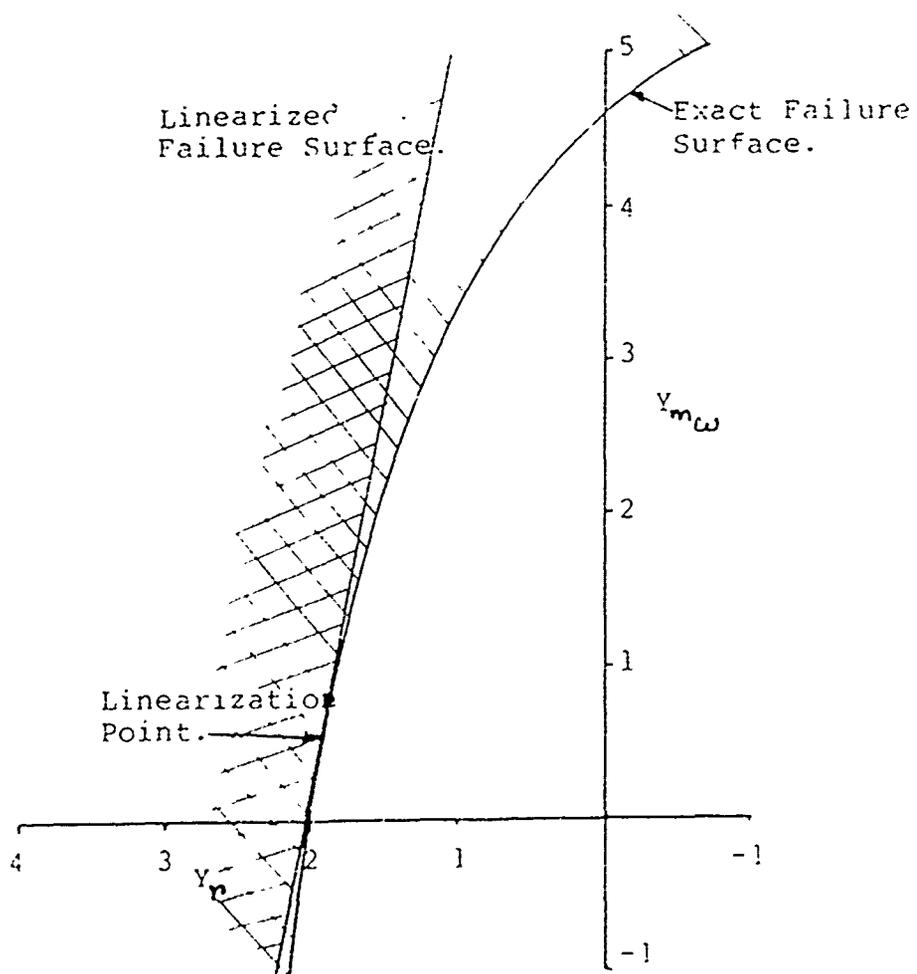
Figure 10.10. Exact and Linearized Failure Surface in Standard Space
(for Sea State 10 in Application Example 3).

286

10.2.4. -- Application to Eighteen Ships Using Level 3, M.V.F.O.S.M. and the Improved First Order Methods:

The same eighteen vessels of the example application given in Chapter 5 are used here to perform a comparison between Level 3, M.V.F.O.S.M. and the improved method. The characteristics of the ships are shown in Table 5.1 (Chapter 5). In Chapter 5 the M.V.F.O.S.M. method has been applied to the eighteen vessels and their safety indices have been determined on that basis. In this example Level 3 and the improved first order (Hasofer/Lind and transformation to normal variables) methods are also applied to the eighteen ships. In Level 3, the following equation was used to calculate the probability of failure (see equation 4.35):

$$P_f \simeq \left[1 - \Phi \left(\frac{\mu_r - m_0}{\sigma_r} \right) \right] + \Phi \left(\frac{\mu_r - m_0}{\sigma_r} - \frac{\sigma_r}{\lambda} \right)$$

$$\cdot e \left\{ -\left(\frac{\mu_r - m_0}{\lambda} \right) + \frac{\sigma_r^2}{2\lambda^2} \right\} \tag{10.6}$$

where μ_r and σ_r are the mean and standard deviation of the resistance, λ is long-term mean value of the wave bending moment (also equal to its standard deviation) and m_0 is the maximum stillwater bending moment (considered deterministic). $\Phi (\cdot)$ is the standard normal distribution function.

In the improved first order method the Hasofer/Lind Safety index discussed in Chapter 5 was used (see equations (5.15) to (5.17). This procedure, however, yields identical results to the M.V.F.O.S.M. method since the performance function is linear ($M_r - M_s - M_w = 0$). What results in a difference between the M.V.F.O.S.M. and the improved method is the inclusion of the distribution information as discussed in Chapter 5 (see equations (5.28) and (5.29)).

The mean value of the wave bending moment "λ" was determined by a long term procedure described in the application example of Chapter 5. Similarly, an initial yield limit state was used to determine the resistance parameters as described in the same application example.

Table 10.5 shows a summary of the comparisons of the safety indices as calculated using the M.V.F.O.S.M. method and the improved method. The safety indices were then converted to probabilities of failure and the results are compared with the direct integration method (Level 3) as shown in Table 10.6. Figure 10.11 shows the absolute value of $\log_{10} p_f$ for the eighteen ships and Figure 10.12 shows the probabilities of failure. In both cases the results are plotted versus ship length. Table 10.7 shows the partial safety factors Δ_r and Δ_t of the resistance and total bending moment, respectively, as calculated from Chapter 6 .

Figures 10.11 and 10.12 show that, in general, the improved method gives results closer to the direct integration method than the M.V.F.O.S.M. method. This is solely because of fitting normal distributions to the non-normal variables. However, the spread can be quite large for some ships.

For these eighteen ships, both the improved method as well as the M.V.F.O.S.M. method overestimate the safety of the vessel as compared to the direct integration method, i.e., they err on the nonconservative side.

The degree of approximation resulting from applying the M.V.F.O.S.M. and the improved methods with respect to the direct integration method varies considerably from one vessel to another (see, for example, vessels no. 1 and 11 in Figures 10.11 or 10.12). Inspection of Tables 10.5 and 10.6 reveals that the spread or "errors" in these two methods as compared with the direct integration method are strongly correlated to the total coefficient of variation of the load; increasing with its increase.

The lack of consistency in the degree of approximation when using the M.V.F.O.S.M. or the improved method and the fact that they lead to optimistic values of ship safety are matters of concern.

Ship #	V_r	V_c	β	β'
1	.13	0.083	5.12	5.11
2	.13	.166	6.09	5.97
3	.13	.221	6.30	6.10
4	.13	.087	4.70	4.66
5	.13	.078	5.10	5.10
6	.13	.074	5.26	5.27
7	.13	.074	5.23	5.24
8	.13	.091	4.87	4.82
9	.13	.099	5.20	5.15
10	.13	.097	4.88	4.82
11	.13	.140	5.25	5.01
12	.13	.072	5.26	5.21
13	.13	.119	5.51	5.43
14	.13	110	4.50	4.37
15	.13	.072	4.48	4.48
16	.13	.123	3.44	3.25
17	.13	.241	5.37	6.15
18	.13	133	5 60	5.49

β • safety index according to MVFOSM
β' • safety index according to the improved method
V_r • C.O.V. of the resistance
V_c • C.O.V. of the combined load

Table10.5

289

Ship #	P_f (MVFOSM)	P_f (Improved)	P_f (Direct Integration)
1	1.528E-7	1.611E-7	3.541E-7
2	6.0E-10	1.2E-9	9.356E-9
3	1.5E-10	5.5E-10	8.398E-9
4	1.301E-6	1.581E-6	3.767E-6
5	1.699E-7	1.699E-7	3.372E-7
6	7.205E-7	6.825E-8	1.233E-7
7	8.48E-8	8.03E-8	1.465E-7
8	5.58E-7	7.178E-7	1.784E-6
9	9.965E-8	1.303E-7	3.868-7
10	5.305E-7	7.178E-7	2.100E-6
11	7.605E-8	2.852E-7	1.586E-6
12	7.21E-8	9.45E-8	1.688E-7
13	1.795E-8	2.82E-8	1.197E-7
14	3.358E-6	6.212E-6	1.968E-5
15	3.732E-6	3.732E-6	7.011E-6
16	2.90E-4	5.770E-4	1.099E-3
17	1.0E-10	4.0E-10	7.438E-9
18	1.075E-8	2.01E-8	1.130E-7

Table10.6

290
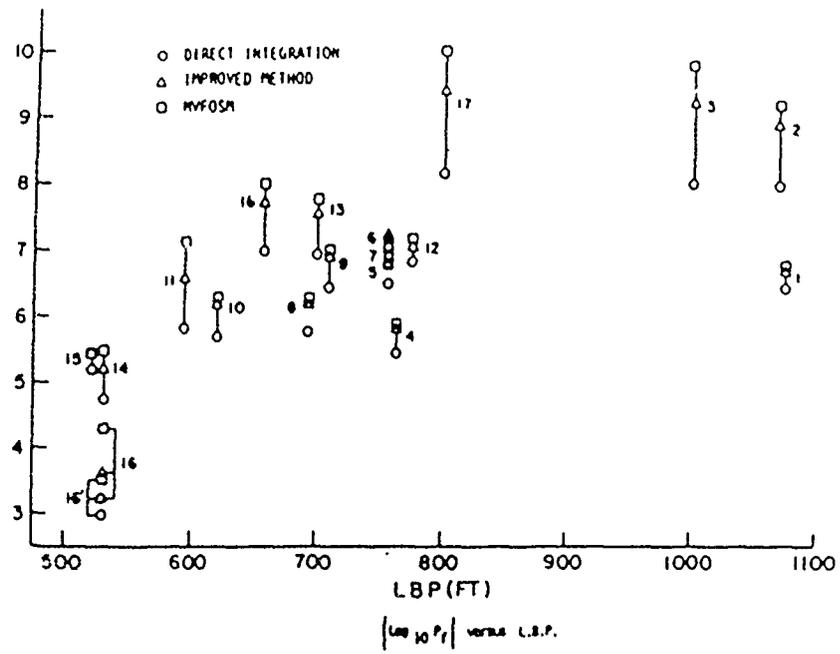
Figure 10. 11

Figure 10.12

291
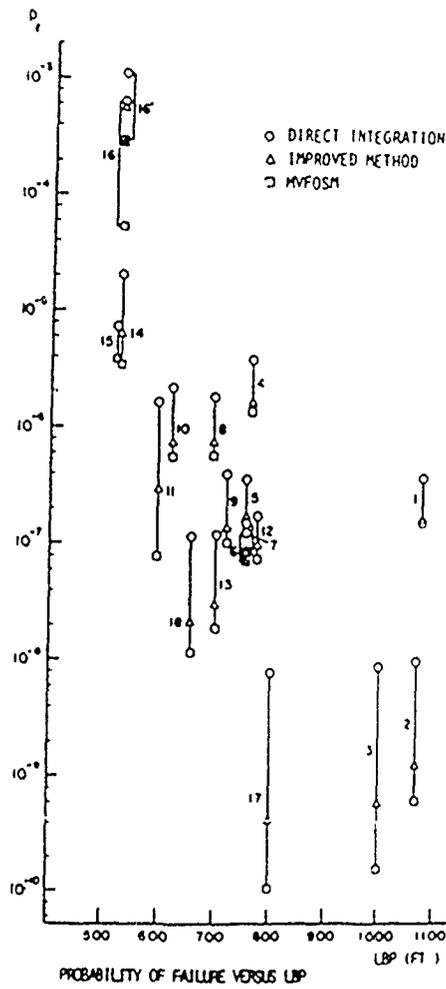
Table 10.7. Partial Safety Factors.

Ship	Based on MVFOSM		Based on Improved Method	
	Δ_r	Δ_t	Δ_r	Δ_L
1	0.348	1.086	0.370	1.135
2	0.230	1.234	0.287	1.391
3	0.208	1.352	0.289	1.596
4	0.407	1.099	0.441	1 156
5	0.349	1.075	0.366	1.116
6	0 326	1.067	0.339	1.103
7	0.330	1.067	0.343	1.103
8	0.385	1.105	0.420	1 166
9	0.342	1.117	0.378	1.189
10	0.386	1 119	0.427	1.190
11	0.249	1.219	0.438	1.354
12	0.326	1.065	0.347	1 099
13	0.304	1.154	0.350	1.252
14	0.444	1.153	0.510	1.243
15	0.432	1.071	0.452	1.109
16	0.596	1.182	0.682	1.263
17	0.200	1 394	0.287	1.671
18	0.294	1.184	0.350	1 302

Δ_r = strength reduction factor.
Δ_t = load magnification factor.

10.2.5. Relative Target Reliability and Partial Safety Factors Implied in ABS Rules for Ship Longitudinal Strength

In developing a new code format, one should compare it with existing practice to insure that the new method has some basis for calibration. One way of doing this is to examine the reliability of existing ships as was done in the previous examples for the eighteen ships. This provides valuable information but has some limitations. Among them are analyzing the ship in the as-built condition rather than the code minimums, and the fact that in any large group of ships, one is probably comparing different codes written at different times.

Another way to tackle this problem is to simply investigate the reliability implicit in the minimum strengths and loadings required by the code. To accomplish this, the safety index β was calculated for ten Series 60 ships, with $C_b = 0.70$ and $L/B = 7.0$. The minimum hull strength and loadings required by the 1982 ABS "Rules for Building

and Classing Steel Vessels" were used to design the ships and the following three assumptions were made:

1. The mean value of the hull strength was assumed to be

$$\mu_S = SM \cdot \bar{\sigma} \qquad (10.7)$$

SM = section modulus from Section 6.3.1.a of the ABS Rules

$\bar{\sigma}$ = average yield stress of steel (assumed to be 31 ksi).

To determine the standard deviation, COV's of both 10 and 12 percent were used. As an example, using the 300 ft ship, the ABS calculated section modulus is 6.243×10^3 in.^{2}-ft; then the hull resistance is 8.640×10^4 ft-ton and the standard deviation is 8.640×10^3 ft-ton for a 10 percent COV.

2. The value of the stillwater bending moment was calculated by Section 6.3.2.a of the ABS Rules. But this value was considered to be an extreme value representing the 95 percent exceedence level; that is, this value would exceeded only 5 percent of the time. To find the corresponding mean and standard deviation, this extreme value was used with COV's of 9.1 and 38.1 percent to cover the range of possibilities suggested by [10.9] and [10.10]. As an example, consider the 300 ft ship for which ABS gives $M_{SW} = 2.662 \times 10^4$ ft-ton. Then the problem is to find μ_{SW} and σ_{SW} such that

$$0.95 = F_{SW} (2.662 \times 10^4) \qquad (10.8)$$

and $\sigma_{SW}/\mu_{SW} = 0.091$ or 0.381 where Fsw (.) is the cumulative distribution function of the normal distribution. Using the standard normal variate

$$t = \frac{X - \mu}{\sigma}$$

293

it is easy to find from standard tables that $t = 1.64$ satisfies (10.8) and using the condition for the COV provides a second equation. Taking the 300 ft ship as an example, the 9.1 percent COV gives $\mu_{sw} = 2.316 \times 10^4$ ft-ton and $\sigma_{sw} = 2.108 \times 10^3$ ft-ton.

3. The value of the wave bending moment was calculated using Section 6.3.2.b of the ABS Rules but again this was considered to be an extreme value. The wave bending is known to fit the exponential distribution where $\mu = \sigma$, that is, COV = 100 percent. It remains now to determine what exceedence level to assign the value derived from the ABS Rules. This uniquely determines λ for the exponential distribution. From references [10.9] and [10.11], values of the expected or average value of the wave bending moment λ, based on rational analysis, were obtained and then were compared with the wave bending moment calculated from the 1982 ABS Rules. For example, using the data from reference [10.9] on the Mariner, $\lambda = 29\ 000$ ft-ton and $M_w = 2.297 \times 10^5$ ft-ton from ABS Rules, one obtains from the exponential distribution

$$P[X \leq 2.297 \times 10^5] = F_X(x) = 1 - e^{-(x/\lambda)}$$
$$= 1 - e^{-(2.297 \times 10^5 / 2.9 \times 10^4)} = 0.9996$$

so the exceedence level is about 0.1 percent. Similar results were obtained from other examples and the exceedence level was set somewhat arbitrarily at 1 percent, which is slightly conservative. Following through on the 300 ft ship example with $M_w = 3.569 \times 10^4$ ft-ton from the Rules, then

$$F_X(3.569 \times 10^4) = 0.99 = 1 - e^{-3.569 \times 10^4/\lambda}$$
$$\text{or } \lambda = 7750 \text{ ft-ton}$$

Now the safety index β can be calculated using

$$\beta = \frac{\mu_s - \mu_{sw} - \mu_w}{(\sigma_s^2 + \sigma_{sw}^2 + \sigma_w^2)^{1/2}} \tag{10.9}$$

Equation (10.9) is the equation for β using both the mean-value first-order second-moment (MVFOSM) as well as the Hasofer/Lind Method (without fitting a normal distribution), since the limit state function is linear. Using the values of the parameters for the 300 ft ship and noticing the $\mu_W = \sigma_W = \lambda$, then

$$\beta \quad = \quad 4.70 \tag{10.10}$$

The partial safety factors can be directly computed using equation (6.5). This results in the following values

$\Delta_S \quad = \quad$ strength reduction safety factor $\quad = \quad 0.66$
$\Delta_{SW} \quad = \quad$ stillwater BM magnification safety factor $\quad = \quad 1.08$
$\Delta_W \quad = \quad$ wave BM magnification safety factor $\quad = \quad 4.10 \tag{10.11}$

It should be noted that these results depend on the validity of the three assumptions discussed previously. Although the values do not change much with large changes in the coefficient of variation of the stillwater bending moment, they are rather sensitive to the wave bending moment exceedence probability (Assumption 2.) If an exceedence probability of 0.1 percent is used instead of 1 percent, the following values result

$$\beta = 5.44, \Delta_S = 0.56, \Delta_{SW} = 1.10, \Delta_W = 3.94$$

instead of the values given by equations (10.10) and (10.11). It is therefore important to regard the values generated in this example for the safety indices and partial safety factors as relative values of the reliability implied in the ABS Rules rather than absolute values. With this in mind, Table 10.8, columns 1 to 4 give the computed safety indices according to the described procedure for strength COV of 10 and 12 percent, and for stillwater bending moment COV of 9.1 and 38.1 percent.

Before calculating all the partial safety factors, one more refinement was possible. This refinement is fitting a normal distribution to the exponential wave load variate at the most likely failure point. This is relevant since the calculation of the safety index implicitly assumes that each variable involved has a normal distribution and thus the safety index can be easily related to a probability of failure.

The equation for the most likely failure point of the wave bending moment in the original space is determined from equation (5.18) as

$$x_w^* = \mu_w + \frac{\sigma_w^2(\mu_s - \mu_{sw} - \mu_w)}{\sigma_s^2 + \sigma_w^2 + \sigma_{sw}^2}$$

(10.12)

The fitted normal distribution parameters can be now determined using equation (10.12) and equations (5.30) and (5.31) as discussed previously. This leads to modified values of the safety indices according to the advanced Level 2 procedure. The results are given in Table 10.8, columns 5 and 6, for stillwater moment COV's of 9.1 and 38.1 percent, respectively. Figure 10.13 shows plots of all the results given in Table 10.8.

Finally, the partial safety factors using the "equivalent" normal wave bending moment distribution were calculated. The computation is straightforward according to the procedure described earlier except for the partial safety factor associated with the mean of the wave bending moment as obtained from the normal distribution. This partial safety factor must be used in conjunction with the fictitious normal distribution mean. Since the normal distribution arises only as a part of the distribution adjustment process, it is more relevant to determine the true partial safety factor associated with the actual mean of the wave bending moment (that is, the mean of the exponential distribution). This is done by stipulating that the true partial safety factor, when multiplied by the mean value of the wave bending moment, gives the same margin in the checking equation as that of the normal mean multiplied by its

partial safety factor; that is, both lead to the same safety index values.

Table 10.9 provides a summary of these results and the target safety indices from which the partial safety factors where computed. It should be emphasized that these results are meant to examine trends and relative magnitudes rather than to be used in the absolute sense.

In general, this analysis of the implicit safety in the ABS Rules is somewhat surprising in two ways. First, the safety index β, is very consistent within each method over the range of ships lengths. Second, the β factor decreases slightly with length while previous results show it increasing. One possible explanation is that the method of calculating the wave moment was not the same. Also, since the previous analyses were done on as built ships, they would reflect more factors changing than just the length. These would include varying degrees of safety margin added by the designer to the code-required minimum as well as different codes from different years and classification societies.

Table 10.8. Safety Indices of the Series 60 Ships

Ship	Length, ft	(1) β	(2) β	(3) β	(4) β	(5) β	(6) β
1	300	4.705	4.728	4.231	4.335	3.420	3 648
2	400	4.650	4.687	4.191	4.303	3 364	3.593
3	500	4.595	4.644	4.150	4 269	3 311	3.530
4	600	4.542	4.600	4.110	4.234	3.265	3.487
5	700	4.489	4.555	4.068	4.196	3.227	3.438
6	800	4.439	4 505	4.025	4 154	3.198	3.415
7	900	4.414	4 480	4.004	4.134	3.179	3 403
8	1000	4.390	4.458	3.983	4.114	3.170	3 389
9	1100	4.367	4.433	3.963	4.092	3 160	3.383
10	1200	4.346	4.411	3.944	4.073	3.149	3.373

(1) COV resistance 10%   COV stillwater bending 9.1%
(2) COV resistance 10%   COV stillwater bending 38.1%
(3) COV resistance 12%   COV stillwater bending 9.1%
(4) COV resistance 12%   COV stillwater bending 38.1%
(5) COV resistance 10%   COV stillwater bending 9.1% adjusted wave bending
(6) COV resistance 10%   COV stillwater bend.ng 38.1% adjusted wave bending
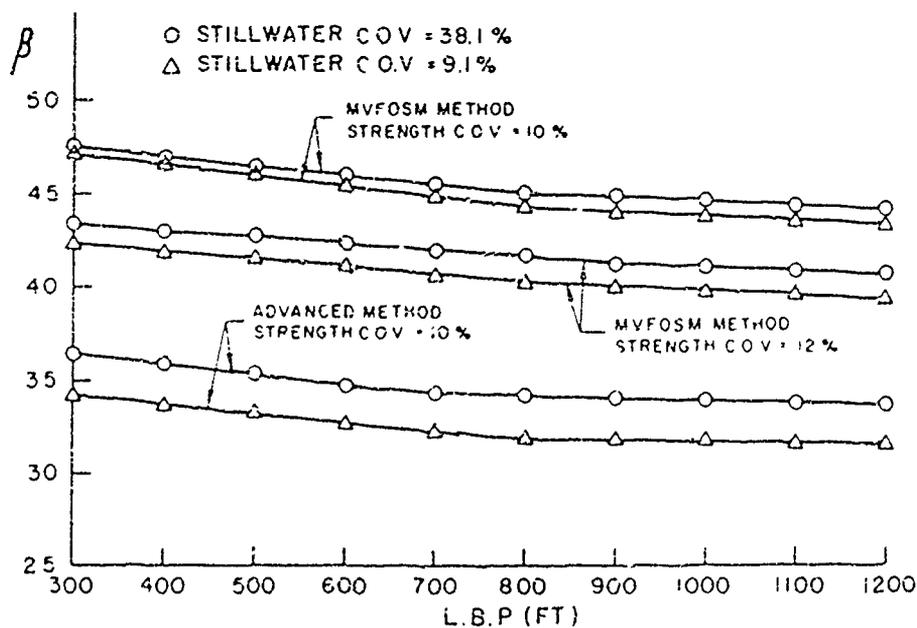
Figure 10.13. Safety Index (ABS) versus length between perpendiculars of Ships

298

Table10.9. Partial Safety Factors and Safety Index of Series 60 Ships

Ship	Length. ft	Δ_s	Δ_{sw}	(1) Δ_w	(2) β
1	300	0.8605	1 031	6.515	3.420
2	400	0.8662	1.029	6.434	3.364
3	500	0.8710	1.028	6.348	3.311
4	600	0.8750	1.027	6.261	3.265
5	700	0.8780	1.027	6.185	3.227
6	800	0.8783	1.027	6.117	3.198
7	900	0.8807	1.027	6.085	3.179
8	1000	0.8808	1.027	6.046	3.170
9	1100	0.8809	1.027	6.018	3.160
10	1200	0.8812	1.027	5.988	3 149

All factors based on strength COV = 10% and stillwater moment COV = 9 1%.
(1) Equivalent partial safety factor, exponential wave moment.
(2) Target safety indices from which all partial safety factors are derived.

299

REFERENCES

10.1 Lankford, W., "The Structural Design of the ASR Catamaran Cross Structure," Naval Engineers Journal, Aug. 1967.

10.2 Hogben, N. and Lumb, F., Ocean Wave Statistics, National Physical Laboratory, Ministry of Technology, London, 1967.

10.3 Pierson, W. and Moskowitz, L., "A Proposed Spectral Form for Fully Developed Wind Seas Based on the Similarity Theory of S.A. Kitaigorodskii," Journal of Geophysical Research, Vol. 69, Dec. 1964.

10.4 Loukakis, T., "Computer Aided Prediction of Seakeeping Performance in Ship Design," Report No. 70-3, Department of Naval Architecture and Marine Engineering, MIT, Aug. 1970.

10.5 Chen, Y.K., Kutt, L.M., Piaszczyk, C.M., and Bieniek, M.P., "Ultimate Strength of Ship Structures," Trans. SNAME, Vol. 91, 1983.

10.6 Mansour, A., "Methods of Computing the Probability of Failure under Extreme Values of Bending Moment," Journal of Ship Research, Vol. 16, No. 2, June 1972.

10.7 Beck, R., "A Computerized Procedure for Prediction of Seakeeping Performance," Report No. 69-2, Department of Naval Architecture and Marine Engineering, MIT, March 1969.

10.8 Ferro. G. and Mansour, A., "Probabilistic Analysis of the Combined Slamming and Wave-Induced Responses," Journal of Ship Research, Vol. 29, No. 3, Sept. 1985, pp. 170-188.

10.9 Mansour, A.E., "Probabilistic Design Concepts in Ship Structural Safety and Reliability," Trans. SNAME, Vol. 80, 1972.

10.10 Soares, C.G. and Moan, T., "Statistical Analysis of Stillwater Bending Moments and Shear Forces in Tankers, Ore and Bulk Carriers," Proceedings, Third Iberoamerican Congress of Naval Engineering, Madrid, 1982.

10.11 Horne, M.R. and Price, P.H., "Commentary on the Level-II Procedure," Supplement to "Rationalization of Safety and Serviceability Factors in Structural Codes," Report 63, Construction Industry Research and Information Association (CIRIA), London, Oct. 1976.

11. CONCLUDING REMARKS AND RECOMMENDATIONS

The powerful tools of the theory of probability provide excellent means for assessing the safety of marine structures under certain conditions of uncertainty. Probabilistic methods have been developed and used in practice for describing the random loads acting on a marine structure and the uncertainties associated with its true strength. The safety margin between an extreme loading combination and the strength of a structure is then assessed through reliability indices and probabilities of failure. Such reliability analysis is only a small but important part of the total probabilistic approach for designing or checking a marine structure. Partial safety factors and safety formats suitable for use in design and for implementation in Codes and Rules have been advanced and used by practitioners as well as Classification Societies and Code Developers. Fatigue analysis has been developed in several reliability formats which allow for the estimation of the probability of failure from the load history and the fatigue strength of the material. Complex redundant structures and structures with multiple failure modes or mechanisms have been treated using system reliability concepts which are being rapidly developed at the present time. In short, powerful and sophisticated probabilistic tools are currently available for use by the marine industry. There are, however, several shortcomings that prevent a wider use of the probabilistic and reliability methods in the design process. These include:

1. Use of reliability analysis in checking and design processes requires more information on the environment, loads and the properties and characteristics of the structure than a typical deterministic analysis. Often such information is not available or may require considerable time and effort to collect . Time and schedule restrictions on the design are usually limiting factors on the use of such sophisticated methods.

2. Application of probabilistic and reliability methods usually require some familiarity of basic concepts in probability, reliability

and statistics. Practitioners and designers are gaining such familiarity through seminars, symposia and special courses. Educational institutions are also requiring more probability and statistics courses to be taken by students at the graduate and undergraduate levels. This, however, is a slow process that will take at least one generation in order to produce the necessary "infrastructure" for a routine use of reliability and probabilistic methods in design.

3. The two shortcomings stated above are not severe drawbacks in connection with development of Codes and Rules based on reliability analysis since such a development requires a "one time" or a more consolidated effort to collect the necessary information. In addition, the "one time" code format and development can be done by experts in the field. But here the "inertia of tradition" comes into play which makes any new approach, reliability or otherwise, difficult to incorporate. This, however, has been changing and more Classification Societies and Code organizations have taken an active interest in the probabilistic methods and developed Rules and Codes based, at least partially, on reliability.

4. On a more technical aspect, the reliability analysis did not deliver what it initially promised, that is, a true measure of the reliability of a structure by a "true and actual" probability of failure. Instead what it delivered is "notional probabilities" of failure and safety indices which are good only as comparative measures. Only notional values are delivered because of the many assumptions and approximations made in the analysis producing such probabilities and indices. These approximations, deficiencies and assumptions, however are made , not only in the reliability aspects, but also in other aspects and disciplines used in the design. Such aspects include determination of loads using hydrodynamics theory and approximations made in the structural analysis and response to the applied loads. When all such assumptions and deficiencies are removed from the design analysis, the resulting probabilities of failure will approach the "true" probabilities.

303

In spite of the shortcomings stated above, use of reliability analysis in design provides advantages and unique features. These include:

1. Explicit consideration and evaluation of uncertainties associated with the design variables.

2. Inclusion of all available relevant information in the design process.

3. Provides a framework of sensitivity measures.

4. Provides means for decomposition of global safety of a structure into partial safety factors associated with the individual design variables.

5. Provides means for achieving uniformity of safety within a given class of structures (or specified nonuniformity).

6. Minimum ambiguity when updating design criteria.

7. Provides means to weigh variables in terms of their significance.

8. Rational guidance for data gathering.

9. Guidance in novel designs.

The advantages seem to outweigh the drawbacks and it is almost inevitable that the probabilistic and reliability aspects will be used in designs where randomness of the variables is an important consideration. Based on these conclusions, the following recommendations are made:

1. The major effort currently progressing in the development and application of reliability methods to marine structure should be continued and expanded. Such efforts will not be wasted since, most likely, some of the developed procedures will, sooner or later, be used in design.

2. In the calculations of the reliability indices and probabilities of failure, the resulting values depend considerably on the methods used in determining the loads acting on the structure (e.g. extreme versus long-term waves loads) and on the method of combining these loads. A need exists for "standardizing" such procedures for use in design.

3. A study of target reliability based on existing ships or minimum Rule requirements for the primary strength should be undertaken based on such a "standardized" load procedure.

4. Studies and additional development of reliability methods are needed for the secondary (stiffened panels) and tertiary (plates between stiffeners) aspects of ship design.

5. There is currently a strong tendency to neglect level 3 reliability analysis in favor of level 2 because of the difficulties stated in Chapters 4 and 5 of the report. Certain simplifications can be made however within level 3 framework which would make it possible for application to marine structures. Such simplifications and further developments of level 3 are worth persuing. Similarly, application of simulation techniques should be further studied.

6. System reliability is an essential aspects of reliability analysis of highly redundant structures such as offshore platforms. Additional work is needed in this area particularly in regard to simplifying and reducing the number of permutations of possible failure paths and the corresponding computations.

APPENDIX 1
HELPFUL INFORMATION

In this appendix some useful information on several aspects of reliability of marine structures are described. They relate to topics which appeared in various chapters in this report where reference is made to this Appendix.

A1.1. Weibull Distribution Parameters - Probability Paper:

The probability density function (p.d.f.) and cumulative distribution function (c.d.f.) of the Weibull Distribution are given by

$$\text{p.d.f.} \quad = \quad f_X(x) \quad = \quad (\ell/k) \left(\frac{x}{k}\right)^{\ell-1} e^{-(x/k)^\ell} \qquad x \geq 0 \qquad (1)$$

$$\text{c.d.f.} \quad = \quad F_X(x) \quad = \quad 1 - e^{-(x/k)^\ell} \qquad x \geq 0 \qquad (2)$$

where k and ℓ are parameters to be determined from data, e.g., data of wave amplitude or wave-bending moment amplitude.

The first two moments (mean and variance) of the Weibull distribution are given by:

$$\text{Mean} \quad = \quad E(x) \quad = \quad k \, \Gamma(\ell^{-1}+1) \qquad (3)$$

$$\text{Variance} \quad = \quad \text{Var}(x) = \quad k^2 \left(\Gamma(2\ell^{-1}+1) - \left(\Gamma(\ell^{-1}+1)\right)^2 \right) \qquad (4)$$

where $\Gamma(t)$ is the Gamma function defined as

$$\Gamma(t) \quad = \quad \int_0^\infty y^{t-1} e^{-y} \, dy$$

The Gamma function is tabulated in many Handbooks, e.g., Handbook of Chemistry and Physics.

Some properties of the Gamma function are described as follows:

$$\Gamma(t) \quad = \quad (t\text{-}1)\,\Gamma(t\text{-}1)$$

$$\Gamma(t+1) \quad = \quad t\,\Gamma(t) = t\,(t\text{-}1)\ldots(t\text{-}r)\,\Gamma(t\text{-}r)$$

i.e., generalization of the factorial function.

$$\Gamma(1) \quad = \quad 1$$

$$\Gamma(n+1) \quad = \quad n!\ \text{for any } n = \text{integer}$$

$$\Gamma\!\left(\frac{1}{2}\right) \quad = \quad \sqrt{\pi}$$

$$\Gamma\!\left(n+\frac{1}{2}\right) \quad = \quad \frac{1\times3\times5\ldots(2n\text{-}1)}{2^n}\ \sqrt{\pi}\quad;\quad n = \text{integer}$$

$$\Gamma\!\left(n+\frac{1}{2}\right) \quad = \quad \frac{1\times3\times5\ldots(n\text{-}1)}{2^{n/2}}\ \sqrt{\pi}\quad;\quad n = \text{even integer}$$

The Weibull distribution reduces to two important special cases as follows:

a. Exponential Distribution

When $\ell = 1$ and $k = \lambda$, the Weibull distribution reduces to the exponential distribution with parameter λ. From equations (1) and (2), the resulting p.d.f. and c.d.f. are

$$f_X(x) \quad = \quad \frac{1}{\lambda}\ e^{\text{-}x/\lambda} \qquad\qquad x \geq 0 \qquad\qquad (5)$$

$$F_X(x) \quad = \quad 1 - e^{\text{-}x/\lambda} \qquad\qquad x \geq 0 \qquad\qquad (6)$$

From equations (3) and (4), the mean and variance of the exponential distribution are given by

$$E(X_e) \quad = \quad \lambda\,\Gamma(1{+}1) \quad = \quad \lambda\,\Gamma(2) \quad = \quad \lambda \qquad\qquad (7)$$

$$\mathrm{Var}(X_e) \quad = \quad \lambda^2\left(\Gamma(2{+}1) - \Gamma(2)^2\right) \quad = \quad \lambda^2\,(2{-}1) \quad = \quad \lambda^2 \qquad\qquad (8)$$

b. Rayleigh Distribution

When $\lambda = 2$ and $k = \sqrt{2E}$ the Weibull distribution reduces to the Rayleigh distribution. Notice that, if the Rayleigh distribution is resulting from a stationary Gaussian process as the distribution of the peaks, then "E" as defined

307

here is the mean square value of the process, i.e., the area under the spectral density of the process. From equations (1) and (2), the Rayleigh distribution is given by

$$\text{p.d.f.:} \quad \hat{f}_X(x) \quad = \quad \frac{x}{E} \quad e^{-x^2/2E} \qquad\qquad x \geq 0 \qquad\qquad (9)$$

$$\text{c.d.f.:} \quad F_X(x) \quad = \quad 1 - e^{-x^2/2E} \qquad\qquad x \geq 0 \qquad\qquad (10)$$

and, from equations (3) and (4), its mean and variance are given by

$$E(X_R) = \sqrt{2E} \; \Gamma\left(\frac{1}{2} + 1\right) = \sqrt{2E} \; \frac{1}{(2)^1} \; \sqrt{\pi} = \frac{1}{2} \; \sqrt{2\pi E} \qquad (11)$$

$$\text{Var}(X_R) = 2E\left(\Gamma(2) - \left(\Gamma\left(\frac{1}{2} + 1\right)\right)^2\right) = 2 \; \left(1 - \frac{\pi}{4}\right) \qquad (12)$$

Estimation of the Weibull Distribution Parameters

Several methods can be used to estimate the Weibull distribution parameters from a set of data. Since the exponential and the Rayleigh distributions are special cases, similar methods can be used to estimate their parameters. The methods include the method of moments, Weibull probability paper, the maximum likelihood method and a method based on order statistics. Only the moment method and the Weibull probability paper are discussed here. The advantage of the probability paper over the moment method is that it provides a mean for checking if the Weibull distribution actually fits the data or not as will be discussed later.

a.   Method of Moment

The mean and standard deviation of a data sample can be determined from the usual equations:

$$\bar{x} = \text{Sample mean} = \frac{1}{n} \; \sum_{i=1}^{n} \; x_i$$

308

$$\sigma_x = \text{Sample standard deviation} = \left(\frac{1}{n} \sum_{i=1}^{n} (x_i - \bar{x})^2 \right)^{1/2}$$

The resulting values for $\bar{x}$ and σ_x can be used in conjunction with equations (3) and (4) to determine the values of k and ℓ, or more conveniently from the ratio:

$$\frac{\Gamma(\ell^{-1}+1)}{\left(\Gamma(2\ell^{-1}+1) - (\Gamma(\ell^{-1}+1))^2\right)^{1/2}} = \frac{\bar{x}}{\sigma_x} \tag{13}$$

which is a function of ℓ only. Thus ℓ can be estimated from (13) and then inserted in equation (3) or (4) to determine k.

b.   Weibull Probability Paper

The Weibull distribution function is given by:

$$F_x(x) = 1 - e^{-(x/k)^{\ell}}$$

therefore,

$$\log \log \left(1 - F_x(x)\right) = -\ell \log (x/k)$$

or,

$$\log \log \left(\frac{1}{1 - F_x(x)}\right) = \ell \log x - \ell \log k$$

Insert

$$w = \log \log \left(\frac{1}{1 - F_x(x)}\right) \; ; \; v = \log x$$

the linear relation results

$$w = \ell v - \ell \log k \tag{14}$$

So if $(1-F_x(x))^{-1}$ or $(1-F_x(x))$ is plotted against x on log log versus log paper a straight line is obtained (if the data fits the Weibull distribution closely). The slope of the straight line is ℓ or $-\ell$, respectively, and the intercept with the axis is $-\ell\log k$. Thus k and ℓ can be determined.

Notice that, in addition to providing a mean for estimating the parameters k and ℓ, the Weibull paper is useful in examining visually the quality of the fit. Goodness-of-fit tests such as Chi-square, W-statistics and Kolmogorov-Smirnov tests may also be used to examine more accurately the quality of the fit and to determine which of several candidate probability distributions fits the data best.
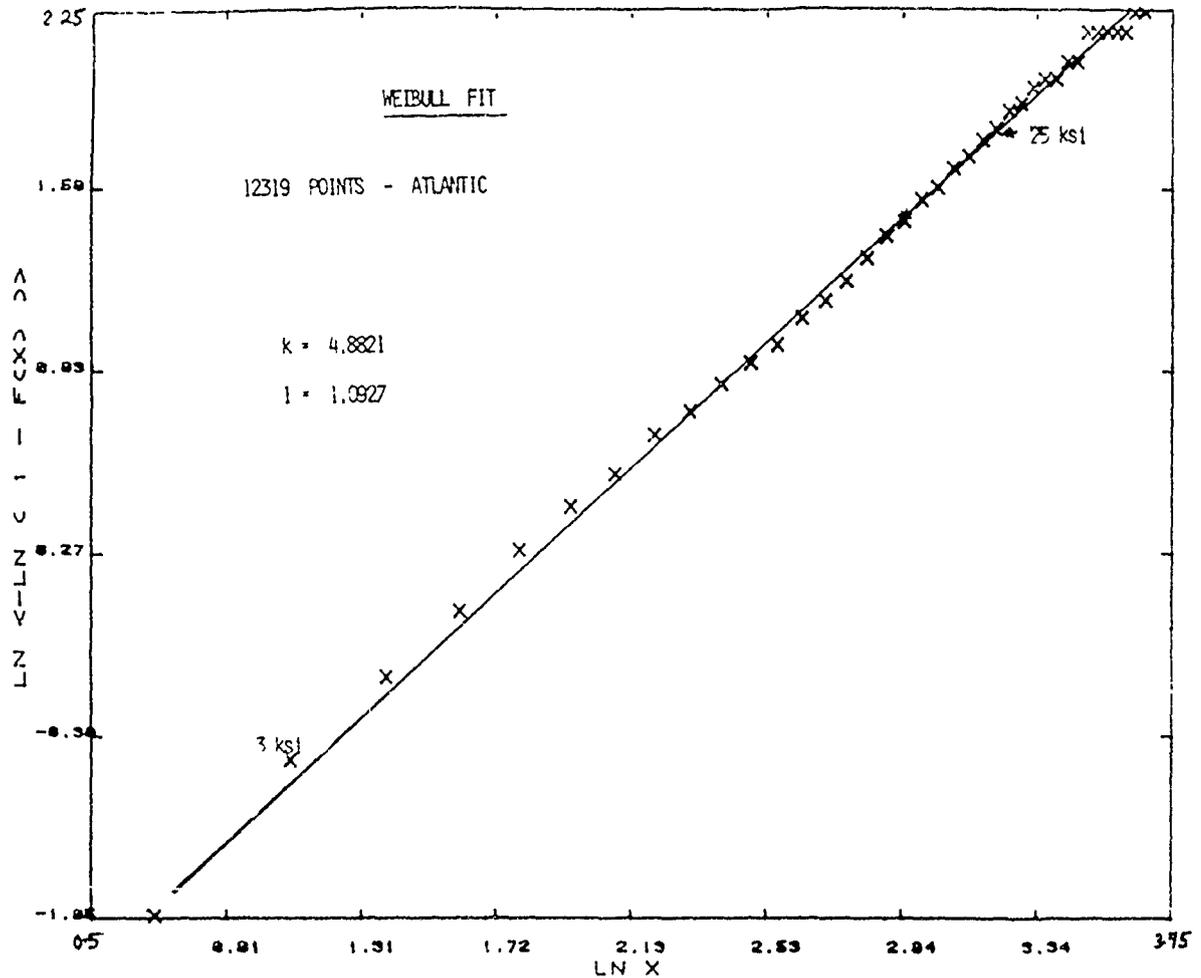
Figure A1. Weibull Plot of SL -7 Five Year Data

More detailed information on these tests and examples of their use in conjunction with wave bending moment data from SL-7 containerships are given in reference [A1]. A sample of Weibull probability paper which shows the fit of 12319 data points from SL-7 containerships is shown in Figure A1 obtained from reference [A1].

A1.2. The Safety of Index Versus Probability of Failure for Normal and Other Distributions:

In Chapter 4 and 5 it was shown that, for the simple margin "M" (or limit state function) given by:

$$M = g(x_1, x_2) = S - Z \tag{15}$$

the probability of failure p_f is given by (see equations 4.4 and 5.5)

$$p_f = \int_0^\infty F_S(z), f_Z(z)\, dz \tag{16}$$

$$= F_G(-\beta) \tag{17}$$

where $F_G(\cdot)$ is the cumulative distribution function of the standardized Margin "G" (see equation 5.4) and β is the safety index defined as the margin mean divided by its standard deviation. If S and Z are both normal, then the margin M defined by (15) is also normal and $F_G(\ )$ becomes the standard normal cumulative distribution function tabulated in many handbooks. Thus the relation between p_f and β can be easily computed.

Figure A.2 obtained from reference [A.2] shows the relation between p_f and β for some other distributions of S and Z and specified values of their coefficients of variation ($v_s = 0.13$ and $v_z = 0.10$). The plot shows that p_f is sensitive to the type of distributions of S and Z in the higher values of β (range of low probabilities of failure).
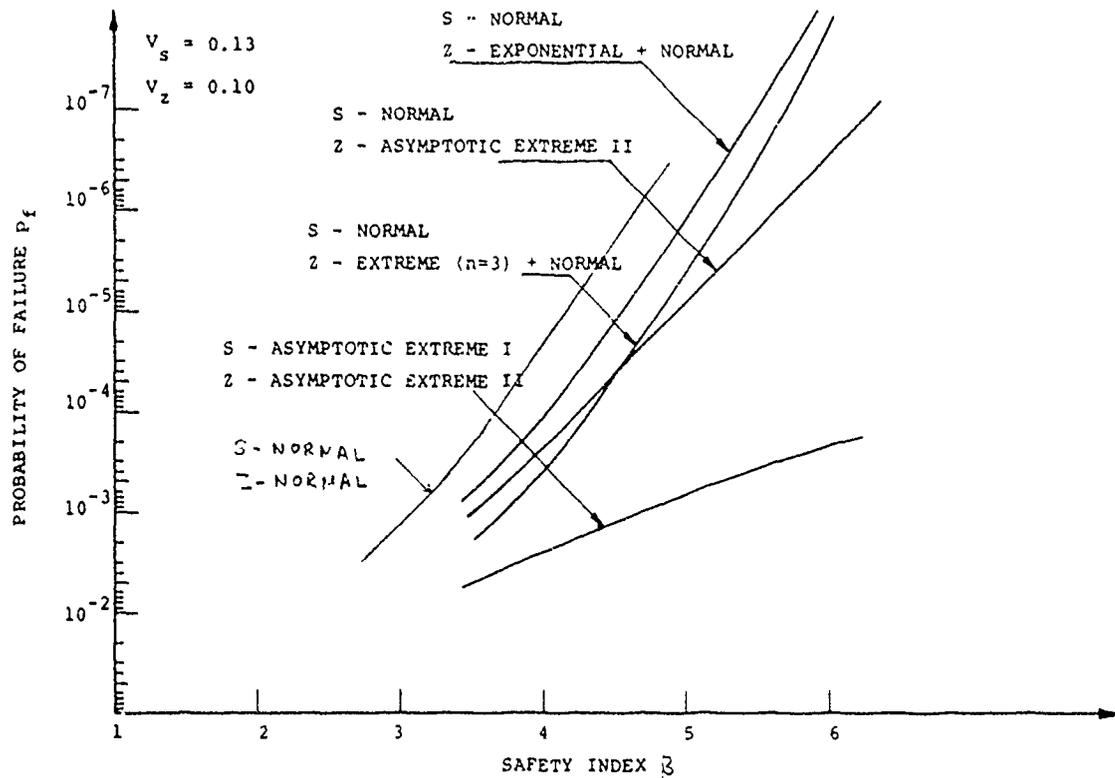
Figure A.2. Probability of Failure Versus the Safety Index

REFERENCES

A.1. Mansour, A. E., Jan, H. Y., Zigelman, C. I., Chen, Y. N. and Harding, S. J., "Implementation of Reliability Methods to Marine Structures," Trans. SNAME, Vol. 92, 1984, pp. 353-382.

A.2 Mansour, A. E., "Approximate Probabilistic Method of Calculation Ship Longitudinal Strength," Journal of Ship Research, Vol. 18, No. 3, September 1974, pp. 203-213.

Appendix 2: Computer Program "CALREL" for Performing Reliability Analysis

A Brief Description of CALREL - A Computer Program for Component Reliability Analysis:

CALREL is a batch processed computer program in FORTRAN language suitable for execution in both mainframe and microcomputers. Given a probabilistic characterization of the basic random variables, and an analytic performance function (limit state equation), the program calculates the Hasofer-Lind reliability index, β_{HL}, in the standard space of uncorrelated variables (u space). The program calculates the probability of component failure if probability distribution (level III method) of basic physical variables are provided. The output includes sensitivity measures of the reliability index and probability of failure with respect to basic variables, deterministic parameters in the performance function and the distribution parameters. Following is a brief description of special options and features of CALREL. The attached 'User's Guide to CALREL' is a self explanatory document of all the other options and features.

Input Description:

The input to CALREL consists of two parts: i) input data and ii) user provided subroutines. The data input defines basic physical random variables, i.e., their mean standard deviation, correlation, etc. and, or parameters of the optional distribution functions. For level-II methods only second moment characterization of random variables are necessary. Both mean value first order second moment (MVFOSM) and Hasofer-Lind first order second moment (FOSM) reliability index can be calculated. For level III characterization of the random variables two options are available: i) first order marginal distribution method [FOMD, ref.A.1] or ii) first order full distribution method [FOFD] using Rosenblatt transformation.

If the basic random variables are independent they can be specified completely by their respective marginal distributions. For dependent variables if only marginal distributions and pair wise correlation among them is known then, a (non-unique) joint distribution model is implicitly assumed that is consistent with the specified marginal distributions and correlation structure [FOMD, ref. A.1]. The marginal distribution function can either be chosen from the program library or can be specified in an analytical form through a user specified subroutine called 'df'. The correlation structure for dependent variables is specified in the input data section.

For full distribution method [FOFD] using Rosenblatt transformation the following conditional distribution functions are analytically specified through a user defined subroutine called 'hfun'. [See Example 3 in User's Manual.]

$$H_i(x_i \mid x_1, ..., x_{i-1}) = P(X_i \le x_i \mid X_1 = x_1, ..., X_{i-1} = x_{i-1}) \quad (A.1)$$

If $f_{\underline{X}}(\underline{x})$ and $F_{\underline{X}}(\underline{x})$, respectively, represent the joint density and joint distribution function of $\underline{X}$, we have:

$$H_i(x_i \mid x_1, ..., x_{i-1}) = \int_{-\infty}^{x_i} f_{X_i \mid X_1,.....X_{i-1}}(x_i \mid x_1, ..., x_{i-1}) \, dx_i$$

$$= \frac{\dfrac{\partial^{i-1}}{\partial x_1.....\partial x_{i-1}} F_{X_1,....X_i}(x_1,...x_i)}{f_{X_1,....,X_{i-1}}(x_1,..., x_{i-1})} \quad (A.2)$$

The program then implicitly uses the following transformations between the basic variables space and the standard normal uncorrelated space :

$$U_1 = \Phi^{-1}[H_1(X_1)] = \Phi^{-1}[F_{X_1}(X_1)]$$

$$U_2 = \Phi^{-1}[H_2(X_2|X_1)]$$

$$U_3 = \Phi^{-1}[H_3(X_3|X_1,X_2)] \qquad\qquad\qquad (A.3)$$

$$U_n = \Phi^{-1}[H_n(X_n|X_1, ..., X_{n-1})]$$

In addition to the above specifications in the subroutine 'hfun' the standard deviation of the basic variables are required as input data for calculatirg iteration steps in the optimization scheme to find the β-point. The user can also specify parameters of the above conditional distributicns (h-functions) through input data.

Performance function: The performance function (limit state equation) in CALREL is specified analytically through a function subprogram 'g'. The subprogram returns a value of the performance function for each call from the main program specifying a value of the basic variable $\underline{X}$. The parameters for the analytic performance function can be passed from the main program, if defined, through the input data.

The main program uses a finite difference scheme to calculate the gradient vector of the limit state surface at the iteration point. Hence, if an analytic performance function is not available the subprogram 'g' can be made to call other programs (e.g., finite element, dynamic analysis program, etc.) to return a value of the performance function. Since finite difference scheme is used to calculate the gradient vector at the β-point, a number of performance function values may be required involving great computational efforts. It is desirable to be able to input the gradient

vector directly when available (either analytically or through numerical values returned by other programs such as finite element etc.). This is beyond the capability of the present version of CALREL but can easily be achieved through minor modification of a subroutine in the main program. The user provided subroutines are provided in a file called 'user.for' which is compiled and linked to the main body of CALREL, each time a new problem is solved.

Output Description

The output of CALREL consists of reliability indices, probability of failure for level-III analyses and various other sensitivity measures. In level-III analyses probability of failure results can be obtained based on both first order (tangential hyperplane) and second order (quadratic hypersurface) approximation of the limit state surface. Two different second order approximations to the actual limit state surface are available, based on point fitting and curvature matching procedures. For an approximated quadratic hypersurface the probability content is calculated by four different approximating formulas. The different sensitivity measures calculated by the program can be described as follows:

$$ 1 \qquad \underline{\alpha} = \nabla\beta(\underline{u}^*), \text{ i.e., } \alpha_i = \frac{\partial\beta}{\partial U_i}\bigg|_{\underline{U}=\underline{u}^*} \qquad (A.4) $$

where $\underline{u}^*$ is the design point (or β-point).

$\underline{\alpha}$ is a sensitivity measure of β_{HL} with respect to the standard variates (U_1, U_2, ..., etc.).

2. Measures of sensitivity with respect to basic variables $\underline{X}$ at a point $\underline{x}^*$ (corresponding to $\underline{u}^*$ in $\underline{u}$ space) is given by

$$ \nabla\beta(\underline{x}^*) = \underline{\alpha}\,\underline{\Gamma}\,\underline{D}^{-1} \qquad (A.5) $$

where $\underline{D}$ = diagonal matrix of standard deviation

and, $\underline{\Gamma} = L^{-1}$, $\underline{R} = \underline{L}\,\underline{L}^T$ and $\underline{R}$ = correlation matrix.

To make variations ∂x_i^*; $i = 1, ..., n$; equally likely $\nabla\beta(\underline{x}^*)$ is scaled by the corresponding standard deviations, i.e.,

$$\nabla\beta(\underline{x}^*)\,\underline{D} = \underline{\alpha}\,\underline{\Gamma}$$

A unit sensitivity vector is now defined as:

$$\gamma = \frac{\underline{\alpha}\,\underline{\Gamma}}{|\,\underline{\alpha}\,\underline{\Gamma}\,|} \qquad\qquad (A.6)$$

Gamma ($\underline{\gamma}$) is a relative measure of importance among basic random variables.

The program also calculates 'delta' and 'eta' normalized (each variation equally likely as in $\underline{\alpha}$ and $\underline{\gamma}$) sensitivity vectors with respect to the mean and standard deviation of the basic physical variables. If desired the program also calculates sensitivity measures of reliability index and probability of failure with respect to other distribution parameters and deterministic parameters of the analytic performance function.

References

A. 1. Der Kiureghian, A. and Liu, Pei-Ling (1986). Structural Reliability Under Incomplete Probability Information. Journal of Engineering Mechanics, ASCE, Vol. -112, No. -1.

User's Guide to
C A L R E L
A First and Second-order Structural Reliability Analysis Program

INPUT DATA

1. Title --- Format (A80)

Column	Variable	Description
1-80	TITLE	Alphanumeric description of the problem

2. Control Data --- Format (5I5/7I5/3I5,4d10.0)

Column	Variable	Description
1- 5	IFO	Type of technique used IFO=1 MVFOSM IFO=2 FOSM IFO=3 FOMD IFO=4 FOFD (Rosenblatt transformation)
6-10	ISO	Type of second-order approximation ISO=0 First-order analysis only ISO=1 Point fitting method ISO=2 Curvature fitting method ISO=3 Both Point and Curvature fittings
11-15	ITG	Type of integration schemes used in second order approximation ITG.eq.0 Breitung formula, Tvedt 3-term formula and Tvedt single integral ITG.ne.0 All above three schemes plus Tvedt double integral
16-20	ISV	Type of sensitivity analysis required ISV=0 No sensitivity analysis ISV=1 distribution parameters ISV=2 performance function parameters ISV=3 distribution and performance function parameters
21-25	IRS	restart code IRS.ne.0 restart analyzing an old, unconverged problem IRS.eq.0 analyze a new problem
1- 5	NX	Number of basic variables
6-10	NP	Number of deterministic parameters in the performance function
11-15	NU	Number of user-provided distributions
16-20	NS	Number of parameters in user-defined full distributions (Applicable when IFO=4)
21-25	NCORR	Flag for correlation matrix (Applicable when IFO.ne.4) NCORR.eq.0 Uncorrelated variables NCORR.ne.0 Correlated variables
26-30	INIT	Flag for initialization INIT.eq.0 Start from mean point INIT.ne.0 Start point specified by user
31-35	IPR	Output code IPR.eq.0 Output all iteration steps IPR.ne.0 Output at every ipr steps

1- 5	IOPT	Type of optimization scheme used
		IOPT=1 HL-RF method
		IOPT=2 Modified HL-RF method
		IOPT=3 Gradient Projection method
6-10	NIT1	Maximum number of iteration cycles
		Default=100, Maximum=100
11-15	NIT2	Maximum steps in line search
		Default=4
16-25	TOL	Convergence tolerance
		Default=0.001, Minimum=0.001
26-35	OPT1	Step size reduction factor in line search
		IOPT=1, Default=1.0
		IOPT=2 or 3, Default=0.5
36-45	OPT2	Optimization parameter
		IOPT=2 Parameter c in descent function
		Default=10
		IOPT=3 Convergence tolerance for line
		search: Default=TOL
46-55	OPT3	Optimization parameter
		IOPT=3 Maximum step size in line search
		Default=4.0

3. User-defined Distribution --- Format (I5,A20)
   Skip this section if NU=0.
   For each user-defined distribution input:

1- 5	NDISU	Type number of user-defined distribution
		NDISU > 20
6-25	UNAME	Name of user-defined distribution.

4. Basic Random Variables
   Skip this section if IFO=4.
   For each basic variable with NDIS < 21: (2I5,5D10.0)

1- 5	NV	Variable number
6-10	ND	NDIS = abs(ND) : Distribution type.
		NDIS=1 Normal
		NDIS=2 Lognormal
		NDIS=3 Gamma
		NDIS=4 Shifted Exponential
		NDIS=5 Shifted Rayleigh
		NDIS=6 Uniform
		NDIS=7 Beta
		NDIS=11 Type-I Largest Value
		NDIS=12 Type-I Smallest Value
		NDIS=13 Type-II Largest Value
		NDIS=14 Weibull
11-20	P1	Distribution parameter 1
		ND>0 P1 : mean value
		ND<0 P1 : as defined in Table 1
21-30	P2	Distribution parameter 2
		ND>0 P2 : standard deviation
		ND<0 P2 : as defined in Table 1
31-40	P3	Distribution parameter 3
41-50	P4	Distribution parameter 4
		Presently, P3 and P4 are applicable
		only when NDIS=7.
51-60	XINIT	Initial value of x; only needed when INIT=0

For each basic variable with NDIS > 20: (2I5,5D10.0/I5,2D10.0)

1- 5	NV	Variable No.
6-10	NDIS	Distribution type
11-20	P1	Distribution parameter 1
21-30	P2	Distribution parameter 2
31-40	P3	Distribution parameter 3
41-50	P4	Distribution parameter 4
51-60	XINIT	Initial value of x; must be defined even if INIT=0
1- 5	IB	Flag for bounds
		IB=0 No bounds
		IB=1 Has lower bound
		IB=2 Has upper bound
		IB=3 Has lower and upper bounds
6-15	BND1	Lower bound of the basic variable Applicable when IB=1,3
16-25	BND2	Upper bound of the basic variable Applicable when IB=2,3

5. Basic Random Variables --- Format (I5,2D10.0,I5,2D10.0)
   Skip this section if IFO=1, 2, or 3.
   For each basic variable input:

1- 5	NV	Variable No.
6-15	SIG	Standard deviation
16-25	XINIT	Initial value of x
26-30	IB	Flag for bounds
		IB=0 No bounds
		IB=1 Has lower bound
		IB=2 Has upper bound
		IB=3 Has lower and upper bounds
31-40	BND1	Lower bound of the basic variable Applicable when IB=2,3
41-50	BND2	Upper bound of the basic variable Applicable when IB=2,3

6. Correlation Matrix --- Format (*D6.0)
   Skip this section if NCORR=0.

1-10	RO	Lower triangle of the correlation matrix
1-10,11-20		excluding the diagonals. Read it row-wise
...		and in triangular shape.

7. Parameters in Full Distribution Function --- Format (8D10.0)
   Skip this section if NS=0.

1-10....	DS	Values of the parameters in the full cumulative distribution function

8. Parameters in Performance Function --- Format (8D10.0)
   Skip this section if NP=0.

1-10,...	DP	Values of the deterministic parameters in the performance function

321

9. Control Flag for Program Execution --- Format (I5)
   1- 5   NEXT   Control flag for program execution
                          NEXT=0   Stop execution
                          NEXT=1   Restart a brand new analysis
                                    All the aforementioned data
                                    should be input after this line.
                          NEXT=2   Re-analyze the old problem
                                    with a different set of parameters
                                    in the performance function.
                                    Only the values of the parameters
                                    in the performance function should
                                    be input after this line.

Notes:

(1) If the nearest point is not found in NIT1 steps, the final
    status of the analysis will be stored in an unformatted
    file 'calrel.sav'. This file must remain unaltered if the
    analysis is to be continued in an ensuing run.

(2) In a restart problem, the program reads only the title and
    the control data from the input file. The initial status
    of the problem are read from 'calrel.sav'.
    In order to be consistent, IFO, NX, NP, NU, NS, and NCORR
    must be the same as the previous run.

(3) To override the restrictions NIT1<100 and TOL>0.001, input
    negative NIT1 and TOL. Their absolute values will be used
    in the analysis regardless of the limits.

322

Table 1.

ndis	name	PDF	parameters	bounds
1	Normal	$\frac{1}{\sqrt{2\pi}\,\sigma}\,\exp\left\{-\frac{1}{2}\left(\frac{x-\mu}{\sigma}\right)^2\right\}$	$P1 = \mu$ $P2 = \sigma \quad > 0$	
2	Lognormal	$\frac{1}{\sqrt{2\pi}\,\zeta x}\,\exp\left\{-\frac{1}{2}\left(\frac{\ln x - \lambda}{\zeta}\right)^2\right\}$	$P1 = \lambda$ $P2 = \zeta \quad > 0$	
3	Gamma	$\frac{\lambda(\lambda x)^{k-1}\,e^{-\lambda x}}{\Gamma(k)}$	$P1 = \lambda > 0$ $P2 = k > 0$	$x \geq 0$
4	Exponential	$\lambda\, e^{-\lambda(x-x_0)}$	$P1 = \lambda > 0$ $P2 = x_0$	$x \geq 0$
5	Rayleigh	$\frac{x}{\alpha^2}\exp\left\{-\frac{1}{2}\left(\frac{x-x_0}{\alpha}\right)^2\right\}$	$P1 = \alpha$ $P2 = x_0$	$x \geq 0$
6	Uniform	$\frac{1}{b-a}$	$P1 = a$ $P2 = b$	$a \leq x \leq b$
7	Beta	$\frac{(x-a)^{q-1}(b-x)^{r-1}}{B(q,r)(b-a)^{q+r-1}}$	$P1 = q > 0, \quad P3 = a$ $P2 = r > 0 \quad P4 = b$	$a \leq x \leq b$
11	Type I Largest Value	$\alpha_n \exp\left[-\alpha_n(x-u_n)-e^{-\alpha_n(x-u_n)}\right]$	$P1 = u_n$ $P2 = \alpha_n > 0$	
12	Type I Smallest Value	$\alpha_1 \exp\left[\alpha_1(x-u_1)-e^{\alpha_1(x-u_1)}\right]$	$P1 = u_1$ $P2 = \alpha_1 > 0$	
13	Type II Largest Value	$\frac{k}{u_n}\left[\frac{u_n}{x}\right]^{k+1}\exp\left[-\left(\frac{u_n}{x}\right)^k\right]$	$P1 = u_n$ $P2 = k > 0$	$x > 0$
14	Type III Smallest Value	$\frac{k}{u_1}\left[\frac{x}{u_1}\right]^{k-1}\exp\left[-\left(\frac{x}{u_1}\right)^k\right]$	$P1 = u_1$ $P2 = k > 0$	$x > 0$
≥ 21	User provided distribution			

```fortran
      function g(x,dp)
c
c.....Function subroutine to compute the limit-state function
c.....x  = vector of basic variables
c.....dp = vector of deterministic parameters
c
      implicit real*8 (a-h,o-z)
      dimension x(1),dp(1)
          .
          .
      g  ....
      return
      end


      subroutine df(par,x,nd,cdf,pdf)
c
c.....Subroutine to compute pdf and cdf of user-defined distributions
c.....par = vector of parameter distributions
c.....x   = value of variable
c.....nd  = distribution number (>20)
c.....cdf = computed cdf value
c.....pdf = computed pdf value
c
      implicit real*8 (a-h,o-z)
      dimension par(4)
          go to (10,20,...) nd-20
10    cdf = ...
      pdf = ...
      return
20    cdf = ...
      pdf = ...
      return
          .
          .
      return
      end


      subroutine hfun(x,ih,ds,hi)
c
c.....Subroutine to compute conditional CDF's for Rosenblatt transformation
c.....x  = vector of basic variables
c.....ih = row number in Rosenblatt transformation
c.....ds = vector of deterministic distribution parameters
c.....hi = value of ith conditional cdf
c
      implicit real*8(a-h,o-z)
      dimension x(1),ds(1)
          go to (10,20,...) ih
10    hi = ...
      return
20    hi   ...
      return


      return
      end
```

324

File User.for

```
function g(x,dp)
implicit real*8 (a-h,o-z)
dimension x(1),dp(1)
g = dp(2)*x(2)**2-dp(1)*x(1)
return
end

subroutine df(par,x,nd,cdf,pdf)
implicit real*8 (a-h,o-z)
dimension par(4)
return
end

subroutine hfun(x,ih,ds,h)
implicit real*8(a-h,o-z)
dimension x(1),ds(1)
return
end
```

$$g = \eta_2 X_2^2 - \eta_1 X_1$$

Input File for Example 1:

$X_1 = $ Type I $(u = 90.9992, \alpha = 0.0641275)$ $\}$ independent

$X_2 = LN(\mu = 20, \sigma = 5)$

$\eta_1 = 1, \quad \eta_2 = 0.5$

```
example 1
    3    3    1    3    0
    2    2    0    0    0    0    1
    1   20    8   -0.0001
    1  -11 90.9992  .0641275    0.         0.
    2    2       20.        5.          0.         0.
       1.0           0.5
    0
```

Input File for Example 2:

X_1, X_2 as above, but correlated with $\rho_{X_1 X_2} = 0.5$

```
example 2
    3    3    1    3    0
    2    2    0    0    1    0    1
    1   20    8   -0.0001
    1  -11 90.9992  .0641275    0.         0.
    2    2       20.        5.          0.         0.
       0.5
       1.0           0.5
    0
```

```
***********************************************************
*        U n i v e r s i t y   o f   C a l i f o r n i a   *
*         Department  of  Civil  Engineering               *
*                    Division of                           *
*       Structural Engineering and Structural Mechanics    *
*                                                          *
*                  F  O  S  R  A  P                        *
*       First Order Structural Reliabilty Analysis Program *
*                                                          *
*                    Developed By                          *
*          Pei-Ling Liu and Armen Der Kiureghian           *
*              Last Revision: September 1986               *
*                                                          *
*              Extended for FOFD and SOSRAP by             *
*                 HONG-ZONG LIN, March 1986                *
***********************************************************


             ***** input data -- problem  1    ****

  example 1
  type of first-order technique used .......ifo=    3
    ifo=1 ...mean-value, 1st order, 2nd moment (mvfosm) method
    ifo=2 ...first-order, second moment (fosm) method
    ifo=3 ...first-order, marginal distribution (fomd) method
    ifo=4 ...first-order, full dist.(Rosenblatt trans) method
  type of second-order technique used .....iso=    3
    iso=0 ..............no second-order approximation
    iso=1 ......................point fitting method
    iso=2 ....................curvature fitting method
    iso=3 .......point and curvature fitting methods
  type of integration schemes used in second-order
  analysis .................................itg=    1
    itg.eq.0 ....Breitung, Tvedt's 2-term and single integral
    itg.ne.0 ...all of the above plus Tvedt's double integral
  type of sensitivity analysis required ...isv=    3
    isv=0 ...................no sensitivity analysis required
    isv=1 ..............sensitivity of distribution parameters
    isv=2 .......sensitivity of perfomance function parameters
    isv=3 ....distribution and performance function parameters
  number of random variables ...............nx=    2
  number of deterministic parameters .......np=    2
  number of user provided distribution .....nu=    0
  number of parameters in user-defined full
  distributions ............................ns=    0
  correlation structure ...................ncorr=   0
    ncorr.eq.0 ................uncorrelated variables
    ncorr.ne.0 ..................correlated variables
  initialization flag ......................init=   0
    init.eq.0 .........initialization at mean point
    init.ne.0 ...............initialization by user
  output flag ..............................ipr=    1
    ipr.eq.0 ...............output only final results
    ipr.ne.0 .............output at every ipr steps
```

326

```
   icpt=1 .........................RF-HL method
   icpt=2 ...................Modified RF-HL method
   icpt=3 ..............Gradient Projection method
maximum number of iteration cycles .....nit1=   20
maximum steps in line search ...........nit2=    4
convergence tolerance ...............tol= 1.000E-04
optimization parameter 1 ..........opt1= 1.000E+00
optimization parameter 2 ..........opt2= 0.000E-01
optimization parameter 3 ..........opt3= 0.000E-01


available probability distributions:
   normal......................ndis=1
   lognormal ..................ndis=2
   gamma ......................ndis=3
   exponential ................ndis=4
   rayleigh....................ndis=5
   uniform.....................ndis=6
   beta........................ndis=7
   type i largest value .....ndis=11
   type i smallest value ....ndis=12
   type ii largest value ....ndis=13
   weibull.....................ndis=14


statistical data of basic varibles:
 var ndis    mean    st. dev.   param1     param2     param3     param4     init. pt
  1   11   1.00E+02  2.00E+01  9.10E+01  6.41E-02                          1.00E+02
  2    2   2.00E+01  5.00E+00  2.97E+00  2.46E-01                          2.00E+01


deterministic parameters in performance function:
  dp (  1) =  1.000E+00
  dp (  2) =  5.000E-01



               ****    solution phase    ****

mvfosm technique:  beta =  0.9806;   failure probability =  1.634E-01
------------------------------------------------------
iteration no.    1
var.      linearization point          unit normal
             x            y              alpha
  1    1.000E+02    1.773E-01          0.1906
  2    2.000E+01    1.231E-01         -0.9817
reliabilty index beta   =        0.2159
------------------------------------------------------
iteration no.    2
var.      linearization point          unit normal
             x            y              alpha
  1    9.992E+01    1.734E-01          0.3046
  2    1.557E+01   -8.930E-01         -0.9525
reliabilty index beta   =        0.9097
------------------------------------------------------
iteration no.    3
var.      linearization point          unit normal
             x            y              alpha
  1    1.040E+02    3.788E-01          0.3697
  2    1.449E+01   -1.185E+00         -0.9292
reliabilty index beta   =        1.2437
```

```
iteration no.    4
var.        linearization point           unit normal
            x           y                     alpha
    1     1.058E+02    4.656E-01              0.3777
    2     1.455E+01   -1.170E+00             -0.9259
reliabilty index beta    =       1.2595
-------------------------------------------------------
iteration no.    5
var.        linearization point           unit normal
            x           y                     alpha
    1     1.060E+02    4.755E-01              0.3781
    2     1.456E+01   -1.166E+00             -0.9258
reliabilty index beta    =        1.2589
-------------------------------------------------------
iteration no.    6
var    design point    unit sensitivity vectors           nearest pt   unit normal
            x*      gamma      delta        eta                y*          alpha
    1     1.060E+02   0.3782   -0.2715    -0.0841          4.761E-01      0.3782
    2     1.456E+01  -0.9257    0.9624    -0.9965         -1.165E+00     -0.9257
-------------------------------------------------------
reliability index beta    =        1.2589
failure probability       =     1.040E-01
```

```
**********************************************************
*                                                        *
*               Sensitivity Analysis                     *
*                                                        *
**********************************************************
```

        *** Sensitivity Analysis on Distribution Parameters ***

```
d(beta)/d(parameter) :
var      mean        std dev      par 1        par 2       par 3        par 4
  1   -1.773E-02  -5.349E-03  -1.773E-02   4.157E+00
  2    2.514E-01  -2.536E-01   3.760E+00  -4.382E+00

d(pf1)/d(parameter) :
var      mean        std dev      par 1        par 2       par 3        par 4
  1    3.202E-03   9.661E-04   3.202E-03  -7.507E-01
  2   -4.540E-02   4.580E-02  -6.791E-01   7.914E-01
```

        *** Sensitivity Analysis on Deterministic Parameters ***

```
par    d(beta)/d(parameter)        d(pf1)/d(parameter)
  1        -1.880E+00                  3.395E-01
  2         3.760E+00                 -6.791E-01
```

```
*****************************************************************
*                                                               *
*        Second Order Structural Reliability Analysis           *
*                                                               *
*                 Point Fitting Method                          *
*                                                               *
*****************************************************************
```

** coordinates and ave. main curvatures of fitting points in rotated space ***

y' 1 = 1.258944   y' 2 = 1.216377
y' 1 = -1.258944   y' 2 = 1.217586
a 1   =-0.2647618E-01

*** second-order approximation ***

	failure probability	generalized reliability index
Breitung asymptotic formula	1.077E-01	1.2390
Tvedt three term formula	1.091E-01	1.2315
Tvedt single integral formula	1.090E-01	1.2316
Tvedt double integral formula	1.090E-01	1.2316

```
*****************************************************************
*                                                               *
*        Second Order Structural Reliability Analysis           *
*                                                               *
*                 Curvature Fitting Method                      *
*                                                               *
*****************************************************************
```

*** curvature matrix at design point in rotated space ***
```
         1
1  -2.740E-02
```

*** second-order approximation ***

	failure probability	generalized reliability index
Breitung asymptotic formula	1.078E-01	1.2383
Tvedt three term formula	1.092E-01	1.2306
Tvedt single integral formula	1.092E-01	1.2306
Tvedt double integral formula	1.092E-01	1.2306

```
***********************************************************************
*          U n i v e r s i t y    o f    C a l i f o r n i a          *
*              Department  of  Civil  Engineering                     *
*                        Division  of                                 *
*      Structural Engineering and Structural Mechanics.               *
*                                                                     *
*                    F  O  S  R  A  P                                 *
*      First Order Structural Reliabilty Analysis Program             *
*                                                                     *
*                        Developed By                                 *
*          Pei-Ling Liu and Armen Der Kiureghian                      *
*              Last Revision: September 1986                          *
*                                                                     *
*              Extended for FOFD and SOSRAP by                        *
*                  HONG-ZONG LIN, March 1986                          *
***********************************************************************
```

```
                ****    input data -- problem  1    ****

example 1
type of first-order technique used .......ifo=     3
   ifo=1 ...mean-value, 1st order, 2nd moment (mvfosm) method
   ifo=2 ...first-order, second moment (fosm) method
   ifo=3 ...first-order, marginal distribution (fomd) method
   ifo=4 ...first-order, full dist.(Rosenblatt trans) method
type of second-order technique used .....iso=     3
   iso=0 .............no second-order approximation
   iso=1 ......................point fitting method
   iso=2 ..................curvature fitting method
   iso=3 .......point and curvature fitting methods
type of integration schemes used in second-order
analysis ..................................itg=     1
   itg.eq.0 ....Breitung, Tvedt's 3-term and single integral
   itg.ne.0 ...all of the above plus Tvedt's double integral
type of sensitivity analysis required ...isv=     3
   isv=0 ...................no sensitivity analysis required
   isv=1 ..............sensitivity of distribution parameters
   isv=2 .......sensitivity of perfomance function parameters
   isv=3 ....distribution and performance function parameters
number of random variables ...............nx=     2
number of deterministic parameters .......np=     2
number of user provided distribution .....nu=     0
number of parameters in user-defined full
distributions ............................ns=     0
correlation structure ................ncorr=     1
   ncorr.eq.0 ..............uncorrelated variables
   ncorr.ne.0 ................correlated variables
initialization flag ......................init=     0
   init.eq.0 ..........initialization at mean point
   init.ne.0 ..............initialization by user
output flag ..............................ipr=    1
   ipr.eq.0 .............output only final results
   ipr.ne.0 .............output at every ipr steps
```

```
optimization scheme used ...............iopt=    1
   iopt=1 ..........................RF-HL method
   iopt=2 ..................Modified RF-HL method
 , iopt=3 ..............Gradient Projection method
maximum number of iteration cycles .....nit1=   20
maximum steps in line search ...........nit2=    4
convergence tolerance ..............tol= 1.000E-04
optimization parameter 1 ..........opt1= 1.000E+00
optimization parameter 2 ..........opt2= 0.000E-01
optimization parameter 3 ..........opt3= 0.000E-01


available probability distributions:
   normal .....................ndis=1
   lognormal ..................ndis=2
   gamma ......................ndis=3
   exponential ................ndis=4
   rayleigh....................ndis=5
   uniform.....................ndis=6
   beta........................ndis=7
   type i largest value .....ndis=11
   type i smallest value ....ndis=12
   type ii largest value ....ndis=13
   weibull....................ndis=14


statistical data of basic varibles:
 var ndis    mean     st. dev.   param1     param2     param3     param4   init. pt
   1   11   1.00E+02  2.00E+01   9.10E+01   6.41E-02                              1.00E+02
   2    2   2.00E+01  5.00E+00   2.97E+00   2.46E-01                              2.00E+01


deterministic parameters in performance function:
   dp ( 1) =  1.000E+00
   dp ( 2) =  5.000E-01


correlation coefficient matrix in original space:
       1      2
   1  1.00   0.50
   2  0.50   1.00


correlation coefficient matrix in normal space:
       1      2
   1  1.00   0.51
   2  0.51   1.00


              ****     solution phase     ****


avfosm technique:  beta =   1.0911;   failure probability = 1.375E-01
------------------------------------------------------
iteration no.   1
var.      linearization point          unit normal
            x           y                 alpha
   1     1.000E+02    1.773E-01         -0.3470
   2     2.000E+01    3.764E-02         -0.9379
reliabilty index beta    =        0.1813
------------------------------------------------------
iteration no.   2
var.      linearization point          unit normal
            x           y                 alpha
   1     9.078E+01   -3.511E-01         -0.2607
   2     1.519E+01   -9.489E-01         -0.9654
reliabilty index beta    =        1.0117
                                            331
```

```
           *** Sensitivity Analysis on Deterministic Parameters ***

par    d(beta)/d(parameter)      d(pf1)/d(parameter)
  1         -2.328E+00                2.732E-01
  2          4.656E+00               -5.563E-01




        ***********************************************************
        *                                                         *
        *      Second Order Structural Reliability Analysis -     *
        *                                                         *
        *              Point Fitting Method                       *
        *                                                         *
        ***********************************************************




** coordinates and  ave. main curvatures of fitting points in rotated space ***

y' 1  =  1.552342     y' 2  =  1.463146
y' 1  = -1.552842     y' 2  =  1.434239
a 1   =-0.32465336E-01
-----------------------------------------------------------------


              ***   second-order approximation   ***

                                failure           generalized
                              probability      reliability inde
Breitung asymptotic formula     6.352E-02            1.5259
Tvedt three term formula        6.443E-02            1.5186
Tvedt single integral formula   6.442E-02            1.5187
Tvedt double integral formula   6.442E-02            1.5187




        ***********************************************************
        *                                                         *
        *      Second Order Structural Reliability Analysis       *
        *                                                         *
        *              Curvature Fitting Method                   *
        *                                                         *
        ***********************************************************

        *** curvature matrix at design point in rotated space ***
           1
  1 -2.272E-02


              ***   second-order approximation   ***

                                failure           generalized
                              probability      reliability index
Breitung asymptotic formula     6.355E-02            1.5257
Tvedt three term formula        6.446E-02            1.5184
Tvedt single integral formula   6.445E-02            1.5195
Tvedt double integral formula   6.445E-02            1.5184
```

```
      function g(x,dp)
      implicit real*8 (a-h,o-z)
      dimension x(1),dp(1)
      g = dp(1) - dp(2)*x(1) - dp(3)*x(2)
      return
      end


      subroutine df(par,x,nd,cdf,pdf)
      implicit real*8 (a-h,o-z)
      dimension par(4)
      return
      end


      subroutine hfun(x,ih,ds,h)
      implicit real*8(a-h,o-z)
      dimension x(1),ds(1)
          go to (10,20) ih
10    h = 1-dexp(-x(1))
      return
20    h = 1-(1+ds(1)*x(2))*dexp(-x(2)-ds(1)*x(1)*x(2))
      return
      end
```

$$g = 5 - X_1 - X_2$$

$$ds(1) = 1.0$$

Input File for Example 3:

```
+*************************************************************
+         U n i v e r s i t y    o f   C a l i f o r n i a   *
*         Department  of  Civil  Engineering                 *
*                   Division of                              *
*    Structural Engineering and Structural Mechanics         *
*                                                            *
*                  C  A  L  R  E  L                          *
*    First and Second Order Reliabilty Analysis Program      *
*                                                            *
*                   Developed By                             *
*         Pei-Ling Liu and Armen Der Kiureghian              *
*              Last Revision: September 1986                 *
*                                                            *
*              Extended for FOFD and SOSRAP by               *
*                 HONG-ZONG LIN, March 1986                  *
+*************************************************************
```

****   input data -- problem 1   ****

```
example 3
type of first-order technique used .......ifo=     4
   ifo=1 ...mean-value, 1st order, 2nd moment (mvfosm) method
   ifo=2 ...first-order, second moment (fosm) method
   ifo=3 ...first-order, marginal distribution (fomd) method
   ifo=4 ...first-order, full dist.(Rosenblatt trans) method
type of second-order technique used .....iso=     3
   iso=0 ..............no second-order approximation
   iso=1 ....................point fitting method
   iso=2 ................curvature fitting method
   iso=3 .......point and curvature fitting methods
type of integration schemes used in second-order
analysis . ..............................itg=     1
   itg.eq.0 ....Breitung, Tvedt's 3-term and single integral
   itg.ne.0 ...all of the above plus Tvedt's double integral
type of sensitivity analysis required ...isv=     3
   isv=0 ...................no sensitivity analysis required
   isv=1 ............sensitivity of distribution parameters
   isv=2 .......sensitivity of perfomance function parameters
   isv=3 ....distribution and performance function parameters
number of random variables ...............nx=     2
number of deterministic parameters .......np=     3
number of user provided distribution .....nu=     0
number of parameters in user-defined full
distributions ...........................ns=     1
correlation structure ...................ncorr=    1
   ncorr.eq.0 ...............uncorrelated variables
   ncorr.ne.0 ................correlated variables
initialization flag .....................init=     1
   init.eq.0 .........initialization at mean point
   init.ne.0 ..............initialization by user
output flag .............................ipr=     1
   ipr.eq.0 ..............output only final results
   ipr.ne.0 .............output at every ipr steps
```

```
    iopt=1 ...........................RF-HL method
    iopt=2 ..................Modified RF-HL method
    iopt=3 ..............Gradient Projection method
maximum number of iteration cycles .....nit1=   20
maximum steps in line search ...........nit2=    4
convergence tolerance ..............tol= 1.000E-04
optimization parameter 1 ..........opt1= 1.000E+00
optimization parameter 2 ..........opt2= 0.000E-01
optimization parameter 3 ..........opt3= 0.000E-01



                 ****    restart solution    ****


-----------------------------------------------------
iteration no.    1
var.     linearization point        unit normal
            x           y               alpha
   1     1.825E-01   -9.669E-01        -0.4254
   2     4.818E+00    2.064E+00         0.9050
reliabilty index beta    =       2.2788
-----------------------------------------------------
iteration no.    2
var.     linearization point        unit normal
            x           y               alpha
   1     1.817E-01   -9.695E-01        -0.4246
   2     4.818E+00    2.062E+00         0.9054
reliabilty index beta    =       2.2788
-----------------------------------------------------
iteration no.    3
var.     linearization point        unit normal
            x           y               alpha
   1     1.823E-01   -9.675E-01        -0.4252
   2     4.818E+00    2.063E+00         0.9051
reliabilty index beta    =       2.2788
-----------------------------------------------------
iteration no.    4
var.     linearization point        unit normal
            x           y               alpha
   1     1.818E-01   -9.690E-01        -0.4247
   2     4.818E+00    2.063E+00         0.9053
reliabilty index beta    =       2.2788
-----------------------------------------------------
iteration no.    5
var.     linearization point        unit normal
            x           y               alpha
   1     1.822E-01   -9.679E-01        -0.4251
   2     4.818E+00    2.063E+00         0.9051
reliabilty index beta    =       2.2788
-----------------------------------------------------
iteration no.    6
var.     linearization point        unit normal
            x           y               alpha
   1     1.819E-01   -9.687E-01        -0.4248
   2     4.818E+00    2.063E+00         0.9053
reliabilty index beta    =       2.2788
-----------------------------------------------------
iteration no.    7
var.     linearization point        unit normal
            x           y               alpha
   1     1.821E-01   -9.681E-01        -0.4250
   2     4.818E+00    2.063E+00         0.9052
reliabilty index beta    =       2.2788
```

```
var.        linearization point            unit normal
              x            y                 alpha
    1     1.820E-01    -9.686E-01          -0.4249
    2     4.818E+00     2.063E+00           0.9052
reliabilty index beta    =        2.2788
----------------------------------------------------------
iteration no.    9
var.        linearization point            unit normal
              x            y                 alpha
    1     1.821E-01    -9.692E-01          -0.4250
    2     4.818E+00     2.063E+00           0.9052
reliabilty index beta    =        2.2788
----------------------------------------------------------
iteration no.   10
var.        linearization point            unit normal
              x            y                 alpha
    1     1.820E-01    -9.685E-01          -0.4249
    2     4.818E+00     2.063E+00           0.9052
reliabilty index beta    =        2.2788
----------------------------------------------------------
iteration no.   11
var.        linearization point            unit normal
              x            y                 alpha
    1     1.821E-01    -9.693E-01          -0.4250
    2     4.818E+00     2.063E+00           0.9052
reliabilty index beta    =        2.2788
----------------------------------------------------------
iteration no.   12
var.        linearization point            unit normal
              x            y                 alpha
    1     1.820E-01    -9.684E-01          -0.4249
    2     4.818E+00     2.063E+00           0.9052
reliabilty index beta    =        2.2788
----------------------------------------------------------

reliability index beta    =        2.2788
failure probability        =    1.134E-02


        **********************************************************
        *                                                        *
        *                 Sensitivity Analysis                   *
        *                                                        *
        **********************************************************


        *** Sensitivity Analysis on Distribution Parameters ***

par    d(beta)/d(parameter)      d(pf1)/d(parameter)
  1           1.825E-02               -5.427E-04


        *** Sensitivity Analysis on Deterministic Parameters ***

par    d(beta)/d(parameter)      d(pf1)/d(parameter)
  1           3.765E-01               -1.119E-02
  2          -6.853E-02                2.039E-03
  3          -1.814E+00                5.393E-02
```

```
**********************************************************
*                                                        *
*      Second Order Structural Reliability Analysis       *
*                                                        *
*             Point Fitting Method                        *
*                                                        *
**********************************************************
```

Σ

** coordinates and ave. main curvatures of fitting points in rotated space ***

y' 1 = 2.278824   y' 2 = 2.545030
y' 1 = -2.278324   y' 2 = 2.999305
a 1 = 0.9042262E-01

*** second-order approximation ***

	failure probability	generalized reliability index
Breitung asymptotic formula	9.542E-03	2.3439
Tvedt three term formula	9.285E-03	2.3541
Tvedt single integral formula	9.291E-03	2.3538
Tvedt double integral formula	9.292E-03	2.3538


```
**********************************************************
*                                                        *
*      Second Order Structural Reliability Analysis       *
*                                                        *
*            Curvature Fitting Method                     *
*                                                        *
**********************************************************
```

*** curvature matrix at design point in rotated space ***

```
        1
1   1.639E-01
```

*** second-order approximation ***

	failure probability	generalized reliability index
Breitung asymptotic formula	8.580E-03	2.3833
Tvedt three term formula	8.212E-03	2.3993
Tvedt single integral formula	8.229E-03	2.3986
Tvedt double integral formula	8.233E-03	2.3984

337

To run CALREL, do the following:

(1) Turn on the power of IBMPC and VCR terminal.

(2) Create a temporary directory in drive C and make it your
    working directory.
       [C:\]> MD CE249
       [C:\]> CD CE249

(3) Copy all files in D:\CE249 to drive C.
       [C:\CE249]> COPY D:\CE249*.* .

(4) Reset the search path.
       [C:\CE249]> START

(5) Edit the three subroutines in user.for such that they work
    in the same manner as indicated in the class handout.
    To edit the subroutines, key in:
       [C:\CE249]> PE USER.FOR
    To display the help file in PE, press <F1> key.

(6) Compile user.for and link the program.
       [C:\CE249]> CUSER
    If there are errors, use 'TYPE ERR' to examine them, and
    correct the errors in user.for. Then compile user.for again.
    Once a correct user.for is compiled, link the program.
       [C:\CE249]> LREL

(7) Create an input data file.
       [C:\CE249]> PE IN
    To exit the editor, type '<F3> IN NOTABS <RETURN>'. If 'NOTABS'
    is skipped, some spaces in the input file will be replaced
    by tab's. That messes up the input file.

(8) Run program CALREL.
       [C:\CE249]> CALREL < IN   (output on screen)
       [C:\CE249]> CALREL < IN > OUT   (output to file 'OUT')
    Make sure you leave spaces between file names and the symbols
    < and >.

(9) Read output file (if the output is routed to a file)
       [C:\CE249]> TYPE OUT   (read the file 'OUT' on screen)
       [C:\CE249]> NETPRINT OUT (get a hardcopy of the output file)
    Before the print queue is submitted, make sure that the line
    printer is online.

(10) Store your files in a floppy disk and delete all files in
     the working directory.
       [C:\CE249]> COPY (your file) A:
       [C:\CE249]> ERASE *.*

(11) Delete the temporary directory.
       [C:\CE249]> CD \
       [C:\]> RD CE249

(12) To shut down the machine, take your diskette out and turn
     off the power.